The Dissertation Committee for Daniel William Klosowski Certifies that this is the approved version of the following Dissertation:

Applications of Enantioselective Halolactonization Reactions, Synthesis of Photocaged Compounds for Identifying Neurons Based on Function, and Progress Towards the Total Synthesis of Alstoscholarisine E

Committee:

Stephen F. Martin, Supervisor

Grant Willson

Eric V. Anslyn

Adrian Keatinge-Clay

Boris Zemelman

Applications of Enantioselective Halolactonization Reactions, Synthesis of Photocaged Compounds for Identifying Neurons Based on Function, and Progress Towards the Total Synthesis of Alstoscholarisine E

by

Daniel William Klosowski

Dissertation

Presented to the Faculty of the Graduate School of

The University of Texas at Austin

in Partial Fulfillment

of the Requirements

for the Degree of

Doctor of Philosophy

The University of Texas at Austin

May 2018

Dedication

To my parents, Robert and Roxanne Klosowski, who have afforded me every opportunity to succeed. Thank you for everything.

Acknowledgements

The success I achieved in graduate school would not have been possible without a number of people who supported me along the way. First and foremost, I would like to thank Professor Stephen F. Martin for all his patience and guidance throughout my graduate career. Thank you for taking me into your group and teaching me all that you have. I could not have made it this far without your wisdom and expertise. You have influenced my career in ways that I will never forget and you truly changed my life for the better. Thank you, Steve, for all that you have done for me.

Next, I would like to thank my family, who unconditionally supported me throughout this difficult time. Especially my parents, Robert and Roxanne, who have always been there with words of encouragement and motivation. I owe everything I have in life to you both, and words cannot describe how grateful I am. To Kym and Brad, thank you for making Austin feel like home. You both were always there, with margaritas and queso, to remind me that everything will be ok. To my brother Tommy, thank you for moving to Austin with me. I know I was not the best roommate but living with you was one of the best times of my life. To my sister Heather, thank you for always being willing to listen. To Bobby and Philippe, thank you for believing in me. And finally, thank you to my grandfather, James Metz, and my uncles, Jimmy, Kenny, Joey, and Gary, for teaching us all to be there for one another.

I also owe a great deal of my success to my fellow Martin group members. From the first day I joined the group, you have all been great friends inside and outside of the lab. Graduate school would not have been the experience it was without all of you. To Caleb Hethcox and Shawn Blumberg, thank you for teaching and helping me. You both

were constant role models and I could not have done it without you. Also, Caleb, thank you for showing me where to find all the best concerts and beer. To Tim Hodges, thank you for your help in planning the route to alstoscholarisine E. You were always ready to help with a research problem, and your enthusiasm for euchre kept the lab's social life intact. To Alex Goodnough, thank you for being a great friend since the first day we met at orientation. I would not have made it through graduate school without you Al, you are the realest dude I know. To Zach White and Lance Lepovitz, thank you for all of the helpful chemistry discussions, supportive conversations, and board game nights over the years. I would also like to thank Alan Meis, who has always been a great colleague and friend. I look forward to working with you again in the future. And thank you to the rest of the current members of the Martin group, Chris Farley, Zhipeng Wang, Michael Wood, and Grant Walby, for making the lab a great place to be.

And finally, I would like to thank Jasmine Mason for all of her support throughout this past year. Thank you for your encouragement and confidence in my ability. I could not have done it without you.

Abstract

Applications of Enantioselective Halolactonization Reactions, Synthesis of Photocaged Compounds for Identifying Neurons Based on Function, and Progress Towards the Total Synthesis of Alstoscholarisine E

Daniel William Klosowski, Ph.D.

The University of Texas at Austin, 2018

Supervisor: Stephen F. Martin

Recently the Martin group developed a bifunctional organic catalyst that promotes highly efficient enantioselective halolactonization reactions for olefinic acids. Using the BINOL-amidine catalyst we invented, our group was able to perform halolactonization reactions on a broad array of substrates. Herein we describe the synthetic utility of this method through a concise synthesis of (+)-disparlure, along with the preparation of F ring synthons for the natural product kibdelone C.

As part of a separate project, in collaboration with the Zemelman research group, we are working to design a system for identifying behaviorally relevant assemblies of neurons in awake animals. This novel technique identifies active neurons and tags them using fluorescent proteins that are expressed upon irradiation of the neuron with visible light. This system hinges on the preparation on light sensitive derivatives of a variety of repressor protein ligands using “cages” or “photocages.” Toward this end, we prepared photocaged derivatives of anhydrotetracycline and vanillic acid.

Finally, we disclose our progress towards the total synthesis of alstoscholarisine E, a natural product isolated in 2014 that was found to be a strong promoter of adult neuronal stem cell proliferation. We envisioned a convergent synthesis where skatole and a hetero-Diels-Alder product could be joined through a metal catalyzed coupling to form the tetracyclic core of the molecule, which could then be easily transformed to alstoscholarisine E through an olefin reduction followed by a reductive cyclization. Accessing our desired hetero-Diels-Alder product quickly was paramount to the effectiveness of this route, and thus, we developed a method to access hetero-Diels-Alder precursors in one step starting from readily available hexahydrotriazines.

Table of Contents

List of Tables xv

List of Figures xvi

List of Schemes xvii

APPLICATIONS OF ENANTIOSELECTIVE HALOLACTONIZATION REACTIONS 1

Chapter 1: Catalytic Enantioselective Halolactonization Reactions 1

1.1 Introduction 1

1.2 Developments in Catalytic Enantioselective Halolactonizations 4

1.2.1 Overview of Reported Catalysts 4

1.2.2 Yeung 11

1.2.3 Summary 15

1.3 Martin Group Halolactonization Methodology 16

1.3.1 Catalyst Development 16

1.3.2 Effects of Catalyst Modification 20

1.3.3 Halolactonization Reactions 23

1.3.4 Mechanistic Aspects 32

1.3.5 Applications to Methodological Problems 34

1.4 Desymmetrization via Asymmetric Halolactonization Reactions 36

1.4.1 Introduction 36

1.4.2 Hennecke 37

1.4.3 Desymmetrization of 1,4-Cyclohexadienoic Acids 38

1.4.4 Johnston 41

1.4.5 Summary 42

1.5 Asymmetric Epoxidation of Unactivated *Z*-Disubstituted Olefins.....43

1.6 Summary and Conclusions 48

Chapter 2: Applications of Enantioselective Halolactonization Reactions 50

2.1 Kibdelone C – Introduction and Isolation.....50

2.2 Previous Syntheses of F-Ring Subunits of Kibdelone C 52

2.2.1 Porco's F-Ring for (+)-Kibdelone C.....52

2.2.2 Hudlicky's Synthesis of Porco's F-Ring 59

2.2.3 Ready's F-Ring for (–)-Kibdelone C 60

2.3 Martin Group Strategy 65

2.3.1 Introduction and Synthetic Approach 65

2.3.2 Strategies for Halogen Atom Installation on Kibdelone F-ring Subunits 67

2.3.2.1 β-Halogenation.....67

2.3.2.2 Hunsdiecker Halodecarboxylation.....69

2.4 Martin Group Synthesis of F-Ring Subunits 74

2.5 Summary of Martin Group F-ring syntheses 94

2.6 (+)–Disparlure – Introduction.....96

2.7 Select Previous Syntheses of Disparlure 98

2.7.1 Iwaki's Synthesis of (+)–Disparlure – Chiral Pool Starting Materials 98

2.7.2 Sharpless' Syntheses of (+)-Disparlure – Asymmetric Epoxidation and Dihydroxylation 100

2.7.3 Tsuboi's Synthesis of (–)-Disparlure – Enzymatic Resolution 103

2.7.4 Kim's Synthesis of (+)-Disparlure – Proline Organic Catalysis 106

2.7.5 Satoh's Synthesis of (+)-Disparlure – Chiral Sulfoxide Auxiliary....107

2.7.6 Summary of Previous Syntheses....109

2.8 Enantioselective Synthesis of (+)-Disparlure Via Asymmetric Iodolactonization....109

2.8.1 Synthetic Approach....109

2.8.2 First Generation Synthesis....111

2.8.3 Carbocupration of Acetylene....115

2.8.4 Second Generation Synthesis....120

2.8.5 Summary....128

2.9 Summary and Conclusions....129

SYNTHESIS OF PHOTOCAGED COMPOUNDS FOR LABELING NEURONS BASED ON FUNCTION....131

Chapter 3: Photolabile Protecting Groups....131

3.1 Introduction....131

3.2 *o*-Nitrophenyl Photolabile Protecting Groups....133

3.2.1 *o*-Nitrobenzyl Photolabile Protecting Groups....133

3.2.1.1 Mechanism of Deprotection....134

3.2.1.2 o-Nitrobenzyl Photolabile Protecting Group Derivatives....137

3.2.2 *2-(2-Nitrophenyl)ethyl* Photolabile Protecting Groups....139

3.2.3 *o*-Nitroanilide Photolabile Protecting Groups....141

3.3 Arylcarbonyl Photolabile Protecting Groups....143

3.3.1 Phenacyl Photolabile Protecting Groups....143

3.3.1.1 p-Hydroxyphenacy Photolabile Protecting Groupsl....143

3.3.1.2 Benzoin Photolabile Protecting Groups....145

3.3.2 Deprotection Via Photoenolization....146

3.3.2.1 2-Methyl-Substituted Acetophenones.....147

3.3.2.2 2-Ethylene-Subtituted Arylcarbonyl Photolabile Protecting Groups.....149

3.3.2.3 Intramolecular Lactonization.....150

3.4 Coumarin Based Photolabile Protecting Groups.....151

3.4.1 Mechanism of Deprotection.....151

3.4.2 Select Examples of Coumarin PPG Derivatives.....153

3.5 Bodipy Derived Photolabile Protecting Groups.....155

3.6 Biological Application of Photocages: Light Controlled Gene Expression.....156

3.6.1 Overview of Small Molecule Regulated Gene Expression Systems.156

3.6.2 Tetracycline Dependent Gene Expression.....159

3.6.2.1 Tetracycline Resistance in Bacteria.....159

3.6.2.2 Tet_{ON} Gene Expression.....160

3.6.2.3 Photocaged Doxycycline: Light Controlled Tet_{ON}.....161

3.6.3 Erythromycin Dependent Gene Expression.....163

3.6.3.1 Erythromycin Antibiotic Resistance.....163

3.6.3.2 Photocaged Erythromycin: Light Controlled Ery_{ON}.....164

3.7 Summary of Photolabile Protecting Groups.....166

Chapter 4: Synthesis of Photocaged Ligands.....170

4.1 Introduction.....170

4.2 Novel Method for Identifying Active Neurons.....170

4.2.1 Overview of Proposed Method.....170

4.2.2 Generic Genetic Components of Neuron Labeling System.....171

4.2.2.1 Transcription Factor and Promoter X.....173

4.2.2.2 Prokaryotic Operator/Repressor Pairs.....174

4.2.3 Implementation of Proposed Method 176

4.3 Design of Photocaged Ligands 178

4.4 Synthesis of CANBP Photocages 183

4.5 Synthesis of Caged Vanilic Acid Derivatives.....185

4.5.1 Caging Vanillic Acid – Ester Derivatization 185

4.5.2 Caging Vanillic Acid – Phenol Derivatization 190

4.5.3 Synthesis of Caged Vanillic Acid Derivatives Summary and Conclusions.....192

4.6 Synthesis of Caged Tetracycline Derivatives 193

4.7 Summary and Future Directions 205

PROGRESS TOWARDS THE TOTAL SYNTHESIS OF ALSTOSCHOLARISINE E 208

Chapter 5: Alstoscholarisines A–E – Isolation and Previous Syntheses 208

5.1 Isolation 208

5.2 Previous Syntheses of Alstoscholarisine A 209

5.2.1 Bihelovic and Ferjancic's Synthesis of (±)-Alstoscholarisine A.....209

5.2.2 Yang's Synthesis of (–)-Alstoscholarisine A.....215

5.2.3 Weinreb's Synthesis of (±)-Alstoscholarisines B and C 219

5.3 Summary.....225

Chapter 6: Progress Towards the Total Synthesis of Alstoscholarisine E.....227

6.1 Synthetic Strategy.....227

6.1.2 Martin Group Previous Work: Intramolecular Hetero-Diels–Alder Reactions.....228

6.2 One-Step Preparation of Hetero-Diels–Alder Precursor 232

6.3 Hetero-Diels-Alder Reaction 236
6.4 Halogenation of Hetero-Diels–Alder Product 237
6.5 Skatole Cross Coupling Efforts 239
6.5.1 Direct C-2 Coupling to Skatole 239
6.5.2 C-2 Lithiation of Skatole 240
6.6 Summary 249
6.7 Future Directions 251
Chapter 7 Experimental Procedures 255
7.1 General Experimental 255
7.2 Experimental Procedures 256
References 290

List of Tables

Table 1.1 Effects of catalyst modification on the conversion of **1.74** to **1.75**[a] 23

Table 1.2 Halolactonization of 4-substituted-4-pentenoic acids[a].....26

Table 1.3 Halolactonization of 5-aryl-4(*E*)-pentenoic acids[a].....27

Table 1.4 Halolactonization of 5-substituted-5-hexenoic acids[a].....29

Table 1.5 Halolactonization of 5-substituted-4(*Z*)-pentenoic Acids[a].....31

Table 1.6 Iodolactonization of 6-substituted-5(*Z*)-hexenoic acids[a] 32

Table 1.7 Desymmetrization of **1.117a–d** via bromolactonization with **1.19**.....39

Table 2.1 Evaluation of catalysts **2.93** and **2.94** for the desymmetrization of **2.58**.....78

Table 2.2 Dihydroxylation of **2.59**.....81

Table 2.3. Conditions screened to prepare **2.101** 86

Table 2.4. Optimization of the preparation of Grignard reagent **2.193**.....121

Table 2.5 Optimization of the carbocupration of **2.200** and **2.201** model systems.....124

Table 6.1. Negishi coupling conditions screened to form **6.60**.....246

Table 7.1 Comparison of ^{13}C NMR peaks of disparlure with reported literature values. 272

List of Figures

Figure 1.1 Select examples of halogenated natural products. 2

Figure 1.2 *Exo*-cyclization mode of 5-aryl-4(*Z*)-pentenoic acids 33

Figure 1.3 Substrate scope of desymmetrizations of cyclohexadienes with **1.19** 40

Figure 1.4. Asymmetric epoxidations of unfunctionalized olefins with **1.147**. 47

Figure 2.1 Kibdelones A–C 51

Figure 2.2 Mechanistic rationale for the observed diastereomeric ratio of **2.16** and **2.17** 56

Figure 2.3 Summary of modifications to the Hunsdiecker halodecarboxylation 71

Figure 2.4. The gypsy moth pheromone disparlure. 97

Figure 3.1. Select examples of *o*-nitrobenzyl photolabile protecting groups. 139

Figure 3.2. Select derivatives of the 2-(2-Nitrophenyl)ethyl PPG class 141

Figure 3.3 Generic examples of expression-ON and expression-OFF systems 158

Figure 3.4 Select tetracycline derivatives. 159

Figure 3.5. Select examples from most common classes of PPGs 168

Figure 4.1 Basic components of the proposed neuron labeling system and their functions. 173

Figure 4.2. Select small molecule/repressor protein pairs 176

Figure 4.3. Summary of the proposed method in practice 178

Figure 4.4. Possible photocages for preparation of caged ligands 179

Figure 4.5. Planned photocaged derivatives of ligands **4.1**, **4.2**, and **4.4**. 182

Figure 4.6 Carbamate linked caged ATc derivative. 206

Figure 5.1. Alstoscholarisines A–E (**5.1–5.5**) 208

List of Schemes

Scheme 1.1 General mechanism for bromonium ion transfer between olefins.....3

Scheme 1.2 Halonium stability studies by Olah.....4

Scheme 1.3 Preparation of catalyst **1.67** from *R*-BINOL (**1.57**).....18

Scheme 1.4 Two-step preparation of enantioenriched epoxides from 4(*Z*)-alkenoic acids. 36

Scheme 1.5. Asymmetric epoxidations of **1.141** and **1.143** with catalyst **1.145**.....46

Scheme 2.1 Porco's synthetic strategy towards (+)-kibdelone C.....53

Scheme 2.2. Porco's synthesis of F-ring fragment **2.16**.....54

Scheme 2.3 Connection of ABCD-rings **2.4** and F-ring **2.5** and E-ring formation.....58

Scheme 2.5 Ready's synthetic strategy for (–)-kibdelone C. 61

Scheme 2.6. Ready's synthesis of F-ring fragment **2.48**.....63

Scheme 2.7 Connection of **2.54** and **2.48** and conversion to **2.57** 65

Scheme 2.8 Martin group synthetic plan for preparing kibdelone F-ring fragments. 66

Scheme 2.9 Bartlett's synthesis of β-chlorinated cyclohexenoate **2.75** 69

Scheme 2.10. General Barton–Hunsdiecker reaction and mechanism of radical decarboxylation.....72

Scheme 2.11. Conjugate addition of *p*-methoxythiophenolate to **2.99** and mechanistic rationale for stereochemical outcome. 87

Scheme 2.12. Halodecarboxylation of **2.105** via formation of **2.108**.....91

Scheme 2.13. Synthesis of F-ring fragments for kibdelone C natural products.....95

Scheme 2.14. Iwaki's enantioselective synthesis of (+)-disparlure. 99

Scheme 2.15 Synthesis of (+)-disparlure via Sharpless asymmetric epoxidation.....101

Scheme 2.16. Synthesis of (+)-disparlure via Sharpless asymmetric dihydroxylation. ..103

Scheme 2.17. Tsuboi's synthesis of (–)-disparlure via enzymatic chiral resolution. 105

Scheme 2.18. Kim's synthesis of (+)-disparlure via proline catalysis. 106

Scheme 2.19. Satoh's synthesis of (+)-disparlure. 108

Scheme 2.20. Martin group synthetic approach to (+)-disparlure. 110

Scheme 2.21 First generation synthesis of (+)-disparlure 114

Scheme 2.22. Synthetic strategy for the one-step preparation of **2.158** 115

Scheme 2.23. Regiochemical outcomes in the carbocupration of alkynes.....116

Scheme 2.24. Theoretical mechanism of carbocupration of acetylene for clustered cuprates ($R_2CuLi•LiX$) as proposed by Nakamura and Morokuma. 118

Scheme 2.25 One-step method for the preparation of *Z*-alkenoic acids reported by Fujisawa. 119

Scheme 3.1. Photodeprotection mechanism of *o*-nitrobenzyl photolabile protecting groups.....135

Scheme 3.2. Photodeprotection mechanism for the 2-(2-nitrophenyl)ethyl-based PPGs.....140

Scheme 3.3. Photodeprotection mechanism for the *o*-nitroanilide class of PPG. 142

Scheme 3.4.Photodeprotection mechanism of the *p*-hydroxyphenacyl PPG. 144

Scheme 3.5. Photodeprotection mechanism for the 3',5'-dimethoxybenzoin class of PPG. 145

Scheme 3.6 Problematic side reactions when protecting alcohols and amines with **DMB**. 146

Scheme 3.7 Photodeprotection mechanism of the 2-methylacetophenone PPG. 148

Scheme 3.8. Photodeprotection mechanism for the ethylene-substituted arylcarbonyl PPG 149

Scheme 3.9. Photodeprotection mechanism of **3.63** via intramolecular lactonization....150

Scheme 3.10 Photodeprotection mechanism for the coumarin PPGs 152

Scheme 3.11. Preparation of photocaged erythromycin derivative **3.92**.....165

Scheme 4.1. Synthesis of **CANBP** photocage **4.21**.....184

Scheme 4.2. Synthesis of nor-methyl **CANBP** photocage **4.25**.....185

Scheme 4.3. Preparation of MOM protected vanillic acid **4.29**. 186

Scheme 4.4. Yamaguchi esterification of **4.29** to prepare **4.30**.....189

Scheme 4.5. Preparation of **4.38** from **4.27**.....191

Scheme 4.6. Acylation of **4.1** with CbzCl in the absence of NMI. 198

Scheme 4.7. Epimerization of ATc during the preparation from **4.55**.....201

Scheme 4.8. Synthesis of caged ATc derivative **4.61**. 204

Scheme 4.9. Release of substrates from a photocage connected by an ethylene diamine carbamate linker.....206

Scheme 5.1. Synthesis of **5.14**.....210

Scheme 5.2. Attempted domino cyclization sequence using **5.15** 211

Scheme 5.3 Successful domino cyclization sequence using **5.14** and **5.18** 212

Scheme 5.4. Equilibration between **5.22** and **5.20**. 213

Scheme 5.5. Elaboration of **5.14** to alstoscholarisine A (**5.1**) 214

Scheme 5.6. Preparation of enantioselective Friedel–Crafts alkylation starting material. 216

Scheme 5.7. Elaboration of **5.33** to **5.38**. 217

Scheme 5.8. Completion of **(–)-5.1** from **5.38** 218

Scheme 5.9. Preparation of the Michael acceptor **5.45** 219

Scheme 5.10 Synthesis of the tetracyclic core **5.50** of **5.2** and **5.3** 221

Scheme 5.11. Elaboration of **5.50** to (±)-alstoscholarisine C (**5.3**) 223

Scheme 5.12. Elaboration of **5.53** to **5.2** 224

Scheme 6.1. Synthetic strategy for the preparation of alstoscholarisine E (**6.1**).....228

Scheme 6.2. Previous Martin group synthesis of intramolecular HDA precursors.....230

Scheme 6.3. Possible transition states for intramolecular HDA cycloadditions for amide tethered trienes. 231

Scheme 6.4 General reactivity of hexahydrotriazines with acyl chlorides and nucleophilic capture of intermediates **6.28** or **6.29**.....232

Scheme 6.5 Proposed mechanism for the halogenation of vinyl ethers by *N*-halosuccinimides and silver nitrate.....239

Scheme 6.6. C-2 -lithiation of skatole derivatives and transmetallation of **6.48**.....241

Scheme 6.7. Proposed one-pot sequence for Negishi coupling of **6.45** and **6.35** or **6.36**.....242

Scheme 6.8. C-2 lithiation of **6.52** and subsequent deuterium quenching. 243

Scheme 6.9. Summary of progress towards the total synthesis of alstoscholarisine E. ..250

Scheme 6.10. Alternative Suzuki coupling strategy for connecting **6.36** and **6.72**.....253

Scheme 6.11. Stille coupling strategy to prepare **6.3**. 254

APPLICATIONS OF ENANTIOSELECTIVE HALOLACTONIZATION REACTIONS

Chapter 1: Catalytic Enantioselective Halolactonization Reactions

1.1 INTRODUCTION

Nature provides a wealth of complex natural products to inspire synthetic chemists. To date, there have been nearly 5,000 halogenated natural products discovered, approximately half of which contain sp^3 hybridized carbon-halogen bonds.[1] Consequently, the introduction of carbon-halogen chiral centers is a critical component for targeting an enormous number of natural products. Natural products such as bromophycolide A (**1.1**), β-snyderol (**1.2**), (–)-kumausallene (**1.3**), and laurencin (**1.4**) have driven an ever-growing field of enantioselective halocyclization reactions (Figure 1.1). To date, enantioselective halolactonizations (**1.5**, Y = O, Z = OH),[2–33] haloetherifcations (**1.5**, Y = O, Z = H_2),[34–43] and haloaminocyclizations (**1.5**, Y = NHR, Z = H_2)[44–52] have been extensively explored (Equation 1.1). Other less explored halocyclization modes include oxazoline formation, oxazolidinone formation, and cyclization of oximes Although, catalytic halo-polyene cyclizations have proven to be particularly challenging, there has been some progress in the area (Equation 1.2).[53–55]

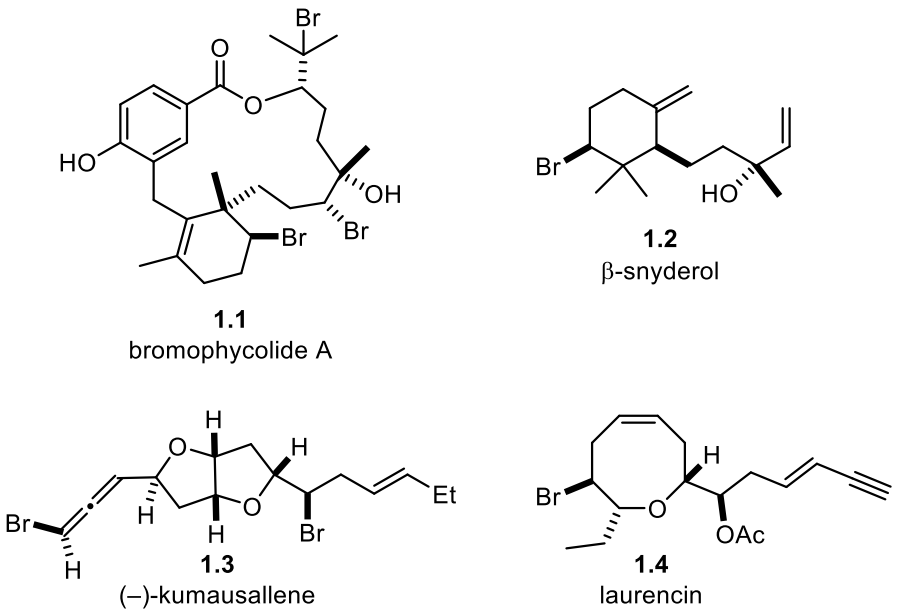

Figure 1.1 Select examples of halogenated natural products.

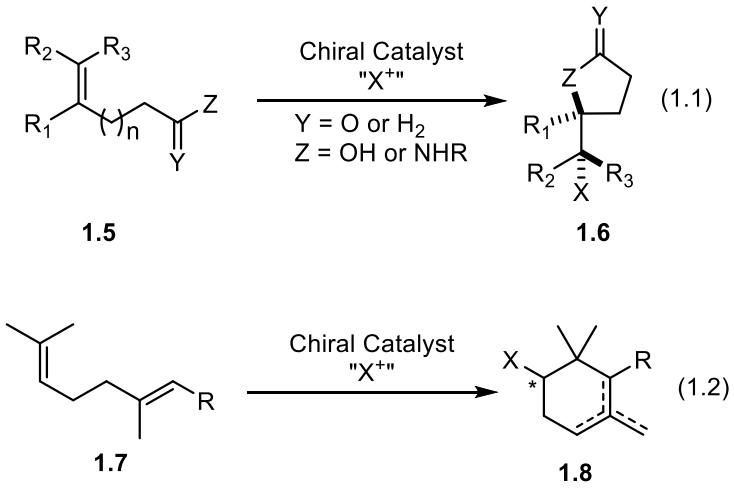

The development of enantioselective halocyclization reactions is inherently difficult due to the propensity of halonium ions to transfer between olefins intermolecularly.[56] Using variable-temperature ^{1}H NMR experiments and computational studies, Brown demonstrated that a rapid olefin-to-olefin transfer process occurs between 2-(2-adamantylidene)adamantane and the isolable halonium ions derived from it (Scheme 1.1).[57,58] In the context of enantioselective halocyclization reactions, this olefin-to-olefin

transfer must be suppressed because of its potential to racemize halonium ions that are generated stereoselectively. Importantly, this transfer process has been shown to be competitive with nucleophilic capture of the halonium ion, and in an achiral environment, the equilibration will result in racemic products, even if the halogen atom is initially delivered selectively.[56]

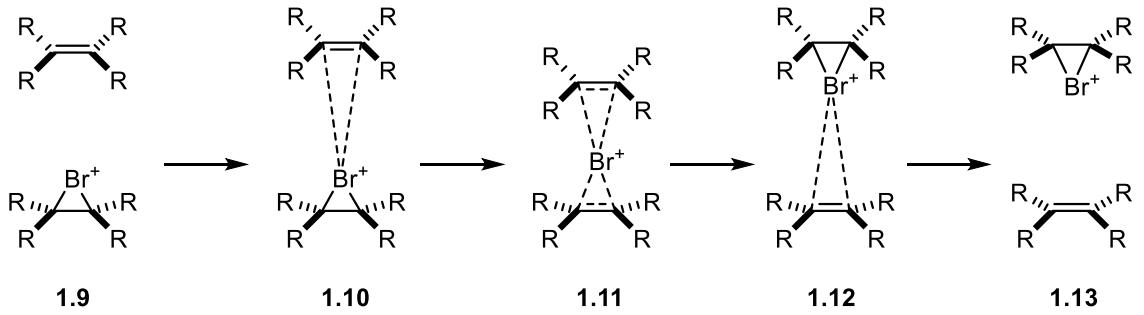

Scheme 1.1 General mechanism for bromonium ion transfer between olefins

Additional challenges arise in the development of chloro- and fluorocyclization reactions because of the instability of the halonium intermediates. Olah studied the stability of halonium ions using **1.14** with varying degrees of methyl substitution at the R groups and found that all iodonium and bromonium ions were cyclic on the ^{1}H NMR time scale at low temperatures, where chloro- and fluoro-substituted substrates of **1.14** existed as the cationic species **1.15** (Scheme 1.2).[59–61] This is potentially detrimental to selectivity in halocyclization reactions because cationic intermediates provide little steric differentiation between either face of the cation, whereas nucleophilic attack onto a fully formed halonium ion would proceed from its opposite face, leading to excellent diastereoselectivity.

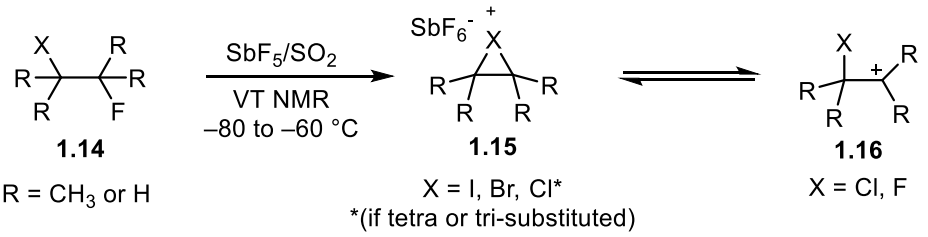

Scheme 1.2 Halonium stability studies by Olah.

Despite these difficulties, considerable progress has been made in the area of catalytic enantioselective halocyclization reactions in the last 10 years. The majority of the work in this area has focused on enantioselective halolactonization reactions, and there has been a number of recent reviews that extensively cover the evolution of this field of research.[56,62–67] The field of asymmetric halolactonization saw rapid development of organocatalysts between 2010–2016, but few new catalysts have been reported since. Herein we will discuss some of the major developments of organocatalytic enantioselective methods that have emerged in recent years.

1.2 Developments in Catalytic Enantioselective Halolactonizations

1.2.1 Overview of Reported Catalysts

Gao disclosed the first catalytic method for an enantioselective halolactonization reaction that provided the halolactones in good yield and with good enantioselectivities.[68] After Gao's seminal reports, other groups quickly joined the effort. Borhan described the first highly enantioselective (up to 95:5 er) chlorolactonizations of a series of 4-aryl-substituted-4-pentenoic acids **1.17** using the commercially available $(DHQD)_2PHAL$ (**1.19**) as the catalyst (Equation 1.3). Chlorolactonization has remained a particularly challenging area of research, in part due to the instability of the chloronium ion as previously mentioned. There have been only two other reported catalysts capable of

promoting enantioselective chlorolactonization reactions, and the substrate scope for these catalysts is limited. Tang reported the modified cinchona catalyst **1.21** which promotes chlorolactonizations of 4-aryl-substituted-4-pentenoic acids **1.17** with similar selectivities as **1.19** (Equation 1.4).[12] Zhou reported the cinchonine-squaramide catalyst **1.25**, which promotes the chlorolactonization of vinylbenzoic acids (**1.22**) with moderate to high enantioselectivities (Equation 1.5).[23] Borhan remains the most active contributor in the area of enantioselective chlorocyclizations and continues to study the mechanistic aspects of these reactions in detail.[21,33,69]

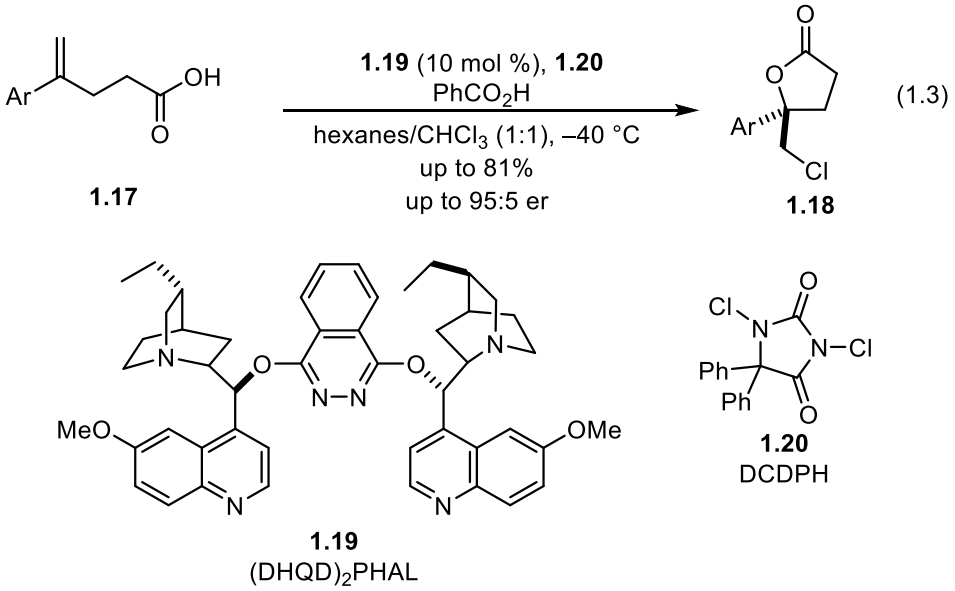

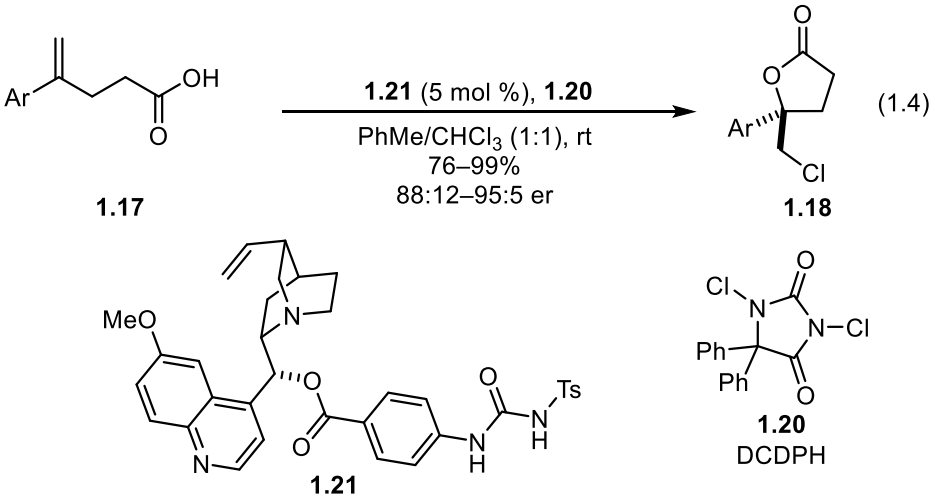
Ar
OH
O
1.17
1.21 (5 mol %), 1.20
PhMe/CHCl3 (1:1), rt
76–99%
88:12–95:5 er
O
O
Ar
Cl
1.18
(1.4)
MeO
N
O
O
N
H
Ts
O
N
1.21
Cl
N
O
N–Cl
Ph
Ph
O
1.20
DCDPH

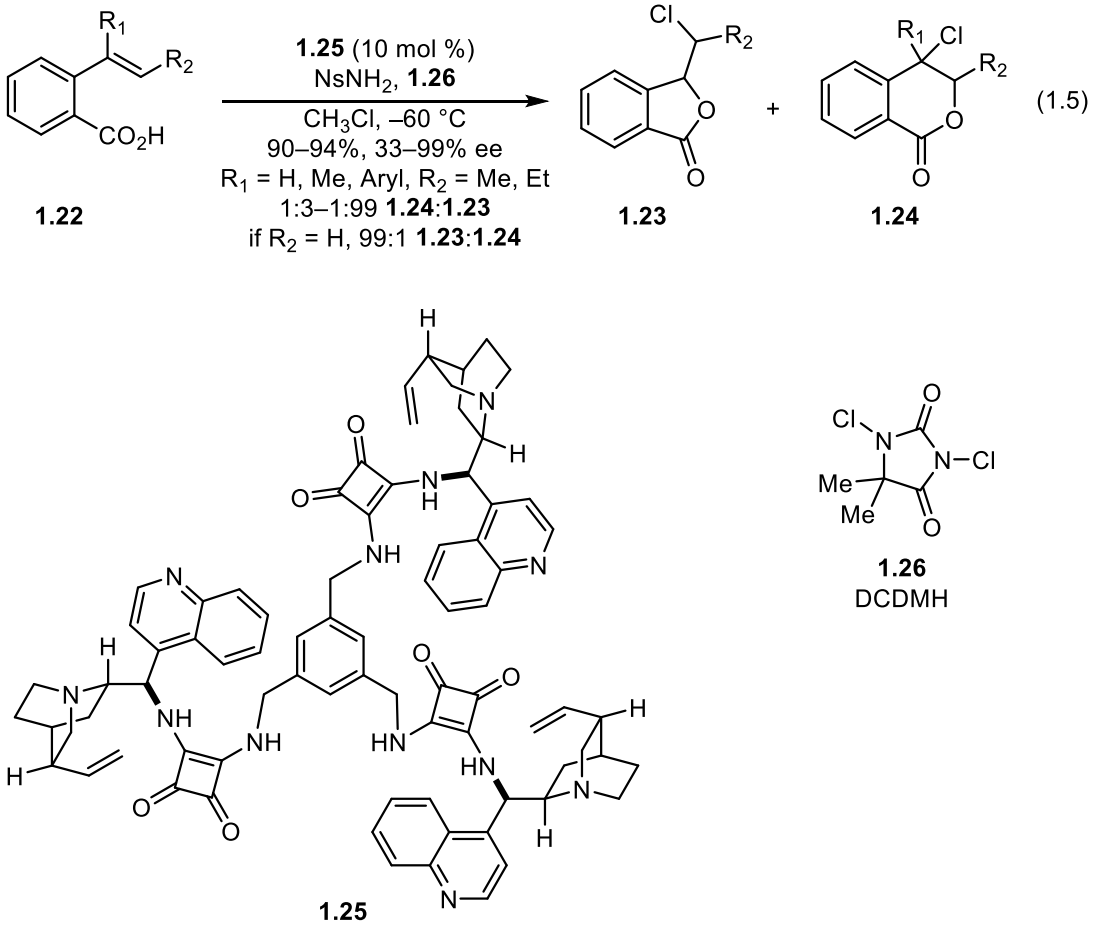

Similar to chlorolactonization reactions, reports of successful catalysts for enantioselective fluorolactonizations have remained scarce. The first example came from Rueping, who utilized a combination of $(DHQ)_2PHAL$ (**1.19**) and Selectfluor® (**1.30**) to generate a fluorinated isobenzofuran in modest yield (50%) and low enantioselectivity (27% ee).[25] The only catalytic, highly enantioselective fluorolactonization using an electrophilic fluorine source reported thus far was achieved by Hamashima using catalyst **1.29**, although the method could only produce fluorinated isobenzofuranones **1.28** (Equation 1.6).[26] Jacobsen recently reported a method for asymmetric fluorolactonization

using a chiral aryl iodide catalyst and a nucleophilic fluoride source that delivered fluorinated isochromanones with generally high enantioselectivity.[27]

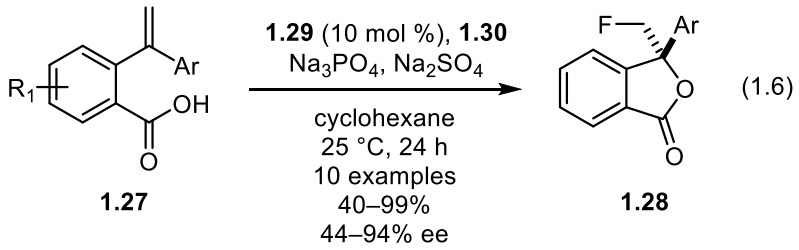

(1.6)

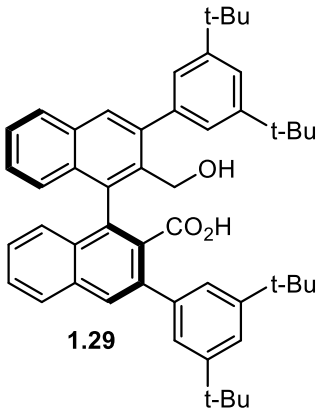

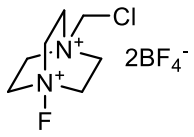

1.30
Selectfluor

Bromo- and iodolactonizations have received much greater attention from the synthetic community, and a wider variety of catalysts have been reported. Since Borhan's initial report, a number of groups have demonstrated the utility of $(DHQD)_2PHAL$ (**1.19**) as a catalyst for bromolactonization reactions. Hamashima and Hennecke both employed **1.19** for the desymmetrization of prochiral substrates through bromolactonization, work that will be discussed later in this chapter. Armstrong surveyed the ability of **1.19** to promote a small variety of olefinic acids that were generally aryl substituted, and in some cases the catalyst demonstrated good enantioselectivity.[19] Yeung has arguably been the largest contributor to the area of organocatalytic enantioselective bromolactonizations, and his work will also be discussed in detail later in this section. Another major contribution

came from Fujioka with his catalyst **1.32**. The C_3-symmetric trisimidazoline catalyst **1.32** was first reported to induce bromolactonizations of 5-aryl-substituted-5-hexenoic acids **1.30** to afford δ-lactones **1.31** via a 6-*exo* cyclization mode (Equation 1.7), and it was later shown to also work well with tri- and tetrasubstituted olefinic acids.[3,13]

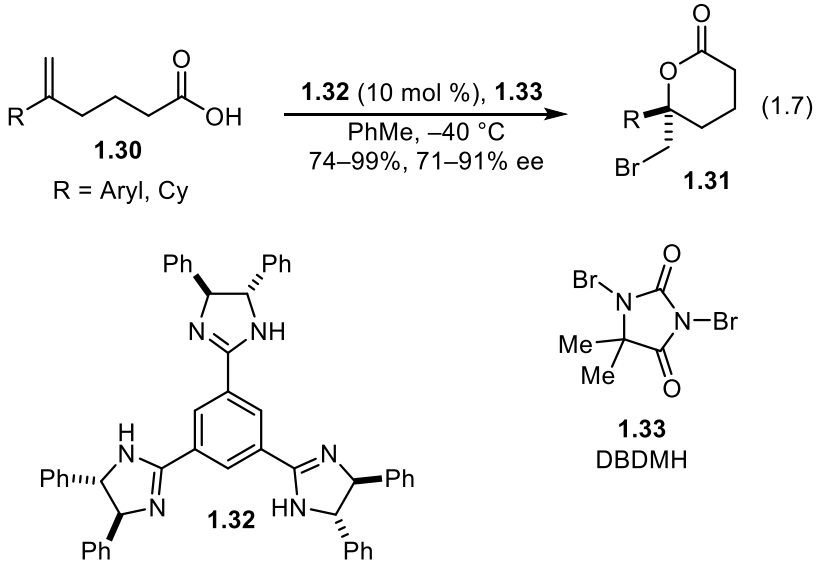

For iodolactonizations, Jacobsen's tertiary aminourea catalyst **1.36** promoted enantioselective iodolactonizations of 5-substituted-5-hexenoic acids **1.34** with moderate to excellent selectivities (Equation 1.8).[4] Hansen later disclosed the squarimide catalyst **1.38**, which also induced iodolactonizations of the same substrates, but the selectivities were lower than with **1.36** (Equation 1.9).[16] Johnston's catalyst **1.41** promoted iodolactonizations of 5-substituted-5-hexenoic acids (**1.30**) with generally high enantioselectivities (Equation 1.10).[11] Ishihara reported the iodolactonization of a unique substrate class using catalyst **1.44**, which promoted the lactonization of benzyl-substituted-4-pentenoic acids **1.42** with good enantioselectivities (Equation 1.11).

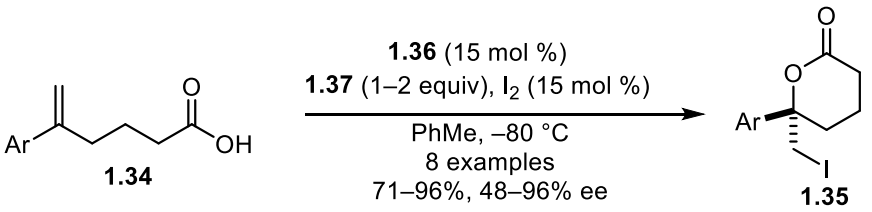
1.36 (15 mol %)
1.37 (1–2 equiv), I2 (15 mol %)
PhMe, –80 °C
8 examples
71–96%, 48–96% ee
Ar
OH
O
1.34
Ar
O
O
I
1.35

(1.8)

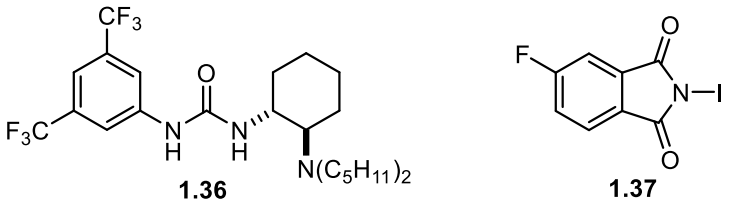
CF3
F3C
N
H
O
N
H
N(C5H11)2
1.36
F
O
N—I
O
1.37

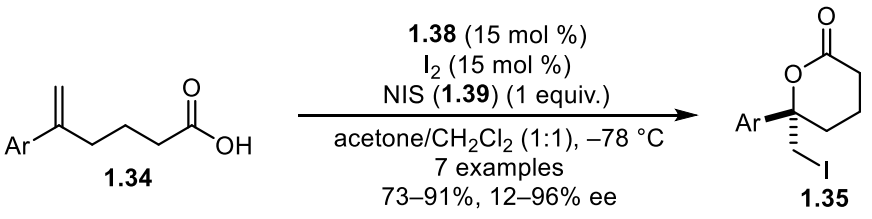
1.38 (15 mol %)
I2 (15 mol %)
NIS (1.39) (1 equiv.)
acetone/CH2Cl2 (1:1), –78 °C
7 examples
73–91%, 12–96% ee
Ar
OH
1.34
Ar
O
O
I
1.35

(1.9)

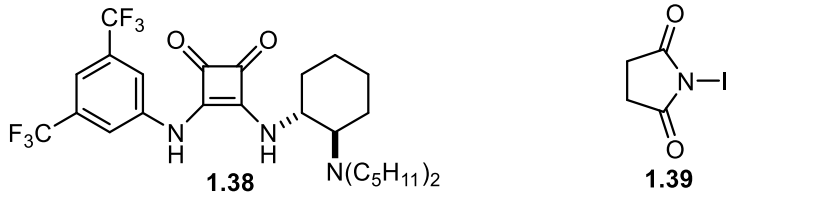
CF3
F3C
O
O
N
H
N
H
N(C5H11)2
1.38
O
N—I
O
1.39
N-iodosuccininimide (NIS)

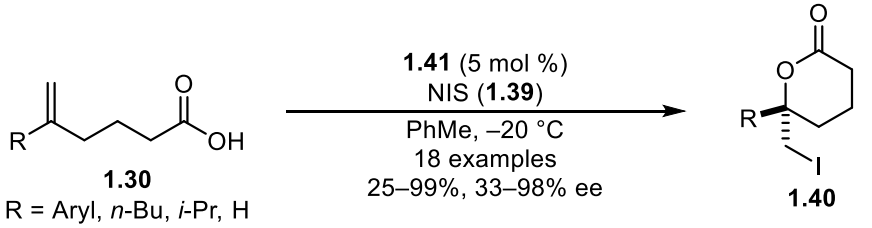
1.41 (5 mol %)
NIS (1.39)
PhMe, –20 °C
18 examples
25–99%, 33–98% ee
R
OH
1.30
R = Aryl, n-Bu, i-Pr, H
R
O
O
I
1.40

(1.10)

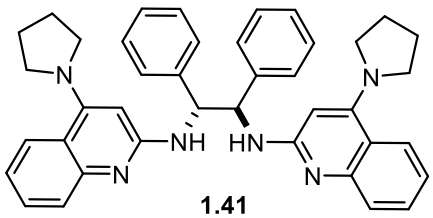
N
NH
HN
N
N
N
1.41

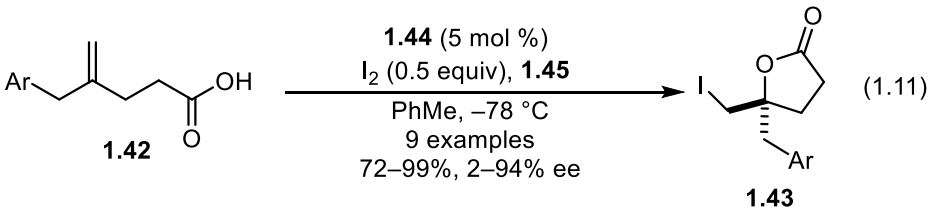

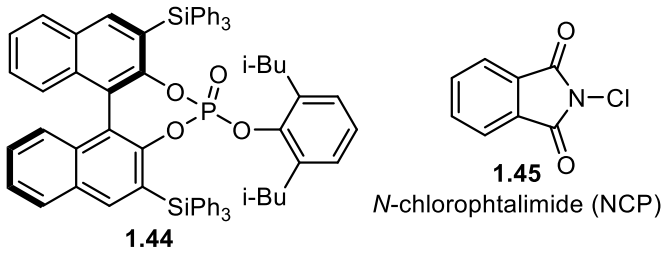

1.2.2 Yeung

Yeung has been the most prolific contributor to the field of enantioselective bromolactonizations, and his work is worthy of discussion in detail because it is the most competitive with the methodology developed in our group. Yeung reported his first-generation catalyst **1.48,** which promoted bromolactonizations of 4-substituted-4-pentenoic acids **1.46** (Equation 1.12).[6] The thiocarbamate cinchona alkaloid catalyst **1.48** was the result of screening a variety of different catalyst structural motifs, as well as a number of different structural modifications of the cinchonidine core features. The majority of alkenoic acid substrates **1.46** investigated were aryl substituted pentenoic acids, and for electron neutral or electron deficient arenes, the enantioselectivity was generally 70–91% ee. However, typical of these reactions, the conversion of substrates that contained electron rich arene rings proceeded with poor enantioselectivity (e.g. R = *p*-MeO-Ph, 28% ee). Yeung also demonstrated a limited number of examples where the olefin was substituted with an alkyl group, and for bulky groups (**1.46**, R = *t*-Bu, Cy) the selectivities were good (82–93% ee), while the methyl substituted substrate (**1.47**, R = Me) was poorly tolerated, and the corresponding lactone was afforded in only 41% ee. Notably, this was the first

report of a highly enantioselective catalytic halolactonization of an alkyl substituted olefinic acid.

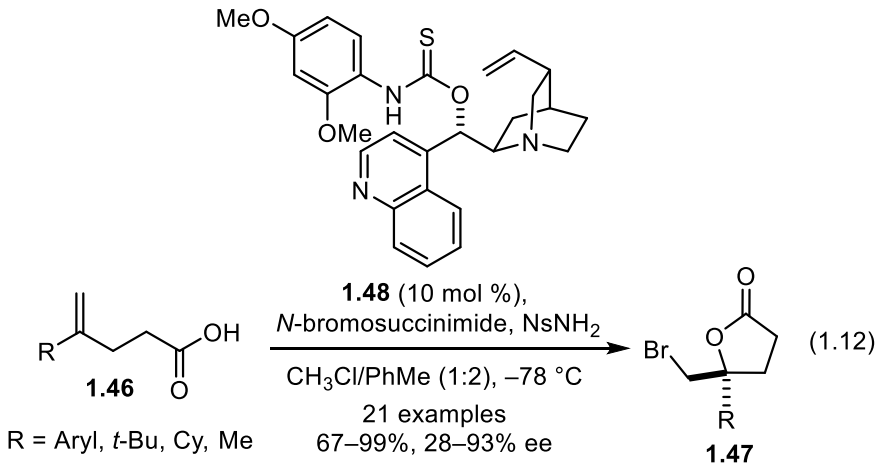

Yeung next investigated the bromolactonization of *E*-6-aryl-5-hexenoic acids **1.49**, another common substrate for halolactonization reactions (Equation 1.13).[7] Yeung discovered that catalyst **1.48** did not provide the same degree of high selectivity it displayed for 4-substituted-4-pentenoic acids **1.46**. Another screen of structural modifications to the catalyst revealed that **1.51** was a superior catalyst for this class of substrates, and the aryl-substituted olefinic acids **1.49** were converted to the corresponding bromolactones **1.50** with 61–94% ee.

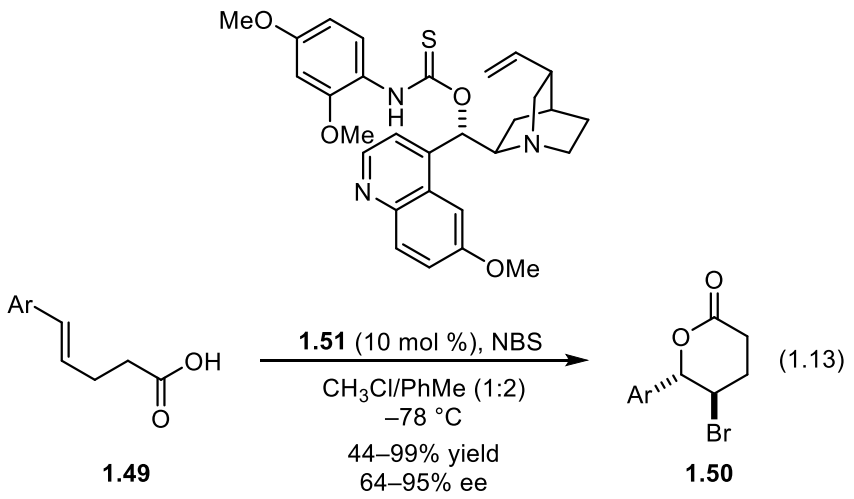

Yeung then explored a subset of 5-substituted-4(*Z*)-pentenoic acids, a substrate class that yet to be explored. Once again, Yeung found that structural modification of the catalyst was required before good selectivity could be achieved. Ultimately, catalyst **1.54** was found to provide the highest degree of selectivity for the bromolactonizations of **1.52**, which proceeded via a 5-*exo* cyclization mode to the corresponding γ-lactones **1.53** (Equation 1.14).[9] Again, mostly aryl substituted alkenoic acids were explored, but Yeung did investigate two alkyl substituted substrates, specifically **1.52** R = *i*-Pr, Cy, which were converted to the corresponding lactones with **1.53** R = *i*-Pr, Cy, 53% and 75% ee respectively.

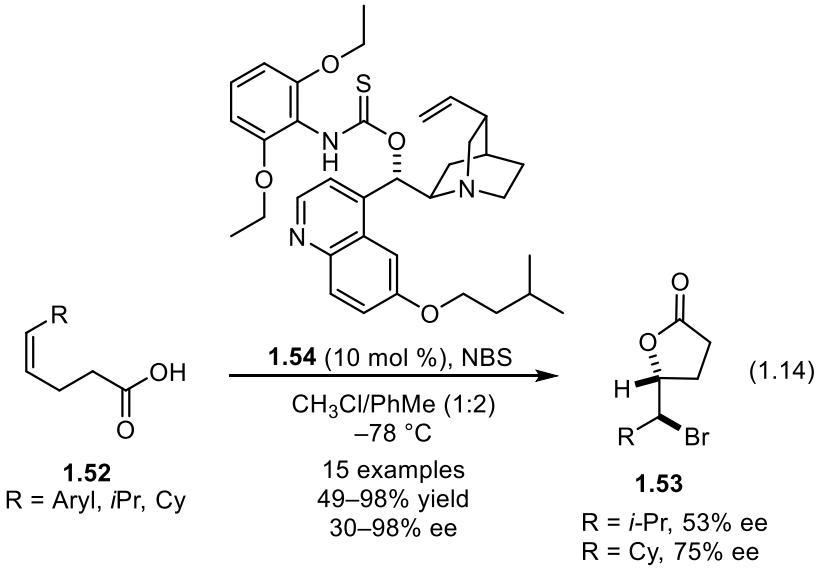

Yeung later developed a new class of proline based second generation catalysts, but again he was unable to find a universal catalyst to promote varied substrates. The *N*-methyl substituted catalyst **1.55** promoted 6-*exo* cyclizations of primarily aryl substituted acids **1.30** with 85:15–96:4 er (Equation 1.15). For pentenoic acids **1.46**, the *N*-allyl substituted catalyst **1.56** delivered the corresponding bromolactones **1.47** with 87:13–96:4 er (Equation 1.16).[14]

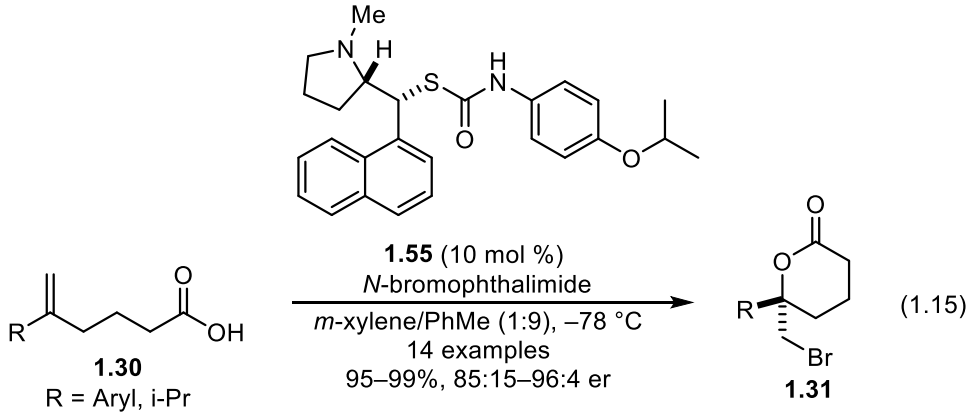

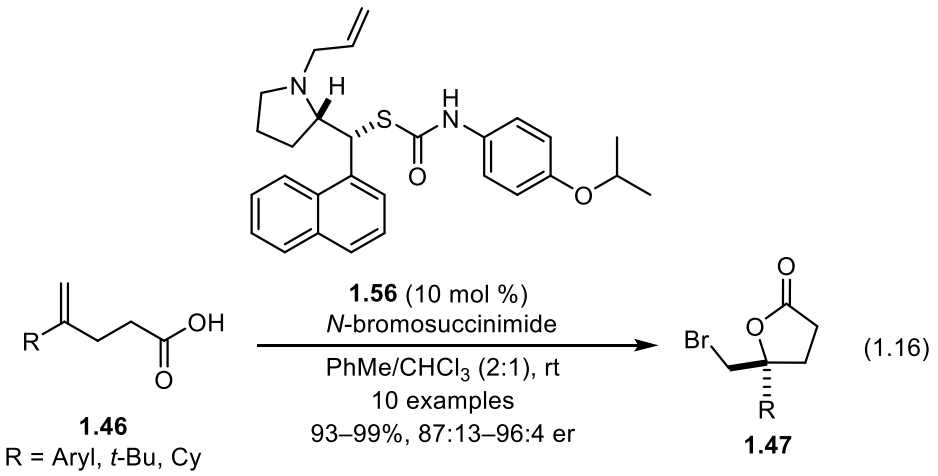

1.2.3 Summary

The introduction of asymmetric C-X bonds is an important and challenging task for synthetic chemists, and in recent years, great strides have been made in developing new catalytic methods to achieve these transformations. The field of enantioselective halolactonization in particular has seen explosive growth. Since the seminal reports of efficient catalytic enantioselective halocyclization by Gao and Borhan, there has been a myriad of new catalysts reported. Despite the many advances in the field and novel catalysts that have been developed, the substrate scope of each is typically limited, especially for fluoro- and chlorolactonizations. Additionally, there were several gaps in the methodology when we initiated our work that we sought to address with a new catalyst. One major deficiency in the art was the lack of examples of a halolactonization that proceeded via an exo mode of ring closure to give a lactone bearing a new C-X bond at a stereogenic secondary carbon atom. Although during the course of our investigations, Yeung disclosed halolactonizations of this type,[9] but he primarily showed aryl substituted alkenoic acids, and in the case of alkyl substituted alkenoic acids, the enantioselectivities were modest (Equation 1.13). Hence, creating a new secondary C-X bond at a stereocenter by halolactonization of an alkene was an unsolved problem. Additionally, there were no

reported catalysts that could perform both bromo- and iodolactonizations. With the exception of **1.19**, all other catalysts were halogenating reagent specific. This presented us with an opportunity to develop a catalyst that would expand the substrate scope and offer a unified approach towards halolactonization reactions. Accordingly, we set to the task of solving these unmet challenges.

1.3 MARTIN GROUP HALOLACTONIZATION METHODOLOGY[1]

1.3.1 Catalyst Development

The development of an enantioselective halocyclization reaction is inherently difficult due to the reversibility of halonium ion formation, and its propensity to transfer X^+ to another olefin prior to bimolecular nucleophilic capture.[56–58,70] The most successful catalysts have addressed this issue through inclusion of both Lewis/Brønsted acid and Lewis/Brønsted base functionalities. The bifunctional nature of these catalysts is a critical component of their design, with the Lewis basic functionality enabling the coordination of the substrate and stabilization of the halonium ion; the Lewis acidic moiety enables the coordination of the halogenating reagent. When we began designing our catalyst, we envisaged incorporating some well-established bifunctional motifs from known catalysts onto a chiral binaphthyl backbone, which despite its ubiquity in enantioselective reactions, had not yet been applied to the development of a halocyclization catalyst (Equation 1.17).

[1] This section is based on the forthcoming publication: Klosowski, D. W.; Hethcox, J. C.; Paull, D. H.; Fang, C.; Donald, J. R.; Shugrue, C. R.; Pansick, A. D.; Martin, S. F. Enantioselective Halolactonization Reactions using BINOL-derived Bifunctional Catalysts: Methodology, Diversification, and Applications *J. Org. Chem.* **2018**, Accepted, In Press. The work in this section was done by the authors Hethcox, J. C.; Paull, D. H.; Fang, C.; Donald, J. R.; Shugrue, C. R.; Pansick, A. D; and Martin, S.F.

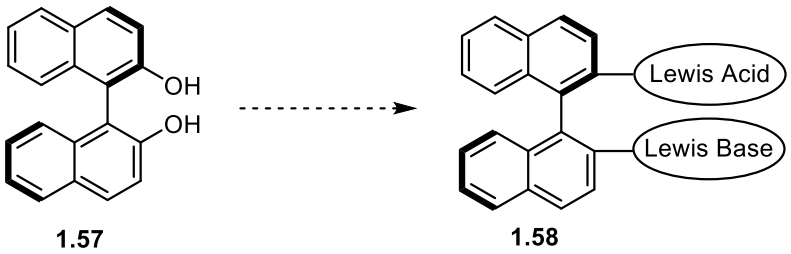

1.57 **1.58** (1.17)

After a survey of reported catalysts, we reasoned that a basic nitrogen atom would be required to coordinate the carboxylic acid, and a Lewis acidic group such as a thiourea, urea, or thiocarbamate would be required to activate the halogenating reagent. The initial goal was to prepare derivatives of catalyst **1.68** (Scheme 1.3), which bears the requisite functionalities previously mentioned. The amidine group was selected rather than a tertiary amine because bromine is known to rapidly oxidize tertiary benzylic amines.[71] Additionally, the phenyl group was included at the 3-position of **1.68** to increase the steric bulk around the proposed catalophore, a strategy that has been shown to enhance stereoselectivity on other BINOL derivatives.[72]

Towards this end, catalyst **1.67** was prepared from *R*-BINOL (**1.57**) in eight steps,[15] beginning with installation of methoxymethyl ether (MOM) protecting groups onto both phenols (Scheme 1.3). Lithiation of **1.59** with *tert*-butyllithium (*t*-BuLi) followed by lithium-halogen exchange with I_2 delivered **1.60**, which was used in a Suzuki coupling with phenylboronic acid to deliver **1.61**. After removal of the MOM protecting groups, the benzylic primary amine moiety of **1.65** was installed through a three-step sequence, first through treatment of **1.62** with triflic anhydride to form triflate **1.63**, which was used in a nickel catalyzed cyanation to afford **1.64**, and the resultant nitrile moiety could be reduced through treatment with borane to finally deliver **1.65**. The amidine moiety could then be easily formed through treatment of **1.65** with **1.66**, affording **1.67** in eight steps and 35% overall yield from **1.57**. Unfortunately, all subsequent efforts to convert the phenol moiety of **1.67** into thiocarbamate **1.68** were unsuccessful.

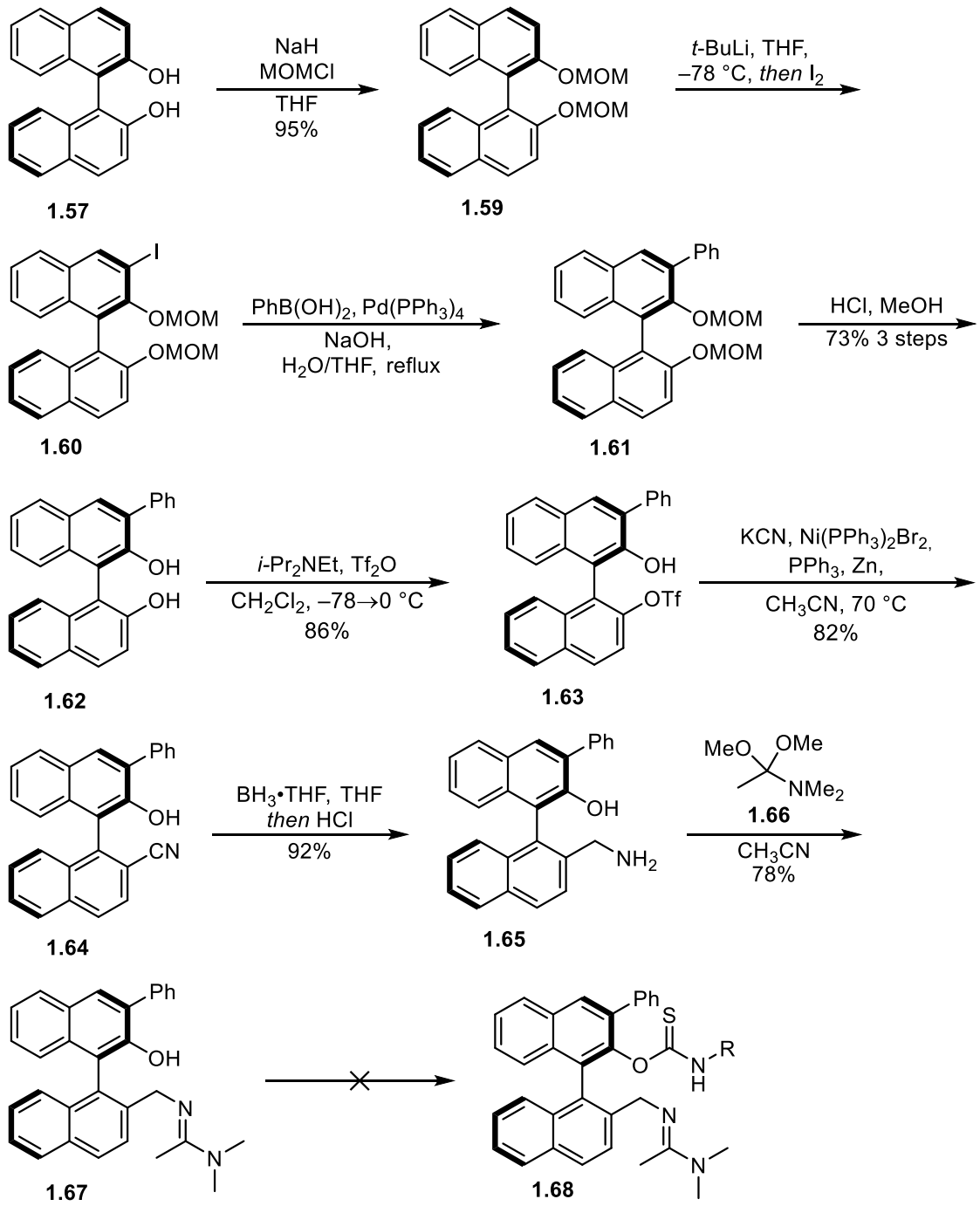

Scheme 1.3 Preparation of catalyst **1.67** from *R*-BINOL (**1.57**)

Despite this initial setback, it was hypothesized that **1.67**, which contains an acidic phenolic hydroxyl group, might serve as an effective catalyst for bromolactonizations. In order to test this idea, however, it was first necessary to identify bromolactonization reaction conditions that gave minimal amounts of background reaction. Initial screenings revealed that stirring solutions of 5-phenyl-4(*E*)-pentenoic acid (**1.69**) in PhMe/CH_2Cl_2 (1:1) containing 2,4,4,6-tetrabromobenzoquinone (TBCO, **1.72**) at temperatures less than –40 °C for 14 h gave negligible amounts of racemic lactones **1.70** and **1.71**, hence, TBCO was determined to be the optimum brominating reagent in our initial studies (Equation1.18).

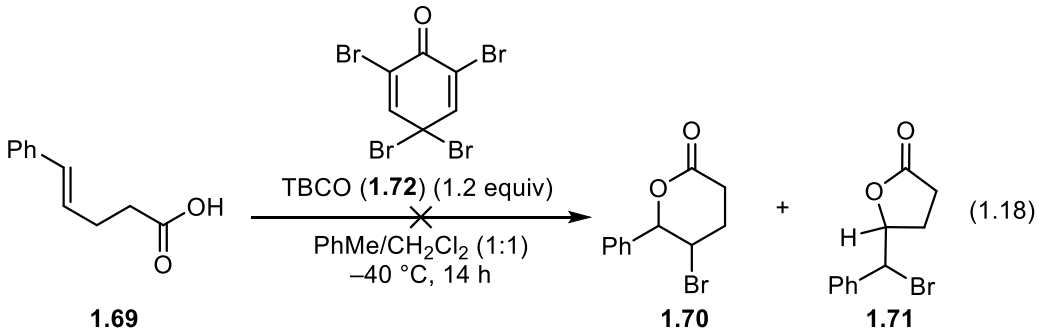

1.69 **1.70** **1.71**

To our delight, we discovered that **1.69**, in the presence of **1.67**, could be converted to **1.73** with some enantioselectivity. A solvent screen revealed that PhMe/CH_2Cl_2 (2:1) provided the highest selectivity, and with optimal reaction conditions identified, **1.69** was converted to **1.73** in 95% yield and 97:3 er (Equation 1.19).

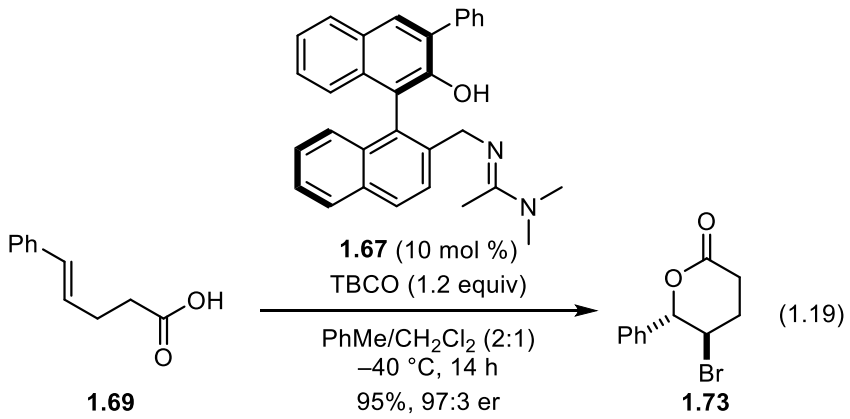

1.3.2 Effects of Catalyst Modification

With the successful conversion of **1.69** to **1.73** with high enantioselectivity, the focus was shifted to olefinic acid **1.74**, another common test substrate for bromolactonizations. Gratifyingly, we found that in the presence of **1.67**, **1.74** was cyclized to **1.75** in 95% yield and a slightly diminished er of 86:14.

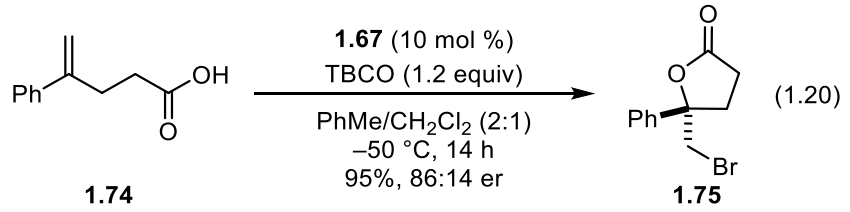

In order to identify analogs of **1.67** that might be superior cataylsts, a series of analogs (**1.76–1.85**) was prepared, and we surveyed their ability to promote the lactonization of **1.74** (Table 1.1). We discovered that under the conditions for bromolactonization, **1.67** underwent facile bromination to give the 6-bromo analog **1.76** in high yield (Equation 1.21). Unsurprisingly, we found that **1.76** catalyzed the bromolactonization of **1.74** with the same enantioselectivity as **1.67** (Table 1.1, Entry 2).

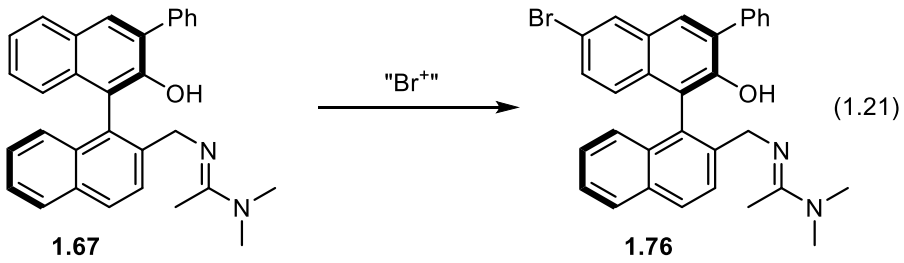

The effect of electron withdrawing groups on the binaphthyl scaffold was evaluated through the 6-nitro analogx **1.77**, which was unable to promote the bromolactonization of **1.74** (Table 1.1, Entry 3). The steric requirements were probed next through analogs with substituents at the 3- and 3'-poisitions of the binaphthyl core, as well as on the amidine group (R_1,R_4, and R_3 respectively). The phenyl group at R_1 of **1.67** was initially included to help create a sterically biased catalytic pocket, but catalyst **1.78** (R_1, R_4 = H, R_3 = Me), which lacks the phenyl group at R_1, promoted the bromolactonization of **1.74** with nearly identical selectivity to that of **1.67** (84:16 vs 86:14), suggesting the phenyl group may not be necessary (Table 1.1, Entry 4). Increasing the size of the R_1 substituent to triphenylsilyl (**1.79**, Table 1.1, Entry 5) or 2,4,6-triisopropylphenly (TRIP) (**1.80**, Table 1.1, Entry 6) led to signification erosion of enantioselectivity. Catalyst **1.81**, which bears an additional phenyl group at the 3'-position (R_1, R_4 = Ph, Table 1.1, Entry 7), catalyzed the bromolactonization of **1.74** with similar selectivity to that of the parent catalyst, and the additional phenyl group was deemed unnecessary. A cursory examination of altering the substituent on the amidine group (R_3) revealed that the methyl derivative provided the best selectivity. Changing R_3 to a phenyl group (**1.82**, Table 1.1, Entry 8) did not significantly enhance selectivity, and incorporation of a *t*-butyl group (**1.83**, Table 1.1, Entry 10) lead to significant erosion of selectivity. Finally, to assess the importance of the bifunctional nature of the catalyst, derivative **1.85** was prepared, where the acidic phenolic group of **1.78** was methylated (Table 1.1 Entry 11). This modification lead to a complete loss of

selectivity, suggesting that the acidic phenol in the catalyst is imperative for enantioselectivity. Although there were a number of catalyst derivatives that showed similar selectivity to the parent catalyst **1.67**, there were instances throughout the method development where **1.67** was superior, and so it was used uniformly in the subsequent experiments.

Table 1.1 Effects of catalyst modification on the conversion of **1.74** to **1.75**[a]

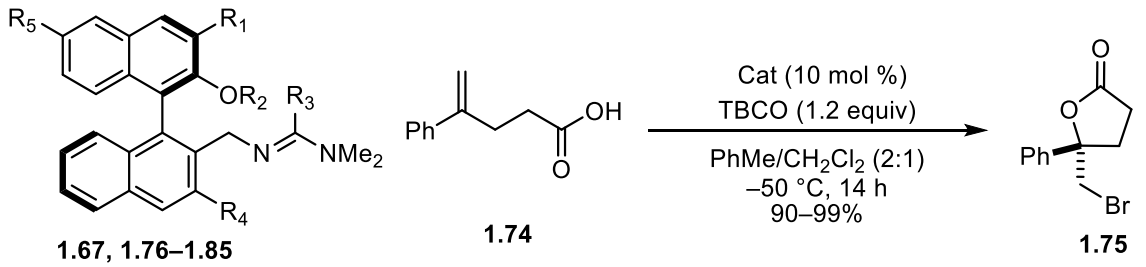

Entry	Cat.	R^1	R^2	R^3	R^4	R^5	er[b]
1	**1.67**	Ph	H	Me	H	H	86:14
2	**1.76**	Ph	H	Me	H	Br	86:14
3[c]	**1.77**	Ph	H	Me	H	NO_2	NR
4	**1.78**	H	H	Me	H	H	84:16
5	**1.79**	Ph_3Si	H	Me	H	H	74:26
6	**1.80**	TRIP[d]	H	Me	H	H	50:50
7	**1.81**	Ph	H	Me	Ph	H	85:15
8	**1.82**	Ph	H	Ph	H	H	82:18
9	**1.83**	H	H	Ph	H	H	87:13
10	**1.84**	H	H	t-Bu	H	H	62:38
11	**1.85**	H	Me	Me	H	H	50:50

[a]Reactions run on 0.10 mmol scale and all reactions gave >90% conversion.[b]er determined by chiral HPLC; absolute stereochemistry of **1.75** was assigned by correlation of optical rotation with those previously reported.[4,6] [c]NR = no reaction. [d]TRIP = 2,4,6-triisopropylphenyl.

1.3.3 Halolactonization Reactions

At the time of these investigations, no catalyst was known to promote enantioselective halolactonizations with more than one halogen. It was therefore intriguing whether or not **1.67** may promote other enantioselective halolactonizations. Initially, the chlorolactonization of **1.74** using **1.67** and **1.76** with N-chlorosuccinimide (NCS) and 1,3-

dichloro-5,5-dimethylhydantion (DCDMH) in a variety of solvents was explored. However, consistent with other reports, the reactions proceeded with low conversions and poor enantioselectivities.[6,9] We then turned our attention to iodolactonizations, and gratifyingly we discovered that the iodolactonization of **1.74** with *N*-iodosuccinimide (NIS) in the presence of **1.67** delivered the corresponding iodolactone in good yield and with high enantioselectivity (93:7 er). Optimization of the reaction conditions revealed that the iodolactonization of **1.74** was slightly faster in the presence of **1.76**, and the reaction times could be further decreased by increasing the temperature to –20 °C from –40 °C with no loss of enantioselectivity (Equation 1.22). This slight operational advantage lead to **1.76** as the catalyst of choice for iodolactonization reactions. Because Jacobsen had reported that use of iodine as an additive in iodolactonization reactions had beneficial effects on selectivity,[4] we tested the effect of adding catalytic amounts of iodine. However, the inclusion of iodine (1–10 mol %) had little to no effect on the iodolactonization of **1.74**. Notably however, the effect of iodine as an additive was not consistent, and some reactions benefitted from catalytic amounts of iodine.

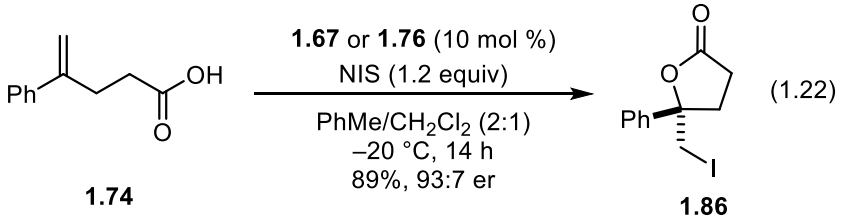

(1.22)

With a standard set of conditions identified for both bromo- and iodolactonizations, we evaluated catalysts **1.67** and **1.76** on a wider variety of benchmark substrates. 4-Substituted-4-pentenoic acids are commonly employed as substrates to demonstrate the efficacy of enantioselective halolactonization reactions, and thus we evaluated the abilities of **1.67** and **1.76** to catalyze the halolactonizations of **1.74** and **1.46a–e**. (Table 1.2). The

bromolactonizations of acids **1.46a** and **1.46b**, substituted with electron withdrawing arene, proceeded in good yield and with high enantioselectivity (Table 1.2, Entries 3,5), showing a slight increase in selectivity compared to alkenoic acid **174** (Table 1.2, Entry 1). This same effect was not observed for the iodolactonization of **1.46a**, which was converted to iodolactone **1.87a** with similar selectivity as its phenyl counterpart **1.86** (Table 1.2, Entry 2); however, the generality of this electronic effect was not rigorously determined. Conversely, an electron donating group (R = *p*-OMe-Ph, **1.46c**) lead to a significant reduction in enantioselectivity for both the bromo- and iodolactonization (Table 1.2, Entries 6,7). 4-Alkyl-4-pentenoic acids also underwent facile iodolactonization, but steric effects are important, and the reaction is more selective for larger alkyl groups (Table 1.2, Entries 8,9).

Table 1.2 Halolactonization of 4-substituted-4-pentenoic acids[a]

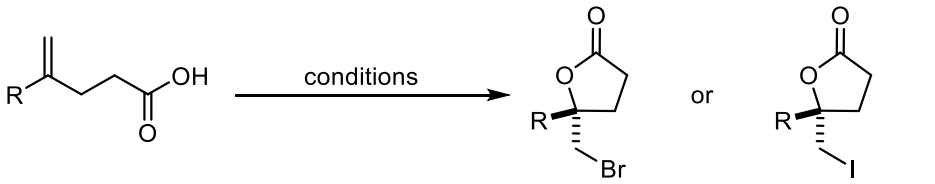

1.74, 1.46a–e **1.75, 1.47a–e** **1.86, 1.87a–e**

Entry	Acids	R	Product	Yield (%)	er[b]
1	**1.74**	Ph	**1.75**	99	86:14
2	**1.74**	Ph	**1.86**	89	93:7
3	**1.46a**	p-NC-Ph	**1.47a**	92	94:6
4	**1.46a**	p-NC-Ph	**1.87a**	73	90:10
5	**1.46b**	m-NC-Ph	**1.47b**	89	91:9
6	**1.46c**	p-MeO-Ph	**1.47c**	70	58:42
7[c]	**1.46c**	p-MeO-Ph	**1.87c**	90	74:26
8	**1.46d**	Me	**1.87d**	96	65:35
9	**1.46e**	t-Bu	**1.87e**	91	83:17

[a]Reactions run on 0.10 mmol scale. Conditions for bromolactonization: 10 mol % **1.67**, 1.2 equiv TBCO in PhMe/CH_2Cl_2 (2:1) at −50 °C. Conditions for iodolactonization: 10 mol % **1.76**, 1.2 equiv NIS in PhMe/CH_2Cl_2 (2:1) at −20 °C. [b]er determined by chiral HPLC; absolute stereochemistry of **1.75** and **1.86** were assigned by correlation of optical rotation with previously reported,[4,6] and other assignments are based upon analogy. [c]Results obtained with 10 mol % I_2, 93% yield, 82:18 er.

In continuation of our evaluation of benchmark substrates, we next examined the halolactonizations of a small variety of *trans*-5-aryl-4-pentenoic acids (Table 1.3). Unsaturated acids **1.88a** and **1.88b** underwent bromolactonizations in the presence of **1.67** and TBCO via 6-endo cyclizations in good yield and with high enantioselectivities (Table 1.3, Entries 2 and 3). Iodolactonization of **1.69** afforded a mixture (1:1.3) of 6-endo and 5-exo products **1.90a** and **1.91a**, respectively (Table 1.3, Entry 1). Iodolactonization of **1.88c** (R = *p*-OMe-Ph) gave the 6-endo product **1.90c** selectively with moderate

enantioselectivity (87:13 er, Table 1.3, Entry 4), whereas the iodolactonization of **1.88d** (R = *p*-NC-Ph) afforded the 5-exo product **1.91d** with very little enantioselectivity (58:42 er, Table 1.3, Entry 5). With the exception of **1.69**, the regioselectivity of the halolactonizations were in accord with the electronic bias of the substrate. Notably, the enantioselectivities obtained with **1.67** and **1.76** for all of the benchmark substrates we evaluated are comparable to those obtained with other catalysts.

Table 1.3 Halolactonization of 5-aryl-4(*E*)-pentenoic acids[a]

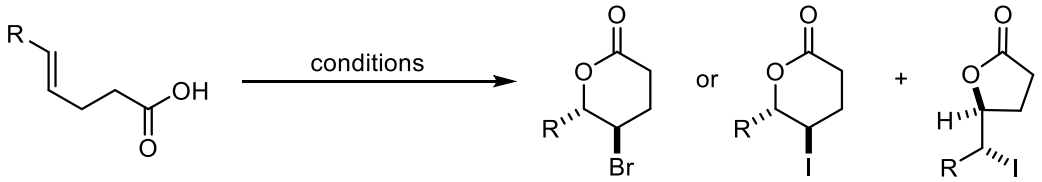

1.69, **1.88a–d** **189a,b** **1.90a,c** **1.91a,d**

Entry	Acids	R	Product	Yield (%)	er[b]
1	**1.69**	Ph	**1.90a + 1.91a**	89[c]	95:5[c]
2	**1.88a**	2-Np	**1.89a**	97	96:4
3	**1.88b**	2-thienyl	**1.89b**	92	94:6
4	**1.88c**	*p*-MeO-Ph	**1.90c**	89	87:13
5[e]	**1.88d**	*p*-NC-Ph	**1.91d**	94	58:42

[a]Reactions run on 0.10 mmol scale. Conditions for bromolactonization: 10 mol % **1.67**, 1.2 equiv TBCO in PhMe/CH_2Cl_2 (2:1) at −50 °C. Conditions for iodolactonization: 10 mol % **1.76**, 1.2 equiv NIS in PhMe/CH_2Cl_2 (2:1) at −20 °C. [b]er determined by chiral HPLC; absolute stereochemistry of **1.89a**,**b** were assigned by correlation of optical rotation with the previously reported values,[7] and other assignments are based upon analogy. [C]ratio of 1.0:1.3 based upon ^{1}H NMR analysis; the er for **1.91a** was 52:48. [e]Reaction performed for 14 h at –20 °C and 48 h at –10 °C in CH_2Cl_2/PhMe (1:1).

The halolactonization of a set of 5-substituted-5-hexenoic acids was evaluated next, and we found that olefinic acids **1.92a–c** cyclized via 6-exo lactonizations to give the corresponding δ-lactones (Table 1.4). The phenyl substituted substrate **1.92a** underwent bromolactonization in good yield (78%), but poor enantioselectivity (62:38 er)(Table 1.4, Entry 1). The iodolactonization of **1.92a** showed improved results, and lactone **1.94a** was

delivered in high yield (98%) and with moderately increased enantioselectivity (76:24 er) (Table 1.4, Entry 2). The halolactonizations of the methyl substituted acid **1.92b** proceeded with similarly enantioselectivity for both the bromo- and iodolactonizations, affording lactones **1.93b** and **1.94c** in 82:18 er and 79:21 er respectively (Table 1.4, Entries 3 and 4). Similarly, the halolactonizations of **1.92c** proceeded to give the the oxanones **1.93c** and **1.94c** with near identical enantioselectivity, 85:15 and 84:16 respectively (Table 1.4, Entries 5 and 6).

Table 1.4 Halolactonization of 5-substituted-5-hexenoic acids[a]

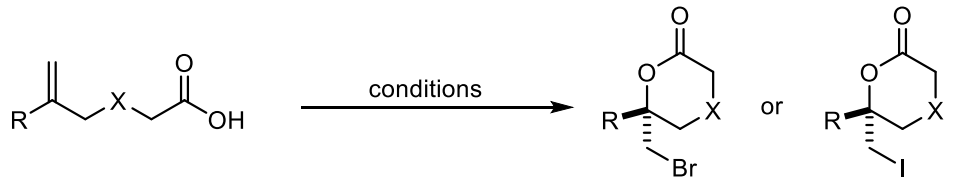

1.92a–c **1.93a–c** **1.94a–c**

Entry	Acids	R	X	Product	Yield (%)	er[b]
1	**1.92a**	Ph	CH_2	**1.93a**	78	62:38
2[c]	**1.92a**	Ph	CH_2	**1.94a**	98	76:24
3	**1.92b**	Me	CH_2	**1.93b**	90	82:18
4[d]	**1.92b**	Me	CH_2	**1.94b**	89	79:21
5	**1.92c**	Ph	O	**1.93c**	94	85:15
6[e]	**1.92c**	Ph	O	**1.94c**	91	84:16

[a]Reactions run on 0.10 mmol scale. Conditions for bromolactonization: 10 mol % **1.67**, 1.2 equiv TBCO in PhMe/CH_2Cl_2 (2:1) at −50 °C. Conditions for iodolactonization: 10 mol % **1.76**, 1.2 equiv NIS in PhMe/CH_2Cl_2 (2:1) at −20 °C. [b]er determined by chiral HPLC; absolute stereochemistry of **194a** was assigned by correlation of optical rotation with previously reported,[4] and the other assignments are based upon analogy. [c]Results obtained with 10 mol % I_2, 95% yield, 85:15 er. [d]Results obtained with 10 mol % I_2, 90% yield, 80:20 er. [e]Results obtained with 10 mol % I_2, 89% yield, 90:10 er.

At the outset of our investigations, the formation of chiral alkyl halides via 6-endo halocyclization modes was known. Our initial exploratory studies showed that our catalyst was similarly effective in promoting these cyclizations to generate C-X containing stereocenters. However, enantioselective halolactonizations in which a new C-X bond is produced at a secondary carbon atom via a 5-exo cyclization was unprecedented at the time of our investigations. We were intrigued if catalysts **1.67** and **1.76** could promote such reactions, and so we investigated the halolactonization of a representative selection of 5-alkyl-4(*Z*)-pentenoic acids (Table 1.5). In the event, the bromo- and iodolactonizations of acids **1.52a–i** proceeded via a 5-exo cyclization to furnish the corresponding γ-lactones in generally high yields and with high enantioselectivities (≥95:5 er). The unsaturated acid

1.52a (R = Et, Table 1.5, Entry 1) was the only substrate that cyclized with a modest er (85:15), suggesting, branching on the carbon atom attached directly to the olefin might play a role in determining selectivity. The iodolactonization of aryl substituted acids **1.52f–i** also underwent cyclization via a 5-exo mode to form the iodolactones (**1.95f–i**) with high enantioselectivity (≥98:2). The γ-lactones **1.53á–e** and **1.95b–i** contain two contiguous stereogenic centers, one of which bears a carbon-halogen bond. Notably, the *Z*-olefin geometry is important for the alkyl substituted olefinic acids, because the corresponding 5-alkyl-4(*E*)-pentenoic acids cyclized with selectivity ranging from 50:50 er to 78:22 er. Collectively, the cyclizations of **1.52a–i** represent the first examples halolactonizations that occur via a 5-exo mode of ring closure to give products in which new C–O and C–X bonds are formed at contiguous stereogenic centers with a high degree of enantioselectivity.

Table 1.5 Halolactonization of 5-substituted-4(*Z*)-pentenoic Acids[a]

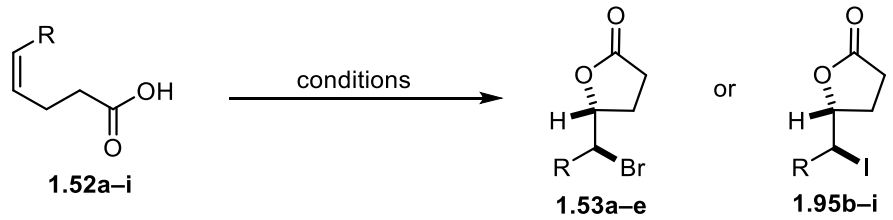

1.52a–i **1.53a–e** **1.95b–i**

Entry	Acids	R	Product	Yield (%)	er[b]
1	**1.52a**	Et	**1.53a**	90	85:15
2	**1.52b**	*i*-Pr	**1.53b**	94	97:3
3	**1.52b**	*i*-Pr	**1.93b**	93	97:3
4	**1.52c**	*i*-Bu	**1.52c**	87	95:5
5	**1.52c**	*i*-Bu	**1.93c**	94	98:2
6	**1.52d**	*t*-Bu	**1.52d**	97	97:3
7	**1.52d**	*t*-Bu	**1.93d**	99	97:3
8	**1.52e**	Cy	**1.52e**	94	98.5:1.5
9	**1.52e**	Cy	**1.52e**	97	98:2
10	**1.52f**	Ph	**1.93f**	93	98.5:1.5
11	**1.52g**	*p*-NC-Ph	**1.93g**	95	99:1
12	**1.52h**	*p*-Cl-Ph	**1.93h**	89	98:2
13	**1.52i**	2-Np	**1.93i**	94	98:2

[a]Reactions run on 0.10 mmol scale. Conditions for bromolactonization: 10 mol % **1.67**, 1.2 equiv TBCO in PhMe/CH_2Cl_2 (2:1) at −50 °C. Conditions for iodolactonization: 10 mol % **1.76**, 1.2 equiv NIS in PhMe/CH_2Cl_2 (2:1) at −20 °C. [b]er determined by chiral HPLC; absolute stereochemistry of **1.53d, 1.95d,** and **1.95f** were determined by X-ray crystallography, and other assignments are based upon analogy.

In a related set of experiments, we briefly examined the iodolactonizations of a set of 6-substituted-5(*Z*)-hexenoic acids **1.96a–d** and found that the corresponding iodo δ-lactones **1.97a–d** were produced in high yields and with excellent enantioselectivities of

≥98:2 er (Table 1.6). Notably, these cyclizations also produce two adjacent stereogenic centers, one of which is a C-I bond.

Table 1.6 Iodolactonization of 6-substituted-5(*Z*)-hexenoic acids[a]

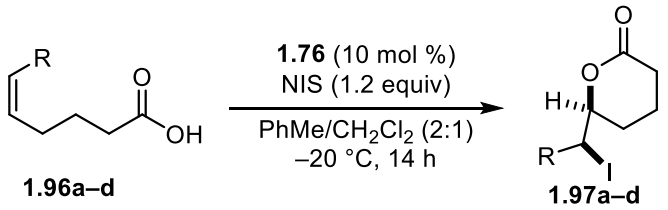

Entry	Acids	R	Product	Yield (%)	er[b]
1	**1.96a**	Ph	**1.97a**	89	99:1
2	**1.96b**	*p*-NC-Ph	**1.97b**	88	99:1
3[c]	**1.96c**	2-Np	**1.97c**	93	98.5:1.5
4[c]	**1.96d**	*t*-Bu	**1.97d**	98	98:2

[a]Reactions run on 0.10 mmol scale. [b]er determined by chiral HPLC; absolute stereochemistry assigned based on analogy with **1.95d** and **1.95f**. [c]Results obtained after 38 h at –20 °C.

1.3.4 Mechanistic Aspects

The 5-exo halolactonization mode of aryl substituted olefinic acids **1.52f–i** is perhaps surprising and worthy of mention. At first, one might anticipate that substrates such as **1.52f** would be electronically biased towards a 6-endo cyclization, but the experimentally observed γ-lactones are consistent with the hypothesized transition state (Figure 1.2). Transition state **1.100** is expected to be favored relative to **1.98**, because of the detrimental steric interaction present in **1.98** that prevents the benzylic stabilization of the iodonium ion or carbocation by the π electrons of the aryl group. The 5-exo cyclization mode is therefore favored due to steric and entropic reasons, and **1.101** is observed as the dominant product, rather than **1.99**.

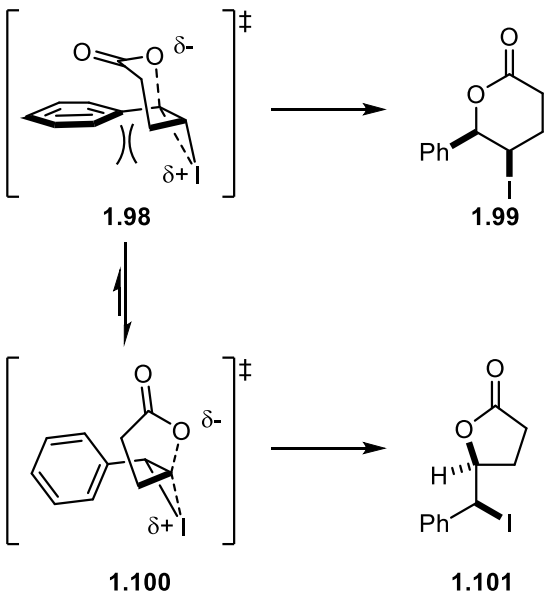

Figure 1.2 *Exo*-cyclization mode of 5-aryl-4(*Z*)-pentenoic acids

Based on the results previously discussed, we devised a tentative working model to rationalize the stereochemical outcome for the enantioselective halolactonizations of unsaturated acids catalyzed by **1.67** and **1.76**. We propose a Brønsted acid/base interaction between the carboxylate of the olefinic acid and either the naphthol moiety (*e.g.* in **1.102** and **1.103**) or the amidinium moiety (*e.g.* in **1.104** and **1.105**). The bridged halonium ion can then be stabilized by a Lewis acid/base interaction with either the amidine (*e.g.* in **1.102** and **1.103**) or the naphthalenoxide moiety (*e.g.* in **1.104** and **1.105**). The reaction pathway is then governed through the minimization of unfavorable steric interactions between the catalyst and the substrate. This can be achieved by orienting the steric bulk of the substrate away from the catalytic pocket created by the binaphthyl core, leading to either **1.102** or **1.104** as the preferred transition states. It is still unclear which is the operative reaction pathway, however, important experimental evidence lends support to the transition state depicted in **1.102**. During the course of our method development, we discovered that TBCO was not required as the brominating reagent during bromolactonizations, and the

bromolactones could be obtained in similar yield and selectivity when *N*-bromosuccinimide (NBS) and 1,3-dibromo-5,5-dimethyl-hydantoin (DBDMH) were used as brominating reagents. Accordingly, amidines are known to transfer bromine from NBS to olefins,[73] and the independence of our catalyst with respect to halogenating reagent offers support in favor of transition state **1.02**, where the halogenated amidine could deliver "X^+" to the olefin and then stabilize the incipient halonium.

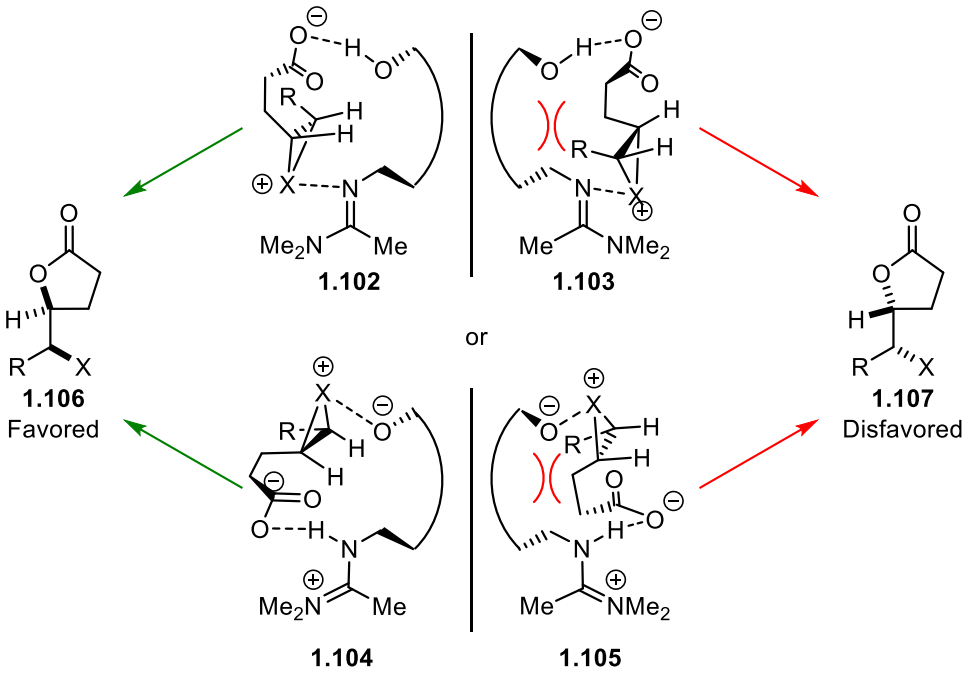

1.3.5 Applications to Methodological Problems

At the beginning of our investigations, we identified a number of unmet synthetic challenges in the context of enantioselective halolactonizations. Inducing cyclizations that produced new C-X bonds at exogenic stereocenters was chief among them, but after achieving that goal, we moved on to other methodological gaps. Other problems that

needed to be solved included the desymmetrization of a prochiral substrate and kinetic resolution of racemic substrates.

The desymmetrization of a prochiral substrate was addressed through the bromolactonization of 1,4-dihydrobenzoic acid (**1.108**) in the presence of **1.67**. In the event, the reaction proceeded to give lactone **1.109** in 73:27 er (Equation 1.23). Although the enantioselectivity of this reaction was initially modest, we discovered that the enantiopurity of **1.109** was easily improved to 99:1 er after a single recrystallization. Importantly, this was the first reported example of the desymmetrization of a prochiral substrate via an organocatalytic halocyclization reaction, although since our initial report, there have been several other examples of desymmetrizing halocyclization reactions (*vide infra*). Additionally, the iodolactonization of **1.108** could be effected using catalyst **1.76**, but the resultant iodolactone was unstable. However, the utility of **1.76** as a catalyst to promote kinetic resolutions of racemic olefinic acids is demonstrated via the iodolactonizations of **1.110** (Equation 1.24) and **1.112** (Equation 1.25), and the corresponding iodolactones were obtained with moderate to good selectivity.

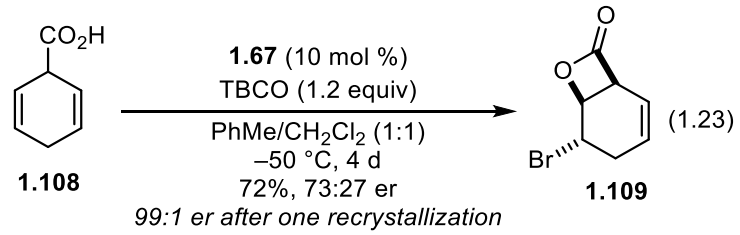

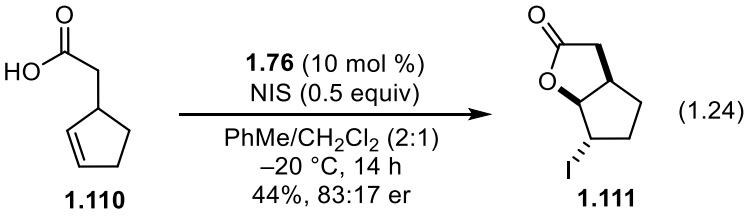

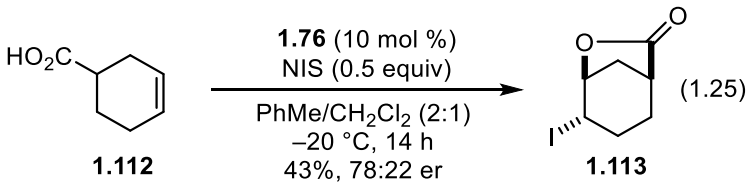

Another important extension of our halolactonization methodology is to the synthesis of enantioenriched *cis*-1,2-disubsubstituted epoxides, a functional group that is typically difficult to access in the absence of directing groups. We discovered that 4(*Z*)-alkenoic acids can be readily converted into the corresponding epoxides by a facile two-step process, first through an enantioselective iodoloactonization, followed by treatment of the enantioenriched iodolactone with a carbonate base in methanol in methanol (MeOH) as exemplified in the conversion of **1.52e** to **1.114** (Scheme 1.4).

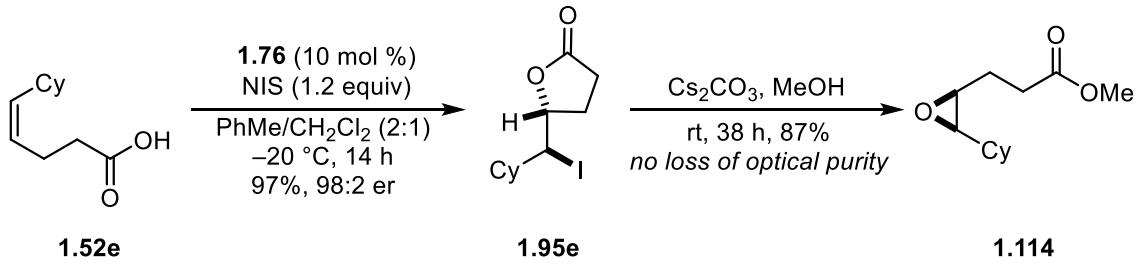

Scheme 1.4 Two-step preparation of enantioenriched epoxides from 4(*Z*)-alkenoic acids.

1.4 Desymmetrization via Asymmetric Halolactonization Reactions

1.4.1 Introduction

The desymmetrization of prochiral substrates through catalytic enantioselective halocyclization reactions has remained a challenging area of interest for organic chemists.[64] This class of reactions represents a powerful tool that offers rapid construction of useful

chiral building blocks. For example, the desymmetrization of 1,4-cyclohexadienoic acids provides chiral molecules with three contiguous stereocenters with dense functionalization.[15,74] The desymmetrization of prochiral substrates through organocatalytic haloetherfication reactions has seen recent advances,[38] but reports of desymmetrizing organocatalytic halolactonization reactions remains scarce.[74–76] During the course of our enantioselective halolactonization method development, we demonstrated the first desymmetrization of a prochiral olefin via catalytic enantioselective halolactonization through the conversion of **1.108** to **1.109** (Equation 1.23). Prior to our work, enantioselective desymmetrizations via halolactonization had only been carried out using chiral auxiliaries, and while some of these methods were able to achieve excellent selectivities,[76–79] the necessity of the auxiliary requires the additional step of attaching it to the substrate. Since our seminal report however, there have been several additional examples of asymmetric catalytic desymmetrizing halolactonization reactions, which will be summarized herein.

1.4.2 Hennecke

As part of his ongoing interest in desymmetrizing halofunctionalization reactions,[35] Hennecke developed conditions for the enantioselective bromolactonization of alkynes,[13] a substrate that previously presented a challenge for enantioselective halolactonizations. Normally the resulting 2-bromoenol lactone would be formed with no new stereocenters, however, a symmetrical starting material made an asymmetric cyclization possible. Hennecke explored a number of organocatalysts from the literature for this transformation, including the trisimidazoline catalyst reported by Fujioka[11] along with other cinchona alkaloid scaffolds. Ultimately, the best results were obtained using $(DHQD)_2PHAL$ (**1.19**),

and Hennecke demonstrated the desymmetrization **1.115** to produce **1.116** in good yield (76–98%) and with high selectivity (86:14–98:2 er) (Equation 1.26). While the exact mechanism of the reaction remains unknown, Hennecke speculates that the brominated quinuclidine of the catalyst delivers a bromonium ion to the alkyne, while the nucleophilic attack of the carboxylic acid is directed through a hydrogen bonding interaction with the pyridizine moiety of the catalyst.

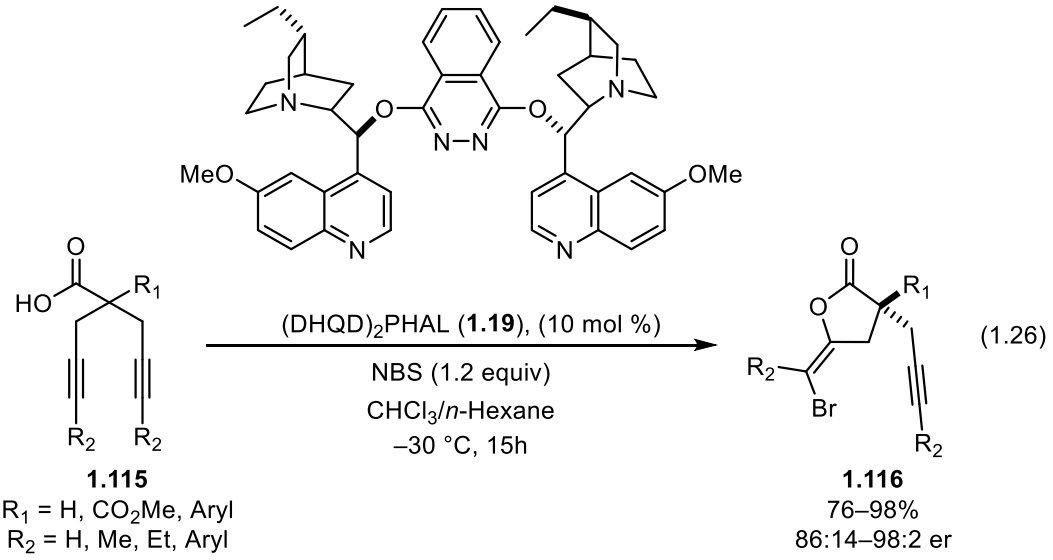

1.115
R_1 = H, CO_2Me, Aryl
R_2 = H, Me, Et, Aryl

1.116
76–98%
86:14–98:2 er

(1.26)

1.4.3 Desymmetrization of 1,4-Cyclohexadienoic Acids

In 2012, Hamashima reported the use of $(DHQD)_2PHAL$ as an effective catalyst for the desymmetrization α-substituted cyclohexadienes.[74] The reaction was optimized on substrates **1.117a–d**, where the alcohol protecting group varied in steric demand. The catalyst did not give any enantio-enriched product when the free alcohol **1.117a** was used (Table 1.7, Entry 1), and the Boc protected **1.117b** provided only modest enantioselectivity (Table 1.7, Entry 2). The catalyst tolerated substrates **1.117c** and **1.117d**, both of which contained alcohols protected with large silyl groups, and the corresponding bromolactones

were delivered with high degrees of selectivity (91 and 88% ee respectively) (Table 1.7, Entries 3 and 4).

Table 1.7 Desymmetrization of **1.117a–d** via bromolactonization with **1.19**.

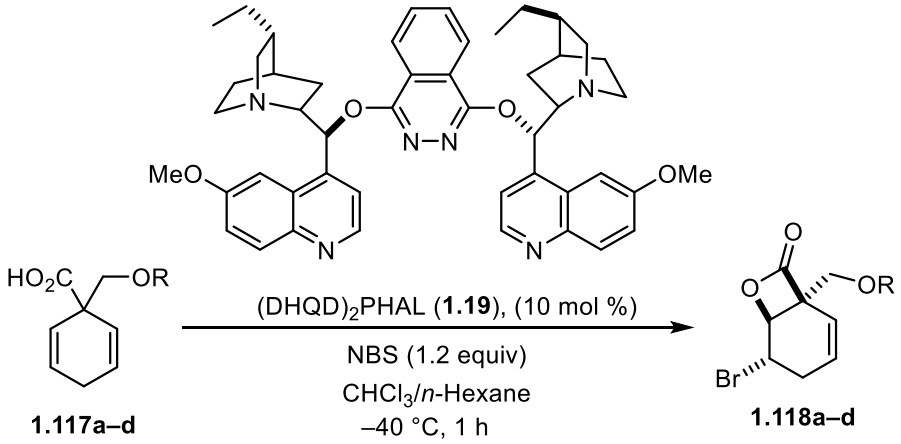

Entry	Acid	R	Product	Yield (%)	ee (%)[a]
1	**1.117a**	H	**1.118a**	70	0
2	**1.117b**	Boc	**1.118b**	84	45
3	**1.117c**	TIPS	**1.118c**	87	91
4	**1.117d**	TBDPS	**1.118d**	93	88

Hamashima then explored the substrate scope of this reaction, probing the catalyst's tolerance of substitution at the 1- and 4-positions of the cyclohexadiene ring (Figure 1.3). Hamashima found the methyl substituted lactone **1.119** could be obtained in good yield and selectivity (89%, 81% ee), but lactones **1.120** and **1.121**, which bore the more sterically demanding OMOM groups, were obtained with good selectivity, but in diminished yields (34% and 46% respectively). Further exploration of substitution at the α-position resulted in lactones **1.222** and **1.23**, both of which were afforded with lower selectivity than **1.117**.

When the substrate was electronically biased towards 5-exo cyclization through methyl substitution at the γ-position, lactone **1.124** was given with only 37% ee.

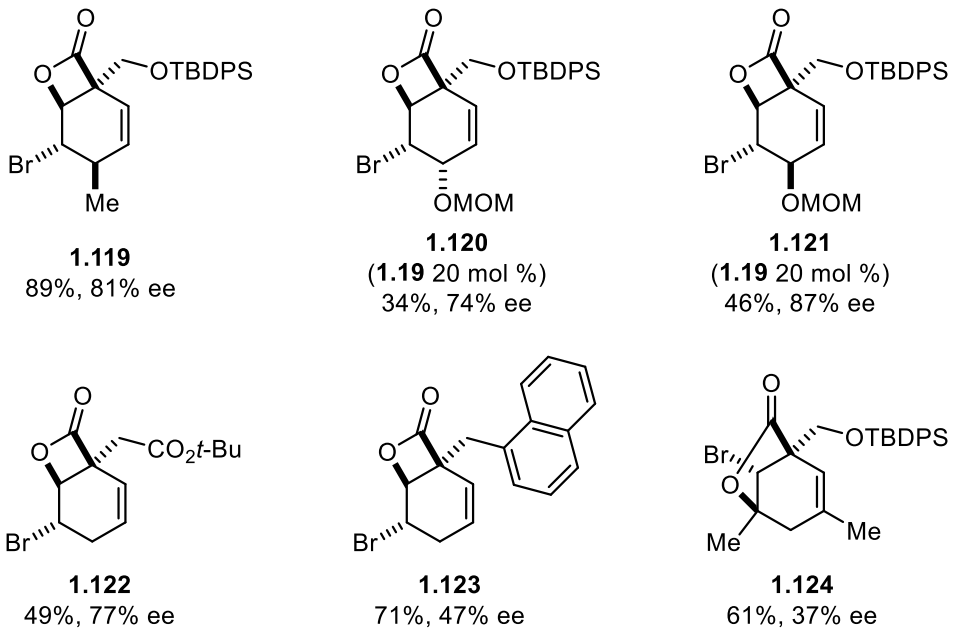

Figure 1.3 Substrate scope of desymmetrizations of cyclohexadienes with **1.19**

Hamashima also demonstrated the formation of a γ-lactone through the one-carbon-homologated cyclohexadiene **1.125** (Equation 1.27). This substrate was converted under his standard reaction conditions to give **1.126** with good enantioselectivity (92% ee). Finally, Hamashima showed an efficient kinetic resolution of **1.127** using catalyst **1.19**, which afforded **1.128** and **1.129** with good enantioselectivities (Equation 1.28).

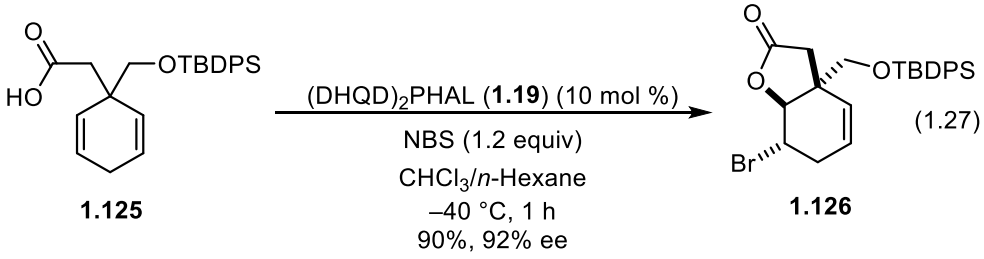

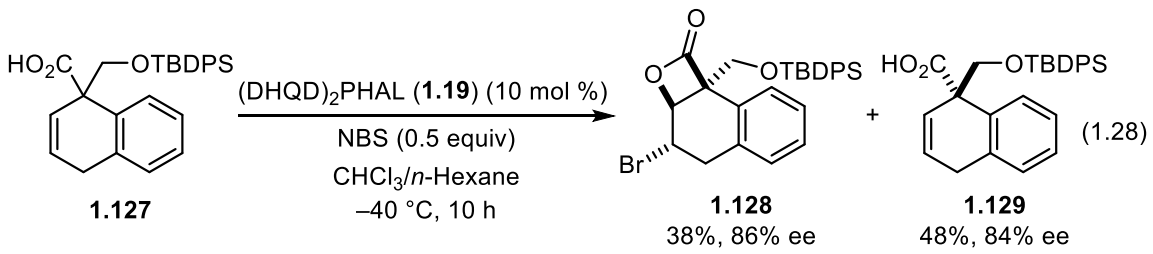

While the substrate scope of Hamashima's desymmetrization is limited, there have been no other reports of catalysts that are able to effect halolactonizations for this substrate class. For comparison to our catalyst, we briefly explored α-substituted cyclohexadienoic acids similar to those used by Hamashima, but a variety of our catalysts were unable to provide the corresponding bromolactones with any enantioenrichment. Hamashima did not report any desymmetrizations of 1,4-dihydrobenzoic acid (**1.108**), but Armstrong disclosed this reaction in 2013 while surveying the ability of **1.19** to promote a small variety of bromolactonizations of alkenoic acids.[75] Under reaction conditions similar to those used by Hamashima, Armstrong found that **1.108** was converted to **1.109** in the presence of **1.19** in low yield (40%) and poor selectivity (30% ee) (Equation 1.29). Even though our catalyst **1.67** could not effectively promote the bromolactonizations of α-substituted substrates, it appears that we have a niche in the ability to promote the desymmetrization of **1.108**.

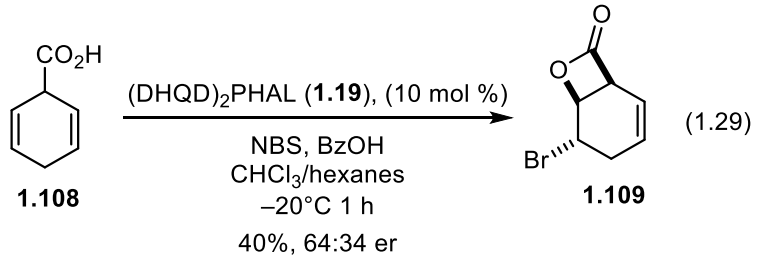

1.4.4 Johnston

Johnston recently reported the desymmetrization of cyclopentenoic acids which were promoted by the chiral Brønsted base catalyst **1.132** (Equation 1.30).[80] Generally, the

catalyst tolerated aryl substituted cyclopentenoic acids (**1.130** R = aryl) well, and the corresponding iodolactones (**1.131**) were delivered with good selectivity (89–94% ee). The catalyst also readily tolerated alkyl substituted acids (**1.130** R = *i*-Pr, Bn, Me) with only slightly diminished selectivities (86–87% ee) compared to the aryl substituted acids. The ester (**1.130**, R = CO_2t-Bu) and thioester (**1.130**, R = C(O)S*t*-Bu) substituted acids however, displayed significantly lower selectivities, and the iodolactones were obtained with 64% and 74% ee respectively. The catalyst did not tolerate unsubstituted cyclopentenoic acids, and in the case of **1.130** R = H, no product was afforded under the reaction conditions.

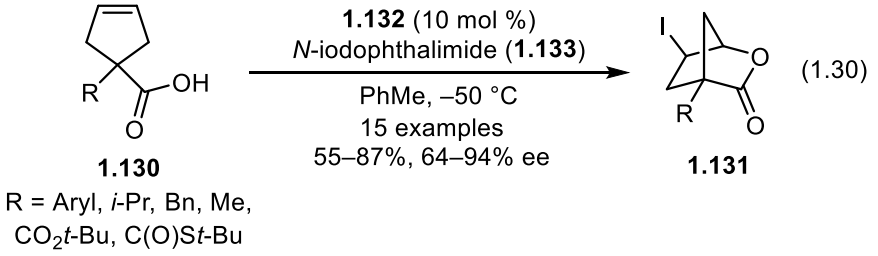

(1.30)

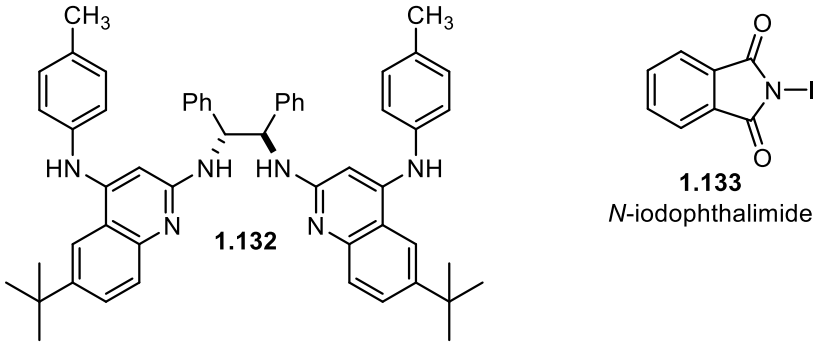

1.133
N-iodophthalimide

1.4.5 Summary

The recent explosion of catalytic enantioselective halolactonizations has paved the way for a variety of novel desymmetric transformations through this reaction mode, allowing the conversion of prochiral or *meso*-compounds to optically active halolactones with good enantioselectivities. Despite recent progress, this has remained a challenging

area in catalytic enantioselective halolactonization research, as evidenced by the relatively few examples of reported desymmetrization methods compared to the number of catalysts capable of promoting asymmetric halolactonizations of alkenoic acids. The desymmetrization of prochiral substrates remains a powerful tool for synthetic chemists however, and the importance of generating stereogenic C–X bonds for the pursuit of halogenated natural products will continue to inspire new developments in this field.

1.5 Asymmetric Epoxidation of Unactivated *Z*-Disubstituted Olefins

In order to better understand the significance of the ability to easily access enantioenriched *cis*-1,2-disubstituted epoxides from the corresponding enantioenriched halolactones obtained from our method, a brief overview of asymmetric epoxidations is required. Epoxides are versatile synthetic intermediates that are one of the most useful building blocks in organic synthesis. Epoxides easily undergo stereospecific ring-opening reactions that can be used to form bifunctional molecules and quickly build structural complexity.[81–83] Additionally, this functional group is prevalent in a wide variety of natural products and biologically relevant molecules. Consequently, there has been great interest in the development of methods for the preparation of enantiopure epoxides. The enantioselective epoxidation of olefins using metal catalysis has seen widespread success and is arguably one of the most important synthetic techniques that has emerged in the last in 40 years.[81] Indeed, Barry Sharpless was awarded the 2001 Nobel Prize as a compliment to his contributions to the field.

Asymmetric epoxidations of *cis*-olefins conjugated to an alkyne, aryl group, or another alkene generally proceed with good selectivity for both organocatalytic and metal based catalytic methods.[81,84] However, the direct asymmetric epoxidation of *cis*-1,2-dialkyl-substitued olefins (**1.134** R_1, R_2 = alkyl) remains a challenging area of research,

and there have been few successful reports of such a transformation (Equation 1.31). Aliphatic substituted olefins are challenging substrates for asymmetric epoxidations in part due to their low reactivity towards electrophilic oxidants. Additional complications arise in the difficulty for catalysts to achieve good enantioface differentiation for substrates of this type.

.

(1.31)

1.134 **1.135**

Jacobsen was the first to describe a highly selective asymmetric epoxidation of a simple *cis*-disubstituted olefin in 1991.[85,86] Jacobsen explored a small variety of aryl substituted *cis*-olefins and showed that substrates such as **1.136** could be converted into the corresponding epoxide using catalyst **1.137** in 65–96% yield and with 92–98% ee. The only non-conjugated alkene that Jacobsen explored was the spirocyclic cyclohexene x, which underwent epoxidation in moderate 65% yield with 89% ee

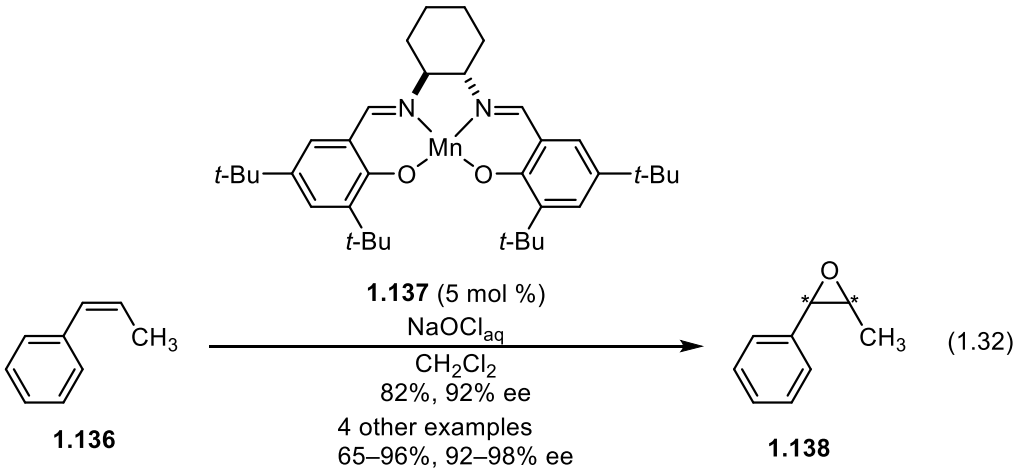

(1.32)

1.136 **1.138**

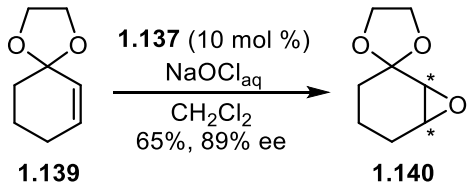

(1.33)

In these initial studies, Jacobsen rationalized the selectivity of these Mn-salen catalysts with a steric model, where the substrate would interact with the catalyst in a manner that would minimize unfavored steric interactions.[83,85] However, later investigations by Katsuki revealed that steric factors alone do not explain the observed enantiomeric ratios, and he hypothesized that the conjugated nature of the olefin plays a role in determining the epoxidation selectivity.[87] Katsuki expanded Jacobsen's investigations into asymmetric epoxidations non conjugated *cis* -1,2- -disubstituted olefins with substrates **1.141** and **1.143** (Scheme 1.5). Substrate **1.141** was converted to **1.142** with good selectivity, 82% ee, but the yield was low at 23%. The straight chain alkyl substituted **1.143** was converted to **1.144** in poor yield of 13% and with poor enantioselectivity, 44% ee.

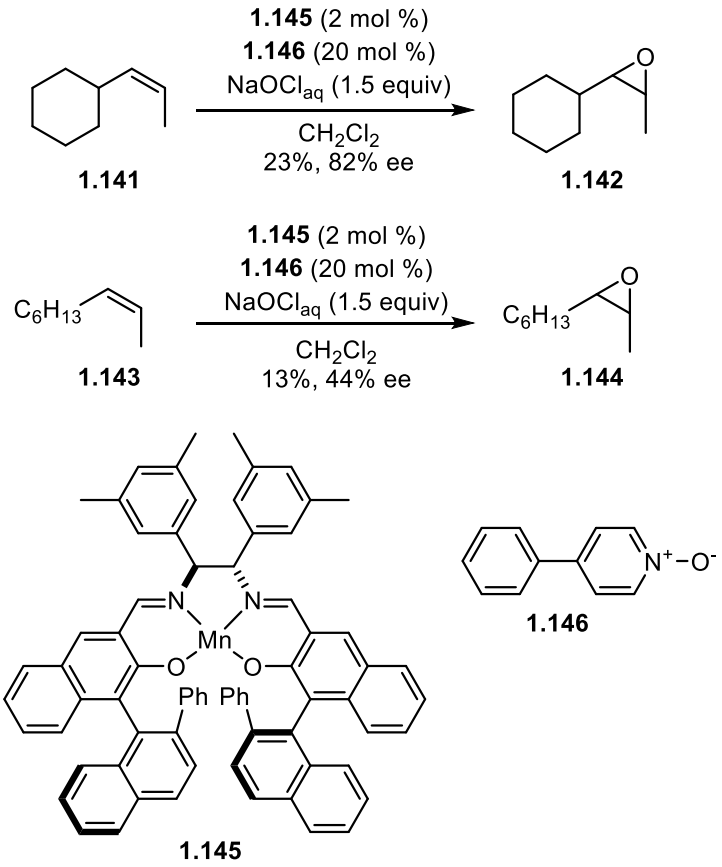

Scheme 1.5. Asymmetric epoxidations of **1.141** and **1.143** with catalyst **1.145**.

Significant progress was not made until years later when Katsuki reported the chiral titanium complex **1.147** as an effective catalyst for asymmetric epoxidations of unfunctionalized olefins (Figure 1.4).[88] Using catalyst **1.147**, Katsuki described epoxidations of a variety of aliphatic olefins, including the *cis*-disubstituted olefins of **1.134** that correspond to products **1.150–1.152**. These substrates were generally converted in 49–85% yield and with 70–92% ee. The catalyst displayed better selectivities for the terminal olefins which led to products **1.148** and **1.149** in 82 and 92% ee respectively. The *cis*-disubstituted olefins were converted with moderate selectivities, exemplified by **1.152** which was obtained in only 70% ee.

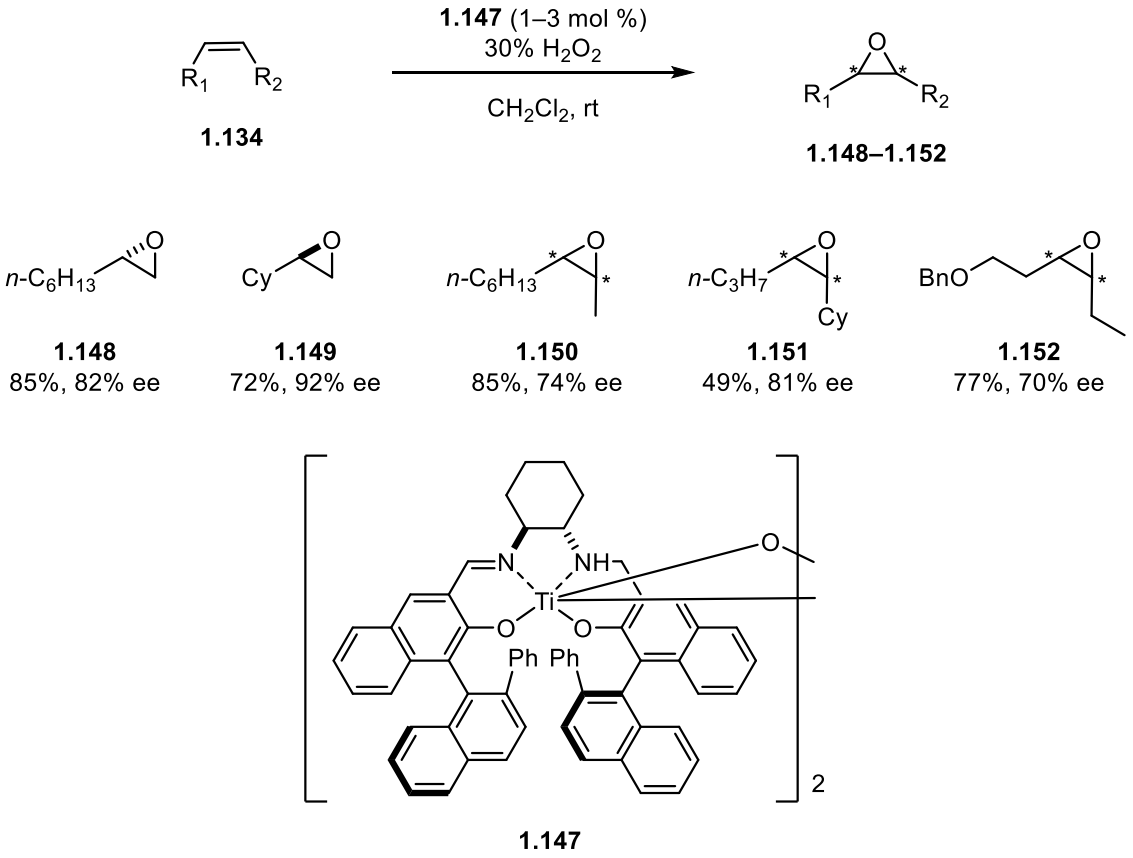

Figure 1.4. Asymmetric epoxidations of unfunctionalized olefins with **1.147**.

Not long after Katsuki's innovations, Shi reported efficient epoxidations using his organic chiral dioxirane catalyst **1.153**. This catalyst was shown to promote the alkyl substituted olefin **1.154** to **1.155** in 52% yield and 64% ee (Equation 1.34). Selectivities improved substrates which were substituted with alcohols or carboxylic acids, as exemplified in equations 1.35 and 1.36. The alcohol containing substrate **1.156** was converted to **1.157** in 89% yield and 82% ee (Equation 1.35). Interestingly, **1.158** underwent an intramolecular cyclization under the reaction conditions to afford the hydroxy lactone **1.159** in 75% yield and 91% ee (Equation 1.36). After probing a variety of other substrates, Shi concluded that the *cis*-olefins required two substituents with

substantially different hydrophobic or electronic properties to obtain good selectivities. Shi's method was lacking in that there was no universal catalyst for all the substrates he explored, and different substitutions required different derivatives of **1.153** to obtain good selectivity.

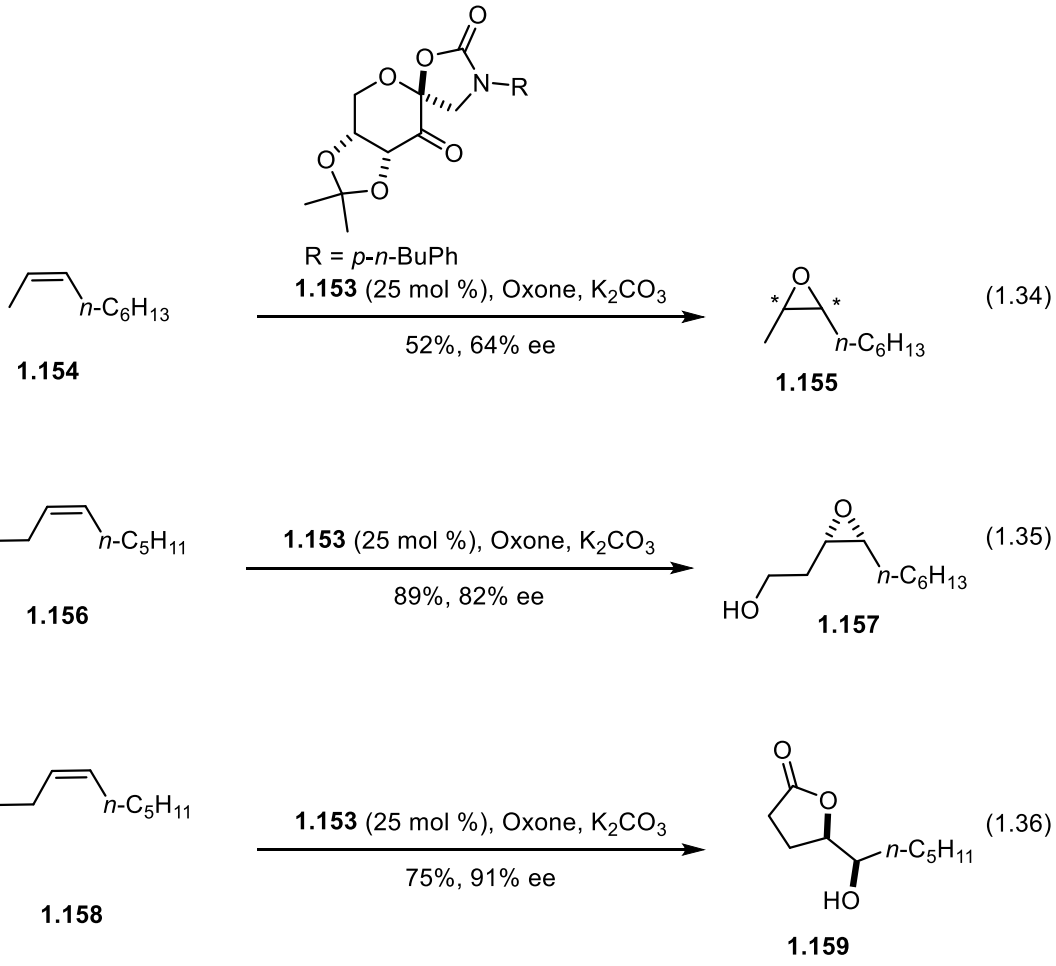

1.6 SUMMARY AND CONCLUSIONS

The bifunctional catalysts **1.67** and **1.76** were the first to incorporate a binaphthyl moiety as part of the catalyst design for an asymmetric halocyclization reaction. We have shown that both **1.67** and **1.76** promote highly selective asymmetric bromo- and

iodolactonizations of a diverse array of olefinic acids. As part of these investigations, we were able to make a number of contributions to advance the field of enantioselective halolactonization reactions. Significantly, these catalysts were the first to induce highly enantioselective halolactonizations of alkyl substituted olefinic acids via exo cyclization modes to give halolactones bearing exogenic enantioenriched secondary C–X bonds. Additionally, with the exception of **1.19**, these are the only catalysts reported that are able to effect more than one type of halolactonization mode, offering the beginnings of a more unified approach to enantioselective halocyclization reactions.

In addition to expanding the substrate scope for enantioselective halolactonization reactions, we were also able to address some of the methodological gaps present in the field when we entered this area of research. Importantly, we demonstrated that **1.67** and **1.76** promote desymmetrizations and kinetic resolutions with good levels of enantioselectivity. We further exemplified the utility of **1.76** by its application to the enantioselective synthesis of (*Z)*-1,2-alkyl epoxides from iodolactones generated from 4(*Z*)-pentenoic acids. As part of our ongoing interest in natural product synthesis, we wished to apply our halolactonization methodology to relevant synthetic problems in the field. Specifically, we planned to demonstrate the utility desymmetrizing 1,4-dihydrobenzoic acid through the enantioselective synthesis of F-ring fragments of the kibdelone natural products. Additionally, we were aware that the asymmetric introduction of epoxides to 1,2-disubstitued *cis* olefins is a challenging transformation in the absence of directing groups. Our halolactonization methodology offered one solution to this problem, and we planned to showcase this strategy through an enantioselective synthesis of (+)-disparlure, an important insect pheromone for the management of gypsy moths.

Chapter 2: Applications of Enantioselective Halolactonization Reactions[2]

2.1 Kibdelone C – Introduction and Isolation

The kibdelones are hexacyclic tetrahydroxanthone natural products discovered by Capon in 2007.[89] They are members of a growing class of natural products that is characterized by their highly oxygenated hexacyclic polyaromatic scaffolds. This class of natural products has attracted considerable attention from the synthetic community due to their interesting structures and biological activities.[90]

Kibdelones A–C (**2.1**–**2.3**) were isolated from a rare Australian actinomycete genus, *Kibdelosporangium* sp (Figure 2.1). The structures were assigned after extensive NMR studies, and the three congeners differed only in the oxidation states of the B (qunione vs hydroquinone) and C (saturated vs unsaturated) rings. The isolation studies also revealed that kibdelone C could spontaneously oxidize to kibdelones A and B under aerobic conditions. Characteristic of this family of natural products, the kibdelones displayed potent biological properties, which included antibacterial and nematocidal activities, as well as cytotoxicity against a panel of human cancer cells. Their potent anticancer activity in particular was striking, as all three compounds displayed GI_{50} values of <5 nm in cell lines derived from lung, colon, ovarian, prostate, breast and other tumor types. The biological mechanism of action for this cytotoxicity remains unknown, and it is

[2] Sections of this chapter are based on previously published work completed by Daniel W. Klosowski that Prof. Stephen F. Martin acted as an advisor for. See: Klosowski, D. W.; Martin, S. F. Enantioselective Synthesis of F-Ring Fragments of Kibdelone C via Desymmetrizing Bromolactonization of 1,4-Dihydrobenzoic Acid. *Synlett* **2018**, *29*, 430–432 and Klosowski, D. W.; Martin, S. F. Synthesis of (+)-Disparlure via Enantioselective Iodolactonization. *Org. Lett.* **2018**, *20*, 1269–1271.

unclear if kibdelones A–C are equally active, or if they interconvert under the conditions of the biological assays.[89,91,92]

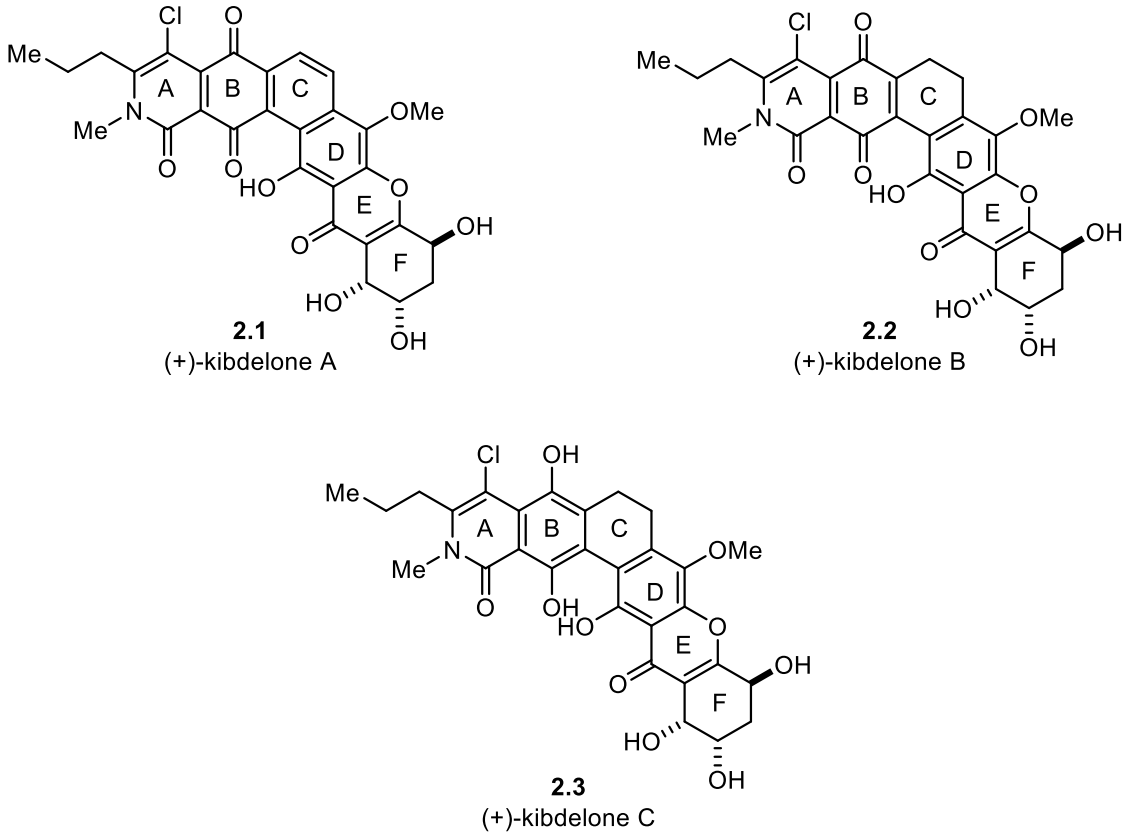

Figure 2.1 Kibdelones A–C

The combination of unique structural features and potent biological activities of the kibdelones drew the attention of the synthetic community, culminating in two enantioselective total syntheses of kibdelone C (**2.3**). Porco completed a synthesis of (+)-kibdelone C,[93] and the antipode (–)-kibdelone C was completed by Ready.[92,94] A major challenge for both groups during their respective syntheses was the preparation of the polyhydroxylated chiral F-ring of the natural product. As part of our work in the area of enantioselective halolactonization reactions, we applied the desymmetrization of 1,4-dihydrobenzoic acid via enantioselective bromolactonization to the synthesis of two

synthons of the F-ring subunits of kibdelone C.[95] In order to provide context for our work in this area, a summary of the previous syntheses of F-ring fragments of kibdelone C as well as the general strategies towards this natural product will be discussed.

2.2 Previous Syntheses of F-Ring Subunits of Kibdelone C

2.2.1 Porco's F-Ring for (+)-Kibdelone C

For his synthesis of (+)-kibdelone C, Porco envisaged a late stage coupling of the ABCD fragment **2.4** and the chiral F-ring **2.7** through an *oxa*-Michael/retro-Michael Friedel–Crafts annulation sequence (Scheme 2.1) The construction of the F-ring **2.5** relied on a diastereoselective intramolecular halo-Michael aldol reaction of ynoate **2.6**, which would ultimately arise from the commercially-available, enantiopure alcohol **2.7**.

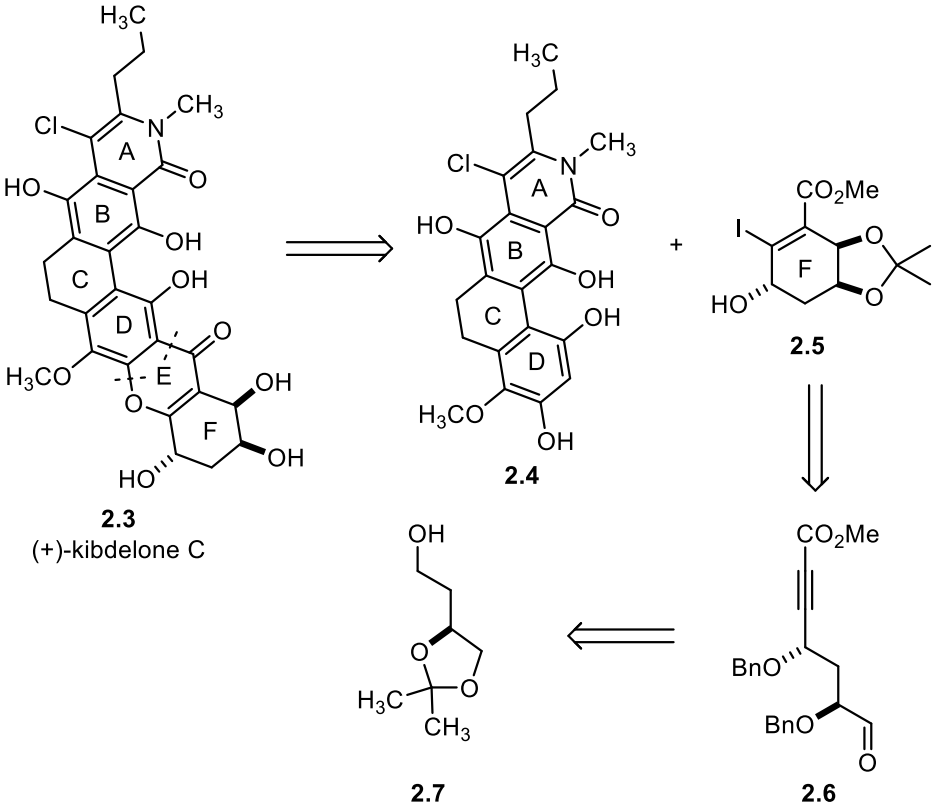

Scheme 2.1 Porco's synthetic strategy towards (+)-kibdelone C.

Porco's synthesis of F-ring fragment **2.5** commenced with a Dess–Martin periodinane oxidation of the enantiopure alcohol **2.7** to give aldehyde **2.8** (Scheme 2.2). Chelation controlled addition of the zinc acetylide **2.9** to **2.8**, followed by benzyl protection of the resulting alcohol and removal of the silyl protecting group with tetrabutylammonium fluoride (TBAF) delivered **2.11** in 60% yield over three steps. The free alcohol of **2.11** was then oxidized to the carboxylic acid through a two-step sequence, beginning with oxidation to the aldehyde with 2-iodoxybenzoic acid (IBX) followed by a Pinnick oxidation. Further treatment with methanol and sulfuric acid (H_2SO_4) delivered the methyl ester **2.12** with concomitant removal of the acetonide protection group. The secondary alcohol of **2.12** was then selectively benzylated, through benzylidene formation with **2.13**, followed by treatment with trimethylsilyl chloride (TMSCl) and sodium cyanoborohydride ($NaCNBH_3$) to provide **2.14** in 76% yield over two steps. The unprotected primary alcohol was oxidized to the aldehyde **2.15**, and the stage was set for Porco to investigate the key step to form **2.16**, which would be achieved through an intramolecular halo-Michael aldol reaction. The desired transformation proceeded smoothly after treatment of **2.15** with magnesium iodide, which delivered the desired diastereomer **2.16** in 78% yield, with only minor amounts of **2.17** being isolated.

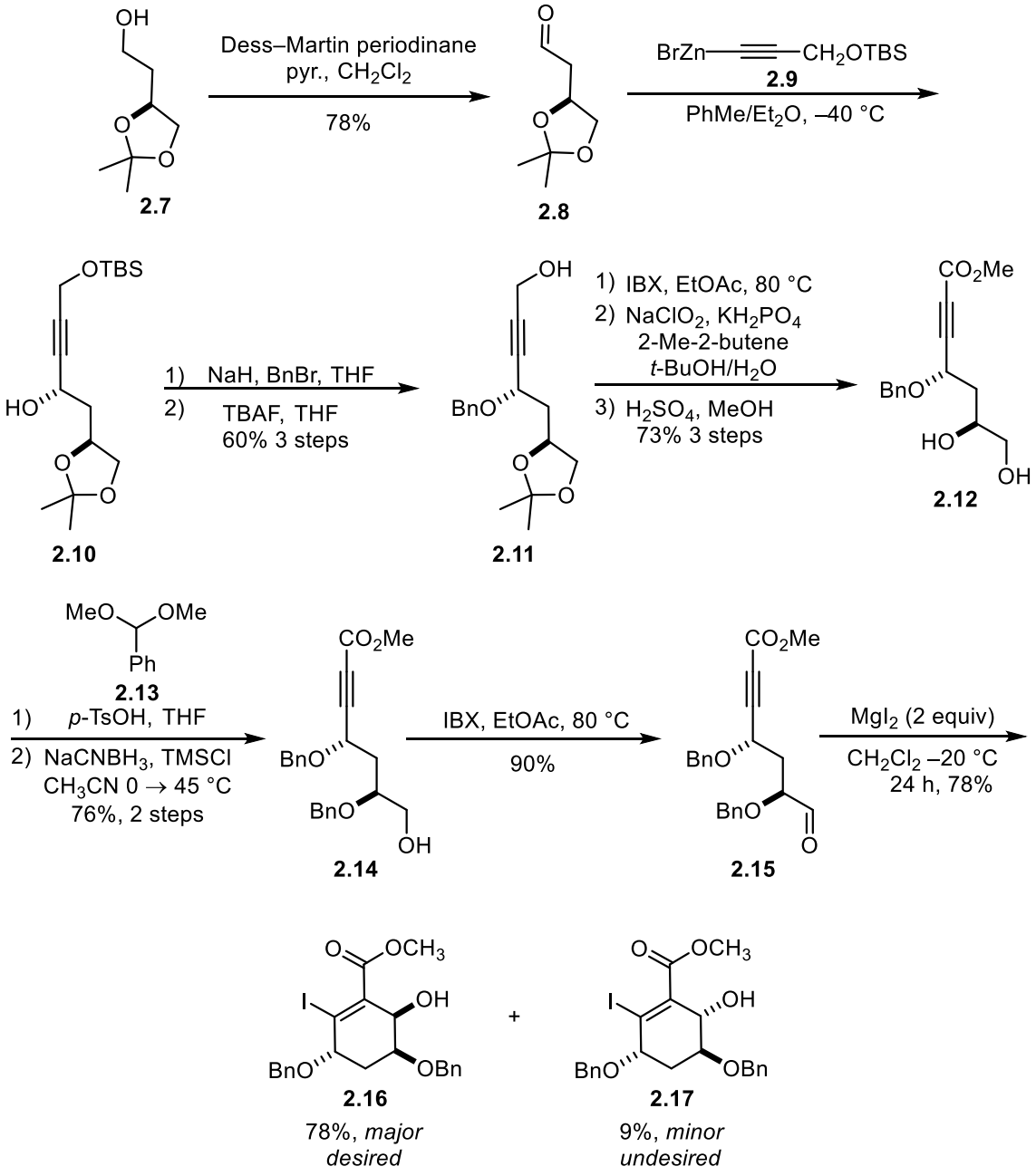

Scheme 2.2. Porco's synthesis of F-ring fragment **2.16**

The diastereoselectivity of this reaction can be rationalized through the proposed transition states **2.18**–**2.21** (Figure 2.2). Michael addition of iodide ion to the ynoate **2.15** leads to the reversible formation of the β-iodoallenoate diastereomers **2.18** and **2.19**, the

former of which can undergo cyclization via transition state **2.20** resulting in the minor product **2.17**.The latter diastereomer **2.19** however can react via intermediate **2.21**, in which leads to the major product **2.16**. Porco speculated that the preference for **2.16** over **2.17** might be due to the stabilizing chelation of the benzyl ether and aldehyde with MgI_2 that is possible in transition state **2.21**. Alternatively, the product ratio could be a reflection of the relative thermodynamic stability of **2.16** and **2.17** if epimerization by a retro-halo Michael aldol process can occur under the reaction conditions.

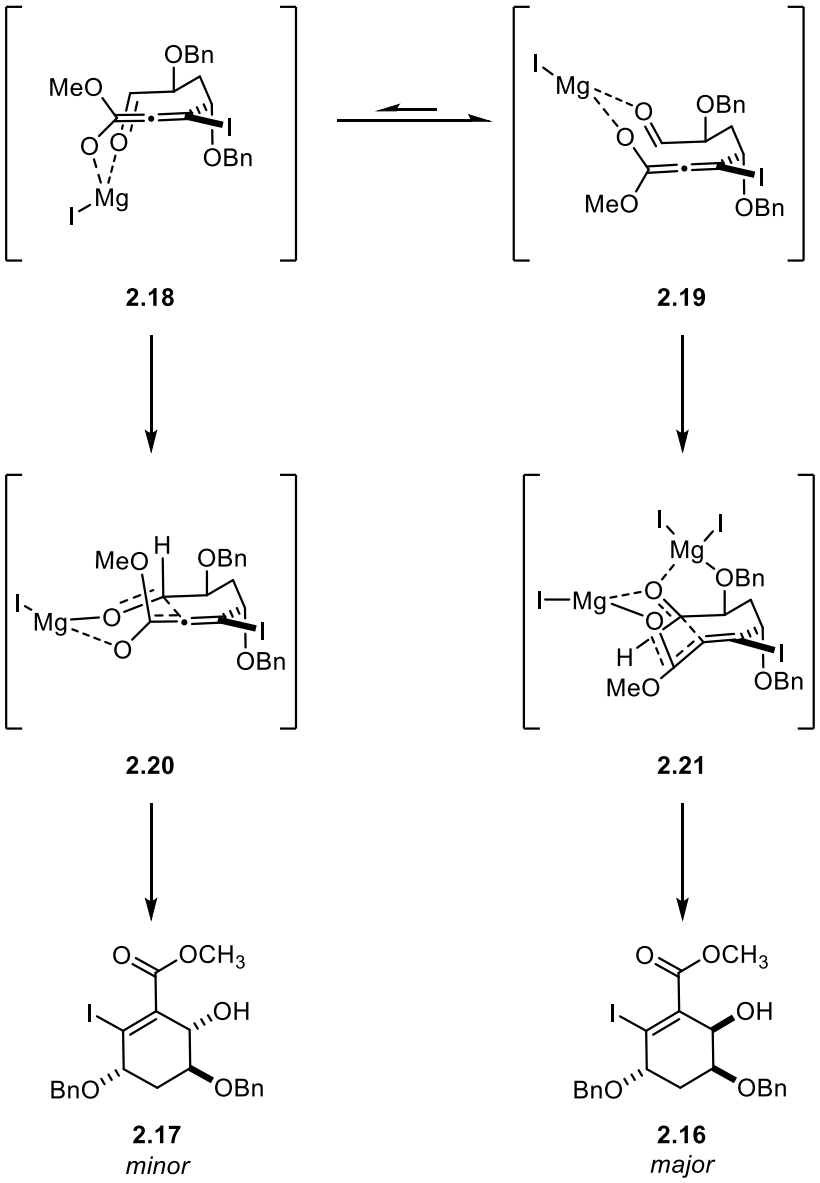

Figure 2.2 Mechanistic rationale for the observed diastereomeric ratio of **2.16** and **2.17**

With F-ring fragment **2.16** in hand, Porco attempted to couple it with **2.4** to generate **2.22**, but unfortunately the reaction was unsuccessful under a variety of palladium- and copper-catalyzed conditions (Equation 2.1).

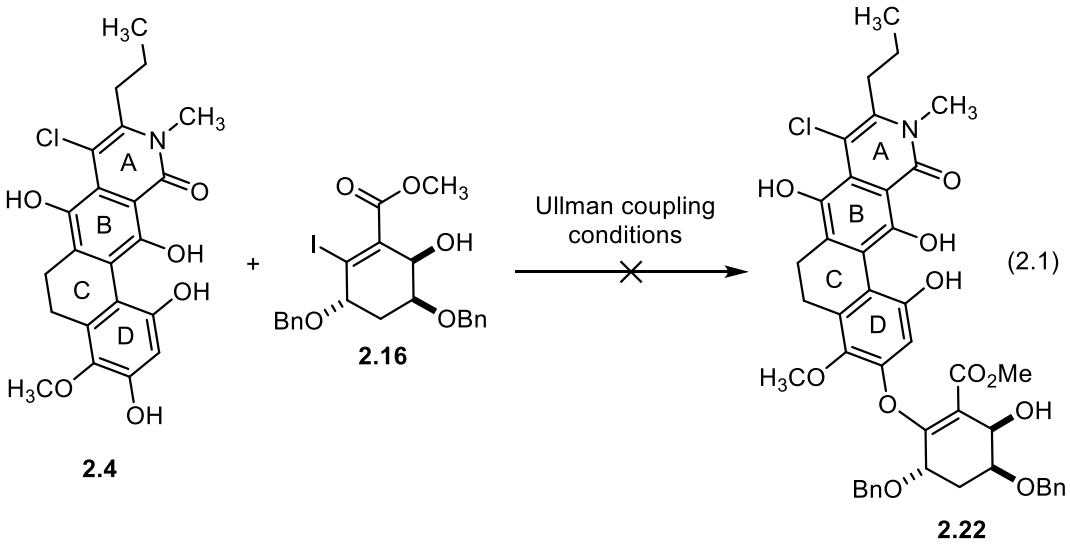

Porco changed his strategy and instead targeted the acetonide **2.5** for use in an *oxa*-Michael reaction, reasoning that the unhindered free allylic alcohol of **2.5** would impart better reactivity than its bulky benzyl protected counterpart **2.16**. After screening a variety of conditions, the protecting group swap was achieved in two steps, beginning with a global debenzylation through treatment with BCl_3, followed by protection of vicinal diol moiety with 2,2-dimethoxypropane under acidic conditions to deliver **2.5** in 87% yield (Equation 2.2).

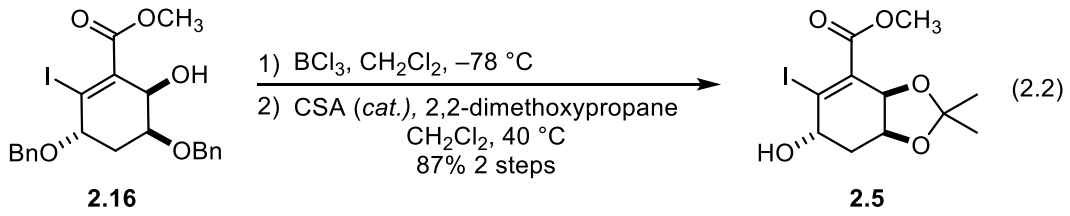

After extensive screening, Porco was able to achieve the *oxa*-Michael/retro-Michael addition elimination sequence to prepare the vinylogous carbonate **2.23**, albeit in moderate yield (44%), through treatment of **2.4** and **2.5** with tribasic potassium phosphate

in DMSO (Scheme 2.3). The final E ring was then formed from **2.23** through a 2 step soaponification–Friedel–Crafts acylation sequence to afford **2.25**.

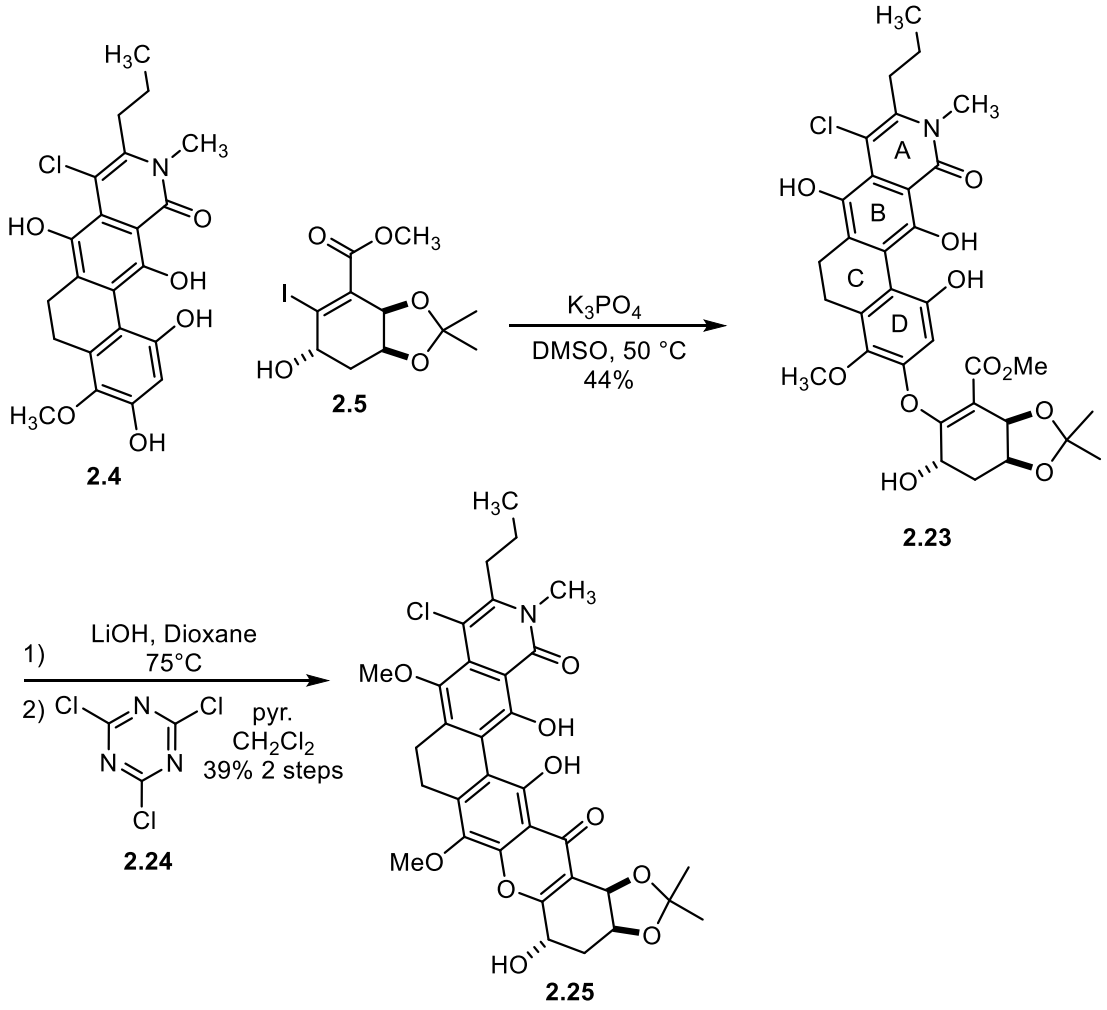

Scheme 2.3 Connection of ABCD-rings **2.4** and F-ring **2.5** and E-ring formation

Porco prepared the F-ring fragment **2.5** in 13 steps and 15% overall yield.[93] The *oxa*-Michael/retro-Michael strategy for preparing the vinylogous carbonate **2.23** relied on the elimination of the halogen atom of **2.5**. The installation of halogen atoms at the β-position of enoates is not a trivial task, and indeed there are no reported methods for a one-step general transformation of this type. Accordingly, the use of **2.5** in his synthesis

required Porco to construct the F-ring fragment from a linear precursor, accounting in part for the lengthy synthetic sequence. Porco relied on a diastereoselective intramolecular halo-Michael aldol reaction (Scheme 2.2, **15** to **16**) as the key step in the preparation of **2.5**, which worked well in terms of yield and diastereoselectivity. Prior to Porco's work, transformations of this type had been previously investigated, but the 1,3-diol moiety of **2.5** does add additional complexity that is not present in earlier examples.[96] Porco's choice of starting materials and strategy allowed him to rapidly construct the framework of **2.5**, which contained all of the requisite carbon atoms after only the second step. However, the rest of the synthesis is mired in oxidation–reduction sequences and protecting group manipulations, with these two types of transformations comprising 11 out of the 13 total steps required to prepare **2.5** from **2.7**.

2.2.2 Hudlicky's Synthesis of Porco's F-Ring

Hudlicky significantly shortened the synthesis of Porco's F-ring fragment **2.5** through a microbial dihydroxylation of methyl 2-halobenzoates (Scheme 2.4). Whole cell fermentation of **2.26** (X = Br) or **2.27** (X = I) with toluene dioxygenase overexpressed in *E. coli* JM 109 (pDTG601A) gave the mixture of diols, **2.28** (desired) and **2.29** (undesired) for X = Br in a 3.5:1 ratio, and **2.30** (desired) and **2.31** (undesired) for X = I in a 1:4 ratio. The interesting selectivity of the diol formation can be explained by Boyd's rule, which states that the largest group directs the enzymatic dihydroxylation.[91] In the case of **2.27** where X = I, the large iodine atom directs the dihydroxylation, resulting in the undesired product as the major diastereomer. For the case of **2.26** where X = Br, the methyl ester is the directing component, leading to greater selectivity for the desired diastereomer.[91] The desired diol **2.28** was carried on and protected as the acetonide through treatment with 2,2-dimethoxypropane under acidic conditions to deliver **2.32**. The final alcohol was installed

using a Mukaiyama hydration to afford **2.33** in only three steps from **2.26**. While the enzymatic dihydroxylation of **2.26** significantly shortened the synthesis to Porco's F-ring fragment, it was low yielding, providing the bromo-analogue **2.33** in only 2.2% overall yield.[97]

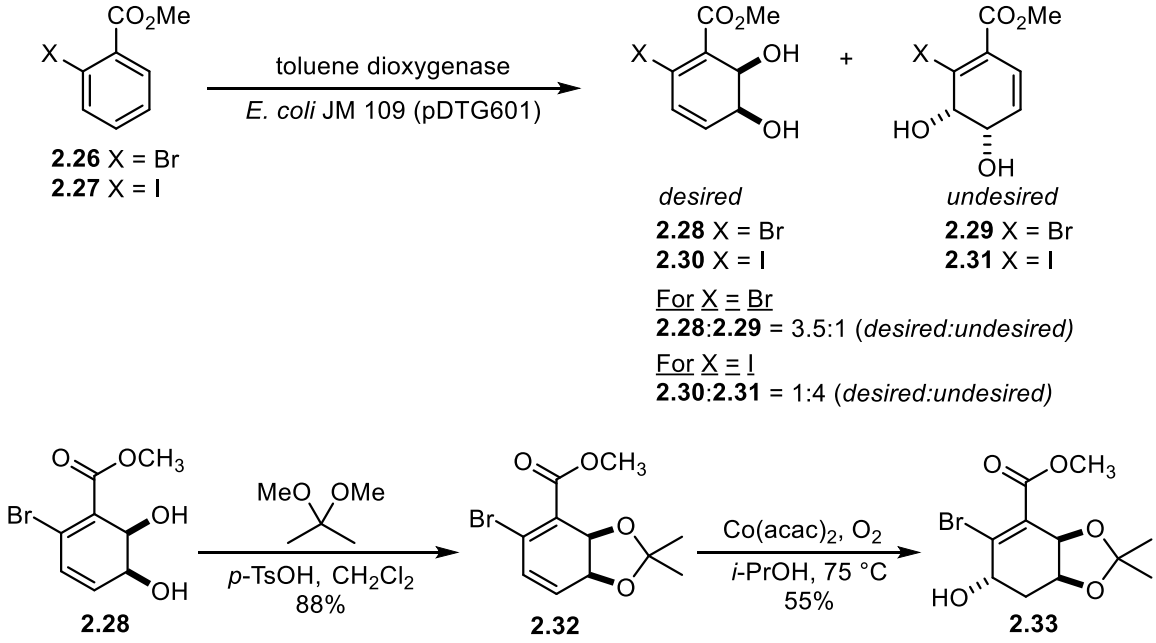

Scheme 2.4 Hudlicky's synthesis of Porco's F-ring fragment.

2.2.3 Ready's F-Ring for (–)-Kibdelone C

Ready planned a convergent approach to (–)-kibdelone C, where **2.34** could be synthesized from the AB-DEF ring system **2.35**, which would be accessed through the smaller subunits **2.36–2.39** (Scheme 2.5). He planned to couple the D and F rings together through lithiation of the iodocyclohexene **2.39**, followed by nucleophilic addition into aldehyde **2.38**.

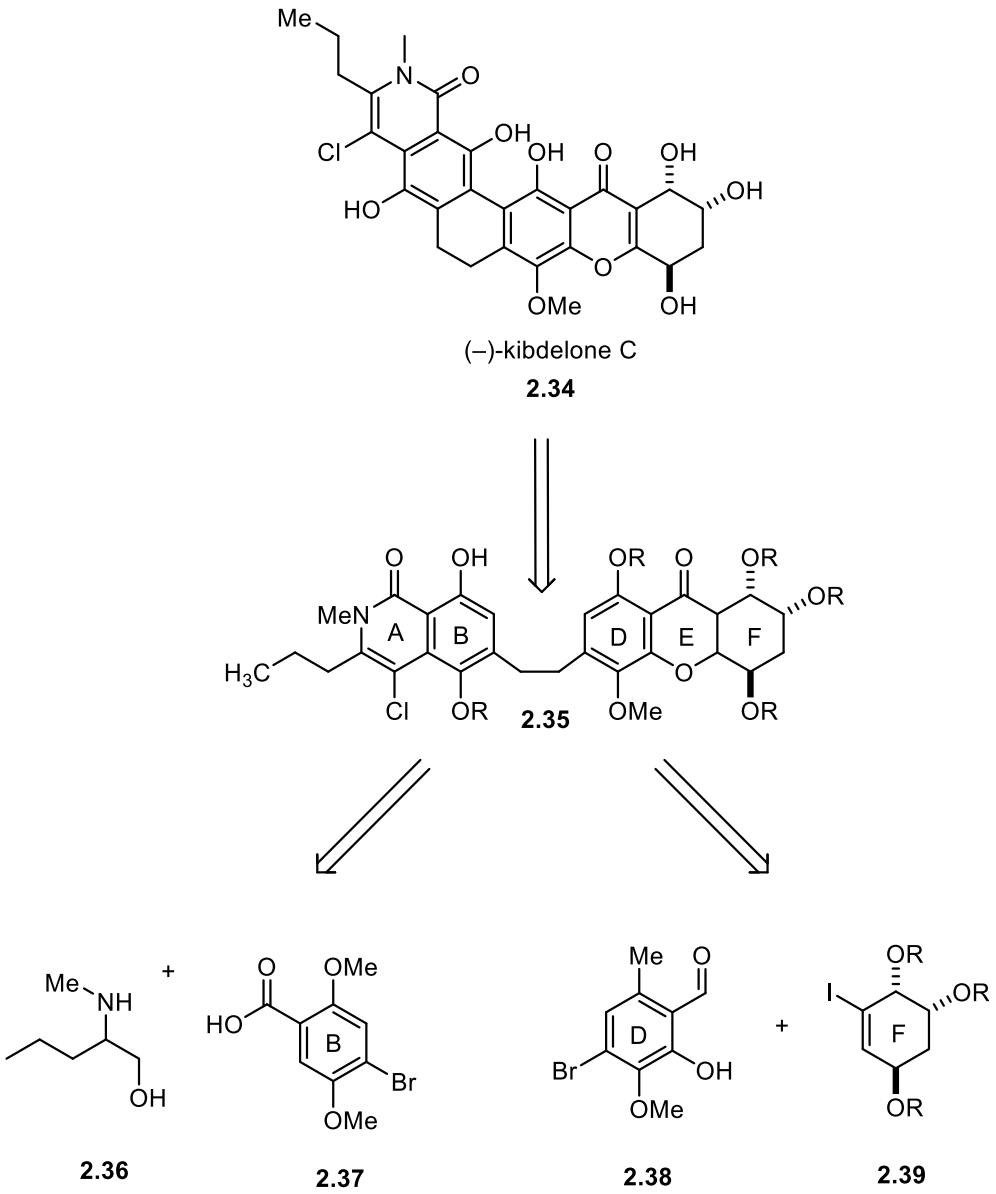

Scheme 2.5 Ready's synthetic strategy for (–)-kibdelone C.

The synthesis of Ready's F-ring fragment began with Birch reduction of **2.40** to give the symmetrical silyl enol ether **2.41** in 82% yield (Scheme 2.6).[92,94] Following work previously established by Myers for the synthesis of trans-diols, the Shi epoxidation of **2.41** with catalyst **2.42** followed by treatment with BH_3•THF smoothly delivered

polyhydroxylated cyclohexane **2.45** in 68% yield, as a single observable enantiomer and diastereomer. The highly selective epoxide reduction proceeds through the proposed intermediate **2.44**, where borane first acts as a Lewis acid to promote the epoxide ring-opening and then delivers a hydride intramolecularly to provide **2.45**. This reaction installed all of the requisite oxygen atoms for the F-ring, with the correct stereochemistry between the C2 and C4 oxygen atoms. The alcohol at C1 was introduced with the incorrect stereochemistry and requires epimerization, while the C5 alcohol provides a handle for introducing the desired olefin. Towards these goals, **2.45** was tosylated to give **2.46** in 71% yield. The C1 alcohol was then oxidized under Swern conditions, which resulted in the β-elimination of the tosyl group to afford the enone **2.47**. Iodination of the α-position of the enone, followed by Luche reduction afforded the desired F-ring fragment **2.48** in seven steps and 30% overall yield from **2.40**. While Ready's synthesis of **2.48** did not contain any novel chemistry, it was an efficient and high yielding preparation of the target F-ring fragment.

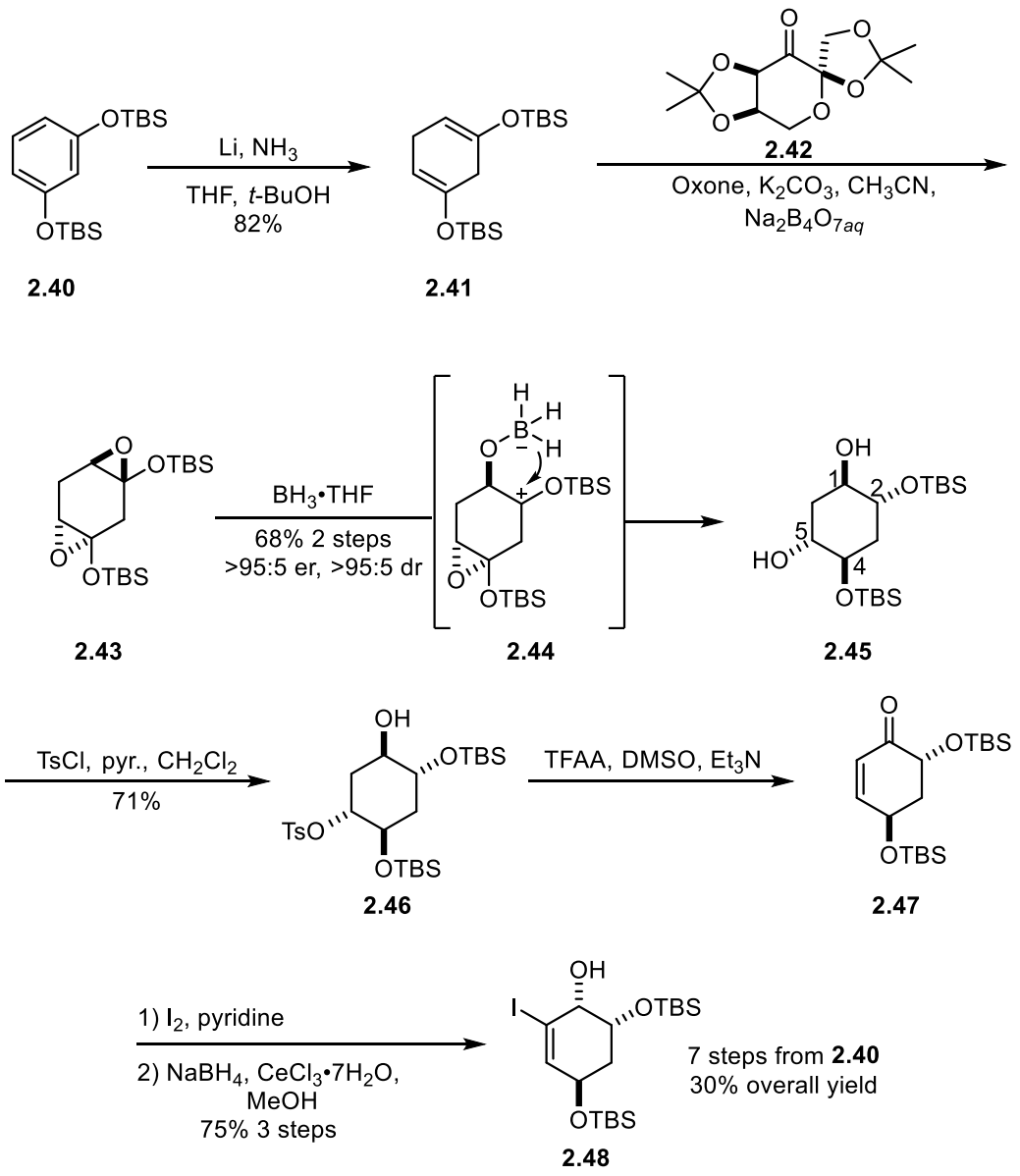

Scheme 2.6. Ready's synthesis of F-ring fragment **2.48**

With the desired fragment prepared, Ready investigated the connection between the D and F rings to construct the tetrahydroxanthone E ring.[92] Preliminary studies revealed that carbonylative Stille couplings between **2.49** and various F-ring precursors **2.50** were ineffective, showing no desired product formation (Equation 2.3). Interestingly, fully

protected F-rings could be metalated to give intermediates such as **2.53**, but no addition to the electron rich, sterically encumbered aldehyde **2.52** was observed (Equation 2.4). It was hypothesized that the protected allylic alcohol of the 1,2-diol moiety might be causing steric crowding during the addition. To test this theory, Ready investigated the use of **2.48** in the nucleophilic addition to aldehyde **2.54**. Deprotonation of the free alcohol of **2.48** with methyl lithium, followed by conversion to the vinyl lithium with *t*-BuLi, generated a nucleophile that was capable of adding to **2.54** to give the benzyl alcohol **2.55** in 80% yield as an inconsequential 1:1 mixture of diastereomers (Scheme 2.7). The tetrahydroxanthone E ring was then cyclized through oxidation of **2.55** followed by immediate treatment with perchloric acid in a *t*-BuOH acetone solvent system to form the acetonide protected **2.56**. The remaining free alcohol of **2.56** was protected as the methoxy methyl (MOM) ether **2.57** in preparation for further elaboration to (–)-kibdelone C.

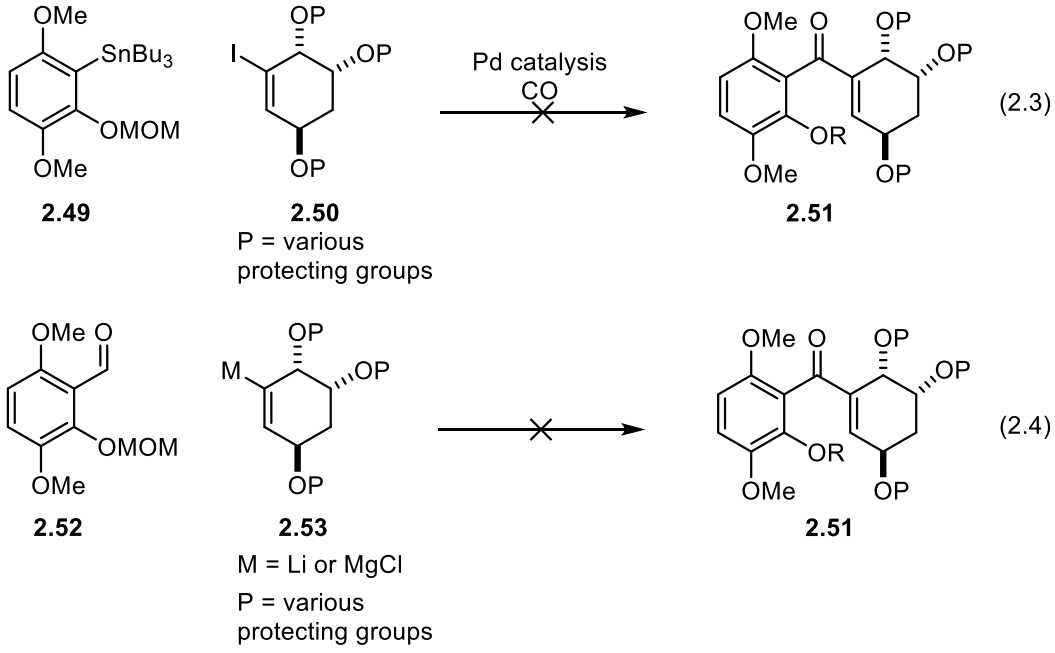

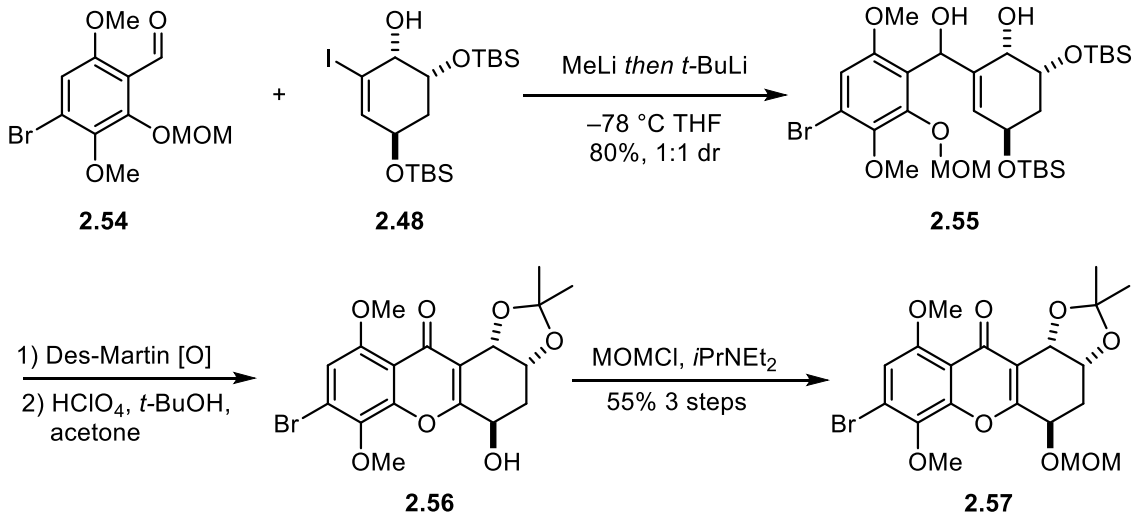

Scheme 2.7 Connection of **2.54** and **2.48** and conversion to **2.57**

2.3 MARTIN GROUP STRATEGY

2.3.1 Introduction and Synthetic Approach

As part of our ongoing interest in polycyclic xanthone natural products such as IB-00208[98,99] and citreamicin η,[100] we planned a synthetic approach to the kibdelone natural products. At the outset of our investigations, it was clear that the F-ring subunits of the kibdelones were not easily accessed, as exemplified by Porco's 13 step sequence to prepare **2.5** (Scheme 2.5). Therefore, we saw ample opportunity to improve upon the previous syntheses of these compounds. We envisaged a strategy that would achieve the two goals of 1) rapidly constructing F-ring subunits that could be applied towards the synthesis of the kibdelone natural products, and 2) demonstrating the synthetic utility of our enantioselective catalytic halolactonization methodology through an application to a synthetic problem. We devised a synthetic plan, where F-ring derivatives such as **2.62** could be accessed in only five steps from 1,4-dihydrobenzoic acid as outlined in Scheme 2.8. We previously demonstrated that we could access the enantiopure lactone **2.59** through

an asymmetric bromolactonization.[15] We planned to install the 1,2-*syn*-diol moiety of the kibdelone F-rings through a dihydroxylation of **2.59**, which we expected to proceed from the least hindered face to give **2.60**. From here, treatment of **2.60** with methanolic base would give access to the enoate **2.61**, which would then only require protecting group installations to complete **2.62**, an F-ring very similar to the one used by Porco. Additionally, it seemed possible that we could elaborate **2.62** further to the halogenated fragments **2.63** and **2.64**, possibly intercepting previously synthesized F-ring fragments.

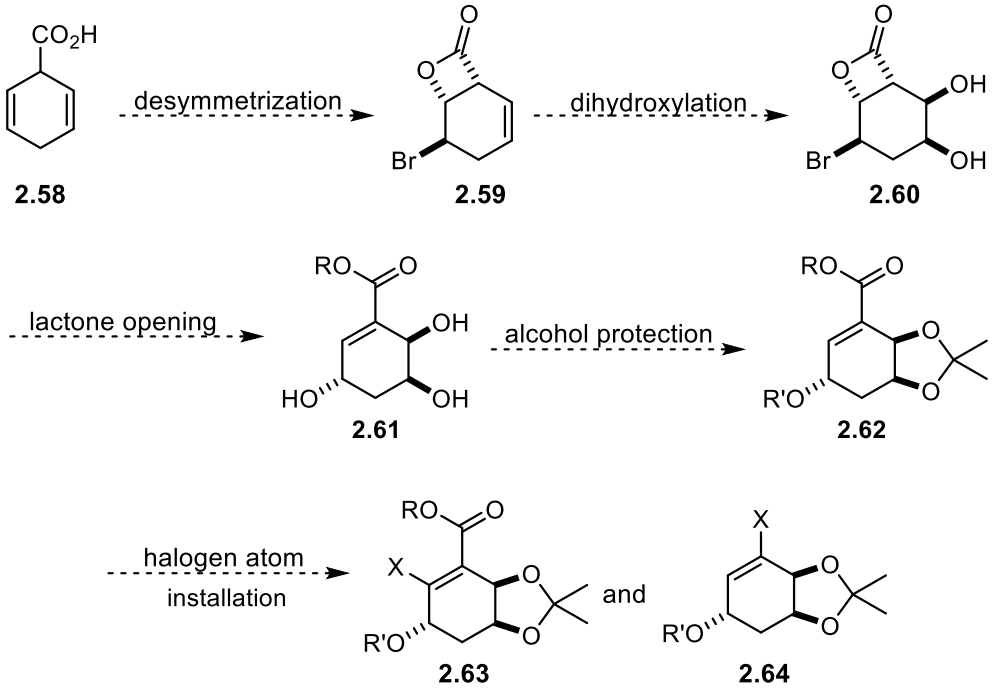

Scheme 2.8 Martin group synthetic plan for preparing kibdelone F-ring fragments.

2.3.2 Strategies for Halogen Atom Installation on Kibdelone F-ring Subunits

2.3.2.1 β-Halogenation

There exists few examples of the direct installation of halogen atoms to the β-position of cyclohexenoates that would allow access to **2.63** from **2.62** in one step, but some limited precedent was available from Nicolaou[101] that suggested the transformation would be possible. The lack of reported methods for this transformation indicated it may be challenging, but this gap in methodology also presented us with an opportunity to develop novel chemistry..

The most relevant example for incorporating a halogen atom at the β-position of intermediate **2.62** in one step came from Nicolaou's syntheses of diversonol and blennolide C (Equation 2.5).[101] The synthesis of these natural products required the preparation of β-brominated cyclohexenoate **2.66**, which was achieved through treatment of **2.65** with bromine followed by triethylamine. While substrate **2.65** is notably different from **2.62** in the hybridization of the γ-position oxygen atom, it provided some evidence that our desired transformation was possible.

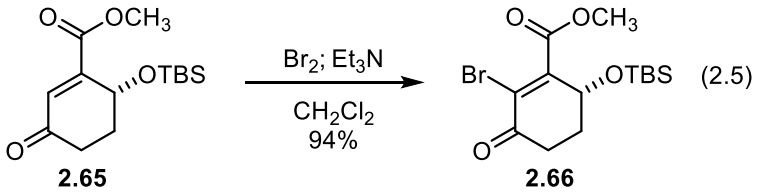

(2.5)

Additionally, we saw an opportunity for the development of novel reaction conditions to achieve this β-halogenation in one step. There were several different speculative strategies that we deemed plausible as outlined in equations 2.6–2.8. Pursuing a strategy similar to that used by Nicolaou, we imagined if halogen addition across the olefin of **2.62** could be achieved through treatment with a dihalogen (X_2), introduction of

a base to the reaction could result in a dehydrohalogenation to form **2.63** (Equation 2.6). Alternatively, if addition of an electrophilic halogen source ("X^+") resulted in formation of a halonium intermediate such as **2.68**, the presence of base in the reaction could result in formation of the desired **2.63** (Equation 2.7). Another possible strategy would be through a nucleophilic addition of I^- to the β-position of the enoate through exposure of **2.62** to trimethyl silyl iodide. This could result in the silylketeneacetal intermediate **2.69**, which could then be oxidized to restore the enoate system (Equation 2.8).

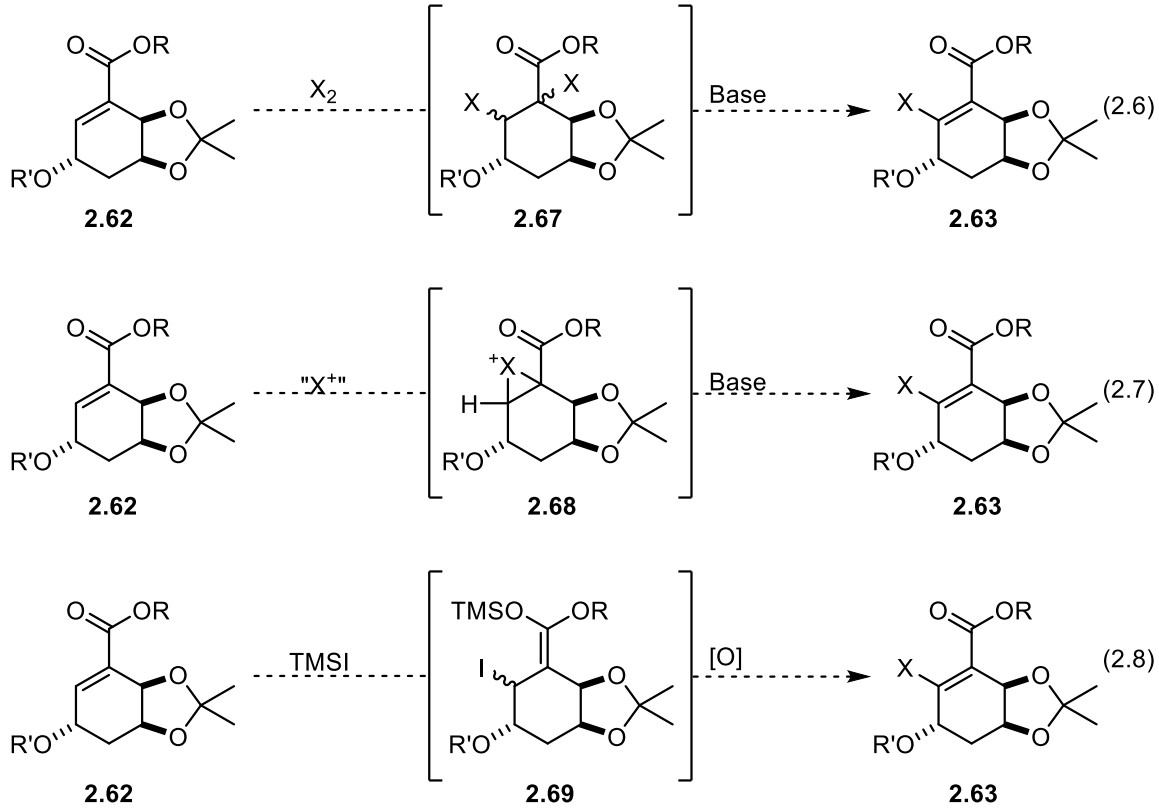

In the event these speculative strategies proved unsuccessful, we had sound precedent for the introduction of a chlorine atom to the β-position of **2.62** from Bartlett's synthesis of (–)-2-chloroshikimic acid.[102] Bartlett installed a vinyl chlorine atom at the β-

position of the structurally related compound **2.70** in four steps, beginning with the conjugate addition of *p*-methoxythiophenol to **2.70** to provide a mixture (7:1) of diastereomers **2.71** and **2.72** in 98% yield (Scheme 2.9). The diastereomeric mixture was treated with sulfuryl chloride and then purified to give **2.73** in 78% yield. Thioether **2.73** was oxidized with *m*-chloroperoxybenzoic acid (*m*-CPBA) to sulfoxide **2.74**, which was thermally eliminated to give **2.75** in 66% yield on a small scale (150 mg), but diminished yields were observed on larger scales (1 g, 32%).[103]

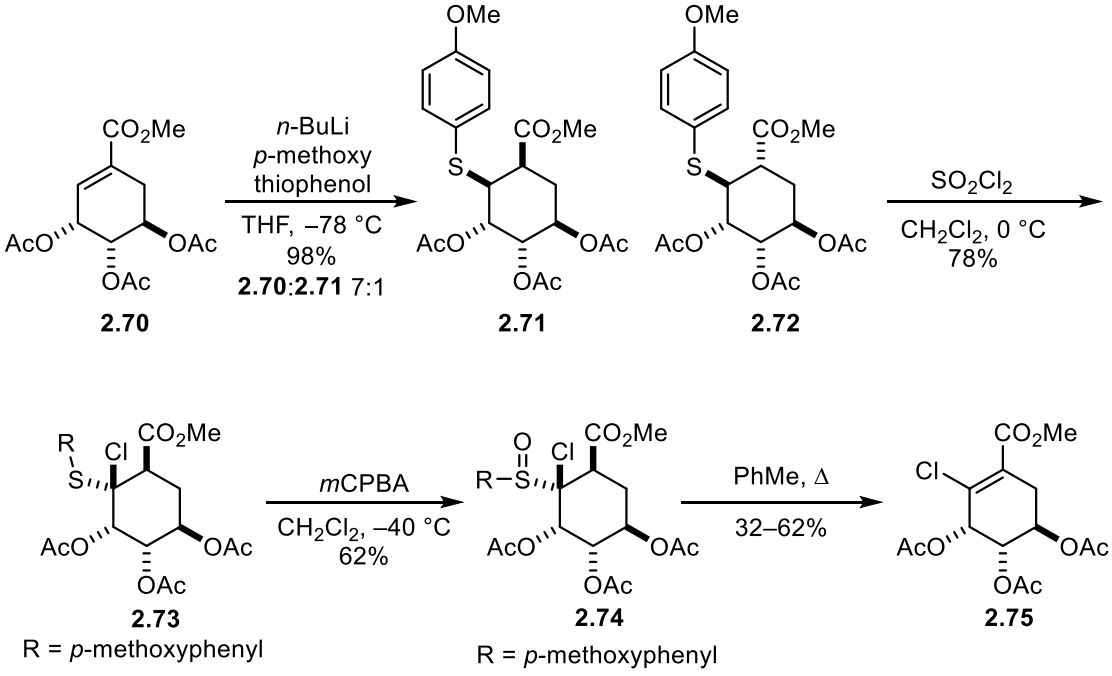

Scheme 2.9 Bartlett's synthesis of β-chlorinated cyclohexenoate **2.75**

2.3.2.2 Hunsdiecker Halodecarboxylation

While the possibility of preparing **2.63** was somewhat speculative, the synthetic path to **2.64** from **2.62** was more apparent. We planned to use a Hunsdiecker

halodecarboxylation reaction to access **2.64**, a compound similar to Ready's F-ring subunit (Equation 2.9).

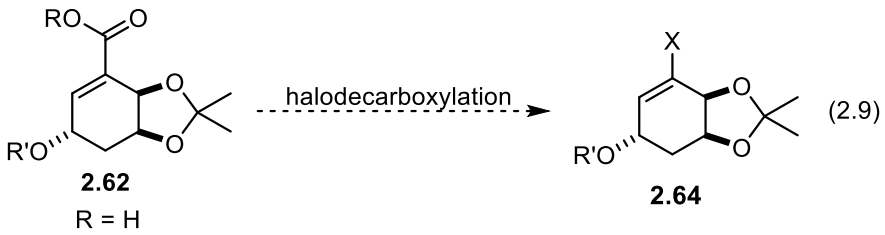

2.62
R = H

2.64

(2.9)

The classic Hunsdiecker reaction involves the preparation of alkyl halides from metal salts of aliphatic carboxylic acids (Equation 2.10).[104] The original methodology was reported using silver carboxylate salts of aliphatic acids, but the reaction has since been shown to work with more stable thallium (I) and mercury (I) salts.[105,106] Treatment of the metal carboxylate salt **2.77** with a dihalogen (X_2) leads to the formation of the unstable acyl hypohalite **2.78**, which undergoes homolytic cleavage of the O-X bond, leading to a radical decarboxylation to produce an alkyl radical. The radical is then trapped by a halogen source to yield an alkyl halide. Halodecarboxylation reactions have a wide substrate scope and generally proceed well for aliphatic primary, secondary, and tertiary carboxylic acids, as well as deactivated aromatic carboxylic acids.[107] While there are numerous examples of halodecarboxylation reactions for cinnamic acids, there have been few successful applications for aliphatic vinylic carboxylic acids. Early reports employing silver salts of small unsaturated aliphatic carboxylic acids showed these substrates typically undergo lactonization or polymerization.[104,108]

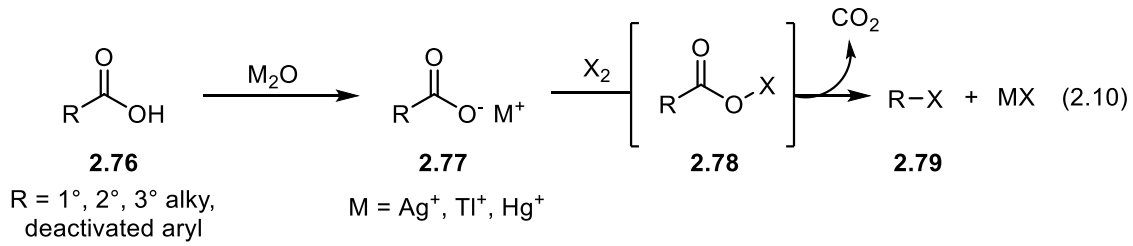

The classic Hunsdiecker reaction is no longer widely used due to the technical difficulties with the preparation and purification of the silver carboxylate salts. The reaction is highly sensitive to trace amounts of water and the silver carboxylate salts are often difficult to dry due to thermal instability.[106,109] There has been a number of improvements to the Hunsdiecker reaction that have led to increased yields and simplified procedures, including the Cristol–Firth,[106] Kochi,[110] and Suárez[111] modifications (Figure 2.3).

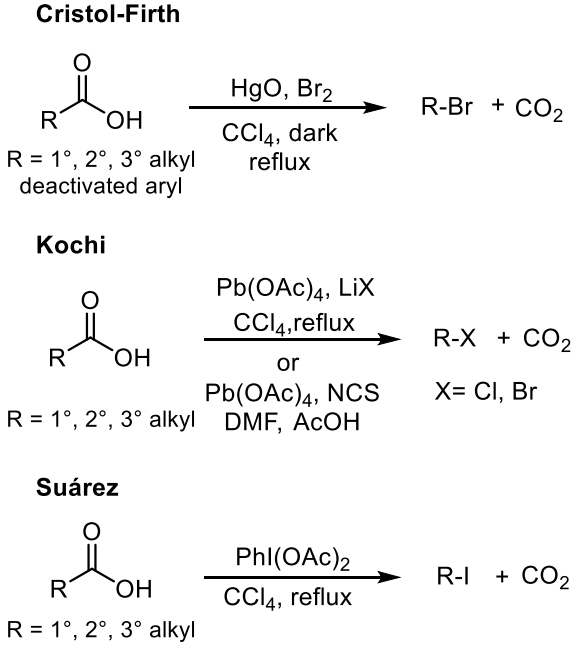

Figure 2.3 Summary of modifications to the Hunsdiecker halodecarboxylation

The Barton–Hunsdiecker reaction has become one of the most commonly used modifications due to its wide functional group tolerance. The Barton modification utilizes

the thermal or photolytic decomposition of thiohydroxamate esters **2.81** to generate carbon radicals that can be trapped by a halogen source to give an alkyl halide (Scheme 2.10).[107] The thiohydroxamate esters are typically prepared by the reaction of acyl chlorides with **2.80** or through a carbodiimide coupling with **2.80**. The Barton–Hunsdiecker method tolerates a wide variety of functional groups due to the mild reaction conditions used to generate the carboxyl radical.

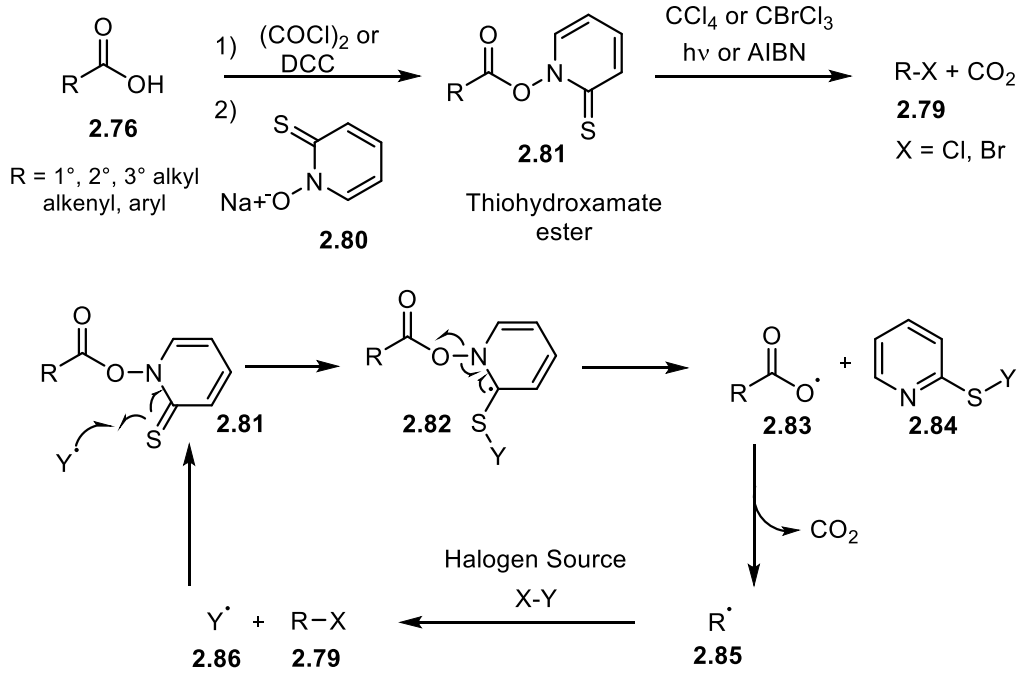

Scheme 2.10. General Barton–Hunsdiecker reaction and mechanism of radical decarboxylation.

Recently Streicher successfully demonstrated an application of the Barton–Hunsdiecker reaction on a cyclohexenoic acid as part of an effort to synthesize shikimic acid derivatives.[112] Streicher initially explored the halodecarboxylation of **2.87** as a model system, and he found that the use of 2,2,2-trifluoroethyl iodide (CF_3CH_2I) gave the best yields of **2.89** (Equation 2.11). Streicher screened a small variety of other halogenating

reagents including CCl_4, CBr_4, and 1,2-diiodoethane, but the yields were generally poor compared to CF_3CH_2I, affording **2.89a–c** in 5–36% yield. In the simple model system, **2.87** was converted to **2.89** in 64% yield, but the method was less successful on more complex substrates such as **2.90**, which was converted to **2.91** in only 39% yield (Equation 2.12).

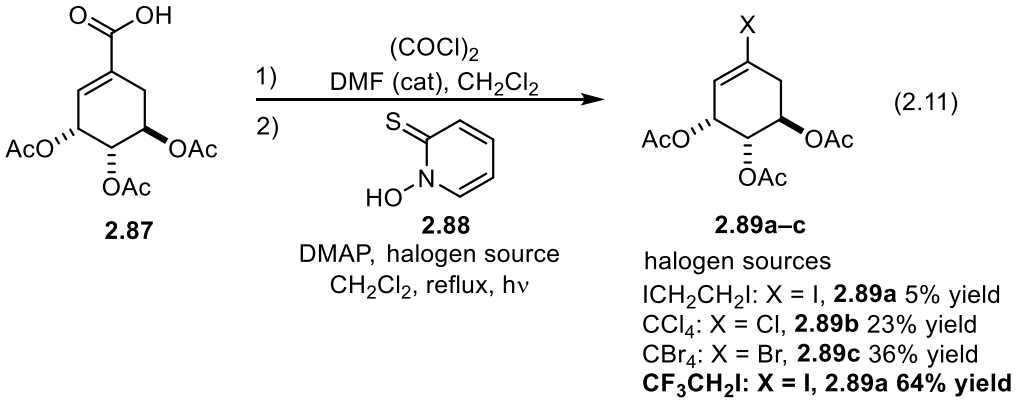

(2.11)

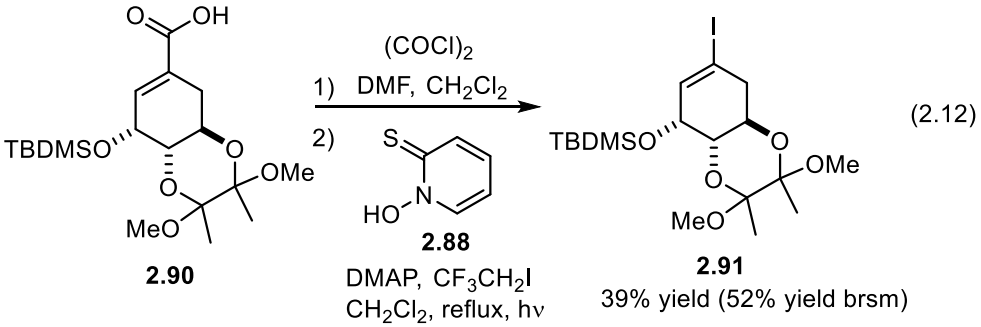

(2.12)

2.4 MARTIN GROUP SYNTHESIS OF F-RING SUBUNITS

Before we could begin our syntheses of enantiopure F-ring fragments of the kibdelone natural products, there were several key questions about the desymmetrization of 1,4-dihydrobenzoic acid that needed to be addressed. We had previously shown that this desymmetrization could be carried out on small scale (0.1 mmol), at dilute reaction concentration (0.01 M), with 2,4,4,6-tetrabromo-2,5-cyclohexadienone (TBCO) as the brominating reagent; under these conditions extended reaction times (4 d) were required (Equation 2.13).

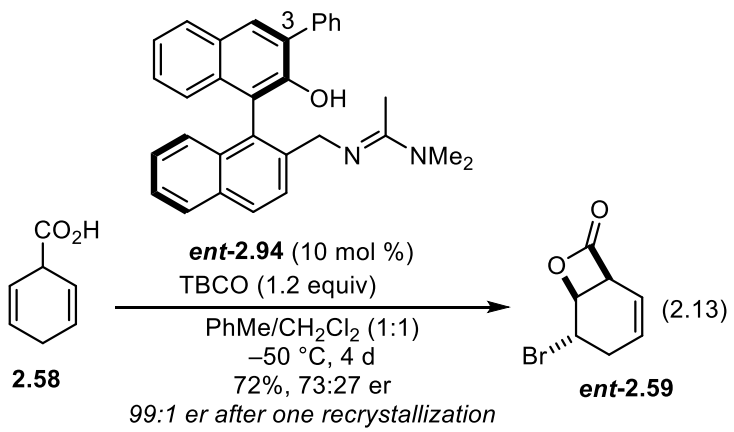

In order for us to use enantiopure **2.59** as a starting material in a multi-step synthesis, optimization of these reaction conditions was necessary. Specifically, it was imperative that we demonstrate the reaction could be carried out on increased scale to produce synthetically useful quantities of **2.59**. Additionally, we had only investigated the desymmetrization of **2.58** using the 3-substituted-phenyl catalyst ***ent*-2.94**. Previous catalyst modification studies revealed that the 3-unsubstituted catalyst ***ent*-2.93** effected enantioselective halolactonizations olefinic acids with similar selectivities as its phenyl substituted counterpart ***ent*-2.94**. From a practical standpoint, **2.93** was a more attractive

catalyst for our method simply because it easier to prepare, requiring only five synthetic operations while **2.94** requires eight. Analysis of the stereochemistry of the F-ring of (+)–kibdelone C revealed that we would need to promote the desymmetrization of **2.58** using the *S*-enantiomer of the BINOL-amidine catalysts. Accordingly, we prepared multigram quantities of catalysts **2.93** and **2.94** starting from enantiopure *S*-BINOL (**2.92**) using the previously established procedures from our lab (Equation 2.14).[15]

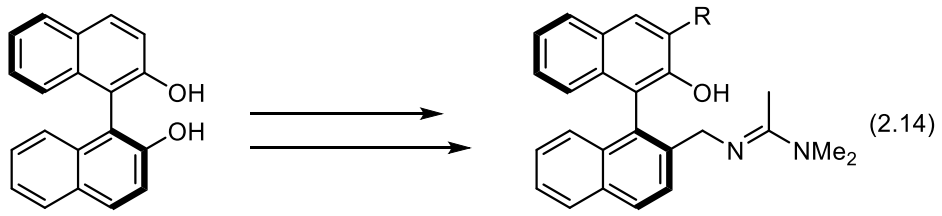

(2.14)

2.92

2.93 R = H, 5 steps
2.94 R = Ph, 8 steps

With catalysts **2.93** and **2.94** in hand, our desymmetrization optimization studies commenced with the Birch reduction of benzoic acid. In the event, treatment of benzoic acid with sodium (3.5 equiv) in liquid ammonia according to a previously established procedure, resulted in only moderate yields of **2.58**,[113] with significant amounts of unreacted benzoic acid (**2.95**) recovered. Fortunately, this problem was easily solved by increasing the amount of sodium (6 equiv) used in the reaction, and 1,4-dihydrobenzoic acid (**2.58)** was obtained in 85% yield without any need for purification (90–95% pure by ^{1}H NMR) (Equation 2.15).

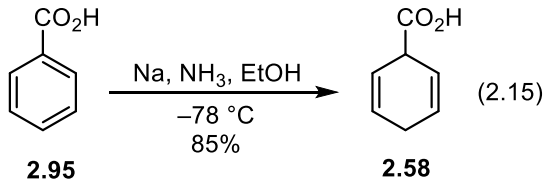

(2.15)

2.95 **2.58**

With an effective protocol for preparing multigram quantities of **2.58** established, we began by simply repeating the previously reported results using catalyst **2.94**. Under the same reaction conditions as before, it was immediately discovered that the reaction did not require four days, instead it went to completion after only 14 hours. Fortunately, the same enantiomeric ratio of 73:27 er was observed, and the enantioenrichment could indeed be increased after recrystallization to a single enantiomer (Equation 2.16).

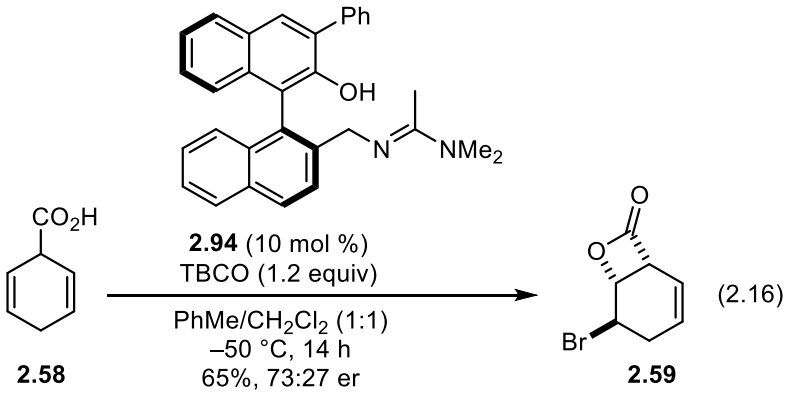

(2.16)

We next compared the ability of catalysts **2.93** and **2.94** to promote the bromolactonization of **2.58** to ascertain if the phenyl group of **2.94** was truly necessary. Additionally, we used the opportunity to probe the effects of the brominating reagent used. Previous studies indicated that the selectivity of the catalysts was independent of halogenating reagent, but to confirm this, we evaluated TBCO and *N*-bromosuccinimide (NBS) in this reaction. The ability to use a more common brominating reagent such as NBS would again improve the value of our method from a practical point of view. While TBCO is commerically available or easily prepared from tribromophenol, NBS is a more common, less specialized reagent. Comparison of catalysts **2.93** and **2.94** in this reaction with 5–15 mol% catalyst loadings revealed that **2.94** universally performed better, with 73:27 er as the best selectivity obtained (Table 2.1). Catalyst **2.94** delivered a consistent 73:27

enantiomeric ratio at 10 mol % catalyst loadings, regardless of which brominating reagent was used (Table 2.1, Entries 4 and 8). The nor-phenyl catalyst **2.93** delivered lactone **2.59** with diminished selectivities, ranging from 60:40 to 67:33, regardless of brominating reagent used (Table 2.1, Entries 1,3,5,7). Reduced selectivities were observed for both catalysts when only 5 mol % loadings were used, presumably due to increased background reaction, but the yields remained consistent throughout the reactions (63–73%) (Table 2.1 Entries 1,2,5,6). Additionally, increasing the catalyst loading to 15 mol % showed no benefit for catalyst **2.94** (Table 2.1 Entry 10) however it did lead to increased selectivity in one instance for **2.93** (Table 2.1 Entry 9). Unfortunately, however, this increased selectivity was not consistent, and we experienced reproducibility issues in general with catalyst **2.93** in this reaction. Therefore, we proceeded with catalyst **2.94** and NBS as the brominating reagent for future experiments.

Table 2.1 Evaluation of catalysts **2.93** and **2.94** for the desymmetrization of **2.58**

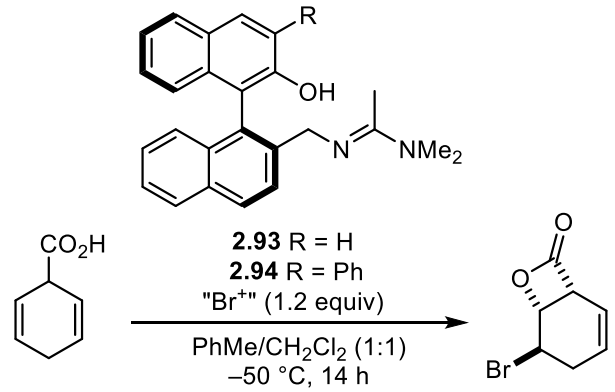

Entry	"Br$^+$"	Catalyst	Mol %	Yield %[a]	er[a]
1	TBCO	**2.93**	5	63	60:40
2	TBCO	**2.94**	5	62	68:32
3[a]	TBCO	**2.93**	10	65	64:36
4[a]	TBCO	**2.94**	10	70	73:27
5	NBS	**2.93**	5	68	60:40
6	NBS	**2.94**	5	62	67:33
7	NBS	**2.93**	10	72	63:37
8	NBS	**2.94**	10	73	73:27
9	NBS	**2.93**	15	68	74:26
10	NBS	**2.94**	15	72	73:27

[a]Determined by chiral HPLC using chiracel OD-H, 1% *i*-PrOH/hexanes, 1 mL/min.

We next probed the tolerance of the reaction to increased reaction concentrations. Gratifyingly, we quickly discovered that increasing the reaction to 0.05 M or 0.1 M concentrations on a small scale (0.1 mmol) had no impact on the selectivity, and **2.59** was still obtained with 73:27 er (Equation 2.17). In retrospect, it would have been interesting to further explore the limits of the reaction concentration, but at the time, 0.1 M concentration was deemed suitable for our needs and we moved onto other, more pressing questions about the synthesis.

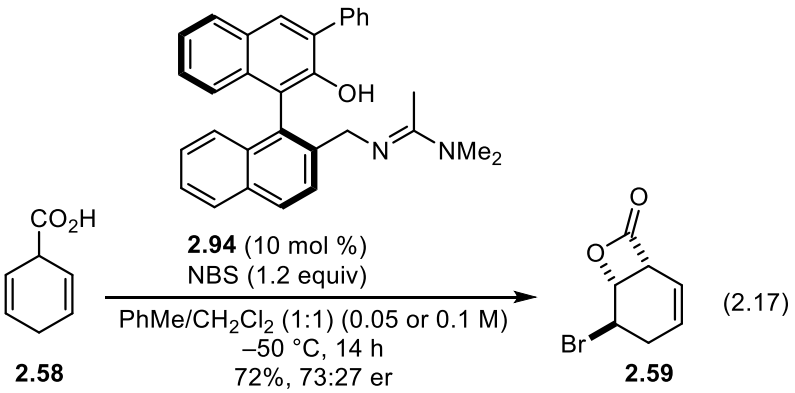

(2.17)

Confident that our desymmetrization methodology would be scalable to synthetically useful quantities to prepare enantiopure F-ring fragments, we investigated the remaining steps of the synthesis using the racemate of **2.59**. The next challenge in the synthesis was the conversion of bromolactone **2.59** to the diol **2.60**. Identifying suitable conditions for the dihydroxylation of **2.59** proved to be non-trivial (Table 2.2). Standard dihydroxylation conditions[114] (Table 2.2 Entry 1) proved to be too basic, and decomposition of the starting material was observed. It was clear that this reaction should proceed via a substrate controlled osmylation to the least hindered convex face of **2.59**, ultimately favoring the desired product. Therefore, it seemed that the reaction should not require chiral ligands and we investigated reaction conditions with simple additives.

Switching to quinuclidine as a ligand and including a phosphate buffer to mitigate the basicity of the reaction conditions gave some of the desired product **2.60**, but it was recovered in low yield (22%) and with low diastereoselectivity (1:1 dr) (Table 2.2 Entry 2). Upjohn dihydroxylation conditions[114] also provided some success, but again low yields due to significant formation of unidentified by-products and poor diastereoselectivity (4:1 dr) were problematic (Table 2.2 Entry 3). Decreasing the reaction temperature to 0 °C with an increased reaction time showed no improvement (Table 2.2 Entry 4). Success was ultimately found through the use of citric acid as an additive, according to modified dihydroxylation conditions for electron deficient olefins reported by Sharpless.[115] At room temperature, the reaction still gave poor yields and dr of **2.60**, but significant unreacted starting material was still observed after three hours, with little to no by-products observed. Further optimization of the reaction conditions through decreased temperature delivered the desired diol **2.60** in 60% yield and >20:1 dr. It is worth mentioning that this reaction does require relatively high osmium catalyst loadings (10 mol %) to maintain the diastereoselectivity. Reactions with decreased catalyst loadings (1–5 mol %) lead to decreased diastereoselectivity. Also worthy of note is that the purification of **2.60** by standard chromatography was initially problematic due to its high polarity. Fortunately, we discovered that the crude material could be purified simply through recrystallization in ethanol, eliminating the need for chromatographic purification.

Table 2.2 Dihydroxylation of **2.59**

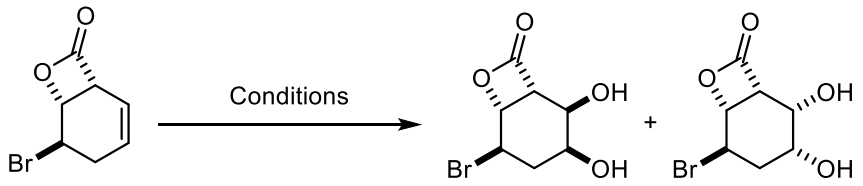

2.59 **2.60** **2.95**

Entry	Reagents	Solvents	Time (h)	T (°C)	Yield (%)	dr[a] **2.60**:**2.95**
1	$(DHQD)_2Pyr$, $K_3Fe(CN)_6$, K_2CO_3, $K_2OsO_4•H_2O$, $MeSO_2NH_2$	*t*-BuOH:H_2O (1:1)	3	rt	NA	NA
2	$K_2OsO_4•H_2O$ $K_3Fe(CN)_6$ $K_2S_2O_8$ quinuclidine Na_2HPO_4 $MeSO_2NH_2$	*t*-BuOH:H_2O (1:1)	3	rt	22	1:1
3	$K_2OsO_4•H_2O$, NMO	acetone:H_2O (1:1)	3	rt	31	4:1
4	$K_2OsO_4•H_2O$ NMO	acetone:H_2O (1:1)	16	0	35	4:1
5	$K_2OsO_4•H_2O$ NMO Citric acid	*t*-BuOH:H_2O (1:1)	4	rt	34	3:1
6	$K_2OsO_4•H_2O$ NMO Citric acid	*t*-BuOH:H_2O (1:1)	18	0	61	>20:1

[a]Ratio determined by ^1H NMR of the crude reaction material.

Fortunately, the next two synthetic steps proceeded with little trouble. When **2.61** was treated with potassium carbonate in methanol, a multi-step cascade commenced,

beginning with the opening of the lactone to form **2.96**, followed by β-elimination of the newly formed epoxide to give the desired triol **2.97** (Equation 2.18). Initial experiments at low temperature (0 °C) delivered mixtures of the epoxide **2.96** and the desired enoate **2.97**. However, warming the reaction to room temperature gave clean conversion of **2.61** to **2.97** with only unreacted potassium carbonate as the by-product.

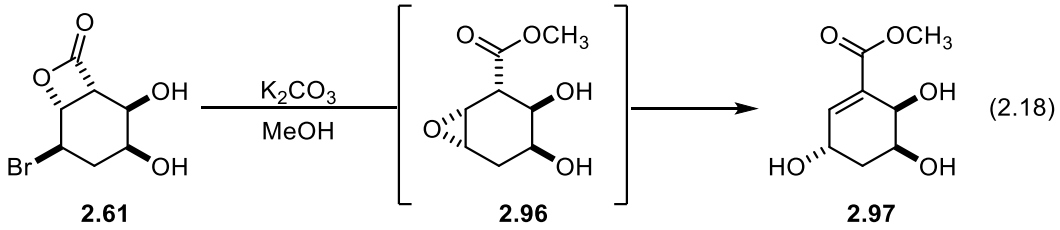

2.61 **2.96** **2.97** (2.18)

Initial efforts to protect the 1,2-diol moiety of **2.97** as an acetonide were low yielding under standard acetonide formation conditions,[93] and **2.98** was obtained in only 32% yield (Equation 2.19). This problem was attributed to the excess potassium carbonate that was being carried into the reaction with crude **2.97**, which upon reaction with camphorsulfonic acid, produced water which inhibited the formation of the desired acetonide. Fortunately, the addition of 4 Å molecular sieves to the reaction led to a significant improvement in yield (75%) (Equation 2.20). With the successful preparation of **2.98**, we had achieved an efficient synthesis to a viable kibdelone F-ring precursor in only five steps from benzoic acid. Notably, the formation of acetonide **2.98** was the first step of the synthesis that required purification by column chromatography. All of the previous reactions were purified by recrystallization, or the crude material was sufficiently pure to carry on to the next step.

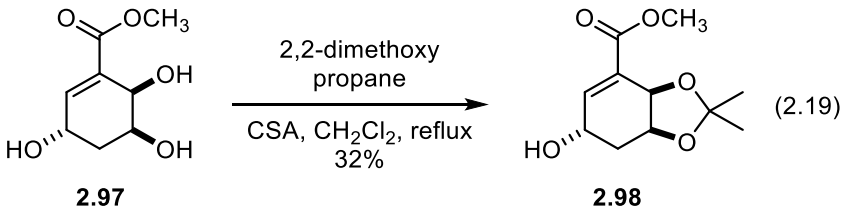

2.97 **2.98** (2.19)

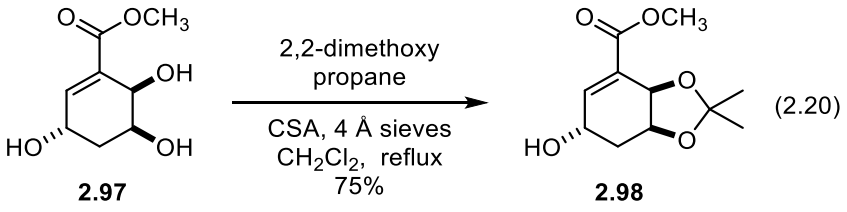

2.97 **2.98** (2.20)

To further demonstrate the utility of this method, we sought to prepare F-ring fragments similar to those used by Porco and Ready in their respective syntheses of kibdelone C. We first investigated the installation of a halogen atom at the β-position of enoate **2.98**. Before proceeding however, we thought it prudent to protect the remaining free hydroxyl group of **2.98** to mitigate the possibility of detrimental side reactions. We planned to install a methoxymethyl ether (MOM) protecting group because it would allow for a global hydroxyl deprotection in the event that the protecting groups needed to be removed. Additionally, we sought to install a *tert*-butyldimethylsilyl ether (TBS) so that if needed, we would have a modular system where one protecting group could be selectively removed. The MOM protection of **2.98** proceeded with little trouble, and treatment of **2.98** with MOMCl gave the desired product **2.99** in 95% yield.

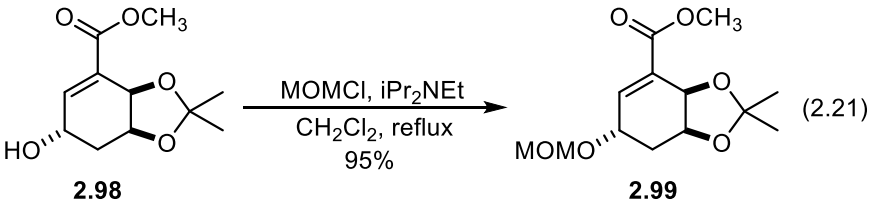

2.98 **2.99** (2.21)

Installing the TBS protecting group, however proved to be more challenging. Initial experiments using TBSCl as the silylating reagent gave **2.100** in only 50% yield with

significant amounts of unreacted starting material being recovered, even after reaction times of 24 hours. This yield was improved by switching to the more reactive TBSOTf reagent, and **2.100** was isolated in 89% yield.

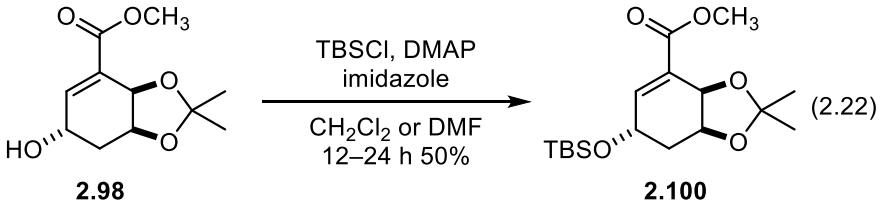

2.98 **2.100** (2.22)

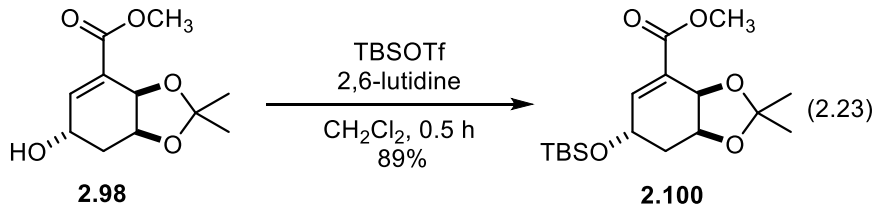

2.98 **2.100** (2.23)

With protecting groups in place, we turned our focus towards the β-halogenation **2.99** and **2.100**. Unfortunately, all of our efforts to achieve this transformation in a single step were unsuccessful (Table 2.3). Attempts to mimic the reaction conditions similar to those Nicolaou used through exposure of **2.99** or **2.100** to Br_2 followed by treatment with triethylamine were unsuccessful and resulted in decomposition of the starting materials (Table 2.3, Entry 1). We suspected that the reaction of **2.99** or **2.100** with bromine led to the removal of the alcohol protecting groups, which could result in further detrimental side reactions, but none of the by-products could be identified. We next investigated electrophilic halogenating reagents, specifically NBS, NIS, and Barluenga's reagent $I(coll)_2PF_6$. These reagents seemed promising in that they could provide an electrophilic halogen atom that would also produce an equivalent of base (succinate or collidine). Unfortunately, we observed no product formation with these reagents and only recovered unreacted starting material (Table 2.3, Entries 2–4), although we did not screen an

extensive number of more forcing conditions. Finally, we attempted a nucleophilic conjugate addition of iodine to the enoate moiety through reaction of **2.99** or **2.100** with TMSI, followed by addition of IBX (Table 2.3, Entry 5). Unfortunately, this reaction was also unsuccessful, and we only observed decomposition of the starting material. We suspect that protecting group stability was issue for these reaction conditions as well. The coordination of TMS to one of the acetal oxygen atoms could result in the removal of the protecting group, and then IBX would be able to oxidize any of the free alcohols.

Table 2.3. Conditions screened to prepare **2.101**

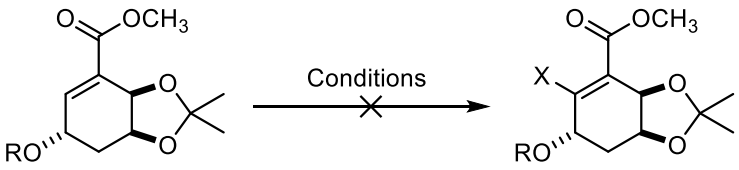

2.99 R = MOM
2.100 R = TBS

2.101
R = MOM or TBS
X = Br or I

Entry	Reagents	Solvent	T (0 °C)	Time	Result[a]
1	Br_2; then Et_3N	CH_2Cl_2	0	15 min	Decomp
2	NBS	THF or CH_2Cl_2	0 to reflux	12 h	NR
3	NIS	THF or CH_2Cl_2	0 to reflux	12 h	NR
4	$I(coll)_2PF_6$	THF	reflux	3 h	NR
5	TMSI; then IBX	CH_2Cl_2	–78 to rt	4 h	Decomp

[a]Decomp = intractable mixtures of products. NR = no reaction

It became apparent that the β-halogenation of **2.99** or **2.100** in one step would be a significant challenge, so we turned our attention to the preparation of a chlorinated analogue through the methods previously established by Bartlett. In the event, the conjugate addition of lithium *p*-methoxythiophenolate to **2.99** proceeded in high yield (89%) to give **2.101** as a single diastereomer (Scheme 2.11). The diastereoselectivity of this reaction can be rationalized through the mechanism depicted in scheme 2.11. The lithium thiophenolate adds to the bottom face of the preferred half chair conformer **2.103**. The resulting ester enolate **2.104** would then be protonated from the convex face, resulting in **2.102**. Analysis of the ^{1}H NMR spectrum of **2.102** reveals the C1 and C2 protons both

possess two coupling constants of 4.5 and 3 Hz respectively, suggesting that the thioether and methyl ester moieties adopt a diaxial configuration with each of the C1 and C2 protons being equatorial.

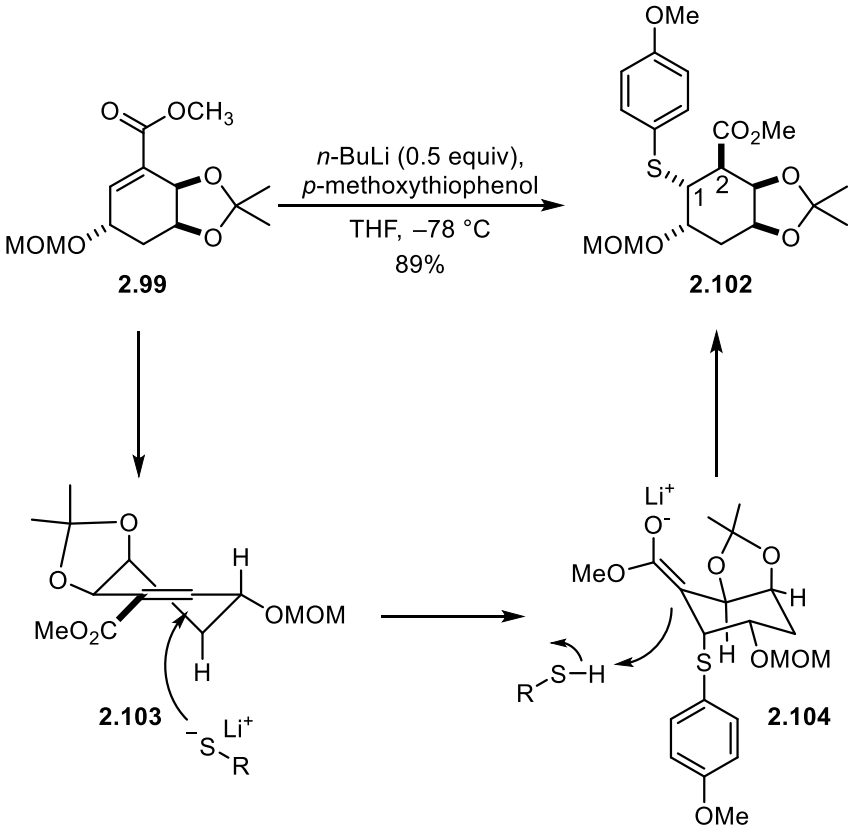

Scheme 2.11. Conjugate addition of *p*-methoxythiophenolate to **2.99** and mechanistic rationale for stereochemical outcome.

Unfortunately, however, we were unable to achieve the Pummerer type chlorination of **2.102**. Treatment of **2.102** with sulfuryl chloride provided no evidence of productformation; only decomposition of the starting material was observed. We speculated that the protecting groups were again not stable to these reaction conditions, and we briefly attempted to achieve the chlorination using NCS, but to no avail (Equation 2.24).

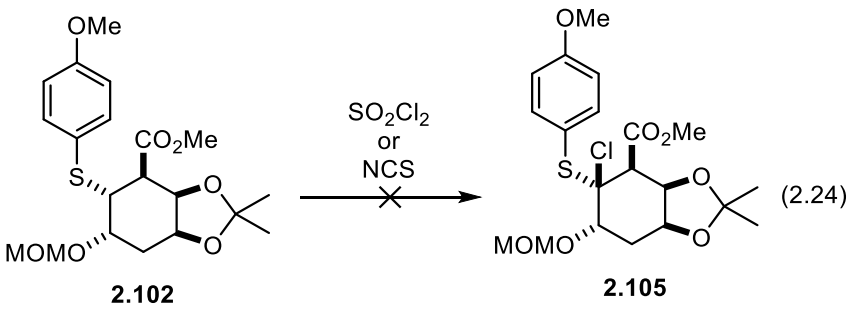

It was clear that the preparation of a chloro analogue of **2.5** was going to be non-trivial and we ultimately decided to abandon our pursuit of intercepting Porco's fragment, becausethe β-halogen of the enoate is not required for **2.98** to be used in a synthesis of a kibdelone natural product. Instead, we transitioned to preparing a vinyl halogenated fragment similar to the one used by Ready.

Our elaboration of **2.99** to **2.110** commenced with the soaponification of methyl esters **2.96–2.98**. This proved to be a surprisingly difficult transformation, due to protecting group instability and problems with epimerization. Initial experiments examining the conversion of the unprotected alcohol **2.96** to **2.104** with either sodium or lithium hydroxide in organic/aqueous solvent combinations resulted in diastereomeric mixtures that were the result of base promoted epimerization at the C6 stereocenter. Similarly, attempts to convert the protected alcohols **2.97** or **2.98** to the corresponding carboxylic acid under these conditions were also plagued by epimerization issues. In the case of **2.98**, the TBS protecting group proved to be unstable and was removed during the soaponification. Cooling the reactions to 0 °C provided no improvement, and still diastereomeric mixtures of carboxylic acid products were observed.

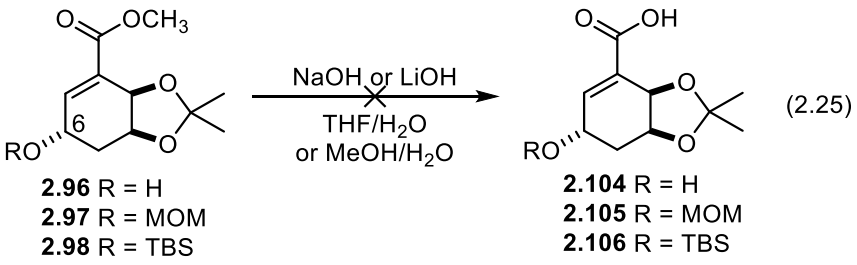

(2.25)

Due to the instability of the TBS silyl ether and the likelihood that the alcohol would need a protecting group for the remaining steps, only the soaponification of the MOM protected alcohol **2.97** was investigated in future experiments. Switching to more mild conditions through treatment with potassium trimethylsilanolate, still resulted in significant epimerization of the C6 center. After screening a variety of conditions, we serendipitously discovered that soaponification of **2.97** with LiOH (1 M aqeous, 2 equiv) in CH_3CN as the primary solvent, cleanly gave **2.105** as a single diastereomer in 87% yield.

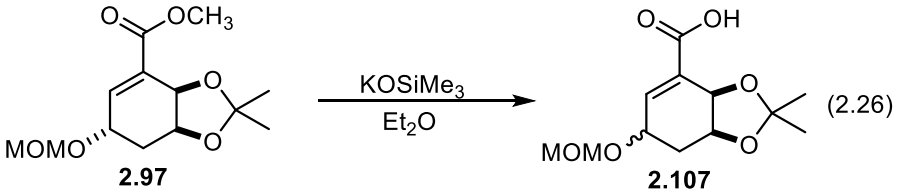

(2.26)

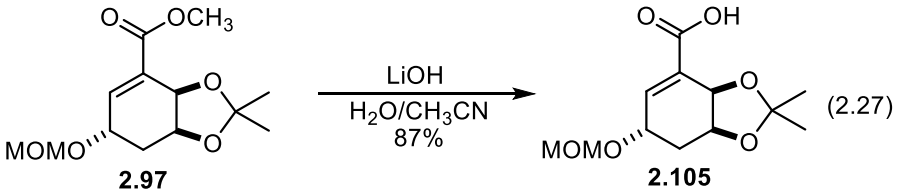

(2.27)

With this fortuitous finding and a route to **2.105** established, we next investigated the key Barton–Hunsdiecker halodecarboxylation reaction. Following the precedent from Streicher, we initially targeted the iodo derivative **2.109,** which we would obtain using trifluoroiodoethane as the halogen source during the irradiation of **2.108**. In an effort to keep the synthesis of **2.109** to as few steps as possible, we initially targeted a three step

one-pot procedure involving: 1) conversion of **2.105** to an acyl chloride; 2) formation of **2.108**; and 3) halodecarboxylation (Equation 2.28). Toward this end, we first investigated each one of these steps individually.

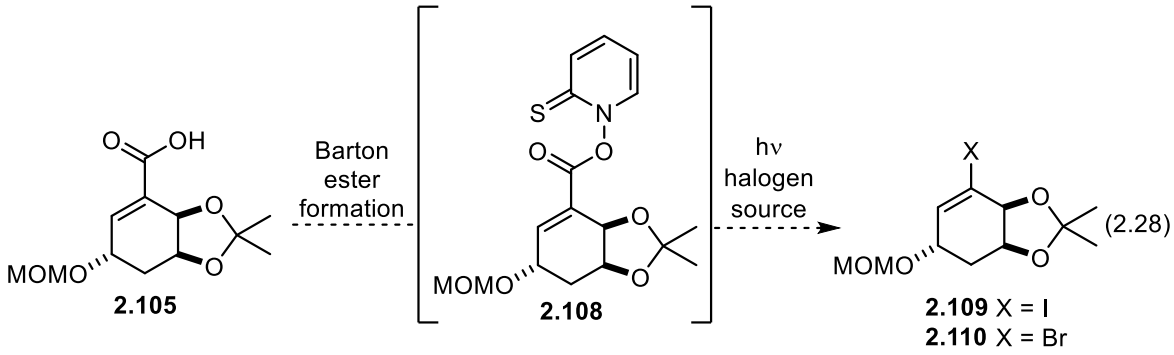

Unfortunately, we discovered that conversion of **2.105** to acyl chloride **2.111** was problematic. Initial attempts to treat **2.105** with oxalyl chloride did not provide clean conversion to **2.111**, and the product was accompanied with various unidentified by-products (Equation 2.29). We speculated that the HCl generated during the reaction was interacting with the acid sensitive protecting groups, leading to deleterious side reactions. To mitigate this problem, the lithium salt of **2.105**, generated from deprotonation with methyllithium, was treated with oxalyl chloride, but the acyl chloride **2.111** was still only obtained in ca. 80% purity by ^{1}H NMR analysis of the crude material (Scheme 2.12). Nevertheless, we carried this material forward in the formation of **2.108**, which was then immediately irradiated with a 150 W electric flood lamp in the presence of CF_3CH_2I to deliver **2.109** in 22% yield.

.

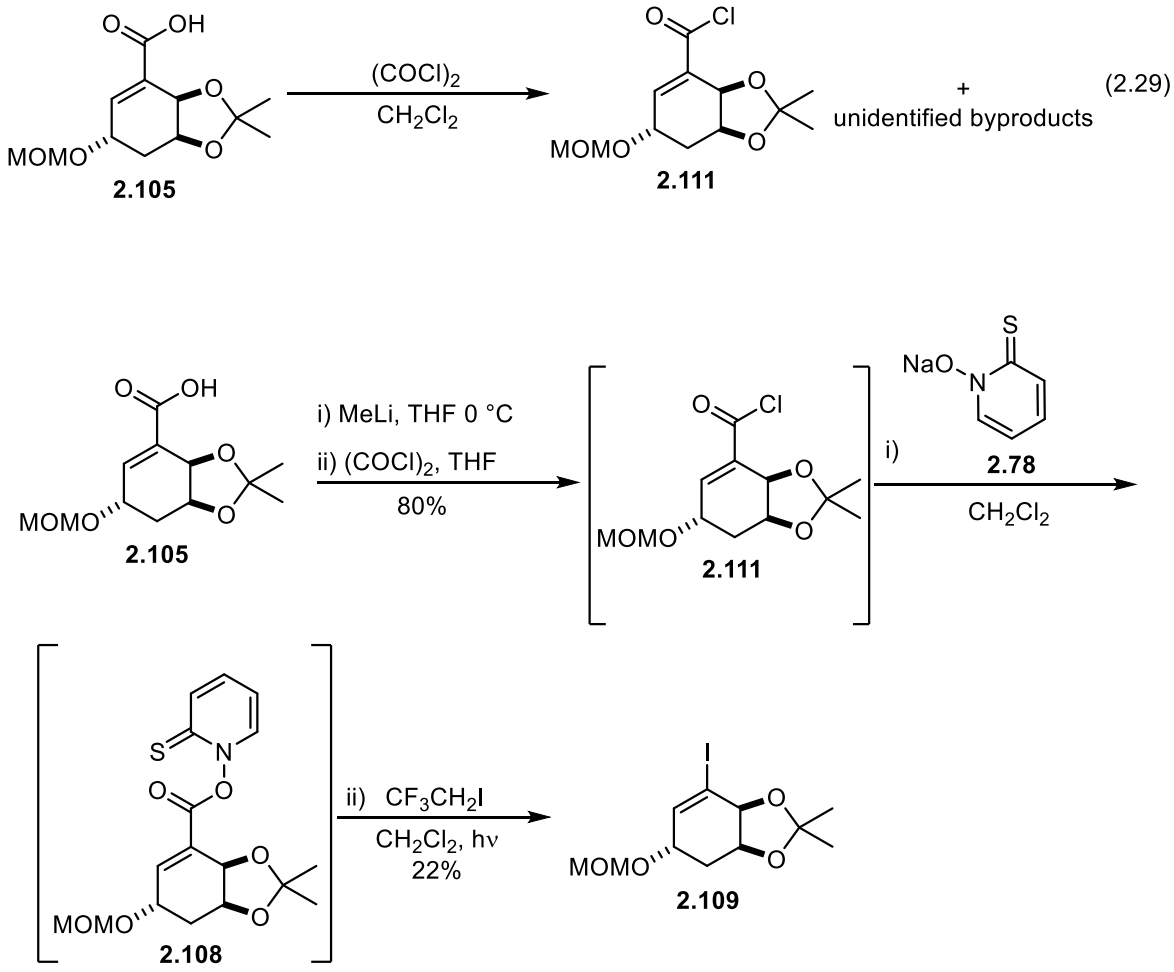

Scheme 2.12. Halodecarboxylation of **2.105** via formation of **2.108**

We were delighted to discover that the halodecarboxylation of **2.105** was possible, despite the poor yield, which we attributed to poor conversion of **2.111** to **2.108**. Accordingly, we set to the task of optimizing this transformation. Fortunately, we found that an EDCI mediated coupling between **2.105** and **2.78** cleanly gave **2.108** in 85% yield, and the by-products from the reaction could be removed through an aqueous work up (Equation 2.30).

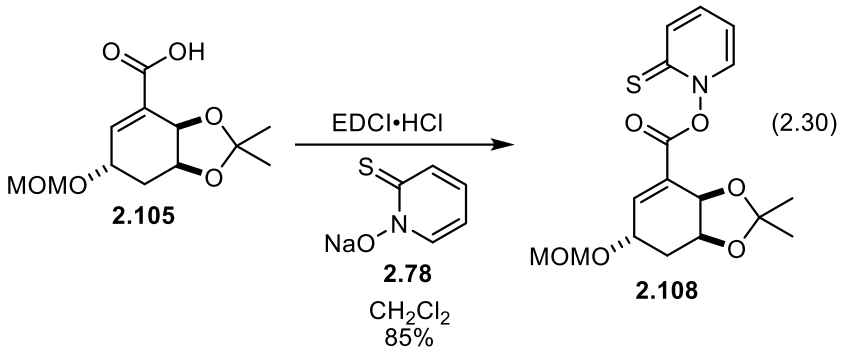

Unfortunately, even with efficient conversion of **2.105** to **2.108**, the yield of the halodecarboxylation was still low, only providing **2.109** in a slightly improved yield of 34%, with the only major identifiable by-product **2.112** being isolated in 15% yield (Equation 2.31).

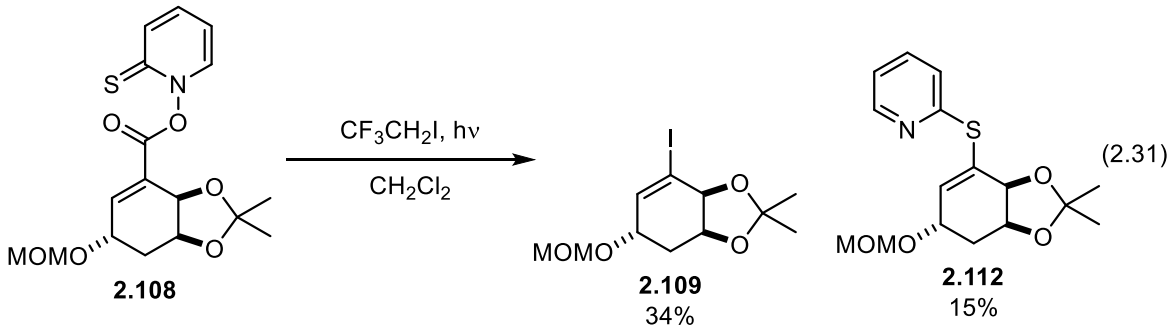

The undesired by-product **2.112** was presumably the result of a radical propagation between the vinyl radical of **2.108** and another equivalent of **2.108**. We speculated that this side reaction could be suppressed by increasing the concentration of CF_3CH_2I, and we attempted the halodecarboxylation using this reagent as the solvent for the reaction. Unfortunately, this led to no improvement in yield, and **2.109** was isolated in 30% yield (Equation 2.32).

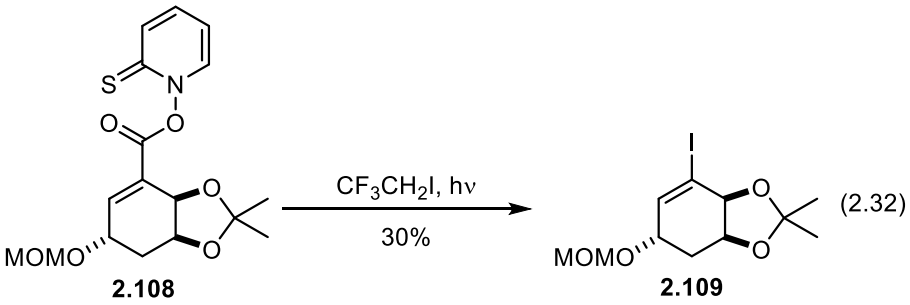

We next sought to make more drastic changes to reaction conditions through screening additional solvents and halogen sources. Unfortunately, despite screening a variety of halogen sources in CH_2Cl_2 or benzene, CF_3CH_2I still provided the best yield, with other reagents only giving minor amounts of product (10–25%) (Equation 2.33). Furthermore, attempts to drive **2.108** to radically decarboxylate under thermal conditions in the presence of AIBN also provided low yields of **2.109** or no product formation at all.

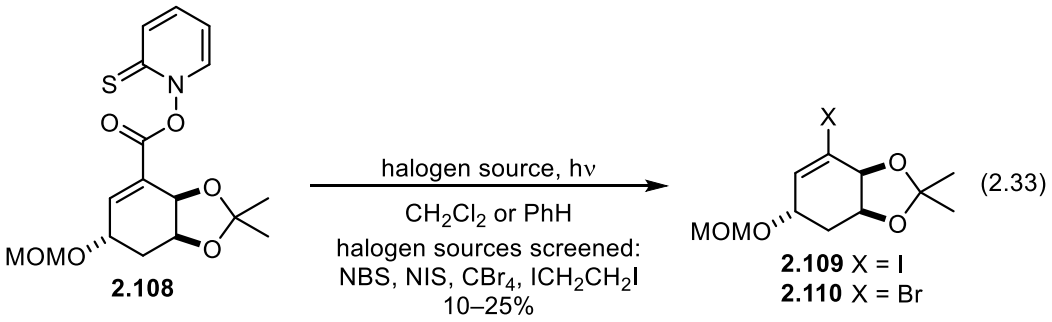

Returning to reports from the original Baron literature revealed the use of Cl_3CBr as a common solvent and bromine source for these radical brominations.[107] Feeling like we had exhausted most other options, we attempted the conversion of **2.108** using this reagent as solvent. To our delight, we found that **2.108** was converted to **2.110** in 65% yield when Cl_3CBr was used as solvent in this reaction (Equation 2.34). We found that the 65% yield was consistent and reproducible for the conversion of **2.108** to **2.110**, but we were unable to improve this yield further.

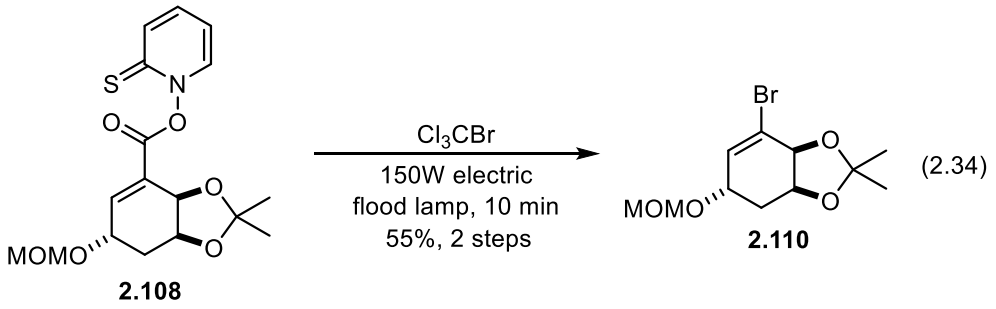

(2.34)

2.5 SUMMARY OF MARTIN GROUP F-RING SYNTHESES

A summary of the optimized transformations leading to the kibdelone fragments **2.98** and **2.110** is provided in scheme 2.13.[95] We have shown that desymmetrization of 1,4-dihydrobenzoic acid (**2.58**) through enantioselective catalytic bromolactonization to give **2.59** using the catalyst **2.94** may be easily upscaled without loss of efficiency or enantiomeric purity. This reaction was used to prepare synthetically useful quantities of **2.59**, which was elaborated into the two kibdelone fragments **2.98** and **2.110** in five (19% overall yield) and eight (9% overall yield) steps, respectively. Notably, only one step in the preparation of **2.98** requires purification via chromatography. Furthermore, the synthesis of **2.110** features a halodecarboxylation of a vinylic carboxylic acid, that proceeds in good yield.

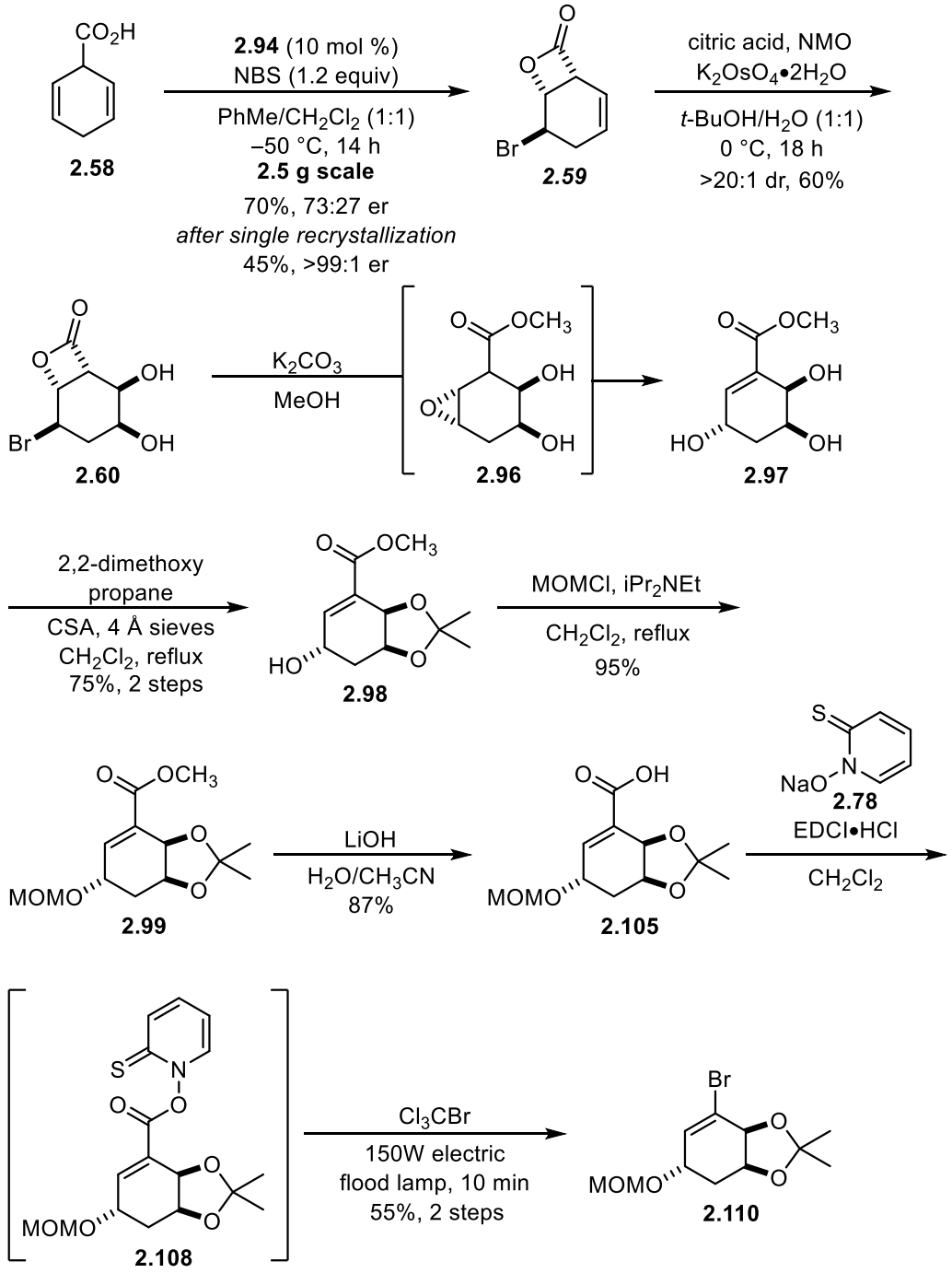

Scheme 2.13. Synthesis of F-ring fragments for kibdelone C natural products.

2.6 (+)–DISPARLURE – INTRODUCTION

The gypsy moth, *Lymantria dispar,* is a widespread forest pest that causes severe deforestation in Europe, Asia, and North America during outbreaks. This invasive insect was first introduced to North America by an amateur entomologist who traveled from France to Medford Massachusetts in 1868 or 1869.[116] It has since become one of the most destructive exotic organisms on the continent, and despite many eradication efforts, the invasive insects persist. Since its introduction to North America, the gypsy moth has spread to small parts of Canada and a large portion of the north- to mid-Atalantic United States. There also exists a secondary population in Michigan that is the result of an independent accidental introduction of the insect.[117] The gypsy moth is capable of causing severe ecological damage to infested areas because the insect is a highly polyphagous herbivore that will consume more than 300 different species of plants and trees. Additionally, the insect can have a serious economic impact in part due to the ecological damage it brings, but also in direct costs associated with managing the gypsy moth populations.[118] For example, the United States spends roughly 12 million dollars annually on controlling gypsy moths. These programs have been successful though and the insects spread has been reduced by 60% since their implementation.[119]

Although gypsy moth outbreaks only occur approximately every 10 years, constant monitoring and controlling the population of the insects remains important to prevent their spread. In the late nineteenth century, strategies for culling gypsy moth populations relied heavily on harmful pesticides such as lead arsenate, but with the many different discoveries of insect pheromones in the 1970s, most programs now rely on target specific mating disruptions to control the spread of gypsy moths.[117] In fact, controlling the spread of gypsy moths in North America has been successful due to the availability of low cost pheromone based traps that are highly effective for detecting low density populations.[119]

Bierl identified disparlure as the sex attractant pheromone of the female gypsy moth in 1970, and Iwaki later proved the absolute stereochemistry of disparlure through the synthesis of both enantiomers, ultimately discovering that (+)-disparlure is more active than (–)-disparlure for the attraction of the insects (Figure 2.4).[120] Interestingly, synthetic (+)-disparlure is able to attract male moths in field studies, but natural sources of the pheromone are more attractive, suggesting that there may be a synergistic effect between the two enantiomers. In its pure form, the antipode antagonizes the effect of (+)-disparlure and is slightly repellant to the male moths.[121] The female moths release the pheromone into the wind in non homogenous plumes, which the male moths are able to detect with their highly sensitive antennae to follow the pheromone upwind to its source. Saturating areas with the moth pheromone can obfuscate the trail left by the female moths, ultimately preventing the male moths from mating and breeding.[117,119]

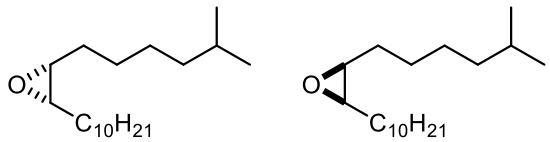

2.111
(+)-disparlure

2.112
(–)-disparlure

Figure 2.4. The gypsy moth pheromone disparlure.

Disparlure has attracted significant attention from the synthetic organic community due to its applications for managing gypsy moth populations and scarcity of natural sources. Since Bierl's seminal reportn, there have been over 50 syntheses of disparlure, the most recent of which was reported in 2017.[114,120–174] The introduction of the two stereocenters on the linear carbon chain of disparlure has been accomplished through a variety of synthetic methods including, asymmetric epoxidation,[128,129,134,142,149,156,171] asymmetric dihydroxylation,[147,151,154] use of chiral stannanes,[160] chiral sulfoxide

auxiliaries,[141,144] enzymatic procedures,[148,150,157] organocatalytic procedures,[165,168] and utilization of chiral pool starting materials.[120,152,164,166,170,173] Herein, we will highlight some syntheses of disparlure that are representative of these different strategies from over the years.

2.7 Select Previous Syntheses of Disparlure

2.7.1 Iwaki's Synthesis of (+)–Disparlure – Chiral Pool Starting Materials

Iwaki reported the first enantioselective synthesis of (+)-disparlure in 1974 (Scheme 2.14).[120] L-glutamic acid (**2.113**) was deaminated with nitrous acid to give lactone **2.114** in 80% yield. The carboxylic acid moiety of **2.114** was converted to the acyl chloride through treatment with oxalyl chloride, condensed with didecylcadmium, and the resulting ketone was reduced with sodium borohydride to give **2.115** as a mixture of diastereomers. The desired diastereomer was purified by column chromatography and recrystallization, and the alcohol protected as the tetrahydropyranyl (THP) ether with **2.116** to afford **2.117**. The lactone moiety was then reduced to the corresponding lactol with diisobutylaluminum hydride (DIBAL-H) and treated with ylide **2.118** to afford Wittig product **2.119** in 74% yield over two steps. Finally, hydrogenation of **2.119** and epoxidation of **2.120** through a three-step sequence delivered (+)-disparlure **2.111** in 12 steps and 9% overall yield

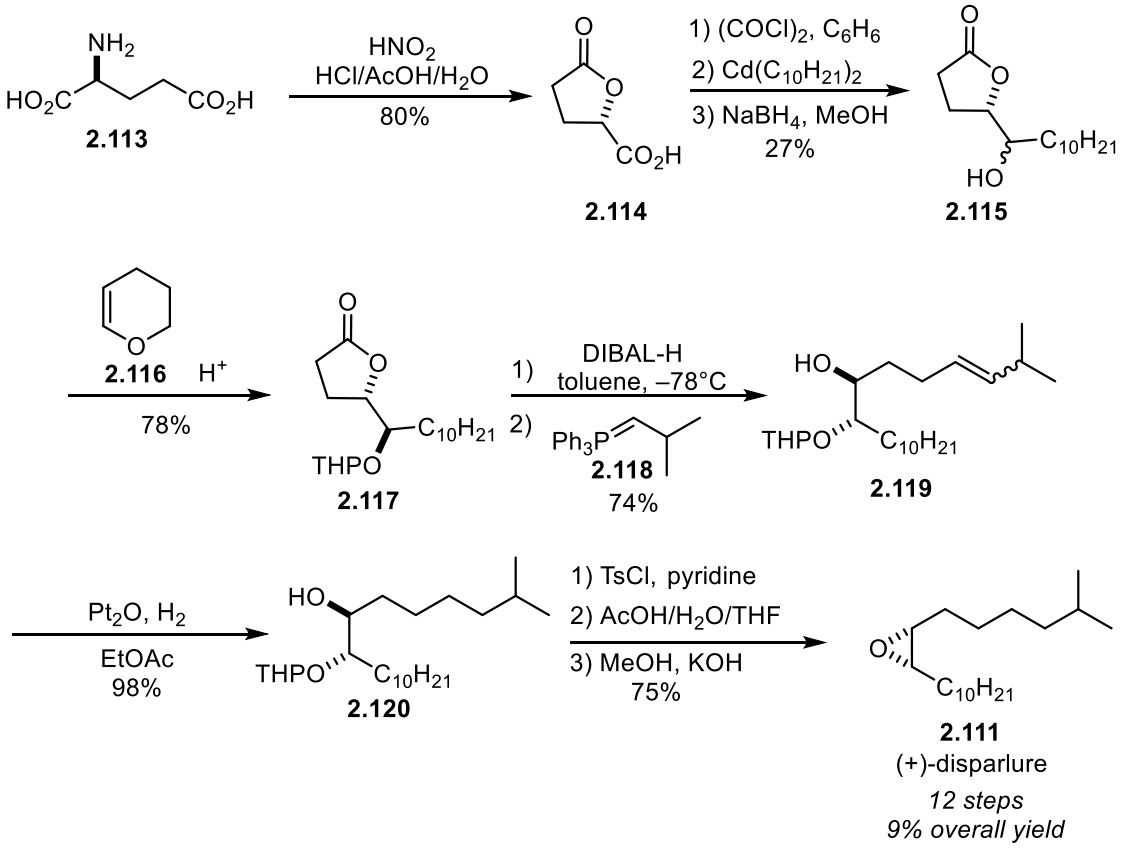

Scheme 2.14. Iwaki's enantioselective synthesis of (+)-disparlure.

. Iwaki managed to complete the first enantioselective synthesis of disparlure, but his synthesis suffered from poor diastereoselectivity, low yield, and lengthy step count. Despite these short comings, his synthesis was still influential for many later approaches to disparlure. The lactone reduction-olefination-hydrogenation three step sequence (conversion of **2.117** to **2.120**) has proven to be a useful strategy that has since been used in a number of syntheses of disparlure. Additionally, utilizing a 1,2-diol moiety as an epoxide precursor has also proven to be a strategy is that is prevalent in many asymmetric syntheses of disparlure.

2.7.2 Sharpless' Syntheses of (+)-Disparlure – Asymmetric Epoxidation and Dihydroxylation

Sharpless reported one of the most efficient enantioselective routes to (+)-disparlure in 1981 utilizing his asymmetric epoxidation methodology (Scheme 2.15).[128] The dianion of propargyl alcohol **2.121** was alkylated with bromodecane to afford **2.122**, which was partially hydrogenated to give the key allylic alcohol **2.123** in 84% yield over two steps. The enantioselective epoxidation of **2.123** proceeded in 80% yield and delivered epoxy alcohol **2.124** in 91% ee. The enantioenrichment of **2.124** was further increased to to >95% ee through recrystallization. Chromium oxidation of **2.124** led to aldehyde **2.125** which was converted to **2.11** through Wittig olefination with ylide **2.126** followed by hydrogenation of the resulting olefin. Sharpless thus prepared (+)-disparlure (**2.111**) six steps and 30% overall yield. The hydrogenation of the resulting allylic epoxide after the Wittig olefination of **2.125** was slightly problematic for Sharpless because the substrate readily isomerized to a ketone by-product under the reaction conditions that was difficult to separate from **2.111**. Isolation of pure **2.111** required treatment of the crude hydrogenation products with sodium borohydride and removal of the reduced ketone by-product via column chromatography.

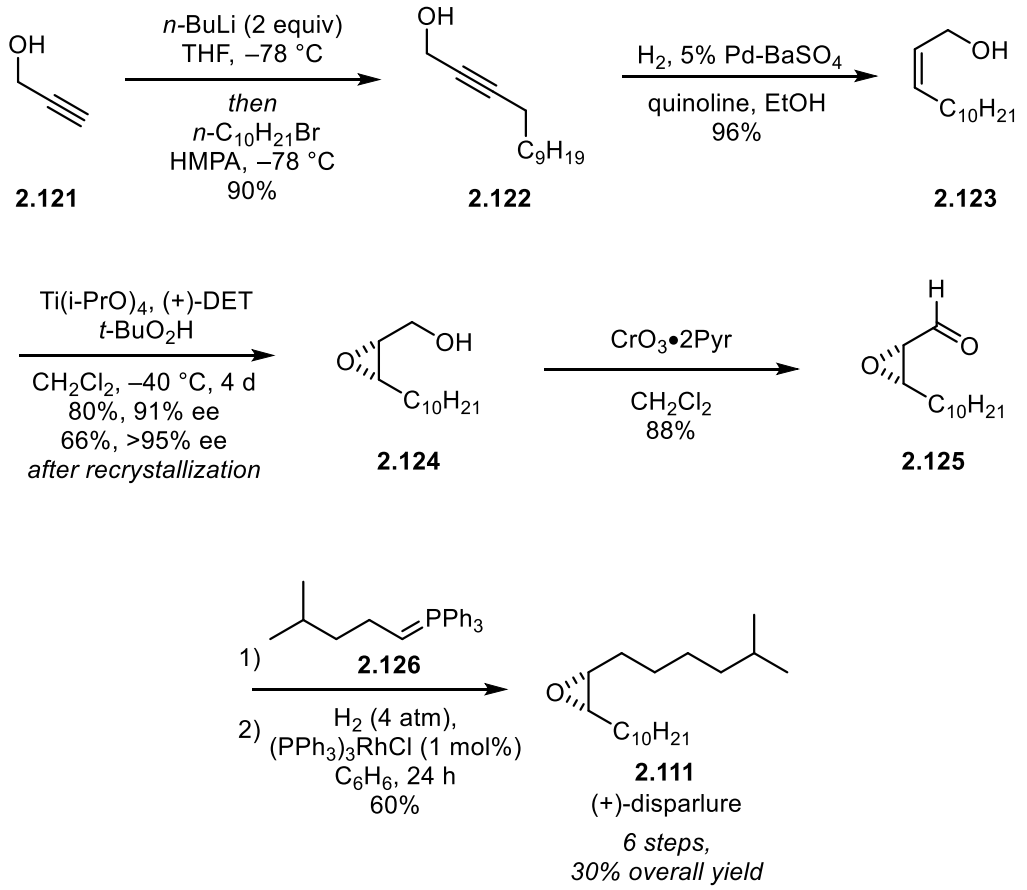

Scheme 2.15 Synthesis of (+)-disparlure via Sharpless asymmetric epoxidation.

Despite complications in the olefin reduction, Sharpless's strategy offers a high yielding efficient route to (+)-disparlure with a high degree of enantiopurity; indeed, this was the shortest catalytic enantioselective synthesis of (+)-disparlure prior to our work. Notably, the synthesis of (+)-disparlure became one of the first industrial applications of the Sharpless epoxidation. There have been a number of other reported syntheses utilizing the Sharpless epoxidation to set the requisite stereochemistry for (+)-disparlure but none have managed major improvements over the original route reported by Sharpless.[156,171]

Sharpless later followed up with another synthesis of (+)-disparlure that utilized his dihydroxylation methodology to set the requisite stereochemistry of the pheromone

(Scheme 2.16).[147] While this synthesis was not as short as his previous one, it offered an improvement in overall yield. The synthesis commenced from undecanal (**2.127**), which was treated with vinyl magnesium bromide to give the allylic alcohol **2.128** in 95%. Heating **2.128** in the presence of triethylorthoacetate and catalytic amounts of acid gave rise to a Johnson-Claisen rearrangement, affording **2.129** in 90% yield. Asymmetric dihydroxylation of **2.129** furnished a hydroxy lactone, the free alcohol of which was protected as a silyl ether to afford **2.130** in 85% yield over two steps. Lactone **2.130** was obtained with selectivity 95% ee, and the enantiopurity was further enhanced through recrystallization to give **2.130** as a single stereoisomer. Since Iwaki's preparation of disparlure, hydroxy lactone intermediates such as **2.130** has become common in strategies towards asymmetric syntheses of disparlure. Sharpless elaborated lactone **2.130** to (+)-disparlure through a commonly employed five step sequence. The lactone moiety of **2.130** was partially reduced to the lactol, which was used in a Wittig olefination with ylide **2.118**, and the newly formed alkene was hydrogenated to give **2.131** in 78% yield over three steps. The synthesis was then completed through mesylation of the free alcohol of **2.131**, followed by epoxidation after removal of the silyl protecting group with tetrabutylammonium fluoride (TBAF), which delivered (+)-disparlure (**2.11**) in nine steps and 43% overall yield from undecanal (**2.127**).

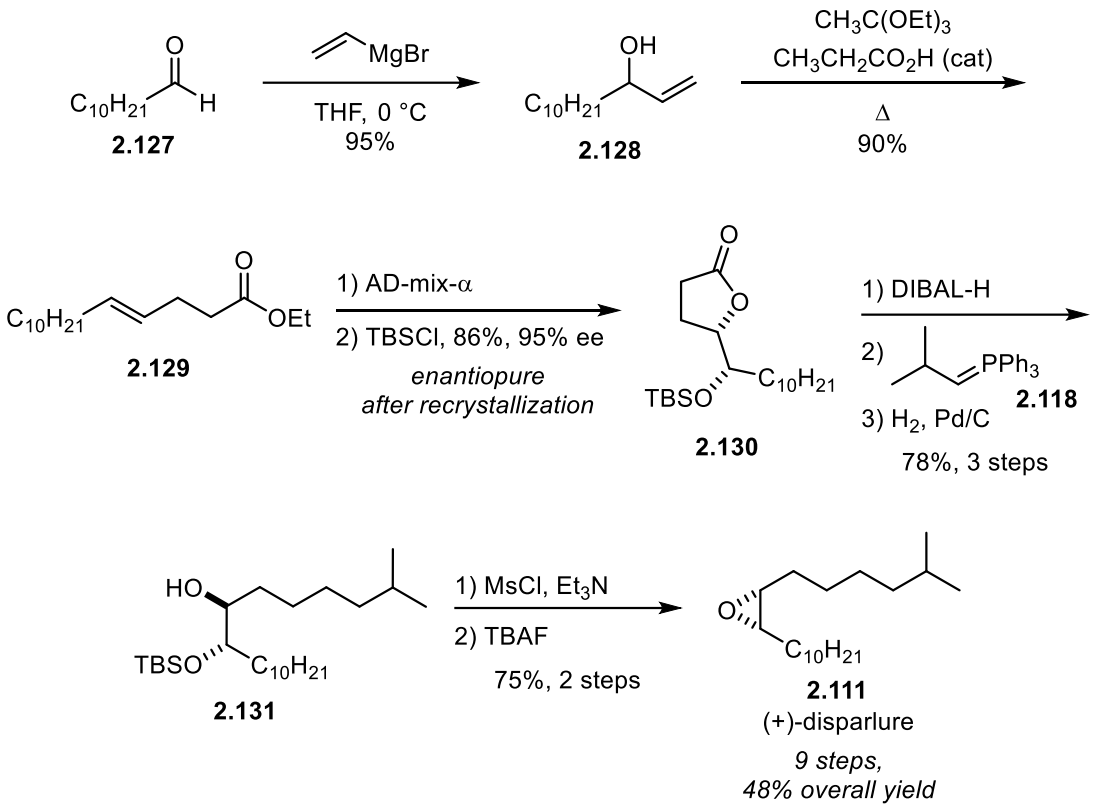

Scheme 2.16. Synthesis of (+)-disparlure via Sharpless asymmetric dihydroxylation.

2.7.3 Tsuboi's Synthesis of (–)-Disparlure – Enzymatic Resolution

Tsuboi's strategy towards (–)-disparlure (**2.112**) utilized an enzymatic chiral resolution of the key intermediate **2.135** to set the epoxide stereochemistry of the natural product (Scheme 2.17). Tsuboi's synthesis commenced with a Darzen's type condensation between undecanal (**2.127**) and dichloroacetate **2.132** which delivered the halogenated epoxide **2.133** in 74% yield. This intermediate underwent smooth thermal rearrangement in the presence of alumina to give **2.134** in 84% yield. The ketone moiety was then reduced with sodium borohydride to give **2.135**, which was subjected to a lipase mediated enzymatic kinetic resolution to afford **2.137** with 91% ee. Reduction of the ester of **2.138** with sodium borohydride delivered the 1,2-diol **2.138**, which upon exposure to NaOEt in

EtOH underwent epoxidation to afford **2.139** in 61% yield over two steps. The free alcohol of **2.139** was activated as a leaving group through tosylation, and then **2.140** was alkylated with cuprate **2.141** to afford (–)-disparlure in eight steps and 9% overall yield.

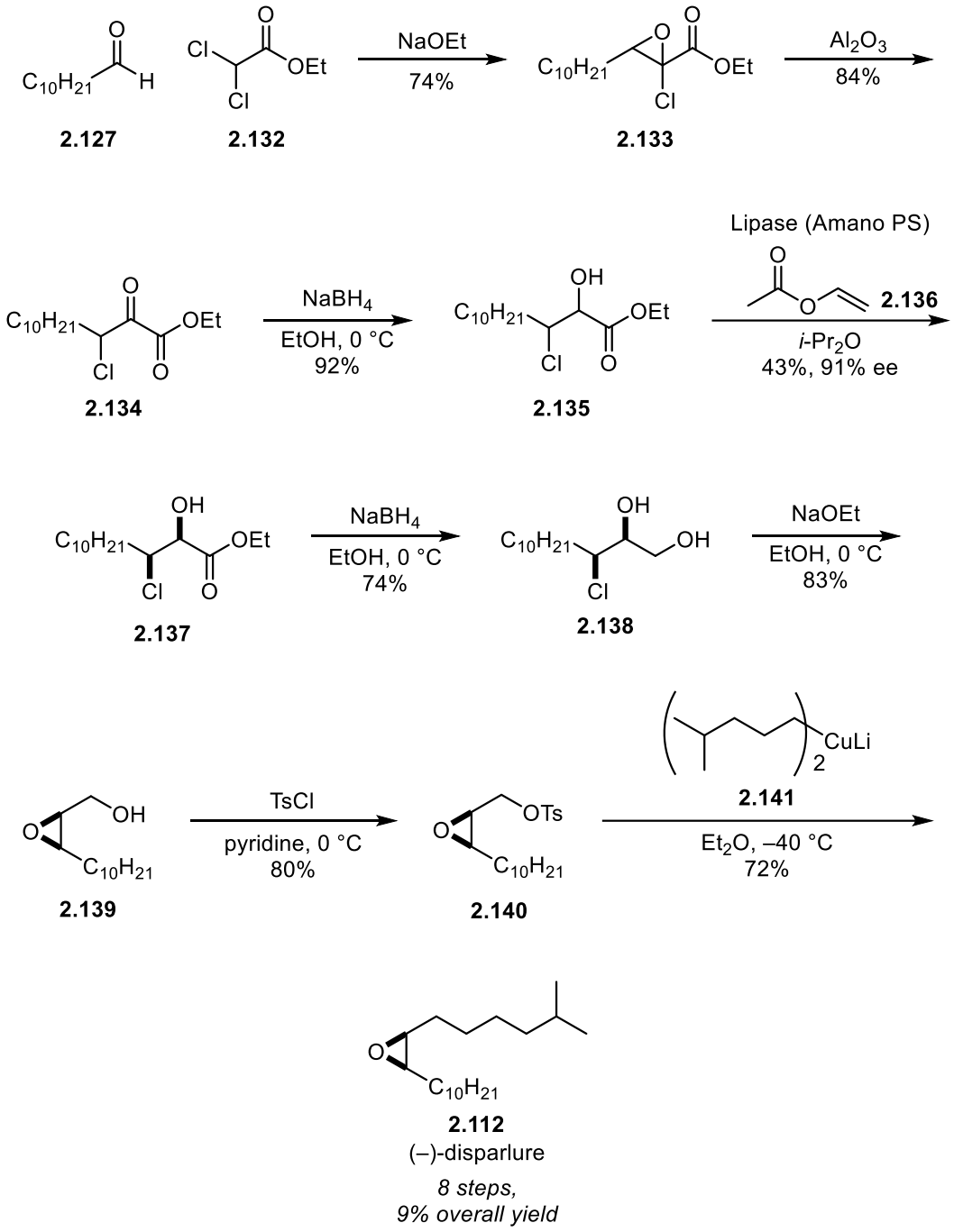

Scheme 2.17. Tsuboi's synthesis of (–)-disparlure via enzymatic chiral resolution.

2.7.4 Kim's Synthesis of (+)-Disparlure – Proline Organic Catalysis

Kim reported an efficient route to (+)-displarlure in 2009 that relied on asymmetric proline catalysis to set the epoxide stereochemistry of disparlure (Scheme 2.18).[168] Kim used a proline catalyzed asymmetric α-aminooxylation of dodecanal (**2.142**) with an in situ indium catalyzed allylation to deliver **2.144** as a 4:1 mixture of diastereomers. The major *anti* diastereomer **2.144** was carried forward through cross metathesis with **2.145**, which was accompanied with N-O bond cleavage to deliver diol **2.146** in 50% yield. Hydrogenation of the alkene moiety of **2.146**, followed by a three step epoxidation sequence afforded (+)-disparlure **2.11** in six steps and 23% yield from **2.142**.

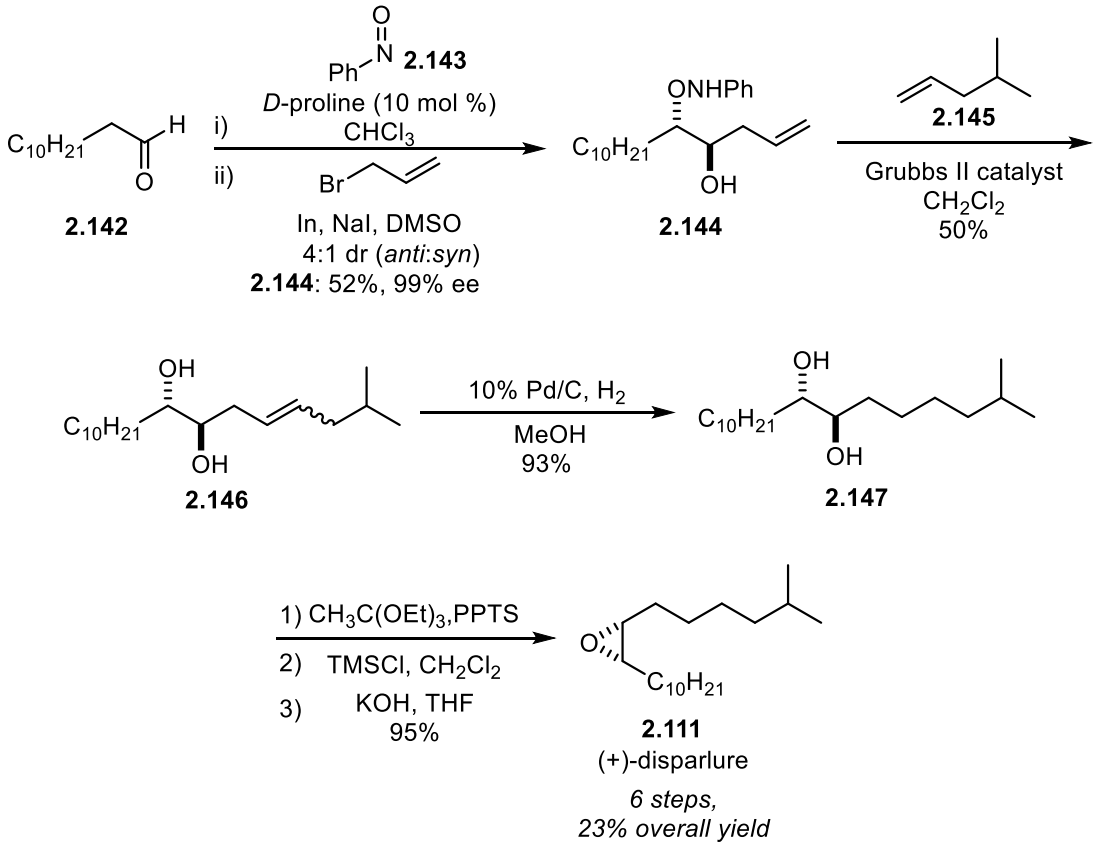

Scheme 2.18. Kim's synthesis of (+)-disparlure via proline catalysis.

Kim's strategy for (+)-disparlure was efficient in step count; it established the requisite stereochemistry and carbon framework of (+)-disparlure in only two steps, but the key step suffered from poor yield and diastereoselectivity. Additionally, the three step epoxidation sequence from the 1,2-diol moiety of **2.147** is a clumsy transformation that has plagued many syntheses of disparlure.

2.7.5 Satoh's Synthesis of (+)-Disparlure – Chiral Sulfoxide Auxiliary

Satoh reported the shortest enantioselective synthesis of (+)-disparlure to date using an optically active sulfoxide auxiliary to impart chirality (Scheme 2.19).[144] Chlorination of **2.148** with N-chlorosuccinimide (NCS) delivered optically pure chloroalkyl sulfoxide **2.149** after recrystallization. Deprotonation of **2.149** with lithium diispropylamine (LDA) and alkylation with iododecane delivered **2.150** in 75% yield as a mixture of diastereomers. Deprotonation of **2.150** with LDA followed by nucleophilic addition to 6-methyl-1-heptanal (**2.151**) delivered **2.152** and **2.153** as a separable mixture of diastereomers, and the desired **2.153** was isolated in 39% yield. Chlorohydrin **2.153** was treated with potassium *tert*-butoxide to give **2.154**, and finally, removal the sulfoxide auxiliary with *n*-butyllithium gave (+)-disparlure **2.111** in five steps and 11% overall yield.

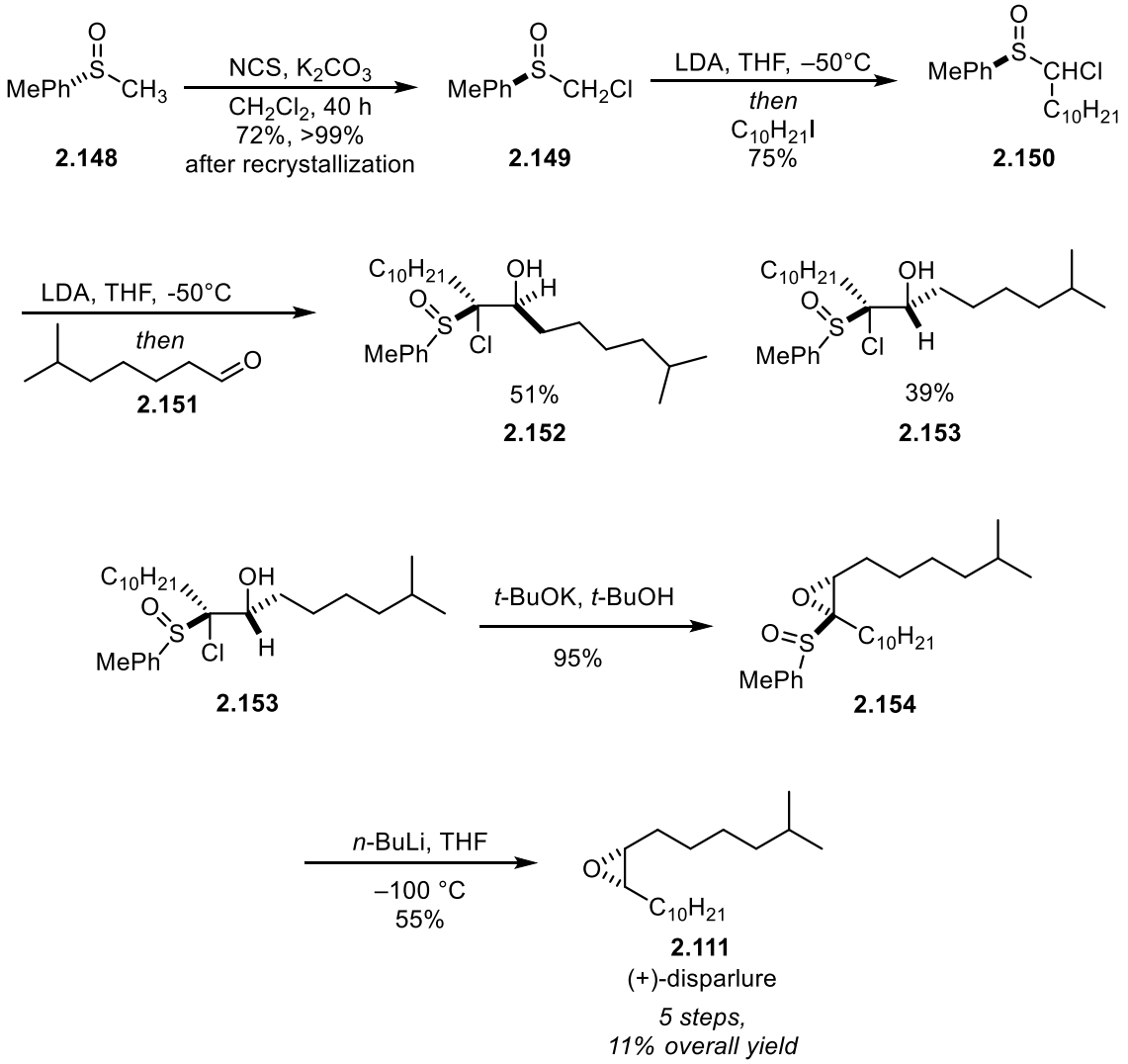

Scheme 2.19. Satoh's synthesis of (+)-disparlure.

Satoh's use of sulfoxide auxiliary offers an expeditious route to (+)-disparlure, however the auxiliary provides poor diastereoselectivity in the alkylation reactions, and the synthesis ultimately suffers from low yield. Additionally, the auxiliary is consumed during the synthesis, further detracting from the efficiency of the synthesis.

2.7.6 Summary of Previous Syntheses

Disparlure has been the target of synthetic investigations for the last 40 years. Despite over 50 syntheses of this natural product, there remains room for improvement. Most approaches to **2.11** that use chiral pool starting materials are lengthy and low yielding, and the enzymatic resolution strategies offer little improvement. Kim's synthesis of **2.11** was efficient in terms of step count, but ultimately suffered from poor diastereoselectivity in the key step, and consequently poor overall yield. Satoh's synthesis represents the shortest enantioselective synthesis to date, but it too suffers from low over yield and poor selectivity in the key step. Satoh's synthesis also suffers from the stoichiometric incorporation of a chiral auxiliary that later requires removal to complete the natural product. Sharpless' syntheses represent the state of the art for enantioselective variants, and indeed these have proven to be powerful methods for establishing stereochemistry of epoxides. Nevertheless, we devised a synthetic sequence to **2.11** that we thought would have an advantage over past syntheses in terms of step count and yield.

2.8 Enantioselective Synthesis of (+)-Disparlure Via Asymmetric Iodolactonization

2.8.1 Synthetic Approach

We planned an approach where (+)-disparlure (**2.111**) could be prepared from the *cis*-epoxde **2.155**, which would be produced from the reductive opening of the enantioenriched iodolactone **2.156** (Scheme 2.20). Our synthesis relied on the ability of catalyst **2.94** to promote the iodolactonization of *cis*-alkenoic acid **2.158** in good yield and with high enantioselectivity.

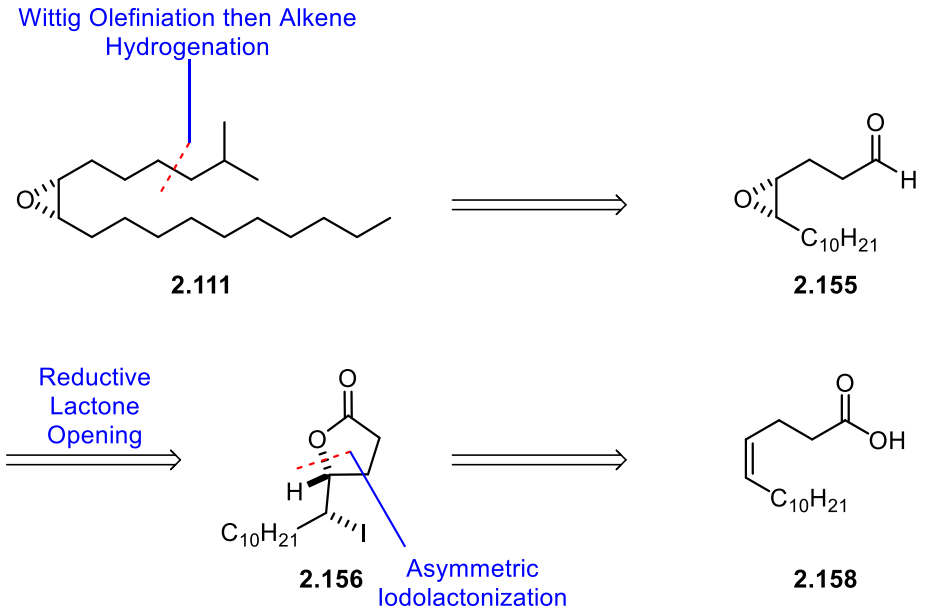

Scheme 2.20. Martin group synthetic approach to (+)-disparlure.

At the outset of our investigations however, it was unclear if **2.158** was would be a suitable substrate for our halolactonization methodology. Previous studies in our group on revealed that unbranched alkyl-substituted *cis*-alkenoic acids such as **2.159** cyclized to iodolactones with only moderate selectivity (85:15 er) (Equation 2.35). Accordingly, we set to the task of evaluating the efficacy of this crucial transformation.

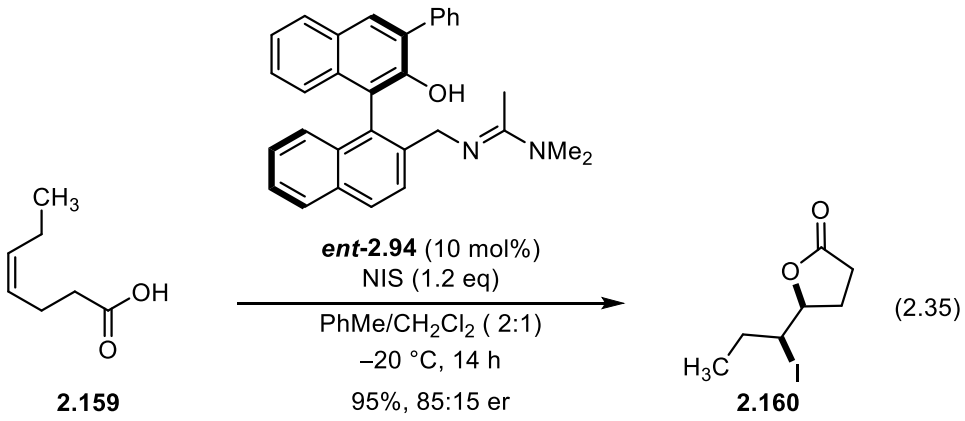

2.8.2 First Generation Synthesis

We first set out to prepare **2.158** through the most straightforward method available in order to test the iodolactonization reaction as quickly as possible. Our first-generation synthesis commenced with the protection of pent-4-yn-1-ol (**2.161**) as the THP ether, followed by the alkylation of the lithiated alkyne of **2.162** with iododecane, which provided **2.163** in 81% yield over two steps (Scheme 2.21).[175] Subjecting **2.163** to the acidic reaction conditions of the Jones oxidation led to *in situ* removal of the THP protecting group and oxidation of the resulting alcohol to the carboxylic acid **2.164** in good yield (82%). Initial attempts to partially reduce the alkyne moiety of **2.164** to the *cis*-alkenoic acid **2.158** with Lindlar's catalyst delivered an inseparable mixture of *cis* and *trans* olefins (~9:1 *cis*:*trans* by ^{1}H NMR). Fortunately, semi-hydrogenation of **2.164** with P2-Ni in a hydrogen atmosphere cleanly gave **2.158** in 85% yield.

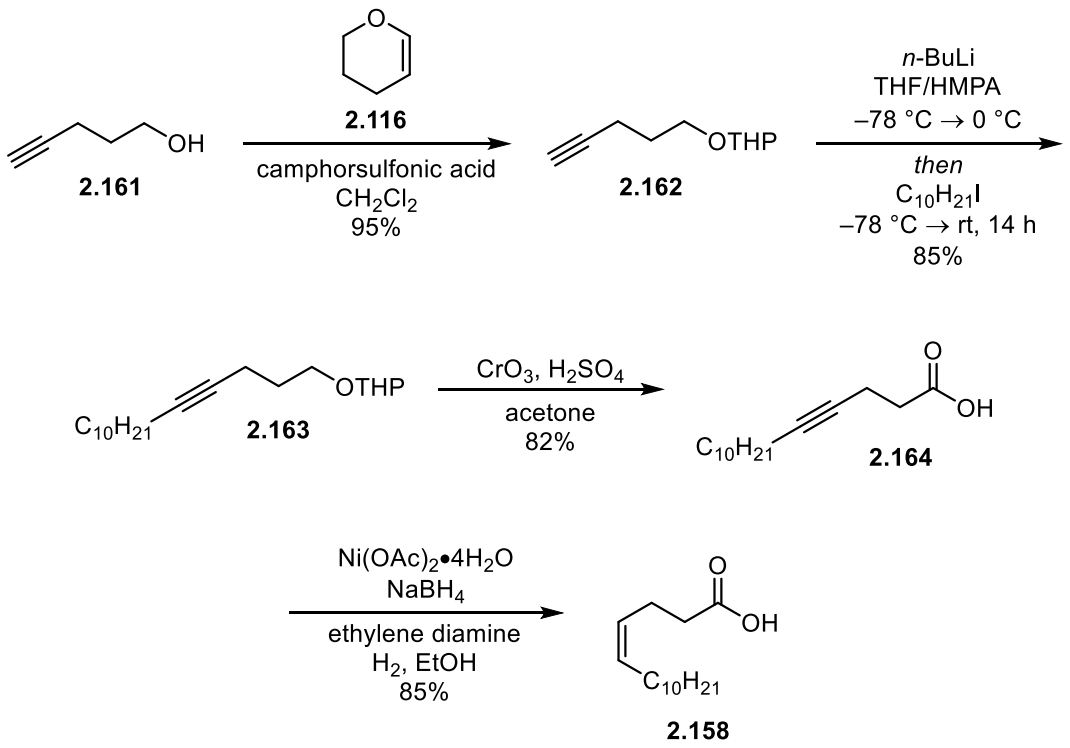

Scheme 2.21. First generation synthesis of **2.158**.

With **2.158** in hand, we investigated the key enantioselective halolactonization. Gratifyingly, we found the iodolactonization of **2.158** in the presence of **2.94** proceeded smoothly to deliver **2.156** in 81% yield and 90:10 er (Equation 2.36). Similar to our previous iodolactonizations,[10] we found that the inclusion of I_2 further enhanced the enantioselectivity of the reaction, and **2.156** was obtained in 85% yield and 95:5 er (Equation 2.37).

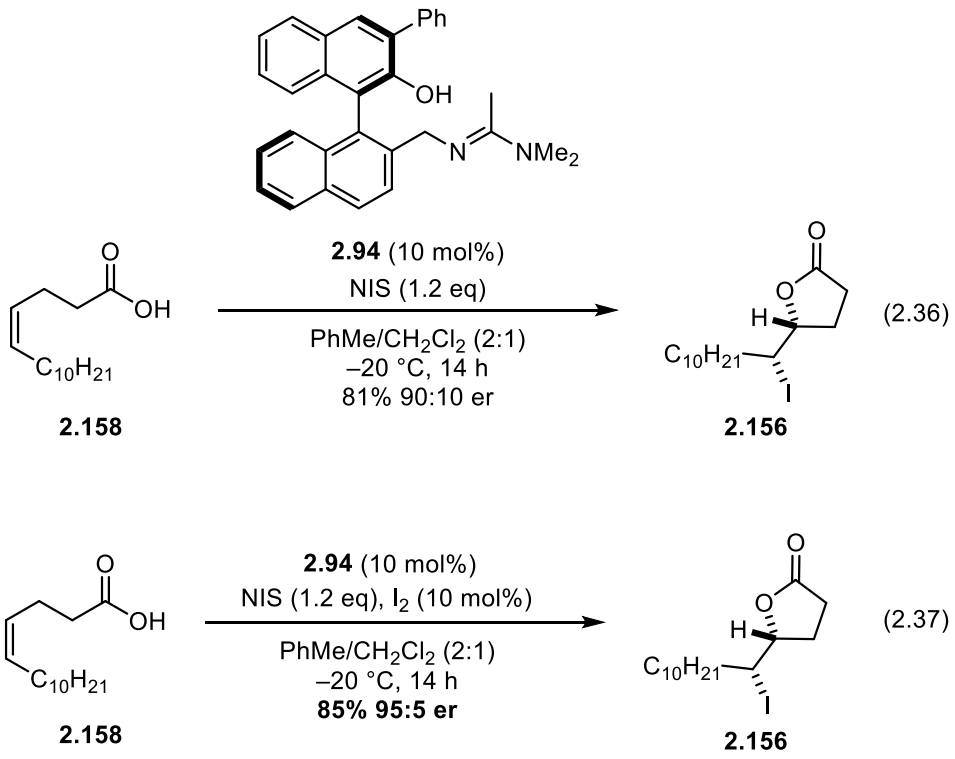

With proof-of-principle for an enantioselective synthesis of (+)-disparlure established, we investigated the remaining steps to elaborate **2.156** to **2.111** (Scheme 2.21). Fortunately, treatment of iodolactone **2.156** with DIBAL led to clean conversion to **2.165**, which was used directly in a Wittig olefination with ylide **2.118** to deliver **2.166** as an inconsequential mixture of *cis* and *trans* isomers. Initially, selective reduction of the alkene moiety of **2.166** was problematic due concomitant opening of the epoxide when Pd/C was used as the catalyst.[176] However, after screening a variety of solvents and reaction conditions, we discovered that the reduction could be achieved using Pt_2O in hexanes to afford (+)-disparlure in 90% yield.

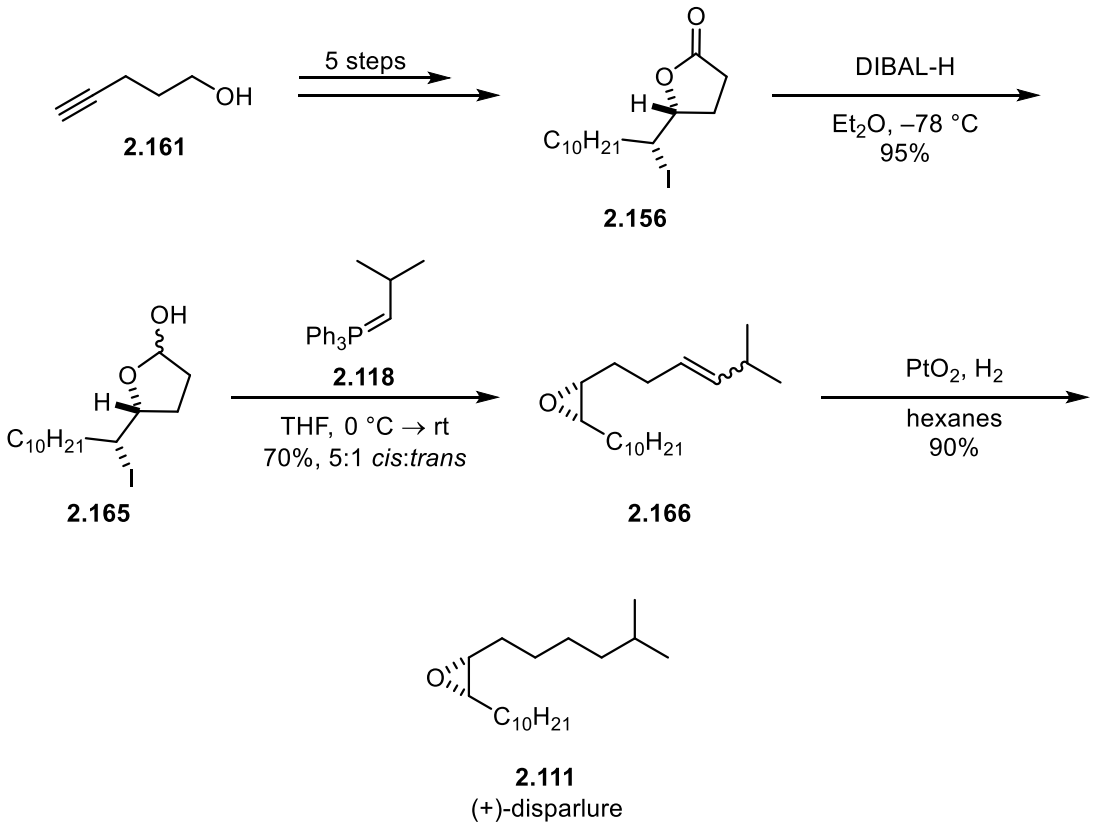

Scheme 2.21 First generation synthesis of (+)-disparlure

In our first-generation synthesis, we prepared (+)-disparlure in eight steps from **2.161**. While this was useful as a proof of principle exercise, a more efficient synthesis was desirable to remain competitive with the plethora of previous syntheses. One area that required improvement was the lengthy preparation of the *Z*-olefinic acid **2.158**, which required four steps from commercial materials. The most appealing approach for preparing **2.158** was inspired by a previously reported one-step procedure for the synthesis of (*Z*)-4-alkenoic acids.[177] We planned a regioselective opening of β-propiolactone (**2.171**) with the vinyl cuprate **2.170**, which would arise from the carbocupration of acetylene with the alkyl cuprate **2.168**, generated from iododecane (**2.167**), ultimately affording **2.158** in one step. (Scheme 2.22)

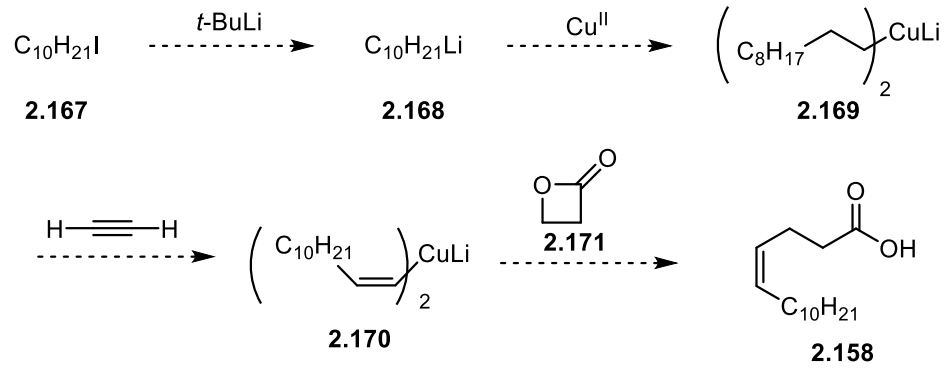

Scheme 2.22. Synthetic strategy for the one-step preparation of **2.158**

2.8.3 Carbocupration of Acetylene

The addition of an organometallic carbon–metal bond to a carbon–carbon unsaturated system, leading to a new organometallic species that can be further functionalized is known as a carbometallation reaction (Equation 2.38). Organocuprate reagents are the most efficient for carbometallation of alkynes, and the addition occurs in *syn* fashion to provide reliable access to vinyl copper derivatives.[178,179] The carbocupration of alkynes generally proceeds with high stereo- and regioselectivity, and consequently, it has become a versatile reaction for the stereospecific construction of di-, tri-, and tetra-substituted olefins.[179] The reaction has been shown to work with various organocopper reagents, including organocopper species derived from Grignard reagents ($RCu{\bullet}MgX_2$), Gilman-type cuprates (R_2CuLi), and organocopper–zinc mixed species (RCu(CN)ZnX).[179]

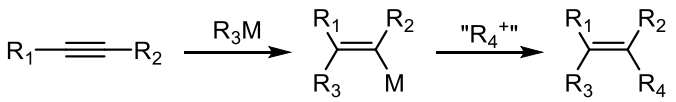

(2.38)

The regioselectivity of carbocupration reactions is determined by the substitution of the alkyne.[178] For the carbocupration of monosubstituted alkynes there are two possible regioisomers, referred to as the "linear" **2.173** and branched" **2.174** products (Scheme

2.24). In the presence of a chelating heteroatom (X = SR', NR'_2, OR'), the linear vinylcuprates (**2.173**) can dominate as the major product of the carbocupration, although the selectivity between linear and branched products can be poor. In the absence of a directing group, (i.e. X = H or alkyl), the reaction is highly selective for the branched products of type **2.174**. Generally, the carbocupration proceeds in a *syn* addition manner, although there can be exceptions.[178,179] The remarkable stereoselectivity of this reaction has made it a valuable synthetic tool for the stereospecific construction of substituted olefins, and it has been implemented in a number of natural product syntheses.[158,180]

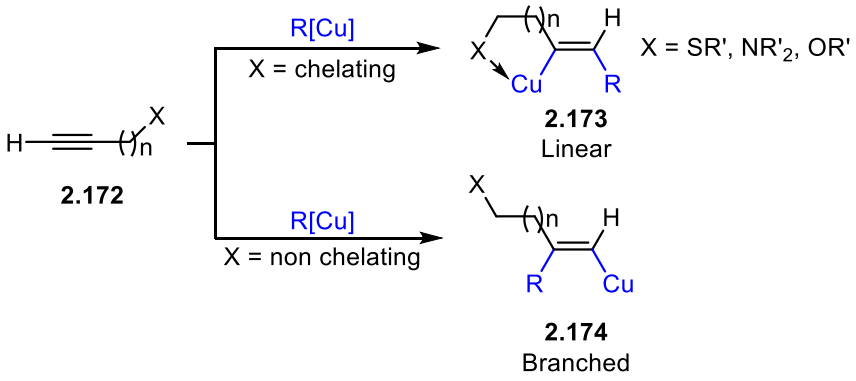

Scheme 2.23. Regiochemical outcomes in the carbocupration of alkynes

For the carbocupration of acetylene, its simplistic nature obviates any concern for regiochemical outcomes of the R–Cu addition, and it has become a useful reaction for the preparation of *Z*-disubstituted olefins. Importantly, Gilman type cuprates exhibit carbocupration reactivity in the presence of acetylene, and deprotonation of the alkyne is not observed.[178,180] The mechanism for the carbocupration of acetylene is still under debate in part due to the lack of information concerning the real structure of organocopper clusters in solution.[181] However, *ab initio* and density functional theoretical investigations from Nakamura and Morokuma have provided evidence for a possible mechanism.[182] They

systematically studied the methylcupration of acetylene using five different organocopper species – MeCu, Me_2Cu^-, Me_2CuLi, Me_2CuLi•LiCl, and $(Me_2CuLi)_2$, – all of which have been invoked in discussions of carbocupration mechanisms. From this study, some general conclusions about the possible reaction pathways can be drawn. The addition of the MeCu organocopper reagent can only occur via a four-centered transition state consisting of nucleophilic addition of anionic methyl group (**2.176**, Equation 2.39). However, the activation energy of C–C bond formation in this pathway is large (43.6 kcal/mol), since the covalent CH_3–Cu bond must be cleaved. Therefore, a neutral RCu organocopper reagent is not a sufficiently reactive nucleophile for the carbocupration of acetylene.[182]

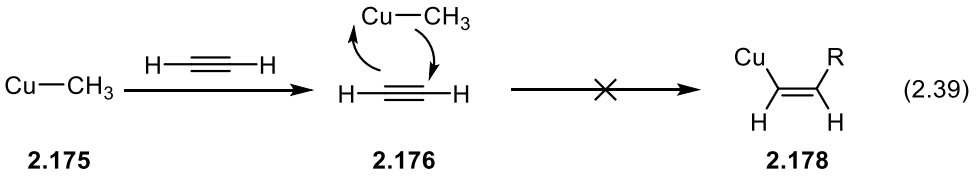

2.175 **2.176** **2.178** (2.39)

For the clustered lithium cuprates, such as R_2CuLi•LiX, a different mechanism appears to be operative.[182] Notably, synthetic copper reagents that are prepared from the reaction of organolithium reagents with copper (I) halides almost always exist as the R_2CuLi•LiX species and are believed to be dimeric in solution.[183,184] The mechanism for these cuprates can be described as a copper-assisted carbolithiation followed by intracluster transmetallation that proceeds via a "trap-and-bite" pathway (Scheme 2.24). The electron rich cuprate first binds tightly to acetylene through a two-electron donation from the copper atom to "trap" the alkyne **2.181**. The binding of acetylene to the copper liberates an R group and opens the cluster, allowing the cuprate to "bite" the alkyne **2.183**. This C–C bond forming reductive elimination is believed to be the rate determining step of the reaction, and after formation of **2.184**, transmetallation results in the vinyl cuprate **2.185**.[182]

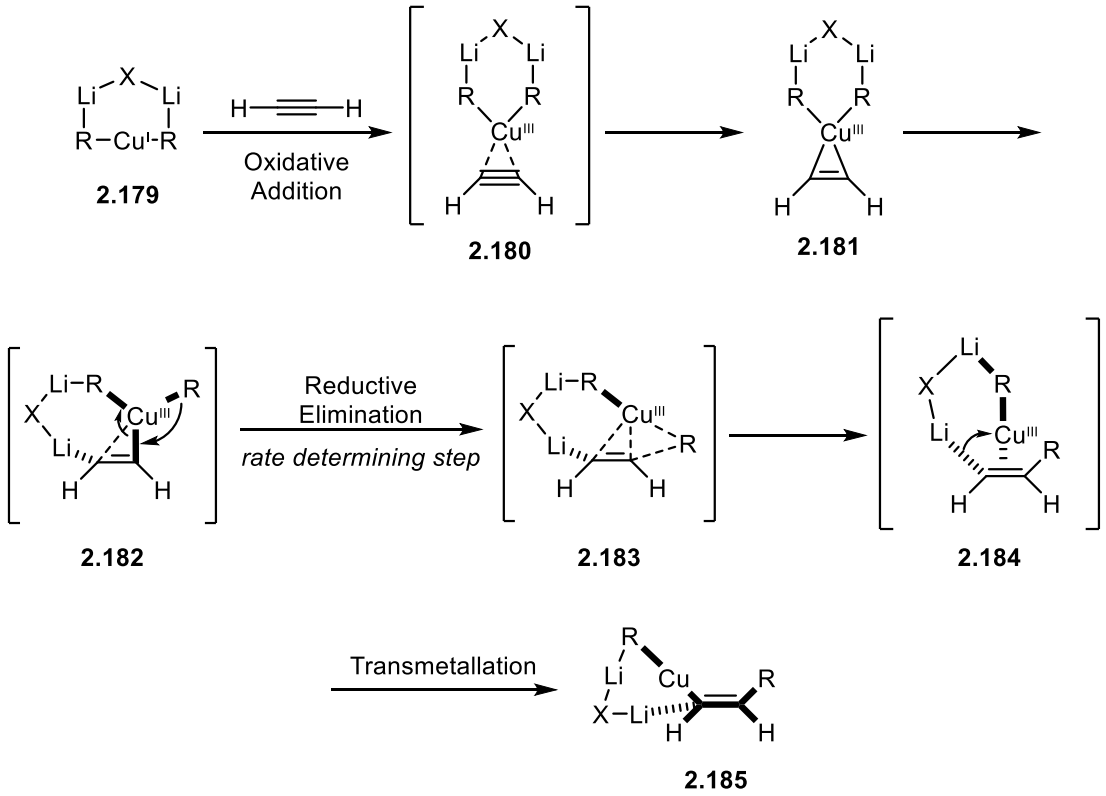

Scheme 2.24. Theoretical mechanism of carbocupration of acetylene for clustered cuprates ($R_2CuLi•LiX$) as proposed by Nakamura and Morokuma.

We became interested in the carbocupration of acetylene as part of a one-step strategy to prepare the key olefinic acid **2.158**. Fujisawa reported a general method for the one-pot synthesis of various (*Z*)-4-alkenoic acids by the ring opening reaction of β-propiolactone with di-(*Z*)-1-alkenylcuprates generated from the carbocupration of acetylene (Scheme 2.25).[177] Fujisawa prepared a series of 5-alkyl-4(*Z*)-pentenoic acids **2.189** substituted with straight aliphatic chains of increasing size, ranging from butyl to nonyl in good yield (80–90%) through this one-pot method. Interestingly, as the size of the alkyl chain increased, it was necessary to increase the number of equivalents of acetylene used to form the cuprate **2.188**, and up to a 6.6:1 molar ratio of acetylene:**2.187** was

required for R = *n*-C_9H_{19}. When the molar ratio of acetylene:**2.187** was < 4:1 for alkyl chains longer than R = *n*-C_4H_9, diminished yields of the desired product was observed, in part due to side reactions that led to **2.190** and **2.191**. By-product **2.190** is the result of the direct reaction of **2.187** with propiolactone **2.171**, which did not first react with acetylene. In contrast, the by-product **2.191** is the result of an additional carbocupration reaction between **2.188** and acetylene, followed by nucleophilic opening of **2.171**.

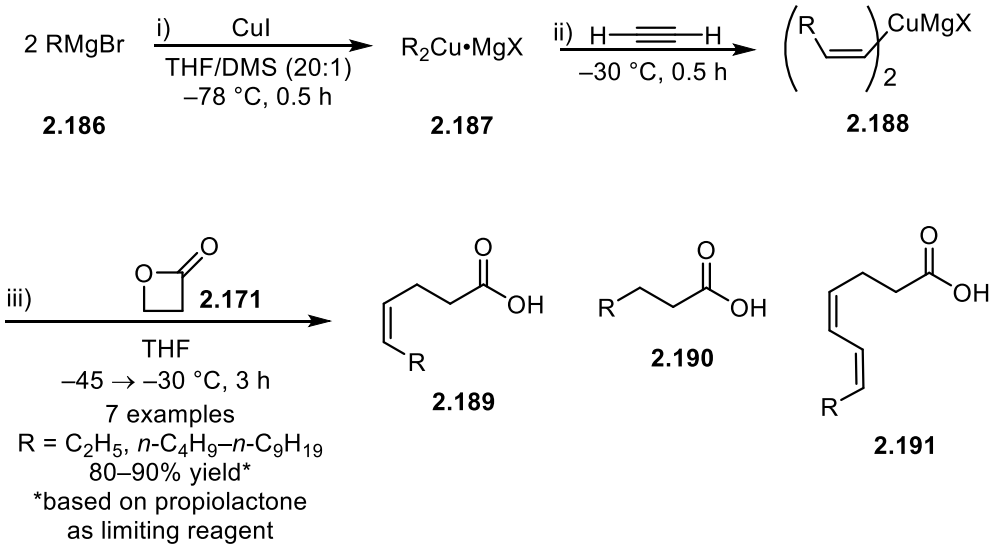

Scheme 2.25 One-step method for the preparation of *Z*-alkenoic acids reported by Fujisawa.

The synthetically useful yields reported by Fujisawa for this reaction prompted us to examine this strategy for the preparation of **2.158**, which would drastically shorten our synthesis of (+)-disparlure (**2.111**). Admittedly, we had a number of concerns about this reaction, specifically, that it was a four-step one-pot operation that relied on highly reactive and sensitive intermediates. The multi-step operation would also be potentially difficult to troubleshoot, as there would be many chances for the reaction to go awry. Despite these

concerns, the promise of a one-step synthesis of **2.158** was too tempting to ignore and we embarked on a carbocupration journey of our own.

2.8.4 Second Generation Synthesis

We began our efforts to optimize our synthesis of (+)-disparlure by attempting to replicate the procedures reported by Fujisawa for the one step preparation of (*Z*)-4-alkenoic acids. Our initial attempts to form the Grignard reagent **2.193** from either bromodecane (**2.192**) or iododecane (**2.167**) revealed that, in our hands, the reagent was not stable at concentrations greater than ca. 0.3 M. Titration of freshly prepared solutions of **2.193** in THF or Et_2O revealed that the actual concentration of Grignard reagent deviated significantly from the targeted concentration (Table 2.3). The formation of the desired Grignard **2.193** appeared to be more reliable when Et_2O was used as solvent and when iododecane (**2.167**) was used as the starting alkyl halide (Table 2.4, Entries 2, 3–5). We speculated that higher concentrations might be resulting in undesired side reactions such as Wurtz type couplings.. Therefore, we instead decreased the targeted concentration to 0.5 M, which proved to be more reliable, and we were ultimately able to reproducibly form **2.193** with concentrations of 0.3 M.

Table 2.4. Optimization of the preparation of Grignard reagent **2.193**

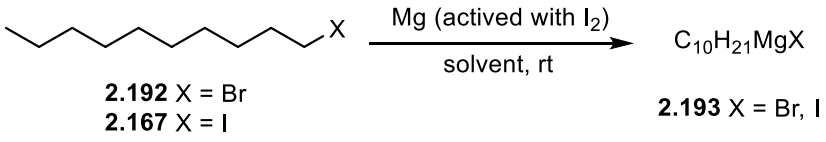

Entry	Reagent	X	Solvent	Target $C_{10}H_{21}MgX$ [M]	Titrated $C_{10}H_{21}MgX$ [M][a]
1	**2.192**	Br	THF	1	0.17
2	**2.192**	Br	Et_2O	1	0.2
3	**2.167**	I	THF	1	0.185
4	**2.167**	I	Et_2O	1	0.25
5	**2.167**	I	Et_2O	0.5	0.3

[a]Reagent titrated using 1,10-phenanthroline and sec-butanol.

With a method established to generate **2.193**, we next investigated the formation of the vinyl cuprate **2.194**. Disappointingly, after treating freshly prepared **2.193** with CuI followed by bubbling acetylene into the reaction mixture, we found no evidence of carbocupration upon quenching the reaction (Equation 2.40). After aqueous work up, only decane was recovered, with evidence of olefin incorporation based on the ^1H NMR spectrum of the crude reaction material.

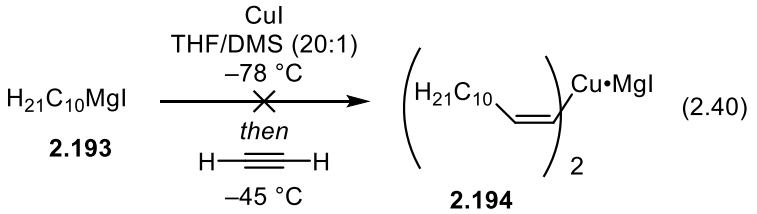

While it was still unclear why we did not observe carbocupration of acetylene, we speculated that the stability of the Grignard reagent may be problematic based on our initial difficulty in forming **2.193**. We changed our strategy and instead, we pursued the Gilman

type cuprate $(C_{10}H_{21})_2CuLi$, which we would prepare from lithiated decane and a copper (I) salt. Gratifyingly, we found the formation of **2.195** proceeded smoothly when iododecane (**2.167**) was treated with two equivalents of *t*-butyllithium (*t*-BuLi) (Equation 2.41). Furthermore, we confirmed the formation of **2.195** through the reaction with an equimolar amount of benzaldehyde (**2.196**), which resulted in near complete conversion to **2.197** based on the ^{1}H NMR spectrum of the crude reaction material (Equation 2.42).

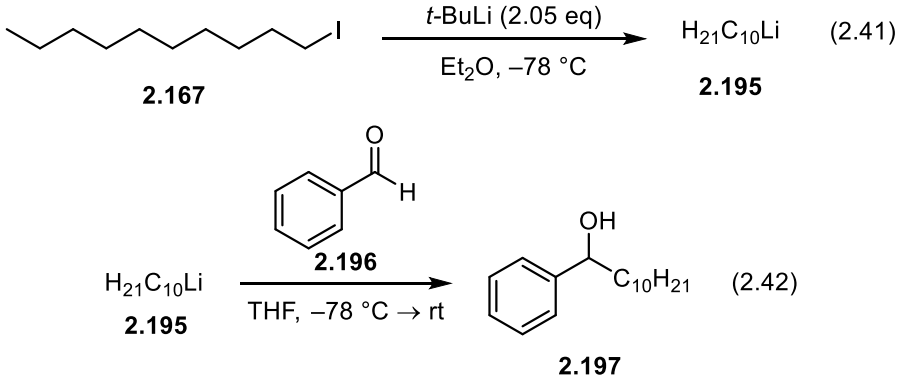

Confident in the nature of our organolithium species, we returned to the carbocupration investigations using reaction conditions similar to those reported by Fujisawa. Unfortunately, we again saw no evidence of carbocupration, and upon quenching the reaction with methanol and removal of the solvent, we again observed no incorporation of vinyl protons in the ^{1}H NMR spectrum of the crude reaction material, and primarily decane was observed (Equation 2.43).

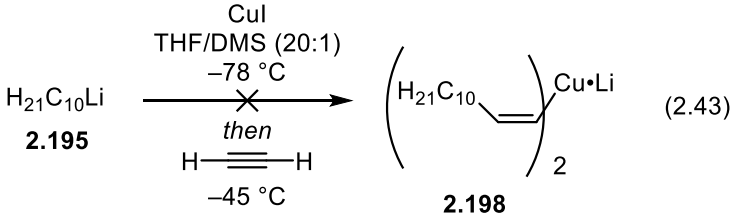

With few clues to ascertain why the reaction was not working, we decided to trouble shoot the problem using phenylacetylene (**2.200**) and 1-hexyne (**2.201**) as model systems. Acetylene was proving to be problematic because it was difficult to precisely control the stoichiometry of the gas introduced to the reaction mixture, meaning we had little control over a reaction parameter that was shown to be important by Fujisawa. Thus, we set to the task of screening conditions for the formation of cuprate **2.199** and the subsequent carbocupration with either **2.200** or **2.201** (Table 2.5). We found that under a variety of conditions, no carbocupration was ever observed when CuI was used as the Cu (I) salt. Attempting the carbocupration of **2.200** or **2.201** in THF, THF/DMS, or Et_2O was universally unsuccessful when CuI was used (Table 2.5, Entries 1–6), which indicated that the formation of the alkyl cuprate **2.199** was problematic. House previously reported the purity of copper (I) salts in the formation of organocurpates from organolithium reagents is critical,[183] and despite using freshly purified and rigorously dried CuI, we suspected this could have been an issue. To solve this problem, investigated the crystalline complex CuBr•DMS as an alternative copper source, which can be easily purified by recrystallization in dimethyl sulfide (DMS).[183] Again however, we observed no carbocupration of **2.200** or **2.201** with **2.199** when the reactions were executed in THF/DMS as the solvent (Table 2.5, Entries 7,8). However, to our delight, we found that the carbocupration of **2.200** with **2.199** proceeded smoothly in Et_2O to provide **2.202** in ca.70% yield (Table 2.5, Entry 9). This model reaction confirmed that **2.199** was indeed being formed as desired, and we could resume our attempts to affect the carbocupration of acetylene.

Table 2.5 Optimization of the carbocupration of **2.200** and **2.201** model systems.

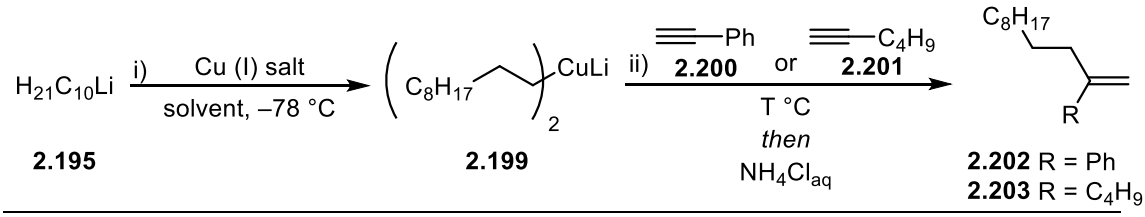

2.195 **2.199** **2.202** R = Ph **2.203** R = C_4H_9

Entry	Cu(I) salt	Solvent[a]	Alkyne[b]	T °C (ii)	Result[c]
1	CuI	THF	**2.200**	–78 to –25	NR
2	CuI	THF	**2.201**	–78 to –25	NR
3	CuI	THF/DMS (20:1)	**2.200**	–78 to –25	NR
4	CuI	THF/DMS (20:1)	**2.201**	–78 to –25	NR
5	CuI	Et_2O	**2.200**	–78 to –25	NR
6	CuI	Et_2O	**2.201**	–78 to –25	NR
7	CuBr•DMS	THF/DMS (20:1)	**2.200**	–45	NR
8	CuBr•DMS	THF/DMS (20:1)	**2.201**	–45	NR
9	CuBr•DMS	Et_2O	**2.200**	–45	~70% **2.202**

[a]Solvents were degassed by sparging with nitrogen gas prior to use. [b]2.1 equivalents of alkyne used. [c]NR = No reaction

Newly confident in our ability to generate **2.199**, we continued our investigations of the carbocupration of acetylene. Disappointingly though, we still did not observe any evidence for acetylene carbocupration, despite the new reaction conditions to form **2.199** (Equation 2.44). Again, we were left with little information as why the reaction was failing, but we speculated that a solvent screen maybe beneficial. Solvents have been reported to play important roles in these reactions,[179] and indeed, we observed this first hand in our own carbocupration model studies. Unfortunately, executing the reaction in a variety of different solvents including THF, Et_2O, and mixtures of THF/DMS and Et_2O/DMS still

resulted in no observable carbocupration of acetylene. We decided that the only variable left to investigate was the source and stoichiometry of acetylene.

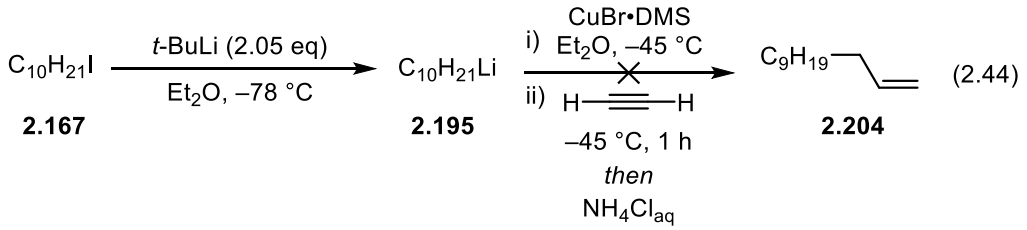

We had been conducting our studies using acetylene obtained from a commercial source stored in a gas cylinder. Acetylene in commercial gas cylinders is typically dissolved in liquid acetone, which aides in safe storage. To introduce acetylene to the reaction mixture, it was first transferred from the storage tank to a balloon, and then passed through two empty flame dried flasks under inert atmosphere that were cooled to –78 °C, which served as condensers to remove any residual acetone. Despite rigorous efforts to exclude air, we reasoned this somewhat elaborate reaction assembly increased the chance for atmospheric oxygen to be introduced to the reaction mixture, which has been shown to oxidize organocuprates.[185] Therefore we sought to change our acetylene source and we planned to introduce acetylene that was generated from the reaction of calcium carbide with water. This approach was also attractive because we would have more control over the stoichiometry of acetylene introduced by controlling the amount of water added to the solid calcium carbide. The gas generated from this reaction could simply be passed through a drying tube prior to being bubbled into the solution of **2.199**.

Gratifyingly, this alternative method for introducing acetylene proved effective. We finally enjoyed some success when six equivalents of acetylene were introduced into a solution of **2.199** over a one-hour period at –45 °C, and we observed ca. 50% formation of

2.204 (Equation 2.45). When larger ratios of acetylene (12:1 acetylene:**2.199**) were used, significant formation of **2.205** was observed.

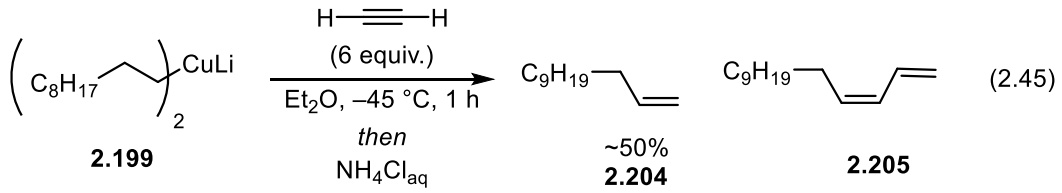

(2.45)

While we only observed modest incorporation of acetylene to **2.199** we were heartened by this success, and eager to see if **2.198** would react with β-propiolactone (**2.171**) to generate **2.158**. Disappointingly though, when **2.198** was treated with **2.171**, only ~10% of the desired product **2.158** was isolated, along with 25% of **2.206**. The remainder of the material recovered was **2.207**, which was formed during the aqueous work up of the reaction. The low yield of **2.158** was attributed to poor formation **2.198**, and despite extensive efforts to optimize the carbocupration, we found the generation of **2.198** to be erratic and difficult to consistently reproduce. Consequently, we were never able to improve the yield of **2.158** via this four-step one-pot method, and we ultimately had to abandon our pursuit of this strategy in our synthesis of disparlure.

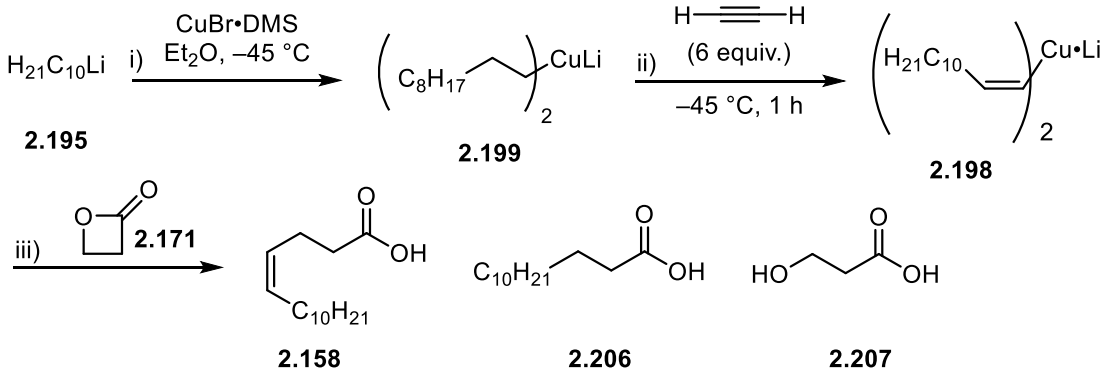

Setting aside our disappointment, we instead pursued a more reliable and practical two step preparation of **2.158**. We planned to alkylate the dianion of commercially available 4-pentynoic acid (**2.207**) with iododecane to provide **2.164**, which could then be reduced to **2.158** as we demonstrated previously. In the event, initial attempts to prepare **2.164** through treatment of **2.207** with *n*-BuLi followed by addition of 1.1 equivalents of iododecane resulted in a mixture of **2.164** and **2.208** with minor amounts of returned starting material (Equation 2.46). We attempted to optimize the yield of **2.164** through screening solvents, as well as temperatures and rates of addition of iododecane, but we were never able to suppress the formation of **2.208**. Rather than attempt to mitigate the formation of **2.208**, we instead increased the stoichiometry of iododecane to 2.5 equivalents to drive the reaction to complete formation of **2.208** (Equation 2.47). We could then soaponify the ester by-product formed *in situ* by addition of 2 M $LiOH_{aq}$ after the starting material had been consumed, and in this fashion **2.164** was obtained in 85% yield.

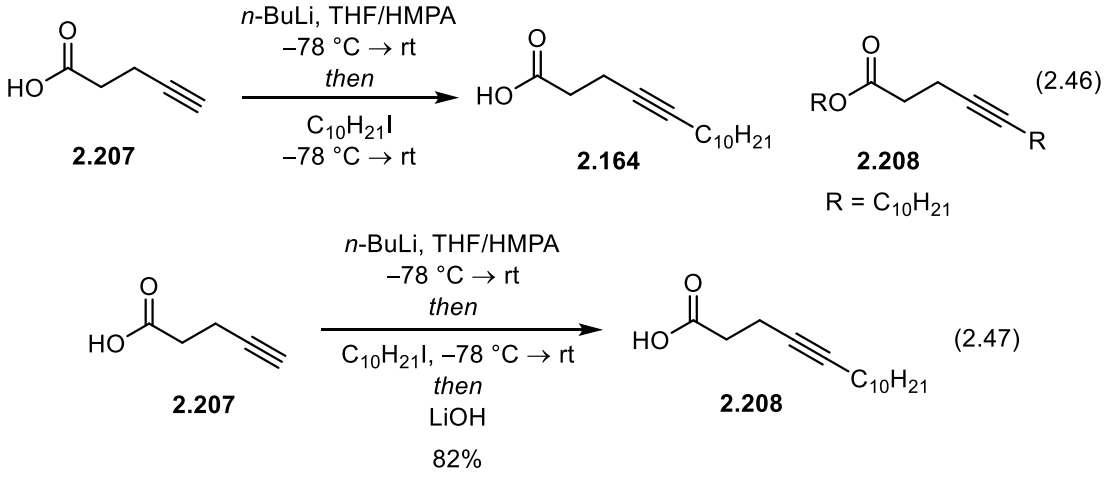

One final innovation we had for the synthesis was the direct preparation of **2.166** from **2.156** (Equation 2.48). The purity by which the DIBAL reduction of **2.156** proceeded,

prompted us to investigate a one-pot transformation of **2.156** to **2.166**. To our delight, we found that after the partial reduction **2.156** was complete, addition of a freshly prepared solution of **2.118** led to formation of **2.166**, albeit in a slightly diminished yield of 62%.

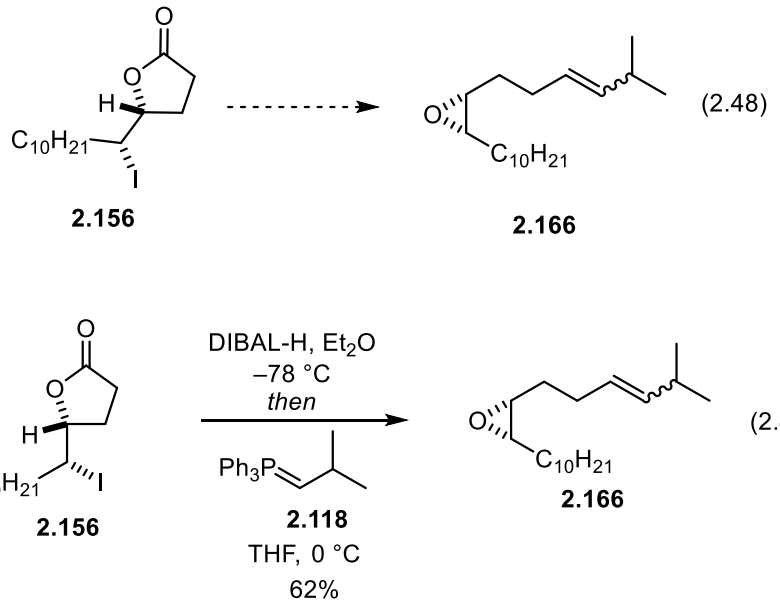

2.8.5 Summary

A summary of the optimized reactions for our enantioselective synthesis of (+)-disparlure is provided in scheme 2.27.[186] The ability of catalyst **2.94** to provide rapid access to enantioenriched *cis*-epoxides is a powerful synthetic method as we have exemplified through the preparation of **2.11**. To the best of our knowledge, our preparation of **2.11** represents the shortest catalytic enantioselective synthesis of this natural product to date, which required five steps from **2.207** and proceeded in 33% overall yield.

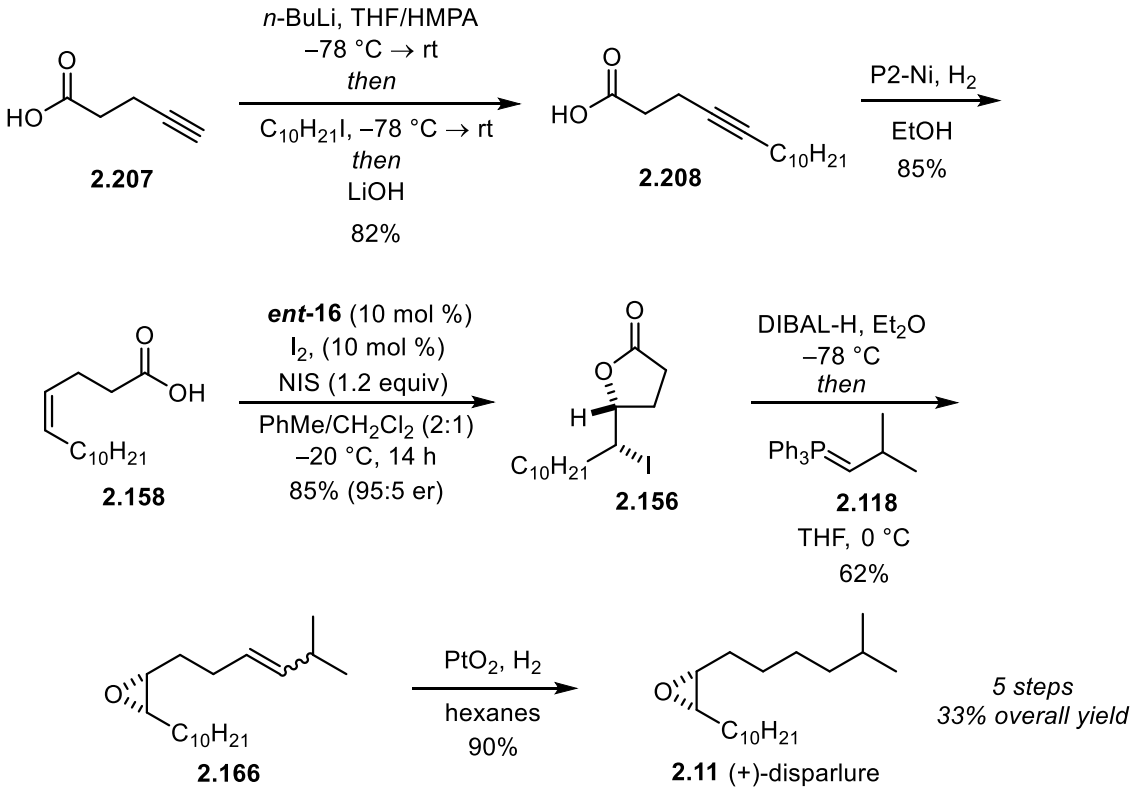

Scheme 2.27. Enantioselective synthesis of (+)-disparlure.

2.9 SUMMARY AND CONCLUSIONS

Enantioselective halolactonization reactions represent powerful tools for synthetic organic chemists. The desymmetrization of 1,4-dihydrobenzoic acid via bromolactonization, for example, converts a prochiral starting material to a complex enantioenriched product which contains three contiguous stereocenters. We demonstrated that this method is readily applicable to synthetically useful scales, and we applied it to efficient syntheses of F-ring fragments of the kibdelone natural products. Furthermore, the ability to prepare enantioenriched *cis*-disubstituted epoxides from enantioenriched halolactones fills a gap in synthetic methodology that has yet to be addressed by direct catalytic methods for epoxidations of olefins. Application of this method to the synthesis

of (+)-disparlure culminated in the shortest enantioselective synthesis to date, despite over 40 years of research around this natural product.

SYNTHESIS OF PHOTOCAGED COMPOUNDS FOR LABELING NEURONS BASED ON FUNCTION

CHAPTER 3: PHOTOLABILE PROTECTING GROUPS

3.1 INTRODUCTION

Photolabile protecting groups (PPGs) are light reactive functional groups that can be attached to a given molecule to render it chemically and or biologically inert. These protecting groups are unique in that their removal is accomplished through irradiation with light without the need for chemical reagents. These unique protecting groups allow for precise temporal and spatial control over chemical reactions and the release of active compounds. Although PPGs were originally designed by synthetic chemists, applications in chemical synthesis have been minimal.[187] However, photoremovable protecting groups, referred to as "cages" or "photocages" by biologists, represent an excellent method for rendering a compound biologically inert that can be activated externally via light. There have been numerous exciting applications of these protecting in the realm of biology including, the control of protein functions, cellular stimulation, regulation of gene expression, and neuronal stimulation or inhibition. These applications have been covered in multiple recent reviews.[188–195]

The photochemical efficiency of the deprotection of a PPG is often described using the quantum yield as a quantitative metric. The quantum yield of substrate release (Φ_{rel}) is equal to the amount of released substrate, n_{rel}/mol, divided by the number of photons absorbed at the irradiation wavelength λ, n_p/mol (Equation 3.1). Alternatively, the quantum yield of release can be described in terms of relative rates for the photochemical processes. That is, the quantum yield of release (Φ_{rel}) is equal to the rate constant of substrate release

from the excited state (k_{rel}) divided by the sum of all of the rate constants of other potential photochemical pathways from the excited state (Σ k) (Equation 3.2).

$$\Phi_{\text{rel}} = \frac{n_{rel}}{n_p} \quad (3.1)$$

$$\Phi_{\text{rel}} = \frac{k_{\text{rel}}}{\Sigma\, k} \quad (3.2)$$

Photolabile protecting groups first appeared in the literature in the early 1960's with the seminal reports from Barltrop,[196] Barton,[197] Sheehan,[198] and Patchornik and Woodward.[199] Barltrop was the first to investigate the first use of a light reactive group as a potential new protecting group strategy. Barltrop described the deprotection of Cbz-glycine (**3.1**) through irradiation with UV-light (254 nm) in aqueous solution, which led to the efficient removal of the carbamate protecting group, yielding benzyl alcohol (**3.2**) and glycine (**3.3**) (Equation 3.3).[200] These early reports set the stage for what has today grown into an extensive field of research, with hundreds of new PPGs reported in the literature to date.[193]

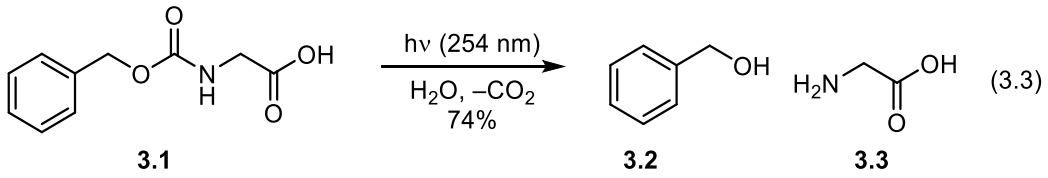

3.1 **3.2** **3.3** (3.3)

The promising biological applications of photolabile protecting groups has reignited the synthetic community's interest in developing novel PPGs. The design of a photoremovable protecting group will depend on its desired application, but for biological systems there are several concerns to address.[193,201]

1) The substrate, the caged substrate, and the photochemical by-products should all have good aqueous solubility and be stable in the targeted media in the absence of light.
2) The photochemical reaction should be efficient with regard to quantum yield and release of the substrate. Furthermore, the departure of the substrate from the protecting group should be a primary photochemical process.
3) The release of the target compound must be faster than the biological response under investigation.
4) The photoproducts should be stable to the photolysis environment and nontoxic or harmful to the biological system under investigation.
5) The PPG should have a strong absorbance above 300 nm, where irradiation is less likely to be absorbed by, and cause harm to, the biological system under investigation.
6) The synthesis of a caged substrate should be high yielding and purification of the caged compound should be facile. It is important that the caged material can be isolated cleanly, with no contamination of uncaged substrate.

While it is difficult for one PPG to meet all of these criteria, they are important to consider when designing novel photocages or planning a biological study involving one. However, the quest to design the ideal photolabile protecting group is ongoing and reports of new classes and derivatives of PPGs are constant. Herein we will highlight some of the most popular PPGs, grouped by common structural features.

3.2 *o*-NITROPHENYL PHOTOLABILE PROTECTING GROUPS

3.2.1 *o*-Nitrobenzyl Photolabile Protecting Groups

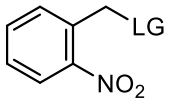

3.4
2-nitrobenzyl (**NB**)

The 2-nitrobenzyl (**NB**, **3.4**) derivatives are the most widely used class of photoremovable protecting groups. Since the pioneering work of Baltrop[200] and Woodward,[199] these groups have been studied in detail and the photodeprotection mechanism is well understood. Numerous analogues of *o*-nitrobenzyl based PPGs have been developed, and their applications spawn a broad array of scientific areas.[193,202] Despite their ubiquity, this class of PPGs has a number of inherent disadvantages, which are better understood through a discussion of the deprotection mechanism.

3.2.1.1 Mechanism of Deprotection

The popularity of the *o*-nitrobenzyl PPGs has led to detailed investigations of the deprotection mechanism over the years.[203–207] The photodeprotection mechanism is highly dependent on solvent, pH, and the nature of the leaving group. The photolysis begins with the photoexcitation of **3.5**, which is followed by rapid (~100 fs) internal conversion to the lowest singlet excited state **3.6** (Scheme 1). The excited state hydrogen transfer (ESHT) then proceeds through either the excited singlet state (**3.6**), or an excited triplet state after inter-system crossing (**3.7**), to form the *aci*-nitro tautomers **3.9** and **3.10**. The barrier for retautomerization of **3.9** back to **3.5** is relatively slow, but in some solvents (MeOH, CH_3CN), the equilibration between **3.9** and **3.10** by proton exchange between oxygen atoms is competitive with reformation of **3.5**. In aqueous solutions the equilibrium between tautomers **3.9** and **3.10,** and the cyclization to give **3.11** is faster than the reverse reaction to reform **3.5**. The cyclization of the *aci*-nitro tautomer **3.10** to **3.11** is irreversible, and this

intermediate will decay via **3.12** to ultimately form the nitroso aldehyde **3.13** with concomitant release of the substrate (X-H).

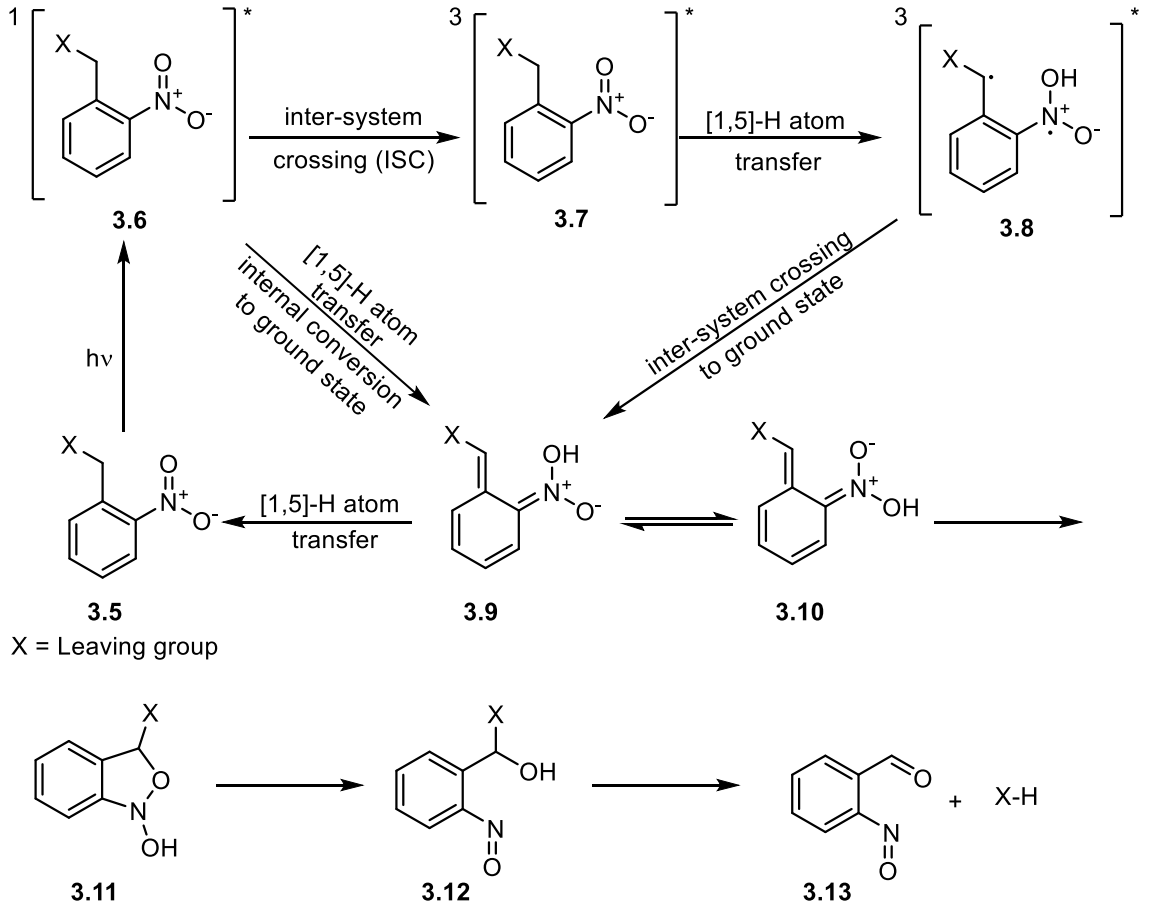

Scheme 3.1. Photodeprotection mechanism of *o*-nitrobenzyl photolabile protecting groups

The mechanism of deprotection for the **NB** class of PPGs reveals a number of problems associated with this photocage, many of which are due to the nitroso by-product 3.13. The *o*-nitroso aromatic aldehydes and ketones typically absorb more strongly than the parent PPG at the deprotection wavelengths. This is problematic in that the nitroso by-products can act as a filter, blocking the irradiation and interfering with the release of the

compound of interest. In some cases, the reactive nature of the **3.13** can result in a number of side-reactions, the most problematic of which is the condensation with primary amines.[208] This becomes problematic for the protection of amino-containing compounds due to the potential for the released substrate to condense with **3.13,** which effectively diminishes the efficiency of the deprotection and prevents the released substrate from participating in the biological response under investigation. Indeed, this undesirable side reaction was observed by Givens and Bayley during their studies of photoreleased peptides.[209,210] Furthermore, the nitroso side products can be toxic towards biological systems, which can limit their applicability in some biological studies.[193]

Part of the appeal of the **NB** class of PPGs is their ability to release a wide range of leaving groups such as phosphates, carboxylates, carbonates, carbamates, thiolates, phenolates, and alkoxides. However, the nature of the leaving group impacts both the rate and quantum yield of the deprotection. For a good leaving group such as a phosphate, release of the leaving group is synchronous with the formation of the *aci* intermediate **3.10** and has kinetics on the order of milliseconds. However, for a poor leaving group such as an alkoxide, the rate of deprotection can be dependent on the collapse of the hemiacetal **3.12**. At neutral pH, the decay of **3.12** was found to be many orders of magnitude slower than the decay of the *aci* intermediates **3.9** and **3.10**.[205,211] Therefore, it is generally not suitable to directly release alcohols from the **NB** photocage in a study of fast biological events. One solution to circumvent the slow deprotection rates of poor leaving groups such as alcohols and amines is to use carbonyl linkers to instead protect them as carbonates or carbamates (**3.14**) (Equation 3.4). In general, these are good leaving groups and will lead to efficient deprotection. After photorelease, the carbonate or carbamate (**3.16**) will undergo thermal fragmentation to provide the parent alcohol or amine (**3.17**).

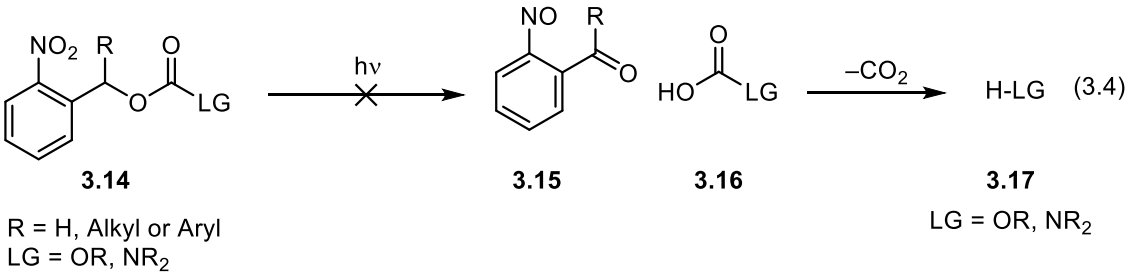

3.2.1.2 o-Nitrobenzyl Photolabile Protecting Group Derivatives

Since the seminal reports of **NB** PPGs, a plethora of derivatives have been developed with aims to improve photochemical properties of this class. These new compounds were developed with the intent to increase quantum yield and release rate and to shift the effective absorbance to longer wavelengths, some of which are highlighted here (Figure 3.1). The structural modifications to the **NB** (**3.4**) class of PPG can be characterized by changes to the aromatic chromophore and substitution at the benzylic carbon. One early effort by Patchornik and Woodward focused on circumventing the formation of the problematic nitroso benzaldehyde **3.13**.[199] Methyl substitution at the benzylic position resulted in the 1-(2-nitrophenyl)ethyl (**NPE**, **3.18**) derivative. Photochemical rearrangement of this derivative led to the corresponding 2-nitrosoacetophenone, which is less prone towards amine condensation. They were able to use this protecting group to demonstrate efficient release of amino acid protecting groups.[199] The 2,6-dinitrobenzyl (**DNB**, **3.19**) derivative was designed to enhance the production of the *aci*-nitro intermediates **3.9** and **3.10**, and ultimately improve the photochemical efficiency of leaving group release. This proved to be an effective strategy and the **DNB** group displayed an improved quantum yield over the classic **NB** PPG, which was attributed to an increase in statistical probability of forming *aci*-nitro intermediates rather than electronic effects from the presence of an additional nitro group.[212,213] The 6-nitroveratryl (**NV**, **3.20**) and the closely related 6-nitropiperonylmethyl (**NP**, **3.21**) derivatives were designed for a

bathochromatic shift of the effective irradiation wavelength. However, the increased absorbance of these groups is not converted to increased photochemical efficiency, and the quantum yield of **NV** is typically an order of magnitude less than that of **NB**. The increased absorbance of the **NV** group is speculated to lead to unproductive photochemical events that do not contribute to release of the leaving group. Nevertheless, the **NV** and **NP** PPGs are among the most widely used **NB** derivatives.[193,202]

The nitrodibenzofuran (**NDBF**, **3.22**) derivative represents a significant improvement in photochemical efficiency compared to the original **NB** PPG. This derivative was first reported by Ellis-Davies for the photochemical release of calcium ions, and it was shown to undergo photolysis 16–160 times faster than other **NB** derivatives.[214] The enhanced photochemical properties of this cage have made it an attractive PPG, and it has since been applied to a number of biological studies including photoregulation of siRNA and peptide activation.[215,216]

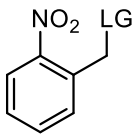

3.4
2-nitrobenzyl (**NB**)

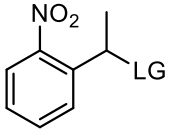

3.18
1-(2-nitrophenyl)ethyl (**NPE**)

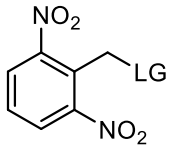

3.19
2,6-dinitrobenzyl (**DNB**)

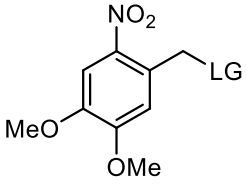

3.20
6-nitroveratryl (**NV**)

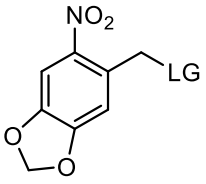

3.21
6-nitropiperonyl (**NP**)

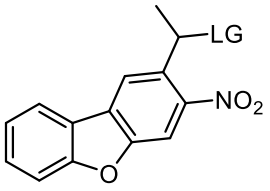

3.22
nitrodibenzofuran (**NDBF**)

Figure 3.1. Select examples of *o*-nitrobenzyl photolabile protecting groups.

3.2.2 *2-(2-Nitrophenyl)ethyl* Photolabile Protecting Groups

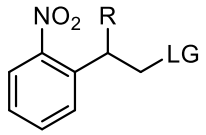

3.23 R = H
3.24 R = CH_3
2-(2-Nitrophenyl)ethyl (**NPE**)

Hasan developed a one carbon homologue of the **NB** protecting groups that, despite structural similarity, has a markedly different deprotection mechanism.[217] The small structural change also resulted in a significant improvement in photochemical efficiency over the **NB** counterparts. Initially, the phenethyl photocage analogues only offered a slight improvement in the release of carbonate leaving groups when compared to **NB** PPGs. However, addition of a methyl group to the benzylic position of the nitro phenethyl photocages considerably added to the efficiency of deprotection.[217] For example, in a photocaging study of 5'-O-nucleoside carbonates, **3.23** released the substrate with a higher quantum yield (Φ_{rel} =0.042) than an **NB** analogue (Φ_{rel} = 0.033). However, caging the substrate with **3.24** added considerably to the efficiency and resulted in a 10 fold increase in quantum yield (Φ_{rel} = 0.35).[218] In addition to the increased photolysis efficiency, the 2-(2-nitrophenyl)ethyl (**NPE**) derived PPGs are also more suitable for the release of amine containing substrates compared to the **NB** PPGs, because the photochemical by-product is unreactive towards amines.

The mechanism of deprotection for 2-(2-nitrophenyl)ethyl (**NPE**) PPGs has not been extensively studied, but the observed nitrostyrene by-product **3.28** is consistent with the proposed pathway.[217] Irradiation of **3.25** leads to intramolecular hydrogen abstraction and from the excited state, and formation of the *aci*-nitro intermediate **3.26**. Deprotonation

of **3.26** by solvent results in the expulsion of the leaving group and the formation of the nitrostyrene by-product **3.28**. The **NPE** groups , the formation of the unreactive nitrostyrene by-product **3.28** rather than the nitroso aldehydes/ketones by-products of the **NB** PPGs makes this class more suitable for the release of amine containing substrates.

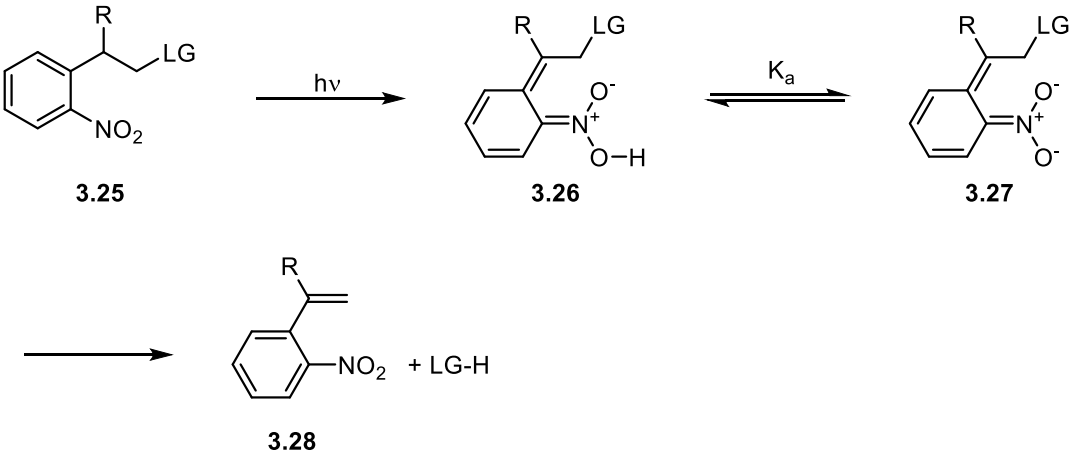

Scheme 3.2. Photodeprotection mechanism for the 2-(2-nitrophenyl)ethyl-based PPGs

Recent modifications to the **NPE** core structure have focused on extending the maximum absorbance to longer wavelengths (Figure 3.2).[219,220] The amino-nitro biphenyl derivatives **3.30** and **3.31**, for example, exhibit a strong absorbance (λ_{max} = 400 nm, ε = 7,500 $M^{-1}cm^{-1}$) in the visible light region. The R groups incorporated at the aniline nitrogen atom serve as effective solubilizing handles for increased aqueous solubility of caged compounds. These compounds have been applied in a recent example of the photorelease of the neurotransmitter GABA. [221]

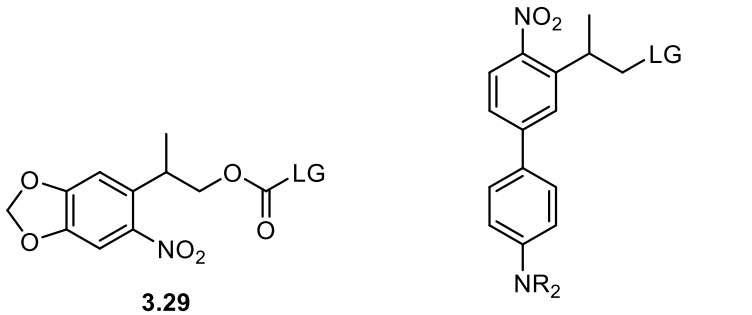

3.29
2-(3,4-methylenedioxy-6-nitrophenyl)-propyloxycarbonyl (**MNPPOC**)

3.30 CANBP R = CH_2CO_2H
3.31 EANBP R = $C_2H_4OCH_3$

Figure 3.2. Select derivatives of the 2-(2-Nitrophenyl)ethyl PPG class

3.2.3 *o*-Nitroanilide Photolabile Protecting Groups

3.32
o-Nitroanilides

The *o*-nitroanilide class of PPG was first reported by Amit and Patchornik in the 1970s as an efficient light sensitive protecting group for esters and carboxylic acids.[222,223] The size of the fused nitrogen heterocycle proved important for the reactivity of the protecting group, and indoline analogues were found to release carboxylic acids very efficiently.[222] Since the seminal reports, the mechanistic aspects of the photo-deprotection have been the focus of a number of studies.[193,224] Early isotopic investigations concluded that the reaction is a rearrangement rather than a solvolysis, as no isotope incorporation was observed upon photolysis in $H_2{}^{18}O$ as solvent.[223] Photoexcitation of **3.33** leads to an acyl migration from the indoline nitrogen atom of **3.33** to one of the nitro group oxygen atoms, forming the highly reactive N–O acyl intermediate **3.34** (Scheme 3.3). Interestingly, the deprotection pathway is solvent dependent, and diverges at this point depending on the reaction media. In organic solution (path A, red arrows), intermediate **3.34** undergoes

nucleophilic attack either by solvent (alcohol or water) or by an external nucleophile to release **3.35** along with formation of the nitro indoline **3.36**. Alternatively, in aqueous solution (path B, blue arrows), a deprotonation occurs at the 2-position of **3.34** to release a carboxylic acid (**3.37**) along with formation of the nitroso indole by-product **3.39**. Substitution of the aromatic ring of **3.33** has been shown to influence the efficiency of deprotection to a certain extent.[225]

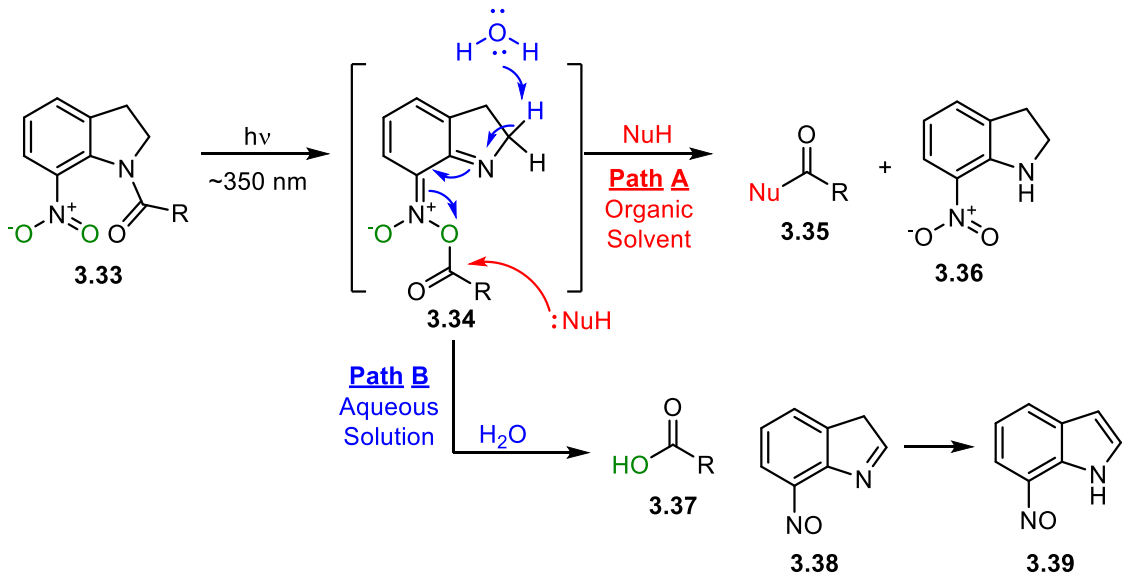

Scheme 3.3. Photodeprotection mechanism for the *o*-nitroanilide class of PPG.

The nitroanilide PPGs have not found widespread application, perhaps due to the limited scope of the functional groups that can be protected. However, their ability to protect carboxylic acids and the reactive nature of **3.34** has resulted in important applications for the protection and synthesis of amino acids.[226] Additionally, nitroanilides have been shown to efficiently release the neurotransmitter GABA, which has proven useful for the interrogation of GABA receptor function.[227]

3.3 ARYLCARBONYL PHOTOLABILE PROTECTING GROUPS

3.3.1 Phenacyl Photolabile Protecting Groups

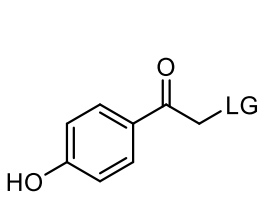

3.40
p-hydroxyphenacyl (**pHP**)

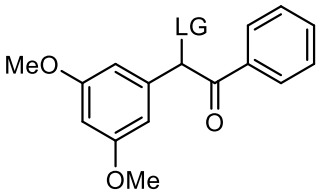

3.41
3',5'-dimethoxybenzoin (**DMB**)

The photocages in this family are grouped based on their structural similarity; they share a common phenacyl core, and the leaving group is attached to the α-position of the carbonyl group. Despite the structural similarities, small variations in substitution at the phenacyl core can alter the deprotection mechanism drastically. The mechanism is also influenced by the nature of the leaving group and the reaction conditions, such as solvent. This class of PPGs can efficiently release good leaving groups such as phosphates, sulfonates, carbonates, and carbamates.[193,194]

3.3.1.1 p-Hydroxyphenacy Photolabile Protecting Groupsl

The *p*-hydroxyphenacyl (**pHP, 3.40**) class of PPG was first reported by Givens[228,229] in 1996, and it has since proven useful in numerous applications including neurobiology and enzyme catalysis.[193,194] The **pHP** group has a number of advantages over other classes of PPGs. First, the release of substrates is very fast, with rate constants on the order of $k_{rel} > 10^8\ s^{-1}$. The deprotection also typically proceeds with high quantum yields, with only one significant by-product. Finally, the hydrophilicity of the **pHP** protecting group typically leads to caged products that have good water solubility, an important property for biological applications.

The photodeprotection upon irradiation of **3.40** at 250-320 nm in neutral aqueous media is proposed to proceed through the excited triplet state, forming the spirodiketone **3.42** and expelling the leaving group (LG-H) (Scheme 3.4). Intermediate **3.42**, deemed the Favorskii intermediate, is prone to hydrolytic ring opening, which yields *p*-hydroxyphenyl acetic acid (**3.43**). The structural rearrangement following the photoexcitation of **3.40** closely resembles the classical ground state Favorskii rearrangement of α-haloketones, hence why this reaction has been coined the photo-Favorskii rearrangement. This unique deprotection mechanism has been the center of a number of studies.[194] The efficiency of the photochemical deprotection is highly dependent on the nature of the leaving group. As a general rule, leaving groups with a pKa < 11 work well, while alcohols and amines with pKa's above that threshold are usually not successfully released.[194]

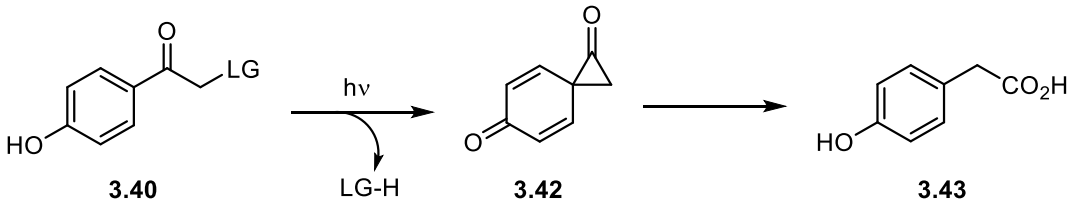

Scheme 3.4.Photodeprotection mechanism of the *p*-hydroxyphenacyl PPG.

Other important advantages of the pHP protecting group are associated with the by-product **3.43**. Unlike the photochemical products of the *o*-nitrobenzyl class, **3.43** is essentially transparent above 290 nm and therefore does not interfere with the absorbance of the starting material (**3.40**). Additionally, *p*-hydroxyphenylacetic acid (**3.43**) is photochemically stable and biologically inert, making the **pHP** group an attractive photocage for biological applications.

3.3.1.2 Benzoin Photolabile Protecting Groups

The benzoin class of PPG was first reported by Sheehan in the 1960s.[228] Early studies quickly revealed that the deprotection efficiency significantly improved through the use of a 3',5'-dimethoxybenzoin group. The release of carboxylates and phosphates from **DMB** (**3.41**) proceeds quickly to quantitatively afford the desired product and **3.47** (Scheme 3.5). The reactions proceed smoothly in both polar and apolar solvents and the deprotection mechanism was found to be independent of the nature of the leaving group. Thus, poor leaving groups such as amines and alcohols can be released directly with the DMB protecting group.

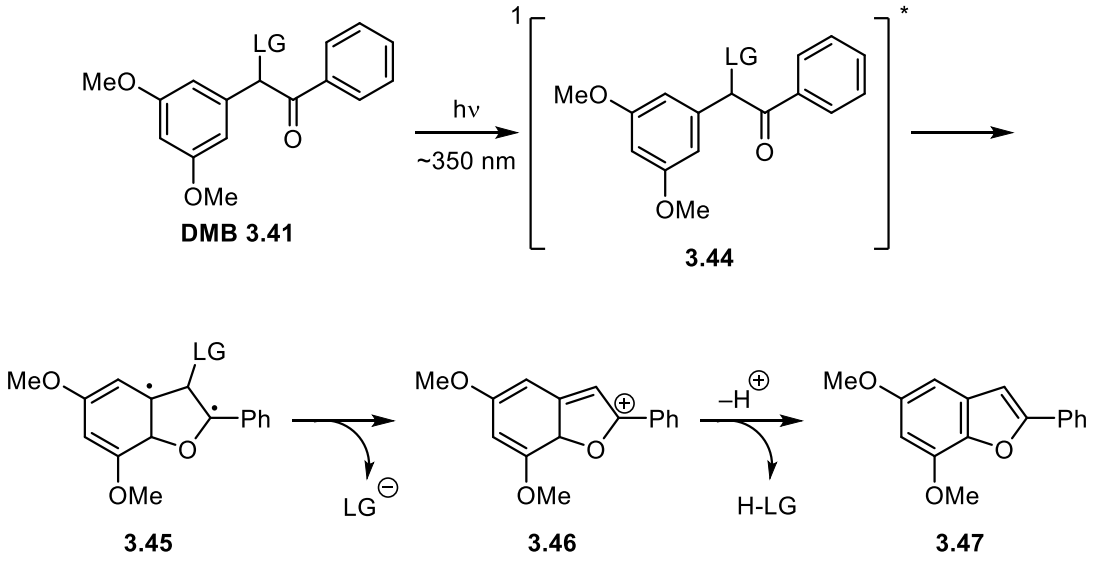

Scheme 3.5. Photodeprotection mechanism for the 3',5'-dimethoxybenzoin class of PPG.

While there are no photochemical reasons that prevent the use of a particular leaving group with **DMB**, the preparation of certain derivatives can be difficult. A common strategy for the protection of alcohols and amines with **DMB** PPGs is to start from **3.48** and convert it to the activated acylating reagent **3.49** through treatment with carbonyldiimidazole or phosgene. However, **3.49** is prone to intramolecular cyclization to

give **3.52**, which is not useful for the preparation of photocaged compounds. Furthermore, the reaction of **3.49** with primary amines will form the carbamate **3.50**, which can also undergo an unproductive intramolecular cyclization to give **3.51**, which is photochemically inert (Scheme 3.6).[188] Additionally, the hydrophobicity of the **DMB** core often results in caged compounds with poor aqueous solubility, thus further limiting the adoption of this PPG for biological studies.[193]

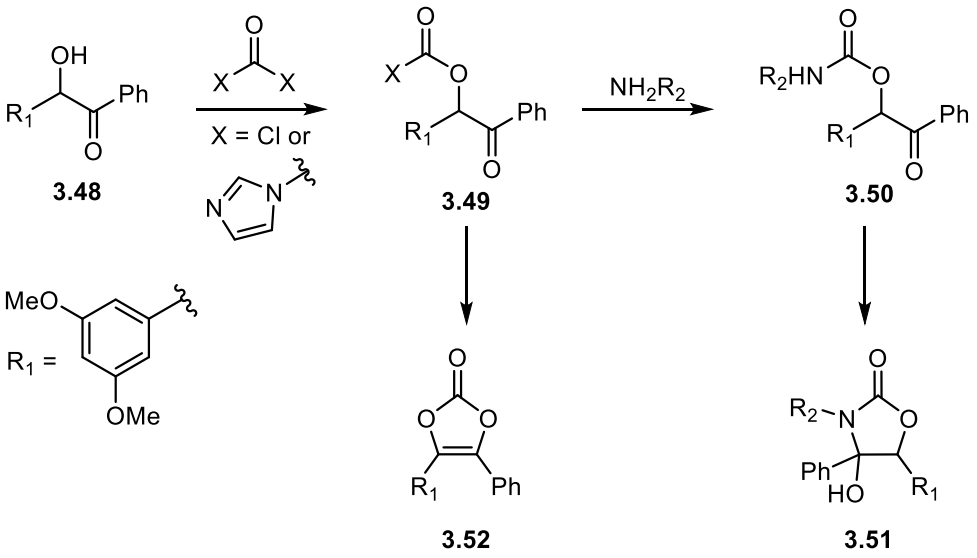

Scheme 3.6 Problematic side reactions when protecting alcohols and amines with **DMB**.

3.3.2 Deprotection Via Photoenolization

The addition of alkyl groups to the aromatic core of the arylcarbonyl class of PPG results in deprotection mechanism that differs from the phenacyl PPGs. Unlike the phenacyl aryl carbonyls, the following protecting groups are classified by deprotection mechanism rather than structural similarity. The releasing mechanism for these PPGs involves hydrogen abstraction, photoenolization, and ground-state transformation to the enol to release the compounds of interest.

3.3.2.1 2-Methyl-Substituted Acetophenones

The 2-alkyl-substituted acetophenones were reported by Klán and Wirz as PPGs for the release of a variety of good leaving groups including carbonates, carbamates, phosphates, and sulfonates.[230,231] Upon irradiation at 250–280 nm, **3.53** is excited to its singlet state **3.54** (Scheme 3.7). After an intersystem crossing (ISC) to the excited triplet state **3.55**, a 1,5-hydrogen abstraction occurs, yielding the biradical **3.56**. This intermediate will decay into the two isomeric enols **3.57** and **3.58**. The (*Z*)-photoenol **3.57** is also formed from the enolization of the excited singlet state **3.54**, but this intermediate is short lived and quickly undergoes a sigmatropic rearrangement to regenerate the starting material **3.53**. The (*E*)-photoenol **3.58** however, requires an intermolecular protonation to quench, and is therefore persistent enough to undergo intramolecular cyclization to afford the deprotection by-product **3.59** and the released substrate (H-LG). The mechanism of deprotection for **3.53** reveals why this class of PPG is best suited for good leaving groups. Given that the leaving group is expelled via S_N2 displacement through an intramolecular cyclization of **3.58**, poor leaving groups such as phenols, alcohols and amines are not good candidates for use with this class of PPG.

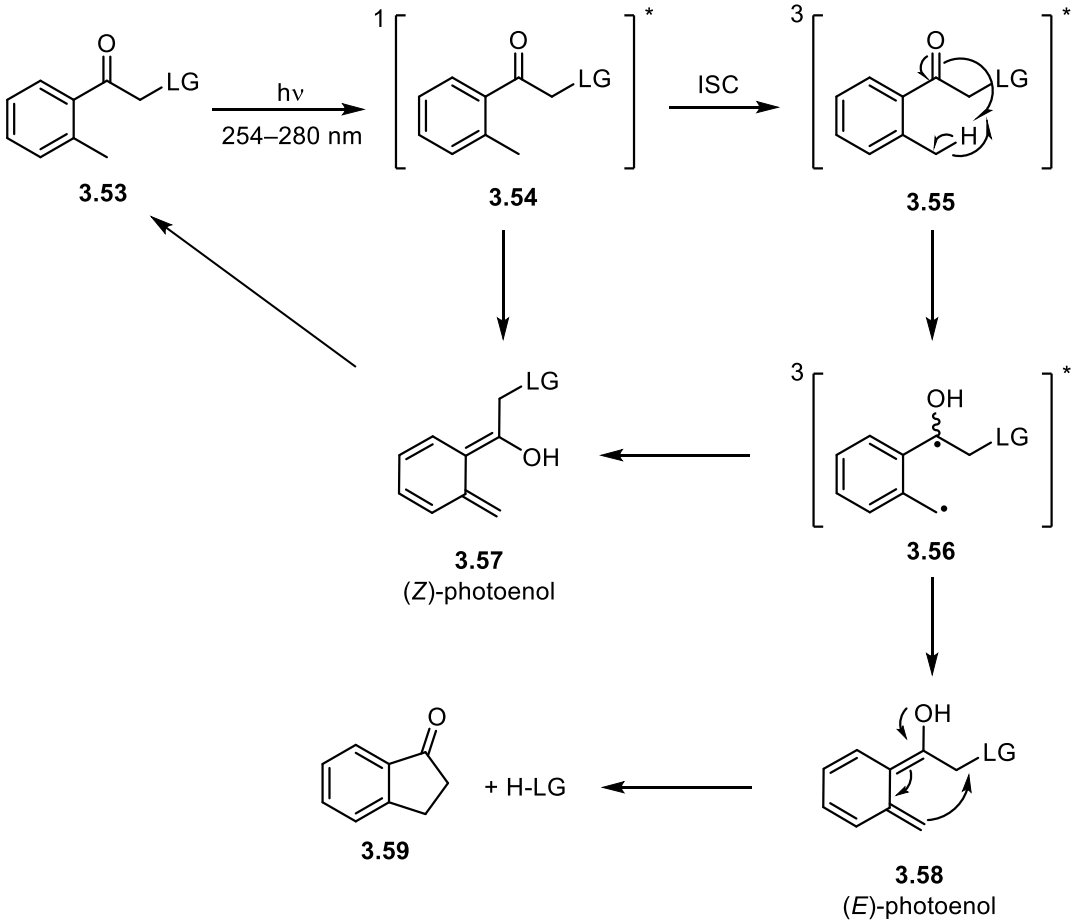

Scheme 3.7 Photodeprotection mechanism of the 2-methylacetophenone PPG.

The 2-methyl-acetophenones have a number of disadvantages associated with them when compared to other PPGs that have limited their applications to only a few examples of photoresponsive polymers.[193,227] Compared to other classes of PPGs, the quantum yields and release rates for the 2-methyl-acetophenones are low. Additionally, the deprotection of **3.53** requires irradiation with UV light, which has limited its use for *in vivo* biological studies because the deprotection wavelength will cause DNA damage to the cells.. The

hydrophobicity of **3.53** typically results in caged compounds that have poor aqueous solubility, which has further limited its applications in biological systems.

3.3.2.2 2-Ethylene-Subtituted Arylcarbonyl Photolabile Protecting Groups

Ullman reported an alternative strategy for the arylcarbonyl PPG core where the leaving group was attached to the alkyl branch of the phenyl group.[232] Irradiation of the 2-ethylene-substitued aryl carbonyl **3.60** leads to the formation of the photoenol **3.61**, which can tautomerize back its keto form, expelling the leaving group (H-LG) and forming the styrene by-product **3.62**.[233] The deprotection is not greatly affected by the solvent, and the reaction is typically slow with low photochemical efficiency. Efficient deprotections can be achieved for some good leaving groups such as tosylates, but with poor leaving groups, elimination of the leaving group is the rate determining step and it is competitive with protonation of **3.61** to reform **3.60**.[202] Attempts to improve the photochemical properties of **3.60** through structural modifications did not result in significantly better PPGs than the parent compound.[234] Consequently, the use of this class of PPG has been minimal since its discovery.

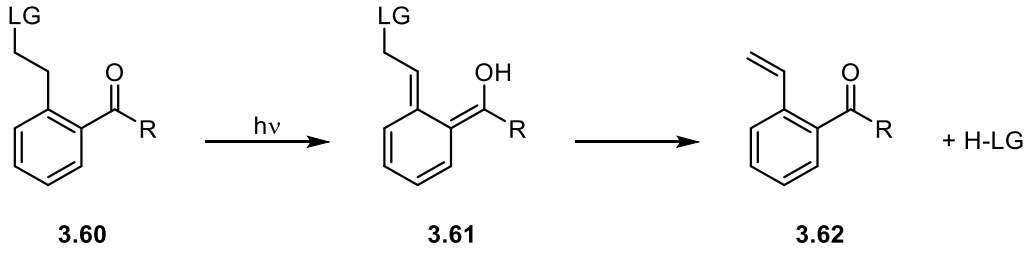

Scheme 3.8. Photodeprotection mechanism for the ethylene-substituted arylcarbonyl PPG

3.3.2.3 Intramolecular Lactonization

A relatively recent example of an interesting photoenolization reliant release of alcohols was reported by Gudmundsdottir in 2003.[235] Upon irradiation with UV light, **3.63** is converted to the photoenol **3.64** via the triplet excited state (Scheme 3.9). This intermediate then undergoes a [2+2] cycloaddition to give the benzocyclobutanol **3.65**. Subsequent intramolecular lactonization results in the release of a free alcohol in high chemical yield (90%) and the formation of **3.66**. The ability to directly release a free alcohol is a rare trait for a photolabile protecting group, however, **3.63** has not been widely applied to many areas, likely due to the long reaction times (hours) to achieve the high yielding release of alcohols.

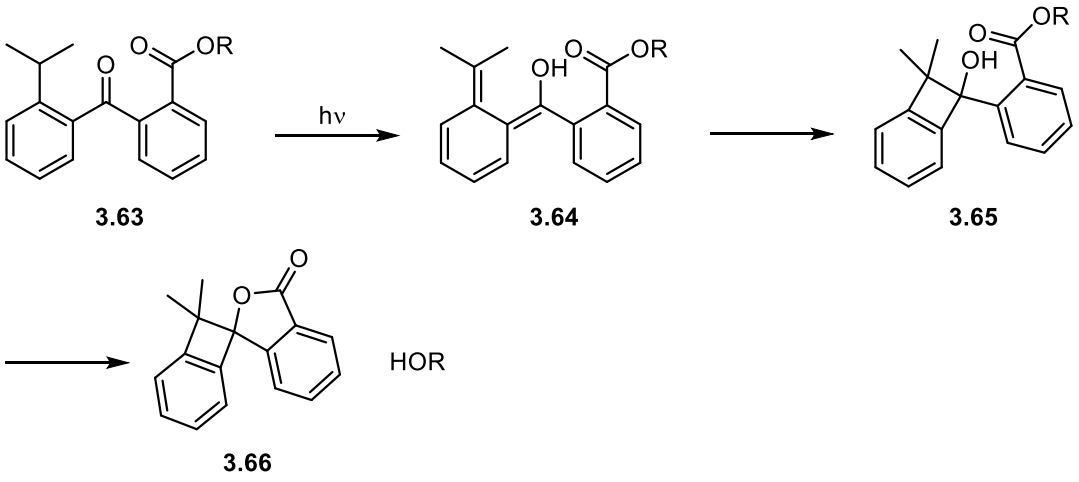

Scheme 3.9. Photodeprotection mechanism of **3.63** via intramolecular lactonization

3.4 Coumarin Based Photolabile Protecting Groups

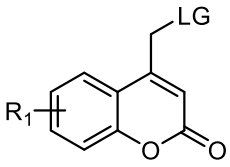

3.67

The coumarin class of photolabile protecting groups was first discovered by Givens in his studies on the photoreactivity of coumarins releasing phosphate esters.[236] This relatively new class of photocages has attracted considerable attention because it offers distinct advantages that include large absorption coefficients at longer wavelengths (λ_{max} = 350–475 nm) and fast release rates. However, these advantages are offset by coumarin's marginal quantum yields and low aqueous solubility. Since the seminal report, there has been a wide variety of modified coumarin PPGs that have sought to address these disadvantages.[193,237]

3.4.1 Mechanism of Deprotection

The mechanism of deprotection for the coumarin protecting groups is proposed to occur via heterolytic bond cleavage from the excited singlet state **3.69** (Scheme 3.10).[238,239] The decay of excited **3.69** back to the ground state **3.68** via fluorescence and nonradiative deactivation is competitive with the productive heterolytic cleavage to give **3.70**. While it is possible **3.70** could arise from the homolytic cleavage of **3.69** followed by single electron transfer, mechanistic studies have revealed little evidence for this pathway. In the event of formation of a singlet radical pair from **3.69**, one would expect hydrogen abstraction products derived from the excited triplet radical pair after intersystem crossing. However, in mechanistic studies of phosphate leaving groups with coumarin protecting groups, only trace amounts of these products were detected. Additionally, no phosphorescence, which

would be characteristic if there were significant population of any triplet states, could be detected.[239] Once the ion pair **3.70** has formed, it is possible for ion recombination to occur and return the starting material **3.68**. Product formation is proposed to occur in two steps, beginning with the escape of the ions from the solvent cage, followed by nucleophilic capture of the coumarin cation **3.71** by solvent to deliver **3.72** and the deprotected material (H-LG).[239]

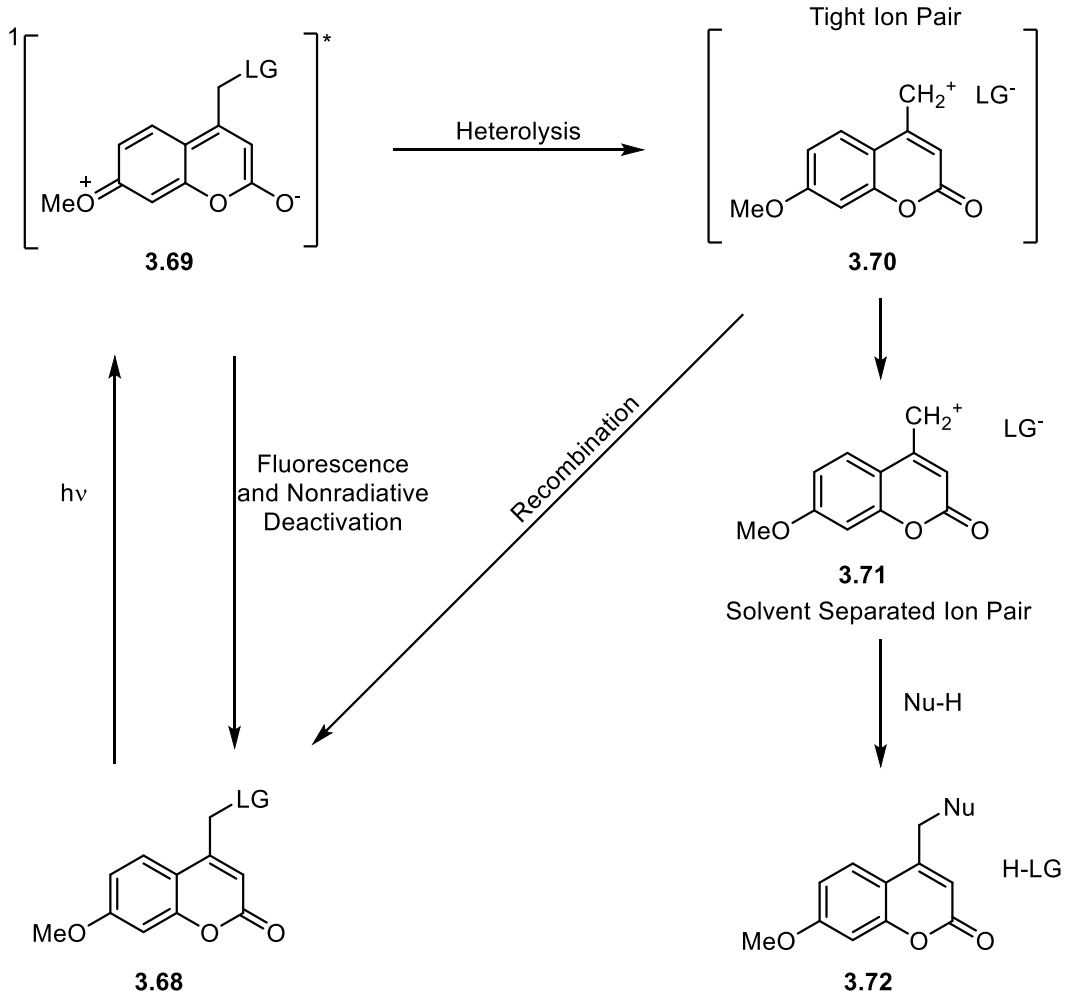

Scheme 3.10 Photodeprotection mechanism for the coumarin PPGs

One major disadvantage of the coumarin PPGs is inherent with the photosolvolytic mechanism of deprotection. The propensity for recombination of the newly formed ions upon heterolytic cleavage of **3.69** is increased with poor leaving groups such as phenols, alcohols, thiols and amines. Masking poor leaving groups through carbonate or carbamate linkers is not always effective because the decarboxylation of the released substrate can be slow and often becomes rate limiting, which significantly reduces the apparent rate of release.[193] Hence, this class of PPG is best suited for good leaving groups such as phosphates and sulfonates. Although, the release rates for these good protecting groups are among the fastest available for a PPG, making the coumarin family a useful group for monitoring very fast physiological events.[187]

3.4.2 Select Examples of Coumarin PPG Derivatives

The utility and distinct advantages of the coumarin family of protecting groups has drawn significant attention to this class of PPG, culminating in the development of a broad array of coumarin derivatives.[193,194,202] The 6-bromo-7-hydroxycoumarin-4-methyl group (**BHCM**, **3.73**) was an interesting early derivative that resulted in a 50 nm redshift of the maximum absorbance (λ_{max} = 370 nm) compared to the methoxy coumarin (**MCM**, **3.68**) (λ_{max} = 320 nm). The **BHCM** derivative also offered the added benefit of increased aqueous solubility due to the acidic phenol moiety.[240,241] Another improvement came from the incorporation of the 7-amino substituent, exemplified by the diethylaminocoumarin (**DEAC**, **3.74**) derivative, which resulted in a further red shift of the maxiumum absorbance (λ_{max} = 390 nm).[242,243]

The innovation of incorporating an amino group to the coumarin core offered a new synthetic handle to install solubilizing groups to address the poor aqueous solubility of the coumarins. The **BCMAC** (**3.75**) derivative was designed with this idea in mind and was

successful in providing significant improvements in aqueous solubility.[193] Ellis-Davies reported the use of **DEAC450** (**3.77**), with a goal to shift the maximum absorbance further into the visible region, as well as address the poor aqueous solubility of the coumarins.[244] The clever design of **3.77** with the extended conjugation of enone moiety in combination with the solubilizing amino acid group resulted in a photocage with a maximum absorbance well into the visible region (λ_{max} = 450 nm) as well as improved aqueous solubility. The **thio-DEAC** (**3.76**) derivative also resulted in a photocage with a high absorptivity in the visible region (λ_{max} = 470 nm). This photocage was successfully used for light regulated protein expression in zebra fish.[245]

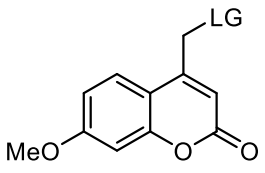

3.68
(**MCM**)

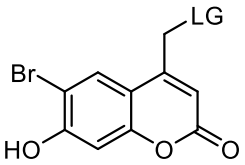

3.73
(**BHCM**)

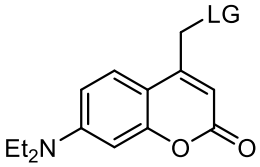

3.74
(**DEAC**)

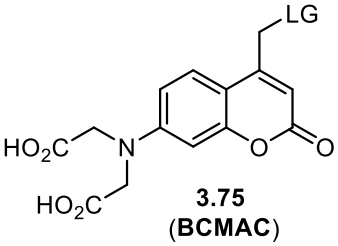

3.75
(**BCMAC**)

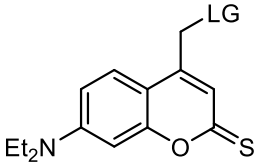

3.76
(**thio-DEAC**)

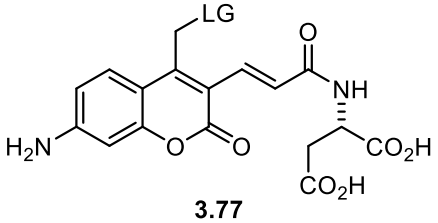

3.77
(**DEAC450**)

3.5 BODIPY DERIVED PHOTOLABILE PROTECTING GROUPS

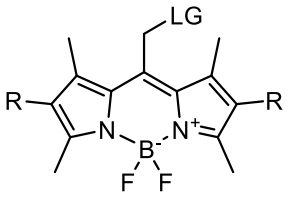

3.78

The BODIPY-based family is an emerging class of PPG that absorbs light in the visible region (λ_{max} 520–560 nm). The photolysis of BODIPY PPGs is proposed to occur via a heterolysis mechanism similar to the coumarin PPGs. Excitation of **3.78** results in heterolytic cleavage, and the cation **3.79** is then trapped by solvent. The nature of the deprotection mechanism leaves the BODIPY with similar challenges as the coumarin PPGs with regard to the release of poor leaving groups.

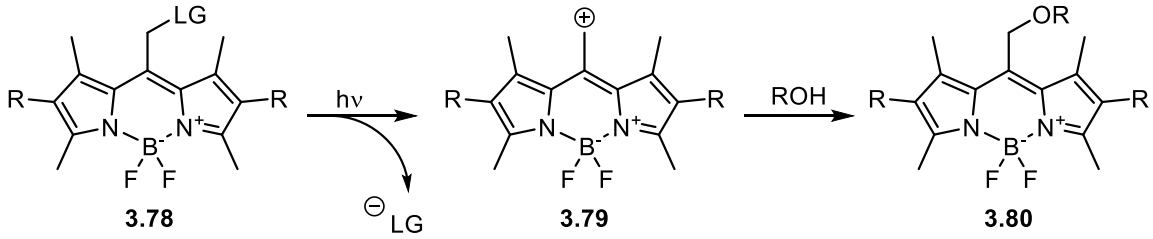

3.78 **3.79** **3.80**

Scheme 3.11. Photodeprotection of BODIPY PPGs via heterolytic cleavage.

Initial reports (Y = alkyl) of BODIPY PPGs disclosed slow (hours) deprotection of carboxylic acids,[246] but Feringa and Szymański recently reported the efficient release of amines through carbamate linkers within 10 minutes of irradiation at 520 nm (Equation 3.5) as monitored by ultra performance liquid chromatography (UPLC).[247] This class of PPG is still new and has yet to be applied to any biological studies, but it strong absorption at longer wavelengths makes it an attractive alternative to other well established classes of PPGs.

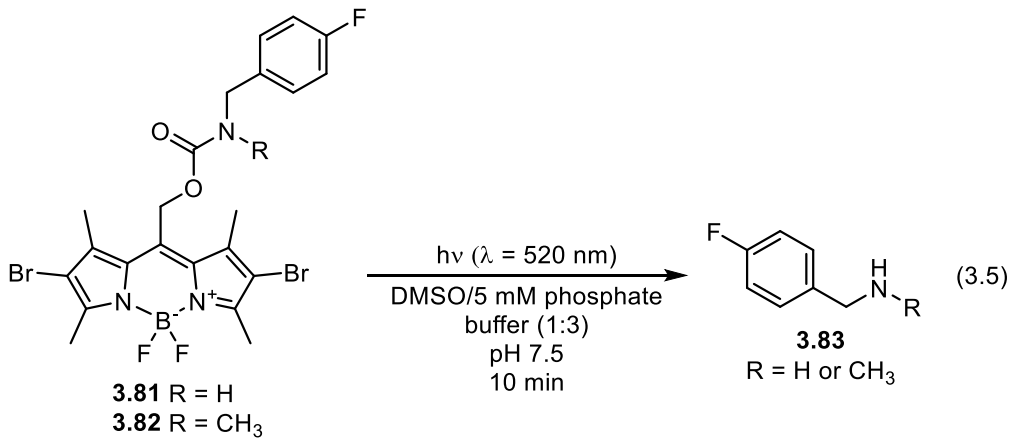

(3.5)

3.6 Biological Application of Photocages: Light Controlled Gene Expression

Light represents a unique tool in the study of genes and regulating cellular processes because of the non-invasive spatial and temporal control it can provide.[248] Photocages have proven to be invaluable tools for the regulation of gene expression via small molecules. Biologically active molecules can be rendered inert through chemical modification with photolabile protecting groups, and upon irradiation with non-damaging light (> 360 nm), the compound can be quickly released and perform its cellular function. The photocaging of small molecules that regulate heterologous gene expression systems has become a powerful tool for controlling cellular processes.[249]

3.6.1 Overview of Small Molecule Regulated Gene Expression Systems

Over the last few decades, a variety of heterologous gene expression systems that are regulated by small molecules have been developed.[250–253] In general, these systems take advantage of specific interactions between prokaryotic repressor protein/operon pairs to create systems where gene expression can be induced in response to specific small molecules in eukaryotic cells. For most of these expression systems there exists both an "expression-ON" and an "expression-OFF" variant. This nomenclature refers to gene

expression being turned on or off in the presence of the repressor ligand. Although mechanisms can vary between systems, typically for an expression-ON system, there is a repressor protein that binds to its operator downstream of a constitutive promoter, thereby inhibiting transcription of the target gene of interest (A, Figure 3.3). Introduction of the repressor ligand leads to a protein binding event that causes a conformational change in the protein, ultimately resulting in the dissociation of the repressor from its operator through a process known as derepression. Once the repressor is removed, transcription of downstream genes is free to occur (B, Figure 3.3).[254]

In contrast, the expression-OFF systems, are designed to prevent transcription of downstream genes in the presence of the repressor ligand. These systems are typically created through fusing a transactivation domain with a repressor protein. The hybrid activator-repressor binds to its operator upstream of a promoter and initiates gene transcription (C, Figure 3.3). When the repressor ligand is present however, it binds to the repressor which results in derepression and inhibition of gene transcription (D, Figure 3.3).[254]

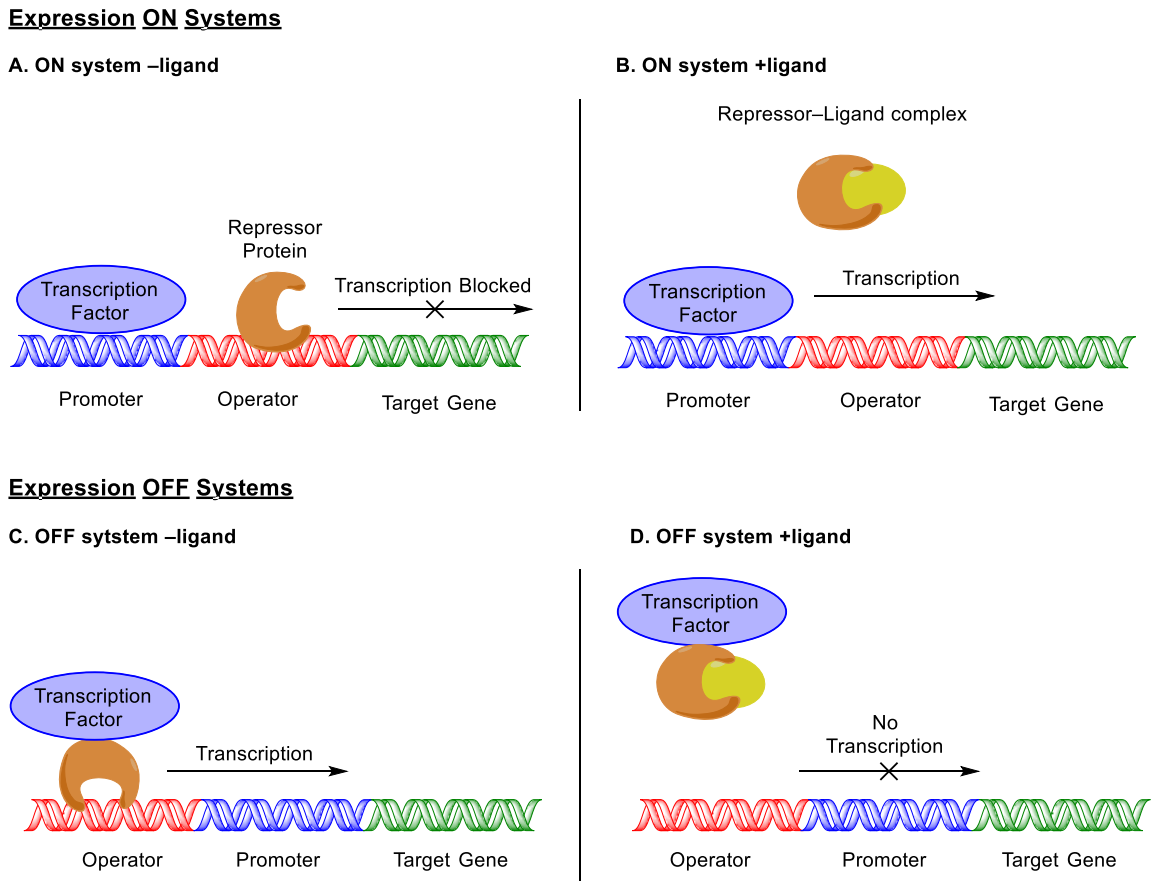

Figure 3.3 Generic examples of expression-ON and expression-OFF systems

A) Expression-ON system in the absence of ligand. The repressor protein binds to its operator downstream of a constitutive promoter inhibiting transcription of downstream genes. **B)** Expression-ON system in the presence of ligand. The repressor ligand binds to the repressor protein resulting in derepression and gene transcrtiption is intiated. **C)** Expression-OFF system in the absence of ligand. The hybrid repressor-transactivator is free to bind to its operator and transcription of downstream genes occurs. **D)** Expression-OFF system in the presence of ligand. The repressor ligand binds to the hybrid repressor-transactivator and causes derepression and thereby inhibiting transcription of genes.

3.6.2 Tetracycline Dependent Gene Expression

3.6.2.1 Tetracycline Resistance in Bacteria

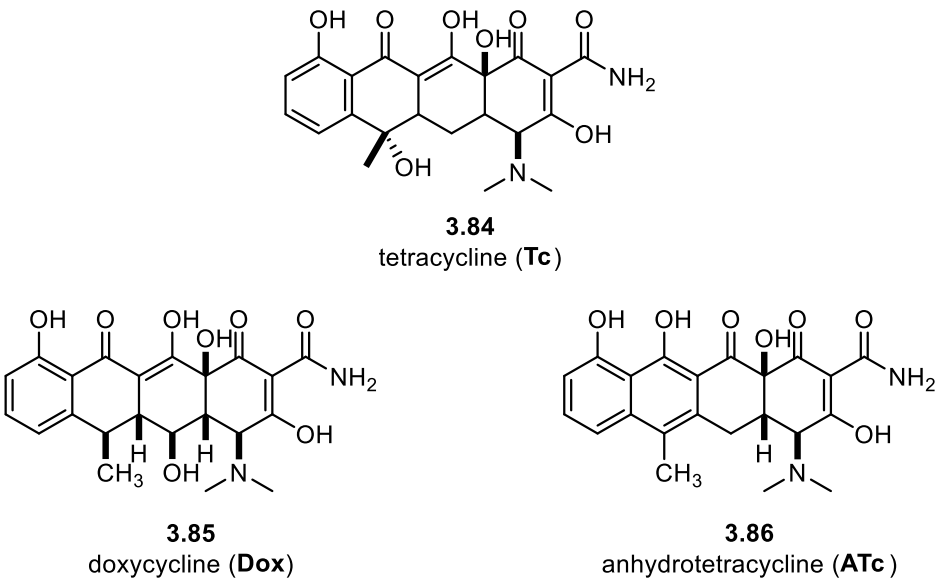

Figure 3.4 Select tetracycline derivatives.

The tetracyclines (Figure 3.4) are a family of antibiotics that act by binding to the bacterial ribosome, which interrupts polypeptide chain elongation and ultimately killing the bacterial cell.[255] Many bacteria have developed mechanisms of resistance to this antibiotic, the most common of which involves a membrane associated protein (TetA) that exports the antibiotic out of the cell before tetracycline (**Tc**, **3.84**) can inhibit translation.[256] The expression of the TetA protein is tightly regulated by the tetracycline repressor protein TetR, which binds with high specificity to two palindromic DNA operators, *tetO*1 and *tetO*2, containing the genetic information for the TetR and TetA proteins. Tetracycline (**3.84**) is believed to enter the cell by diffusion across the cytoplasmic membrane in its

neutral form, after which, the keto-enol moiety forms a complex with Mg^{2+} to give the bioactive **[Tc-Mg]**$^{+}$ complex **3.87** (Equation 3.6). The **[Tc-Mg]**$^{+}$ complex (**3.87**) binds to the TetR protein with high affinity, inducing a conformational change in the protein and causing a rapid disassociation from the DNA operators, ultimately allowing transcription of TetR and TetA. The induced TetA protein integrates into the cytoplasmic membrane where it can export **3.87** from the cell.[255]

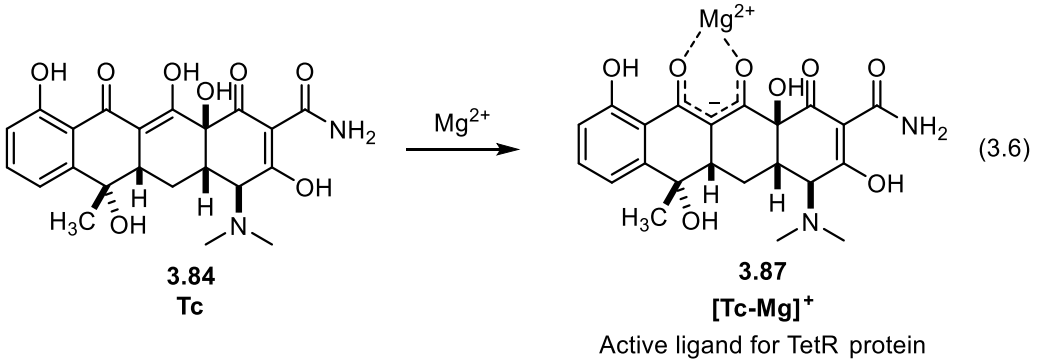

(3.6)

3.6.2.2 Tet$_{ON}$ Gene Expression

Gossen took advantage of the highly specific **[Tc-Mg]**$^{+}$ -TetR-*tetO* interactions of bacteria cells to develop the "TET$_{ON}$" expression system as a tool to regulate gene expression in eukaryotic cells.[257–259] Four DNA sequences of the wild type TetR protein were mutated so that the protein's binding to the *tetO* operon could only occur when a tetracycline antibiotic was bound to the protein. This reverse TetR (rTetR) protein was then fused with the transactivator protein VP16 from the Herpes simplex virus to create a hybrid protein (rtTA) that would initiate gene transcription upon its binding to the *tetO* operator. Thus, binding of a tetracycline ligand to the rtTA protein results in the protein-ligand complex biding to the *tetO* operator, and transcription of downstream genetic information

is initiated. Target genes of interest, such as fluorescent reporter proteins, can be placed downstream of the *tetO* operon, and their transcription will ultimately be controlled by the presence of a tetracycline antibiotic.

Gossen demonstrated control over expression of luciferase, a fluoresecent reporter protein, in HeLa cells with his tetracycline dependent system. He tested several tetracycline analogues and he found that doxycycline (**Dox**, **3.85**) and anhydrotetracycline (**ATc**, **3.86**) were the most potent stimulators of luciferase activity, while tetracycline (**Tc**, **3.84**) was a only moderate effector.[257,259]

The TET_{ON} system has since become a powerful tool for regulating gene expression in cells and transgenic animals. The low toxicity of the tetracyclines and their high affinity for the TetR protein, has enabled the use of these antibiotics at concentrations that cause no appreciable adverse effects in transgenic animals, avoiding the problems associated with many other gene regulation systems.[250]

3.6.2.3 Photocaged Doxycycline: Light Controlled Tet_{ON}

Cambridge developed a light-controlled variant of the TET_{ON} system using doxycycline (**3.85**) caged with the UV-labile **NV** (**3.20**) *o*-nitrobenzyl PPG.[260,261] The synthesis of these protected **Dox** compounds was non-trivial however, owing to the many different reactive unprotected functional groups of **3.85**. The **NV** protecting group was converted into a reactive alkylating agent through condensation with hyrdrazine, followed by oxidation of the resultant hydrazone with MnO_2 to afford the diazo compound **3.87** (Equation 3.7). Treatment of **3.85** with freshly prepared **3.87** afforded **3.88** as a mixture (1:1) of diastereomers in 8% yield (Equation 3.8).

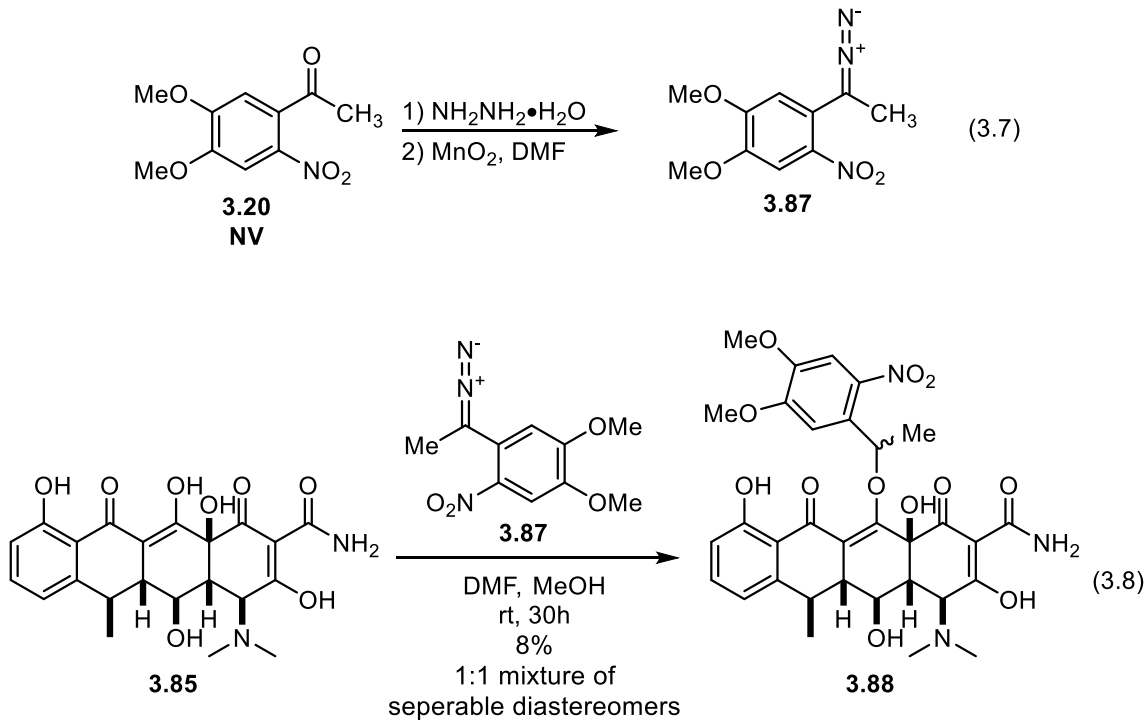

The caged doxycycline derivatives **3.88** were then incubated with hippocampal cells obtained from transgenic mice that were designed for tetracycline dependent expression of green fluorescent protein (GFP). Surprisingly, Cambridge found that one of the caged doxycycline diastereomers of **3.88** maintained bioactivity, inducing significant expression of GFP even in the absence of light, despite only differing in the stereochemistry of the benzylic methyl group of the photocage. Fortunately, the diastereomers could be separated via HPLC and the bioinactive isomer was used in the gene expression studies.[260,261] Incubation of the hippocampal cells with **3.85** led to widespread expression of GFP, whereas incubation with the bioinactive diastereomer of **3.88** resulted in little to no expression of the fluorescent reporter. Irradiation of the cell cultures incubated with inactive **3.88** using a 290–370 nm pulse of light resulted in photolysis of the **NV** cage, release of active **3.85**, and expression of GFP.

Cambridge was also able to demonstrate light activated expression of GFP in embryos of the transgenic mice using the whole-embryo culture system. After removal of 10.5 day old embryos, and incubation with **3.85**, widespread expression of GFP was observed. Incubation with the bioinactive isomer of **3.88** resulted in some background expression of GFP, but it was minimal. However, photoactivation of the embryos incubated with **3.88** through UV irradiation resulted in significant expression of GFP.

Cambridge's work with light activated Tet_{ON} indicates that the system should be applicable wherever the standard Tet_{ON} system is functional. This light activated variant is valuable in that it offers a high degree of spatial and temporal control over expression of target genes. This could be a valuable tool for probing and manipulating complex biological systems.

3.6.3 Erythromycin Dependent Gene Expression

3.6.3.1 Erythromycin Antibiotic Resistance

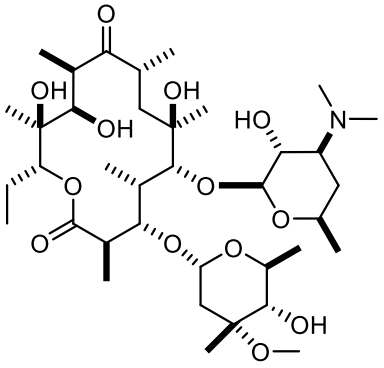

3.89
Ery

Erythromycin (**3.89**, **Ery**) is a 14-membered macrolactone antibiotic that exhibits antibiotic activity by altering ribosome function in a manner that prevents prokaryotic protein synthesis.[262] Many strains of bacteria have developed resistance to macrolide antibiotics through mechanisms that include ribosome modification, efflux of the drug, and

enzymatic modification of the antibiotic itself.[263] One method of resistance found in *E. coli* relies on a 2'-phosphotransferase enzyme, Mph(A), that inactivates erythromycin through phosphorylation of the 2'-desoasamine hydroxyl group. The *mphA* gene is regulated by the repressor protein MphR(A) that binds to its operator (ETR) upstream of its own promoter, PmphR, and the *mphA* gene cluster to regulate transcription of Mph(A) and itself. Erythromycin binds to MphR(A) to induce a conformation change that causes disassociation from the operator, initiating transcription of Mph(A) and MphR(A), conferring the bacteria with erythromycin resistance only when the antibiotic is present.[262,263]

3.6.3.2 Photocaged Erythromycin: Light Controlled Ery$_{ON}$

Deiters used the specificity of the MphR(A)/ETR/PmphR interactions to create an expression-ON system for bacterial cells where the transcription of target genes was controlled by the erythromycin antibiotic (A,B Figure 3.3).[262] The PmphR promoter was placed upstream of the ETR operator so that the repressor MphR(A) inhibited transcription of target genes in the absence of **3.89**. This system was further enhanced to achieve spatial and temporal control over gene expression through incorporation of a photocaged erythromycin derivative, which ultimately created an inducible gene expression method controlled by light. Dieter's efforts towards the goal of a light activated Ery$_{ON}$ system began with attempts to prepare photocaged derivatives of **3.89** directly, but he was unable to do so for reasons not specified.[262] Instead, he directed efforts towards caging the 9-oxime analog of erythromycin **3.90** that was confirmed to retain biological activity. Towards this goal, the ketone moiety of **3.89** was condensed with hydroxyl amine to give **3.90** in 50% yield. Alkylation of **3.90** with 6-nitropiperonyl chloride (**3.91**) delivered the caged erythromycin derivative **3.92** in 87% yield (Scheme 3.11).[262]

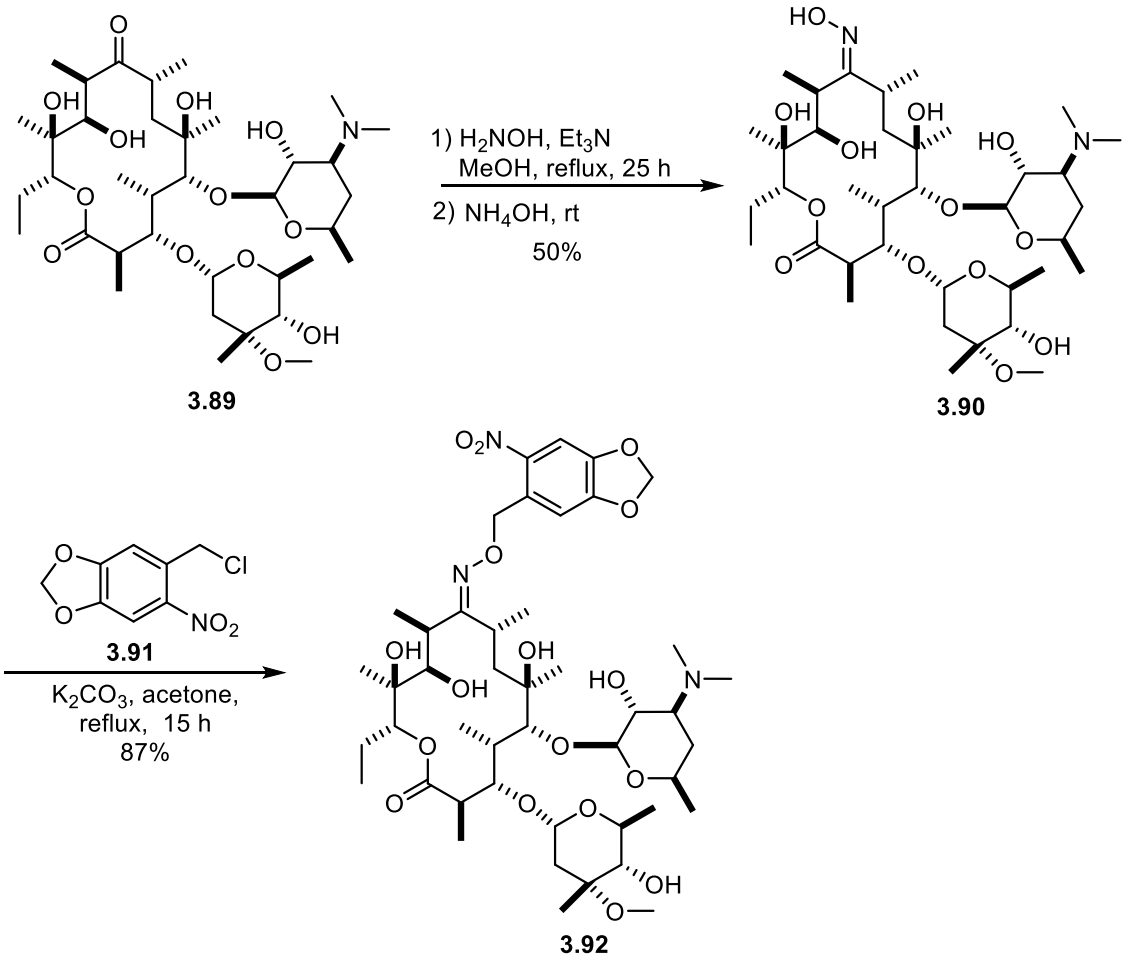

Scheme 3.11. Preparation of photocaged erythromycin derivative **3.92**.

Deiters then used **3.92** to demonstrate light controlled expression of GFP in *E. coli* cells. The oxime **3.90** was shown to induce expression of GFP in the absence or presence of UV irradiation, while the caged derivative **3.92** only displayed significant expression of GFP in the presence of UV irradiation. While Deiters only demonstrated this light activated Ery_{ON} system in prokaryotic cells, there have been several other examples of MphR(A) regulated systems in mammalian cells.[251,264] Therefore, it is possible that this light activated

variant demonstrated by Deiters could be applied to mammalian systems for investigating more complex biological environments.

3.7 Summary of Photolabile Protecting Groups

Since the seminal reports of photolabile protecting groups, the field has grown dramatically and the applications of PPGs now span many different scientific disciplines.[193,202] Photolabile protecting groups have been widely adopted in the field of biology because of their potential to elucidate better understandings of complex biological systems. PPGs have become invaluable tools for time-resolved studies of chemical processes in living cells. The potential biological applications of PPGs have been one of the main driving forces for the invention of new protecting groups and chromophores. Addressing the demands of dynamic *in vivo* events in living organisms will be a constant motivator and source of inspiration for new photocages. The recent upsurge in development of new PPGs has been driven by demands for better sensitivity, faster release rates, increased aqueous solubility, and better absorption properties. Furthermore, new photocages are constantly being developed because there exists no one PPG that will meet the demands for every application. A wide selection of PPGs is therefore important, so that an appropriate PPG will be available for a given application.

Select examples from some of the most common classes of PPGs are shown in Figure 3.5. The *o*-nitrobenzyl groups **3.20** and **3.21** remain the most popular PPGs by far. Their inherent disadvantages are offset by their ability to release a wide variety of groups and the ease by which caged substrates can be prepared from readily available commercial precursors. Nitrodibenzofuran **3.22** represents an important innovation for this class of PPG that will likely see continued use in the future. The 2-(2-nitrohpenyl)ethyl PPGs exemplified by **3.30** are gaining popularity as well.[221] These cages typically display

efficient deprotections and the aniline nitrogen provides a functional handle for the installation of solubilizing groups. The phenacyl cages **3.40** and **3.41** are especially useful in photochemical electrophysiology studies due to their fast release rates[194,234] Applications of these cages remain somewhat limited however due to the lack of derivatives that decage upon irradiation with visible light. Finally, the coumarin and BODPIY cages **3.77** and **3.78** both represent promising new classes of PPGs. Their fast deprotection rates and absorbance of long wavelengths make them attractive choices for biological applications. However, both of these classes are limited by their photosolvolysis mechansim, making them only applicable to good leaving groups. Nonetheless, the coumarins have already been applied to a number of biological studies, and it is likely that the BODIPY cages will as well.

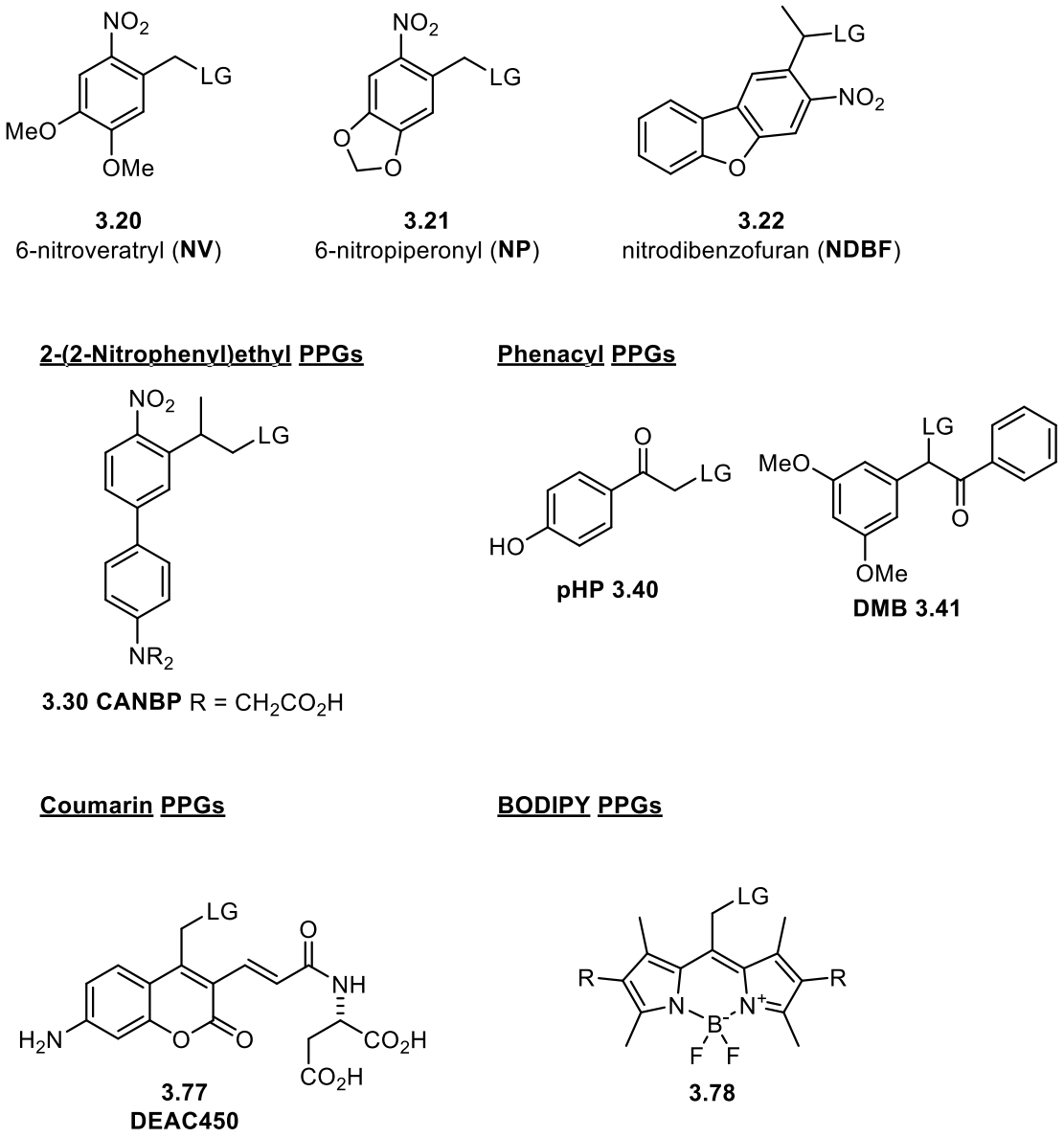

Figure 3.5. Select examples from most common classes of PPGs

The design of sophisticated and more demanding biological applications will continue to drive discovery of new derivatives and classes of PPGs. Increasing the usefulness of photocages will lead to exciting advances in the fields of drug delivery,

materials science, molecular biology, and neurobiology. With regard to neurobiology, we are currently working towards a genetic method for light controlled labeling of active neurons as part of a collaborative effort with Dr. Boris Zemelman. This system will rely on a gene expression gate that is controlled by photocaged small molecules, which has given us first-hand experience in designing and synthesizing caged molecules for use in a biological investigation. If successful, this method could lead to an unprecedented understanding of the brain and neural networks associated with cognitive and behavioral states.

Chapter 4: Synthesis of Photocaged Ligands

4.1 Introduction

Recent developments in the field of neuroscience have indicated that collections of individual neurons work together to form larger structures, and it is these ensembles of neurons that are the true units of function that make up neural circuits.[265] Consequently, the elucidation of groups of neurons that are responsible for cognitive and behavioral events has become a fundamental goal of neuroscience.[265] However, identifying the underlying cellular ensembles that support mental states is not a simple task. Although there have been great advances in recent years for non-invasive brain imaging techniques such as positron emission tomography (PET) and functional magnetic resonance imaging (fMRI), these methods lack the spatial and temporal resolution required to study intricate neuronal circuitry. Therefore, new methods for interrogating the brain at the cellular level are critical for us to gain a deeper understanding of its functions.[266]

4.2 Novel Method for Identifying Active Neurons

4.2.1 Overview of Proposed Method

In collaboration with the Zemelman research group, we are working on the development of a novel method to label neurons with spatial and temporal control using light. We plan to employ this system in live, awake mice to identify the neuronal networks that support specific behaviors and cognitive events. To achieve this goal, we will gate the gene expression of neurons that is normally carried out by the cyclic adenosine monophosphate (cAMP) response element-binding protein (CREB) using prokaryotic repressor protein/operator pairs. The expression gate will be controlled by the presence of the small molecule repressor ligands that bind to these repressor proteins to open the gate

and allow transcription of downstream genes. We will prepare light sensitive derivatives of the repressor ligands to ultimately create a gene expression gate that is regulated with light. The labeling of active neurons is achieved by placing genetic information encoding for reporter proteins, such as green fluorescent protein (GFP), downstream of the operators. Consequently, if the neuron is active and the expression gate is open, it will be tagged through the expression of a fluorescent reporter. The control over cellular transcription with visible light in this fashion grants this system a high temporal resolution that will allow for the labeling of neurons on a behaviorally relevant time scale.

4.2.2 Generic Genetic Components of Neuron Labeling System

The genetic construct to label active neurons, which is currently being designed and developed by Dr. Boris Zemelman, consists of three main generic components; 1) Promoter X, 2) Operator X, and 3) a reporter (A, Figure 4.1). The Promoter X is a DNA sequence that acts as a secure binding site for a particular transcription factor. Upon activation of the neuron, the transcription factor will bind to Promoter X in order to initiate the transcription of downstream genes. Operator X is a DNA sequence that acts as a binding site for a specific repressor protein, and will be placed immediately downstream of Promoter X. In the absence of repressor ligand, the repressor protein will remain bound to its operator, blocking transcription of downstream gene sequences. Introduction of a repressor ligand will result in a binding event that induces a conformational change in the protein, liberating the repressor from the DNA sequence, ultimately allowing transcription of downstream genes. This creates a gene expression "gate" where the repressor protein acts as a gate that prevents gene expression when it is bound to the DNA operator, or that is to say, the gate is "closed" (B, Figure 4.1). The repressor ligand acts a "gate key" where binding of the ligand to its protein releases the repressor from the DNA binding site and "opens" the gate,

and gene transcription can occur (C, Figure 4.1). Finally, for the purpose of this work, the reporter will be represented by green fluorescent protein (GFP). While the basic functions of all three of these components will not change, this system is versatile in its design. Any number of specific genes can be substituted for each generic component to best fit our goals as the project progresses.

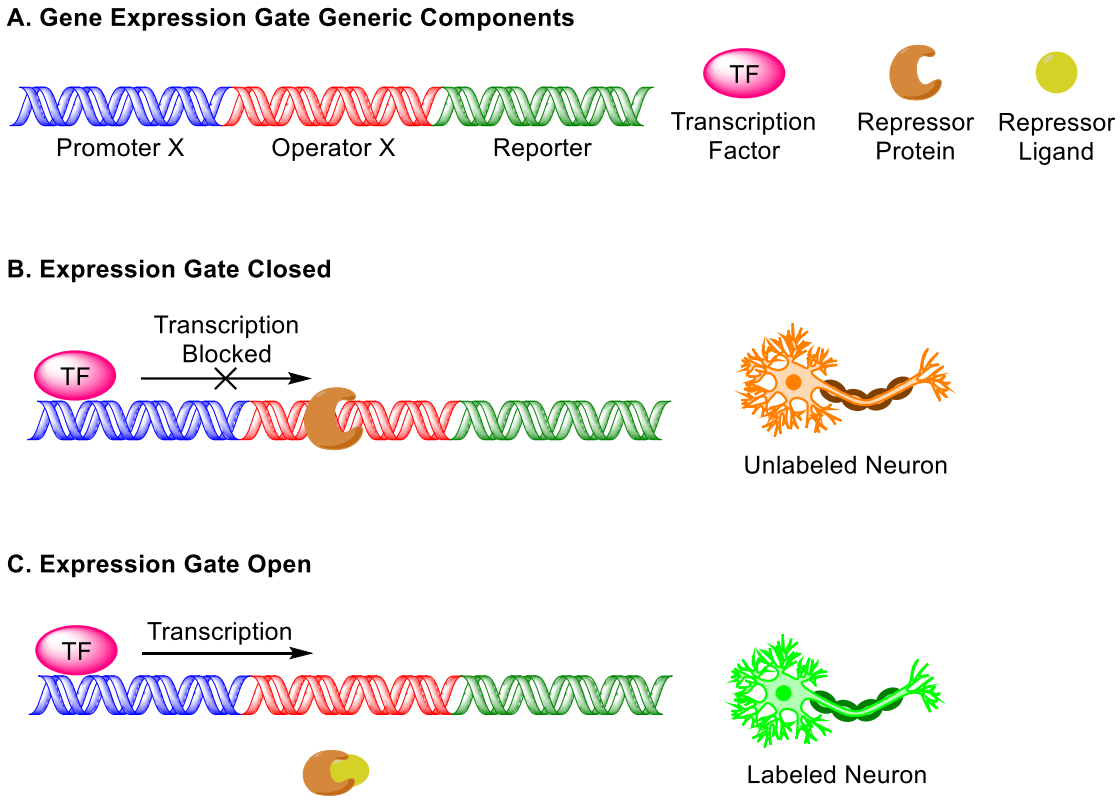

Figure 4.1 Basic components of the proposed neuron labeling system and their functions.

A) The gene expression gate consists of three generic components: 1) Promoter X, 2) Operator X, and 3) a reporter protein. Upon activation of the neuron, the transcription factor binds to Promoter X to initiate gene transcription. The repressor protein acts as a "gate" and binds to Operator X. The repressor ligand acts as a "gate key" and will liberate the repressor protein from its DNA binding site to "open" the gate and allow gene transcription. **B).** Depiction of the repressor protein bound to its operator and the gate is "closed" preventing transcription. **C).** Depiction of the repressor ligand binding to the repressor protein, thereby releasing it from its binding site and "opening" the gate, allowing gene transcription to occur.

4.2.2.1 Transcription Factor and Promoter X

For our investigations, we plan to use the cAMP response element binding protein (CREB) as the transcription factor and the cAMP response element (CRE) as Promoter X.

CREB is found in all neurons, and is phosphorylated in response to a number of cellular signals such as cAMP or elevated calcium upon activation of the neuron.[267] The phosphorylated CREB (pCREB) then binds to the cAMP response element (CRE) DNA sequence to initiate transcription of downstream genes. However, by placing a prokaryotic operator immediately adjacent to CRE, we can create a system where the gene expression of neurons is gated by the presence of a repressor protein. Gating the expression of genes by pCREB offers a distinct advantage in that the presence of pCREB is a near universal indicator of neuronal activation. Therefore, the use of pCREB in this labeling method should ensure that all active neurons are tagged during the behavioral event under investigation.

4.2.2.2 Prokaryotic Operator/Repressor Pairs

The operator/repressor component of the system is critical for exerting control over expression of the reporter protein. At the outset of our studies, we identified a number of possible prokaryotic operator/repressor protein pairs with ligands that control derepression that would be applicable to our gated gene expression system (Figure 4.2).[253,268,269] Specifically, we wished to investigate the tetracycline dependent repressor TetR, the erythromycin dependent repressor MphR, and the vanillic acid dependent repressor VanR. All of these repressor proteins have been modified and incorporated into expression-ON and expression-OFF type systems for use in mammalian cells,[251,253,257] some of which were discussed previously (Chapter 3, Section 3.6). However, in contrast to those gene expression systems, gene expression in this labeling method is not initiated by the presence of the repressor ligand. The prokaryotic operator/repressor pair will simply gate gene expression that has been initiated in response to a cellular event that has triggered the phosphorylation of CREB. This is an essential element of the labeling method that will

allow us to identify neurons that are activated in response to behavioral events. Therefore, we wish to take advantage of the natural prokaryotic mechanisms and only use the wild type operator/repressor pairs in our system.

While the origins of the tetracycline and erythromycin repressor/operator pairs were described in the previous chapter (Chapter 3, Section 3.6), the VanR protein has not yet been discussed and is worth mentioning. The VanR/VanO repressor/operator pair originates from the metabolic pathways of the fresh water bacterium *Caulobacter crescentus*.[253] Vanillic acid (**4.4**) is produced as a by-product of the fungal oxidative cleavage of lignin of decaying plant material.[270] *C. crescentus* can convert vanillic acid (**4.4**) into useful metabolites that can ultimately be converted into energy.[271] This metabolic pathway is inert in the absence of vanillic acid due to the transcriptional repressor protein VanR, which remains bound to its respective operator, VanO, upstream of the genes that encode for the corresponding monooxygenase required to metabolize vanillic acid. However, when *C. crescentus* encounters vanillic acid (**4.4**), the ligand will bind to VanR causing derepression and transcription of downstream genes can occur. The specific interactions of the VanR/VanO pair have since been exploited for control of gene expression in mammalian cells.[253]

While were interested exploring all of the repressor/small molecule pairs shown in Figure 4.2 for our gene expression gate, only doxycycline and erythromycin have been previously rendered biologically inactive with respect to their repressor proteins through chemical modification with a photolabile protecting group.[261,262] Hence, these two repressor protein/ligand pairs represent promising start points for our investigations. While anhydrotetracycline (**4.2**) has not been previously rendered inert with respect to TetR, it was shown to be a strong binder to the repressor protein and is a possible alternative to **4.1**.[272] Additionally, the vanillic acid/VanR system was an attractive alternative because

the relative simplicity of **4.4**, in contrast to the complex chemical environments of **4.1**, **4.2**, and **4.3**, would facilitate the preparation of caged derivatives. While the task of preparing photocaged erythromycin was a concurrent, independent investigation within our lab,[273] we also investigated the preparation of photocaged derivatives of vanillic acid, doxycycline, and anhydrotetracycline (*vide infra*).

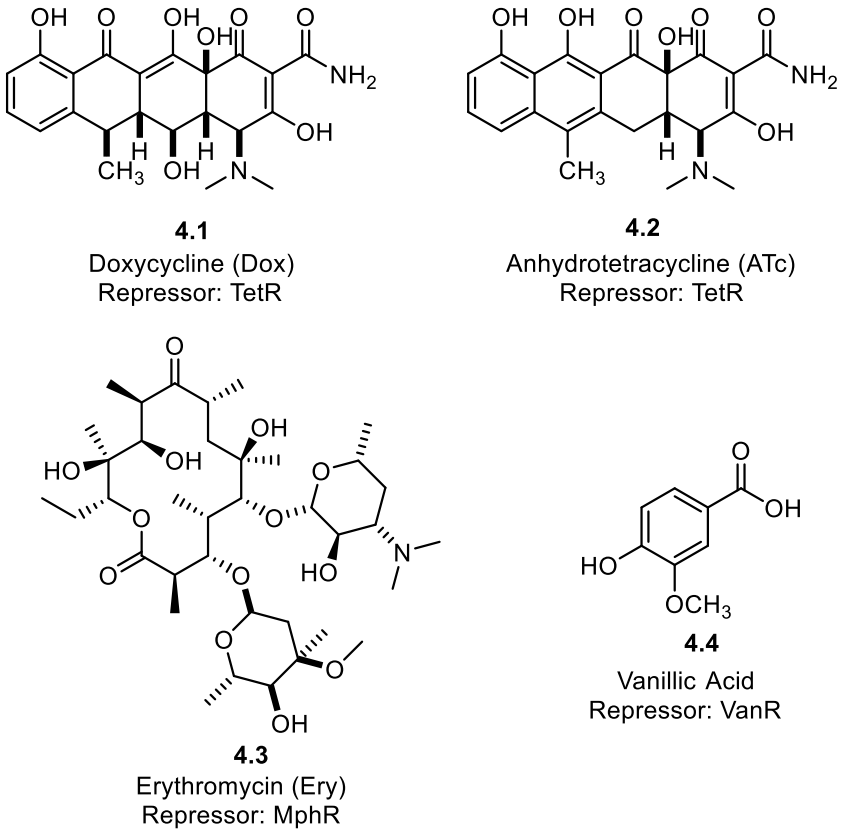

Figure 4.2. Select small molecule/repressor protein pairs

4.2.3 Implementation of Proposed Method

A summary of the proposed neuron labeling method is depicted in Figure 4.3. We plan to use *CRE*, *tetO*, and GFP as the generic components Promoter X, Operator X, and the reporter (Figure 4.1) respectively. The genetic information for these components can

be introduced into the neurons of mice via virus, and with this neuron labeling method in place, we will be able to study their brain function on a cellular level. The mouse neurons will be activated in response to a cognitive or behavioral event of interest, resulting in the formation of pCREB and its binding to CRE to initiate gene transcription. However, the gene expression will be gated by the TetR protein which will bind to the *tetO* operon upstream of the GFP reporter and prevent transcription (A, Figure 4.3). The caged-Dox ligand can then be introduced via local injection. The concentration of the caged ligand will be a critical parameter to explore. It is important that there is enough ligand present to elicit a sufficient signal from the reporter upon uncaging, however, excess ligand will result in over reporting of the fluorescent protein leading to false labeling. Furthermore, low concentration of the ligand will also be important so that it can quickly diffuse away after binding to the repressor protein, thereby reestablishing the expression gate and turning off gene transcription. In the absence of light, introduction of the caged Dox ligand will not induce transcription of the fluorescent reporter. However, upon illumination of the mouse brain with visible light, Dox will be released from the cage and will be free to bind to TetR. This will induce a conformational change in the protein, causing it to dissociate from the DNA sequence, and the expression gate will be opened. After TetR is removed, pCREB will be free to transcribe protein in activated neurons (B, Figure 4.3). Put simply, if the neuron is active and the caged-Dox is present in the cell, irradiation with visible light will result in GFP production, labeling the active neuron (C, Figure 4.3). However, in the absence of light, the neuron will remain unlabeled.

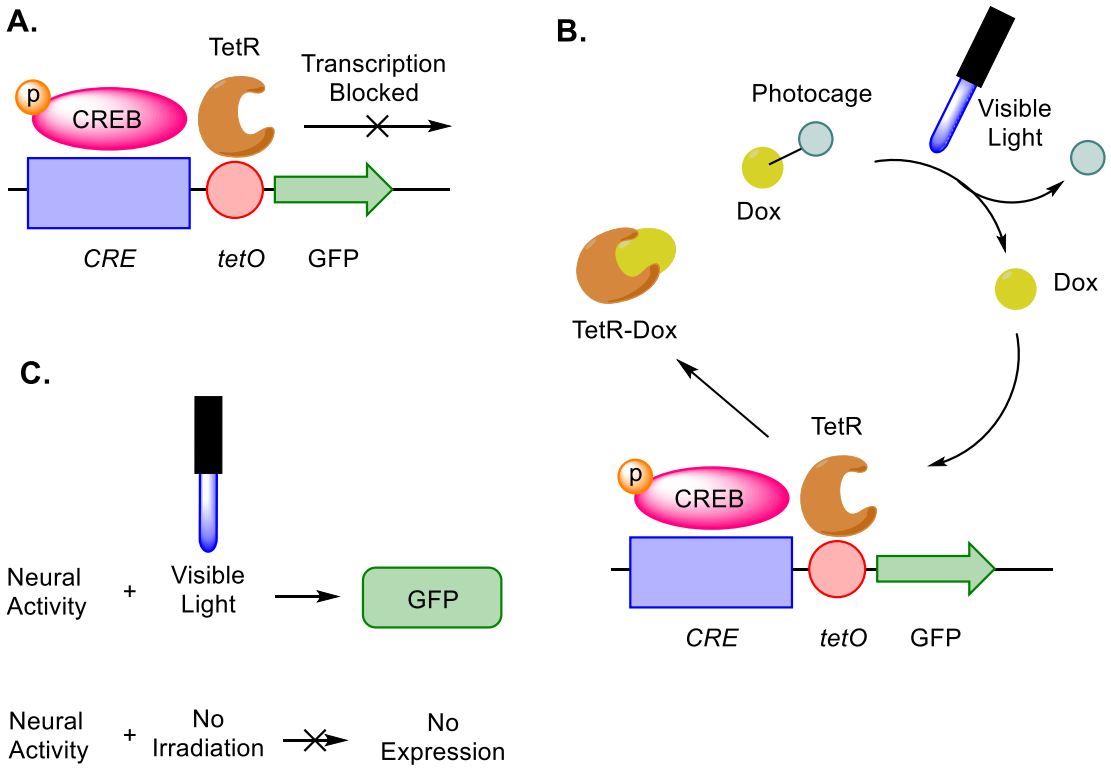

Figure 4.3. Summary of the proposed method in practice

A) Depiction of the closed expression gate where transcription is blocked by the repressor protein TetR. **B)**. Depiction of the labeling method in action. Uncaging of the ligand with visible light allows it to bind to the repressor protein to open the expression gate and allow gene transcription. **C)**. Simple summary of the proposed method. If there is neural activity in the presence of light and the caged ligand, expression of GFP will occur. However, in the absence of light, the neuron will remain unlabeled.

4.3 Design of Photocaged Ligands

As shown in the previous chapter, there exists a wide variety of photocages available for use in rendering the repressor ligands **4.1**–**4.4** biologically inert.[193] It is important for our system however, that the photocage can be removed with low energy visible light because we plan implement the caged molecules *in vivo*, where even brief exposure to near-UV irradiation can cause DNA damage to neurons. Furthermore, it is

important that our caged compounds display good aqueous solubility, and that they are stable in the absence of light. Upon consideration of these requirements, the selection of photolabile protecting groups is more limited. We identified three photolabile protecting groups that would be suitable for our system. These photocages are **DEAC450** (λ_{max} = 456 nm), **CANBP** (λ_{max} = 397 nm), and **NDBF** (λ_{max} = 330 nm) (Figure 4.4).[214,216,221,237]

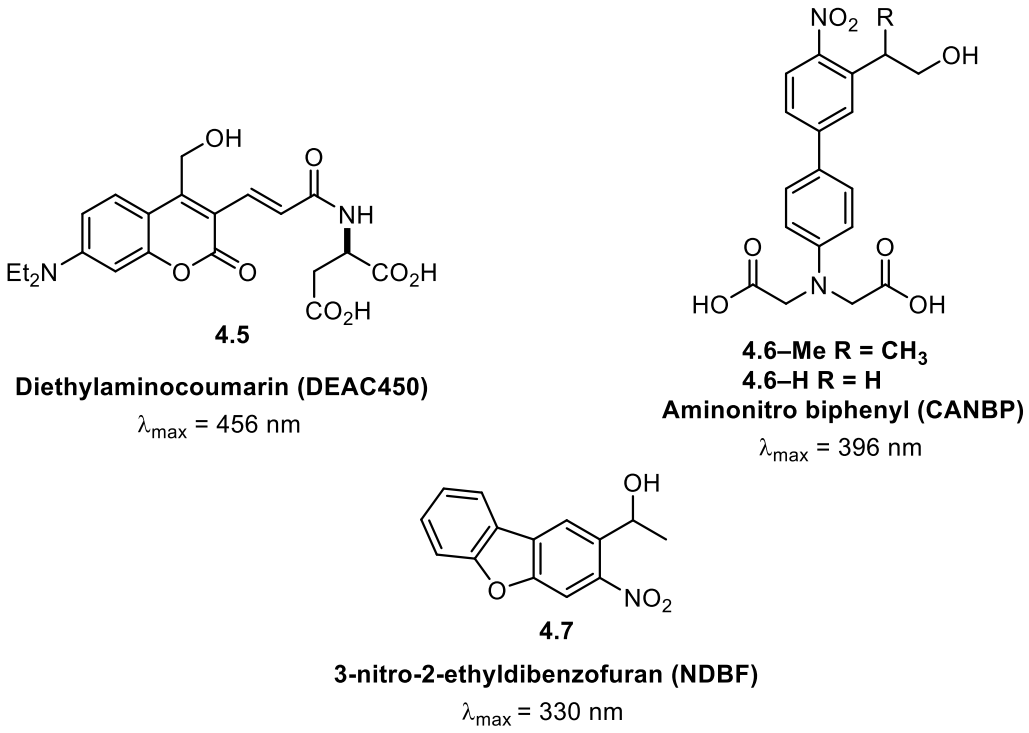

Figure 4.4. Possible photocages for preparation of caged ligands

Each of these photocages offered distinct advantages that could be beneficial to our system. The strong absorbance in the visible region and the water solubilizing functional groups of the **DEAC450** cage were attractive features, but, we were also aware that this cage is typically best suited for good leaving groups such as phosphates, meaning it may not be an appropriate cage for use with **4.**1, **4.2**, or **4.4**. The *o*-nitro-based cages **CANBP** and **NDBF**, however, are capable of efficiently releasing a wider variety of leaving

groups,[193] which made them appealing alternatives. Ultimately, the **CANBP** protecting group[221] seemed to be the most suited for our goals. This photocage possesses a number of desirable traits including, strong absorbance at long wavelengths (λ_{max} = 397 nm), fast deprotection rates (minutes), and the water solubilizing carboxyl groups should ensure good aqueous solubility of the caged ligand. Hence this cage was selected as the PPG of choice for our studies.

Doxycycline had been previously rendered unable to bind to the rtTA protein of the TET_{ON} system through caging of the keto enol moiety of the molecule (**NV-Dox**, **4.8**) (Figure 4.5).[261] While the biological function of the rtTA protein is distinct from TetR, the ligand binding domain of the modified rtTA protein was left unchanged and is the same as with TetR.[257] Therefore, compounds that were rendered inert with respect to rtTA should also be inert with respect to TetR. Furthermore, this keto-enol functionality has been shown to be important for the binding of tetracycline derivatives to the TetR protein.[274,275] Based on this precedent, we set out to cage **4.1** or **4.2** in a similar fashion through the preparation of **4.9** and **4.10**. We anticipated potential complications related to the benzylic stereocenter of the **CANBP** photocage. Caging a tetracycline derivative with **4.6** would result in a mixture of diastereomers (e.g. **4.9-Me** or **4.10-Me**) that could complicate the purification of the caged compounds. Furthermore, Cambridge found that one of the diastereomers of **4.8** remained bioactive, despite being caged.[261] With these potential pitfalls in mind, we planned to prepare the **4.6–H** variant of the **CANBP** cage that does not possess the benzylic methyl group. We were aware that this compound may have diminished deprotection efficiency,[193] but we anticipated that the deprotection would still be sufficient for our needs.

For vanillic acid (**4.4**), there were no previous examples of rendering the ligand biologically inert with respect to the VanR protein via chemical modification. Furthermore, there exists no crystallographic data for vanillic acid bound to the VanR protein. Therefore,

it was unclear if vanillic acid would require caging at the phenol moiety or the carboxylic acid moiety to prevent it from binding to VanR. Hence, we planned to prepare two caged derivatives for this compound, **4.11** and **4.12** so that we could probe its binding to the VanR protein.

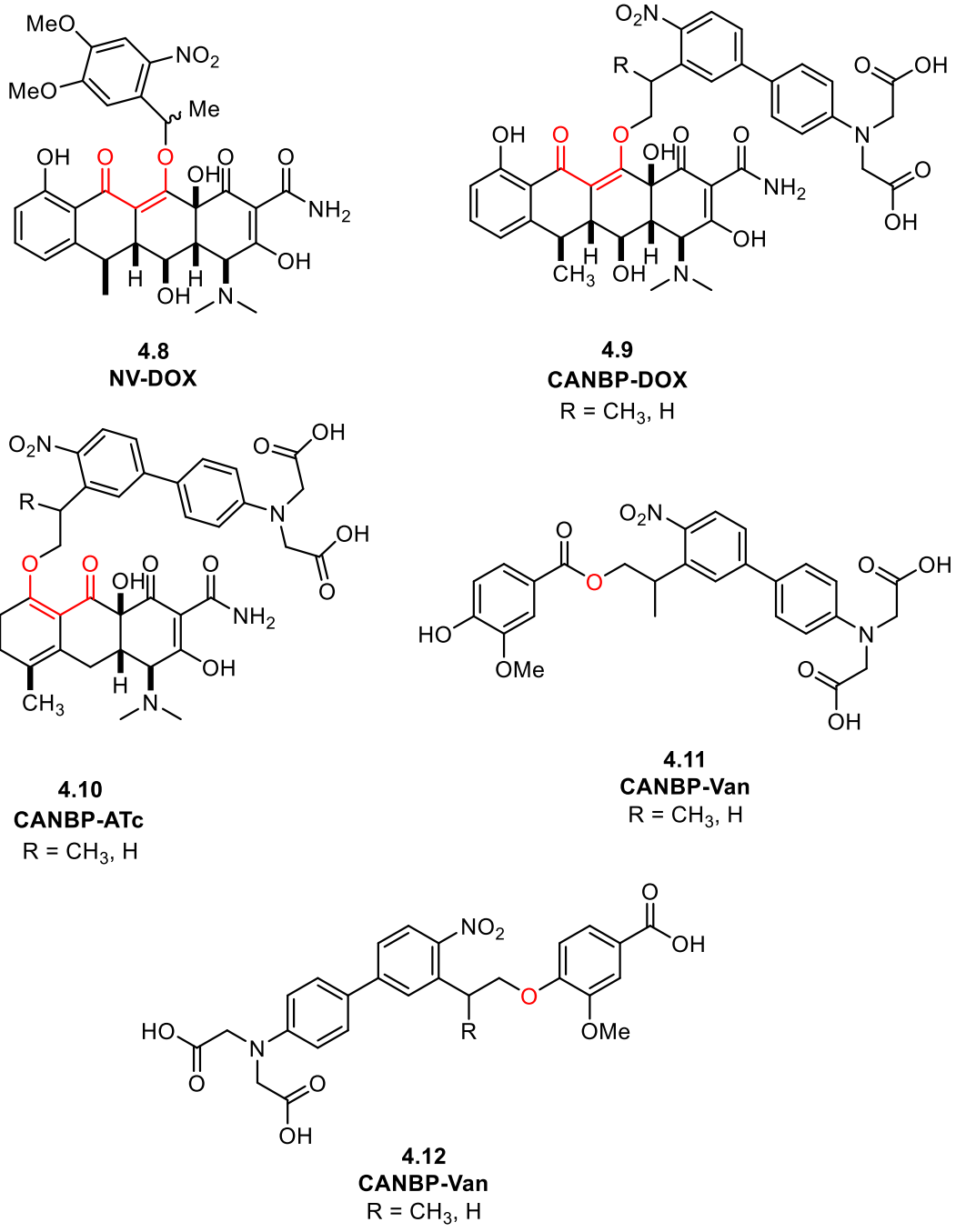

Figure 4.5. Planned photocaged derivatives of ligands **4.1**, **4.2**, and **4.4**.

4.4 Synthesis of CANBP Photocages

Our efforts to prepare photocaged derivatives of **4.1**, **4.2**, **4.4**, commenced with the synthesis of the known **CANBP** photocage.[221] Commercially available 4-nitrobromobenzene (**4.13**) was alkylated via vicarious nucleophilic substitution with *tert*-butylchloroacetate (**4.14**) to afford **4.15** in 90% yield. Methylation of the benzylic carbon through treatment with sodium hydride and methyl iodide, followed by reduction of the *t*-butyl ester with diisobutylaluminum hydride (DIBAL-H) delivered **4.17** in 72% yield over two steps. Construction of the biaryl ring was accomplished through a Suzuki coupling with **4.18** which delivered **4.19** in 85% yield. Final installation of the solubilizing carboxyl groups onto the aniline nitrogen of **4.19** was the only low yielding step in the preparation of the **CANBP** photocage. Alkylation of **4.19** with **4.20** delivered the desired compound **4.21** in only 45% yield, and the remaining material consisted of the monoalkyated analogue **4.22**. While extensive effort has not been undertaken to optimize this reaction, some attempts of increasing the equivalence of **4.20**, extending the reaction time, or inclusion of sodium iodide for an *in-situ* Finkelstein reaction, offered no improvement on the product distribution. Nevertheless, **4.21** was prepared in five steps and 25% overall yield.

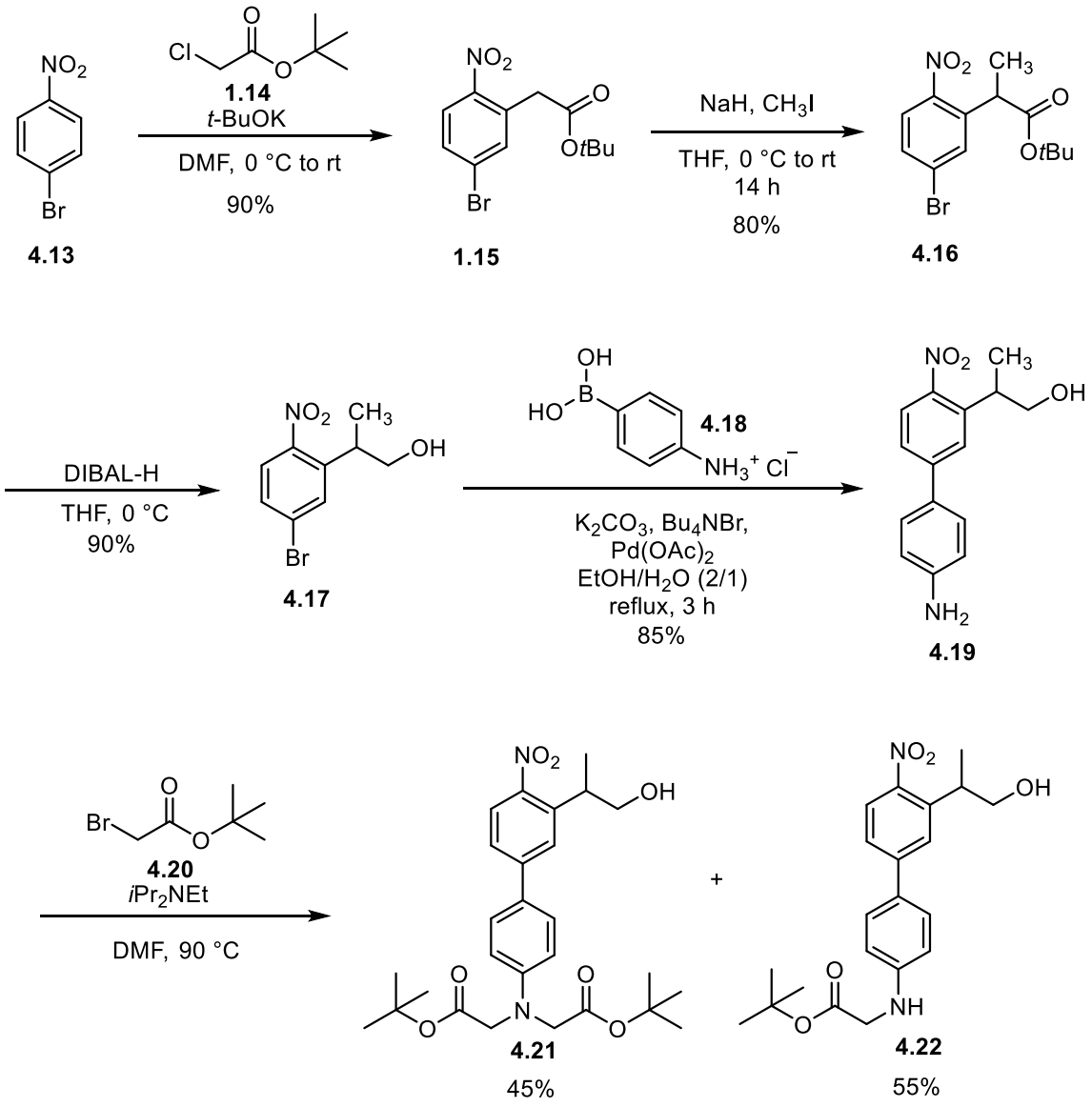

Scheme 4.1. Synthesis of **CANBP** photocage **4.21**.

We prepared the novel nor-methyl **CANBP** photocage **4.25** in an analogous manner to **4.21**, but omitting the alkylation with methyl iodide. In this fashion, the nor-methyl photocage **4.25** was prepared in four steps and 31% overall yield (Scheme 4.2).

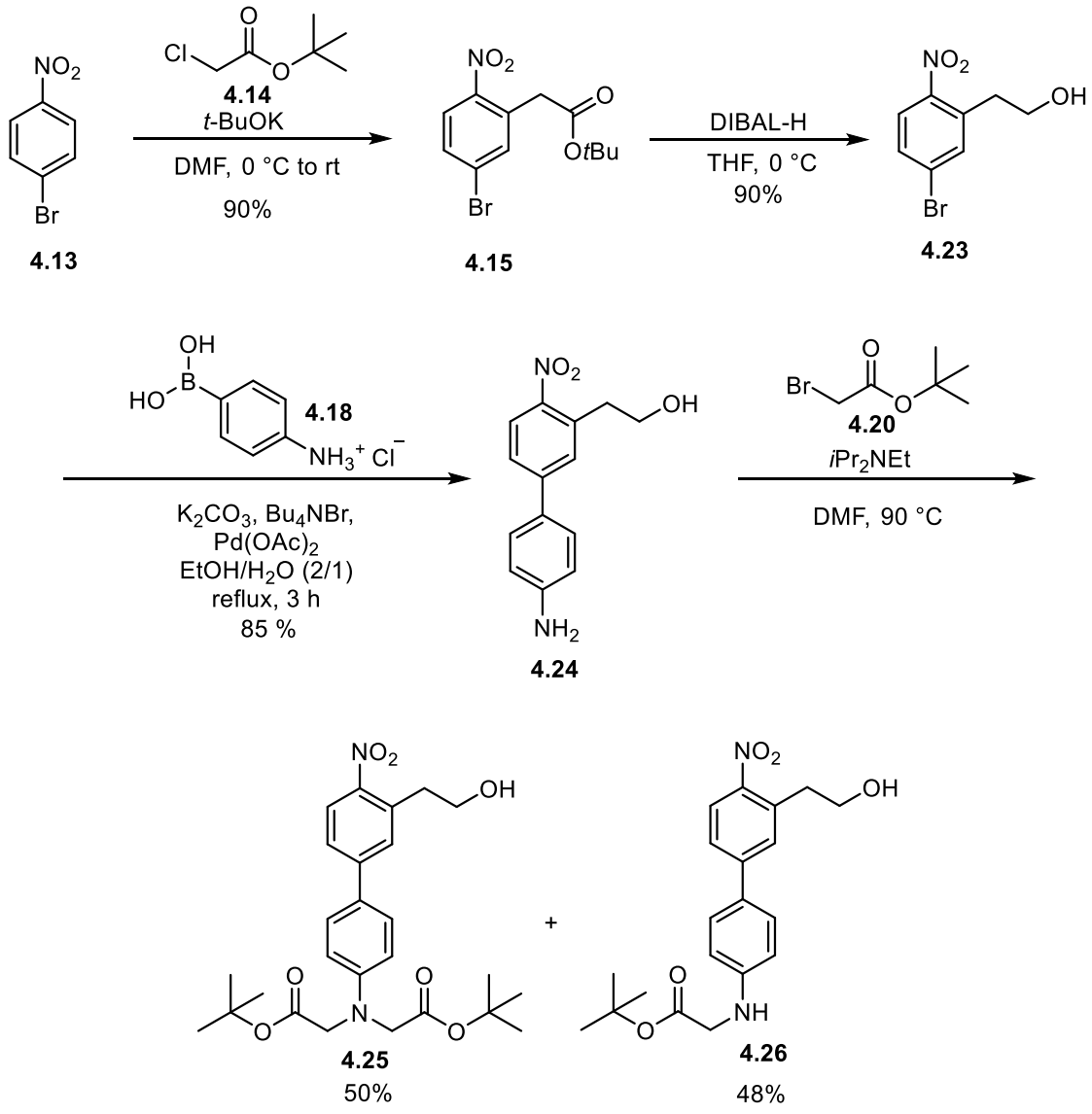

Scheme 4.2. Synthesis of nor-methyl **CANBP** photocage **4.25**.

4.5 Synthesis of Caged Vanilic Acid Derivatives

4.5.1 Caging Vanillic Acid – Ester Derivatization

We planned to cage the carboxylic acid of **4.4** by first installing an acid labile blocking group on the phenol and then activating the carboxylic acid towards ester bond

formation with photocage **4.21**. The methoxymethyl acetal (MOM) protecting group was strategically chosen to enable a global removal of protecting groups upon unmasking of the carboxylic acid moieties of **4.21** through treatment with acid. Thus we prepared a MOM protected analogue of vanillic acid (**4.4.**) in two steps from vanillin (**4.27**). Alkylation of the phenol moiety of **4.27** followed oxidation of the aldehyde with $KMnO_4$ delivered **4.29** in 84% yield. We next sought suitable conditions to esterify **4.29** with the **CANBP** cage using intermediate **4.16** as a model system.

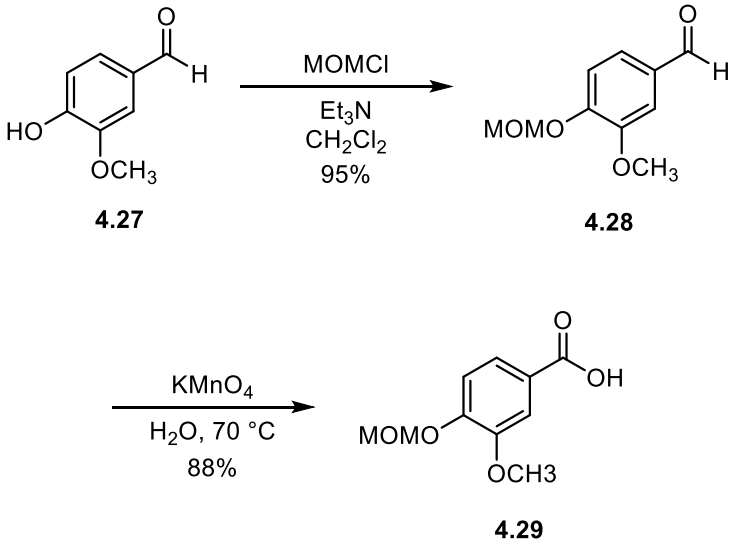

Scheme 4.3. Preparation of MOM protected vanillic acid **4.29**.

We commenced our efforts to esterify **4.29** with **4.16** through carbodiimide mediated couplings. We first attempted a Steglich type esterification[276] between **4.29** and **4.16** using DCC and DMAP, but no product was observed and unreacted **4.16** was recovered (Equation 4.1). Previous reports in the literature showed that EDCI promoted esterifications worked well for the **CANBP** photocage during the preparation of caged

GABA derivatives,[221] but unfortunately, application of these conditions to our system did not provide any of the desired product.

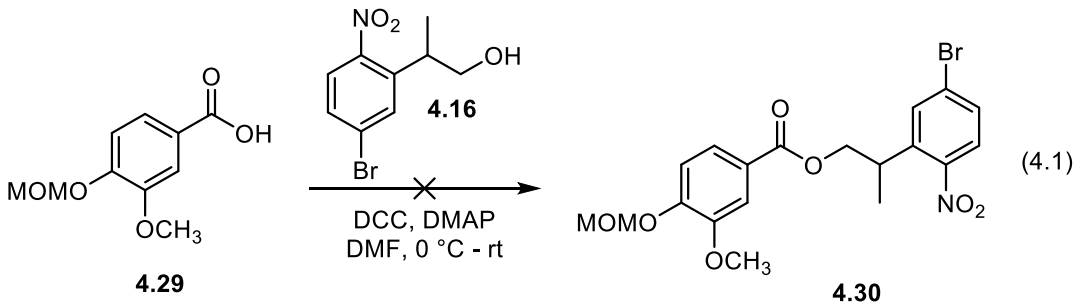

(4.1)

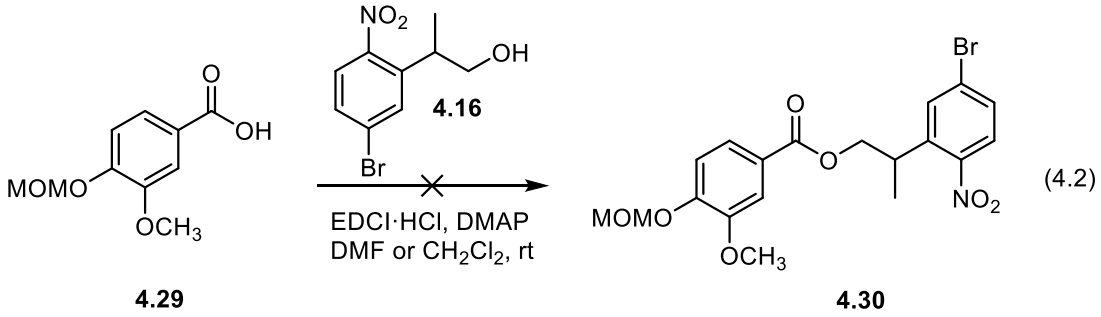

(4.2)

We next attempted to form **4.30** through activation of **4.29** as a carbonate or an anhydride. Introduction of **4.16** and 4-dimethylaminopyridine (DMAP) to a solution of freshly prepared mixed anhydride of vanillic acid derived from pivaloyl chloride (**4.31**) or isobutyl chloroformate (**4.32**) gave no desired product, and again, only unreacted **4.16** was recovered (Equation 4.3). The initial conclusion was that the mixed anhydride intermediates were never formed during the first step of the reaction sequence; however, control experiments revealed there was clean conversion to the desired anhydride intermediates by ^{1}H NMR and TLC analysis of the reaction mixtures. Attempts to drive the reaction to completion through increased reaction times and temperatures were unsuccessful, and only unreacted **4.16** was recovered.

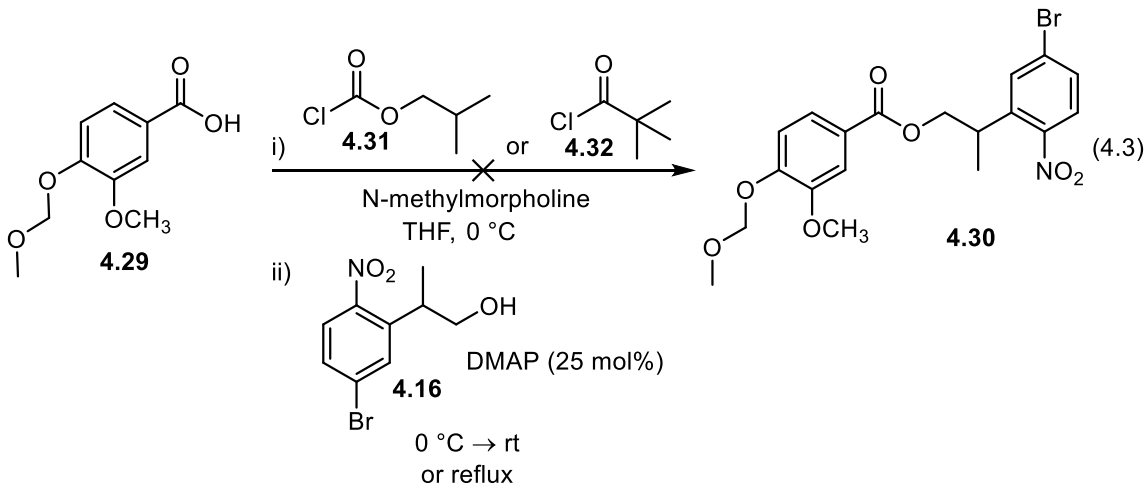

We at last found success when we used the Yamaguchi reagent **4.29**[276] to form the more reactive mixed anhydride **4.34**, which upon reaction with **4.16** and DMAP delivered **4.30** in 33% yield along with the undesired ester **4.35** in 12% (Scheme 4.4). We recovered ca. 50% unreacted **4.16** from this reaction, but we had finally identified conditions to esterify **4.29**. We speculated that the yield could be improved through increased equivalence of the photocage and longer reaction times. We applied this logic to the esterification of **4.29** with **4.21** using the Yamaguchi esterification conditions, and we obtained **4.30** in 57% yield (Equation 4.4).

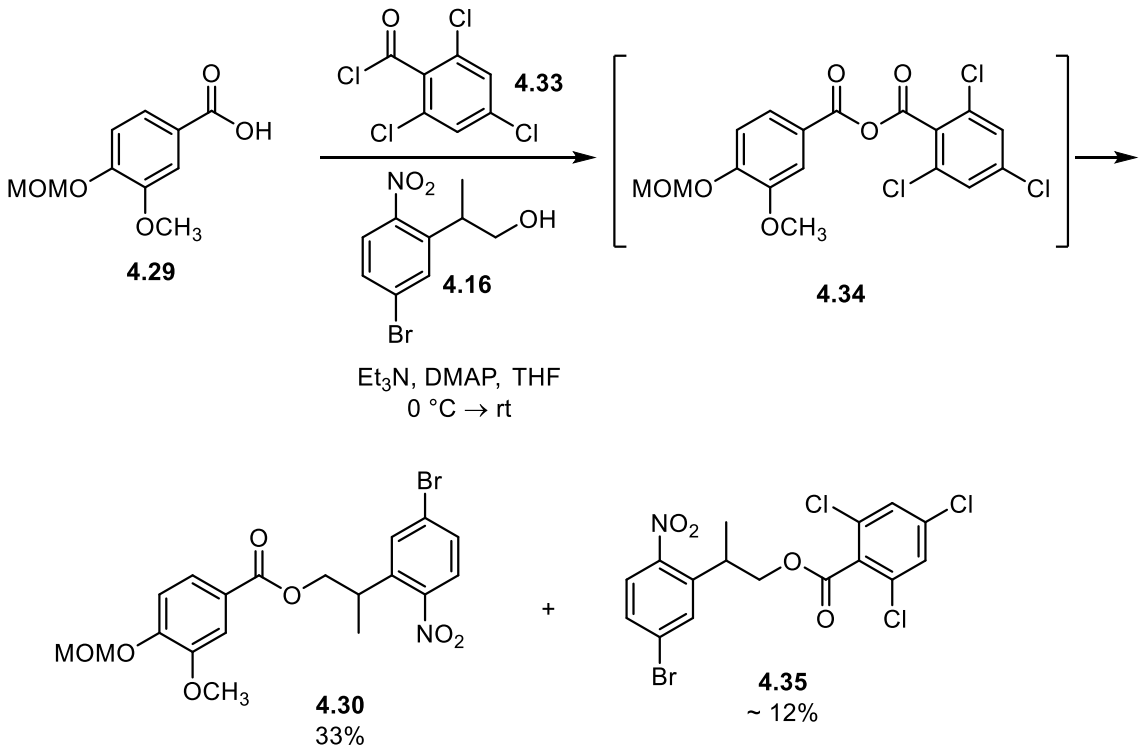

Scheme 4.4. Yamaguchi esterification of **4.29** to prepare **4.30**.

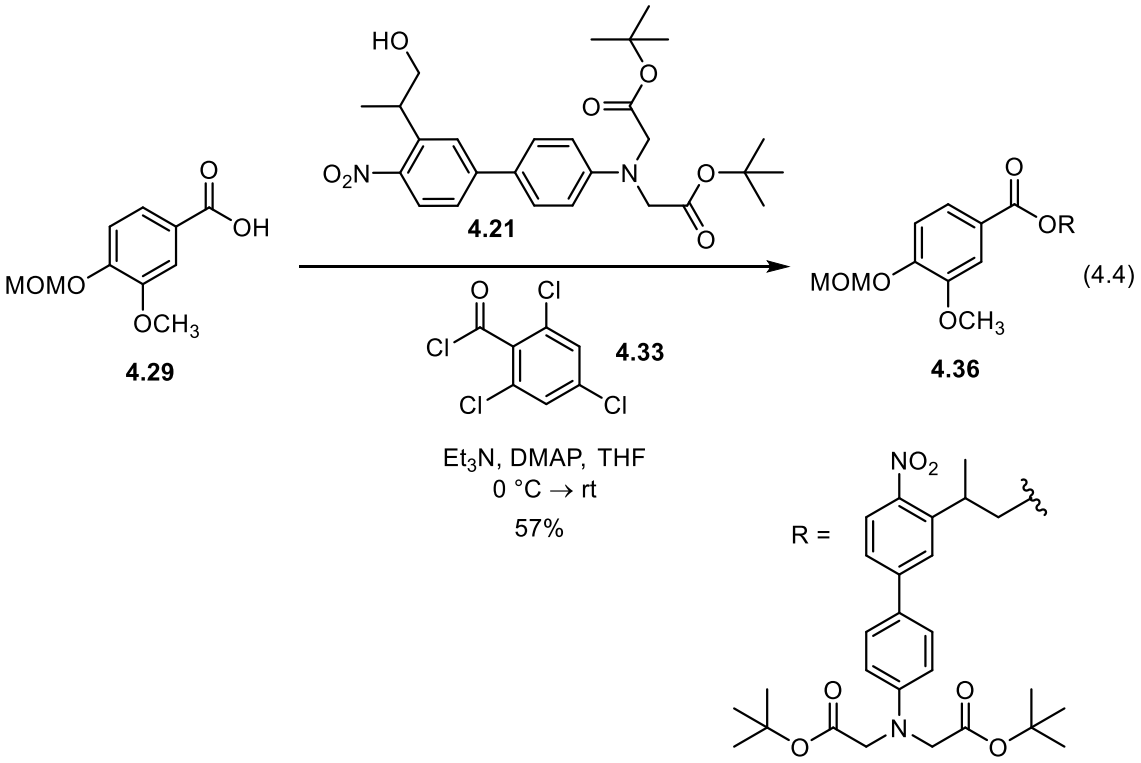

4.5.2 Caging Vanillic Acid – Phenol Derivatization

With the successful preparation of **4.36**, we next attempted to derivatize the phenol moiety of vanillic acid. Applying similar logic as before in choosing a protecting group for vanillic acid, we aimed to prepare the *t*-butyl ester of vanillic acid, which would enable a global removal of *t*-butyl groups from the caged derivative when necessary. Accordingly, vanillic acid (**4.4**) was prepared by silver oxide oxidation of vanillin (**4.27**), and it was subsequently converted into the *t*-butyl ester **4.38** through a Steglich esterification with *tert*-butanol as solvent (Scheme 4.5).

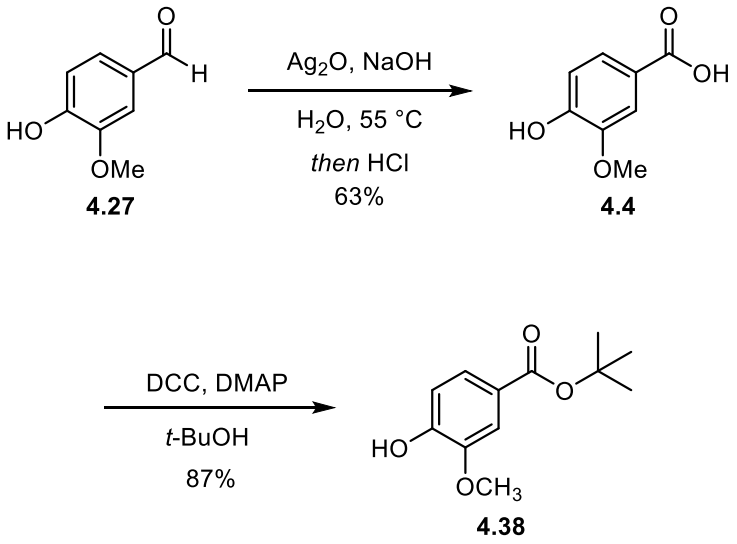

Scheme 4.5. Preparation of **4.38** from **4.27**.

Fortunately, alkylating the phenol of **4.38** proved less difficult than preparing **4.36**. We discovered that a Mitsunobu reaction between **4.38** and model cage **4.16**, delivered the desired alkylated product **4.39** in 60% yield (Equation 4.5). We next appended the full nor-methyl **CANBP** cage **4.25** via the same Mitsunobu reaction conditions used on the model system that afforded **4.40** in 63% yield.

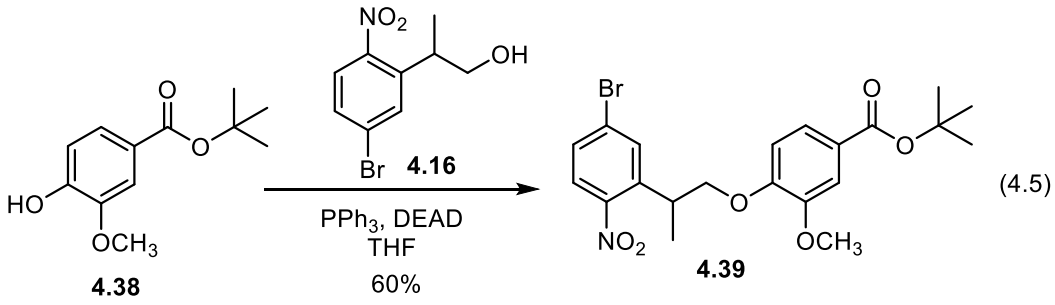

(4.5)

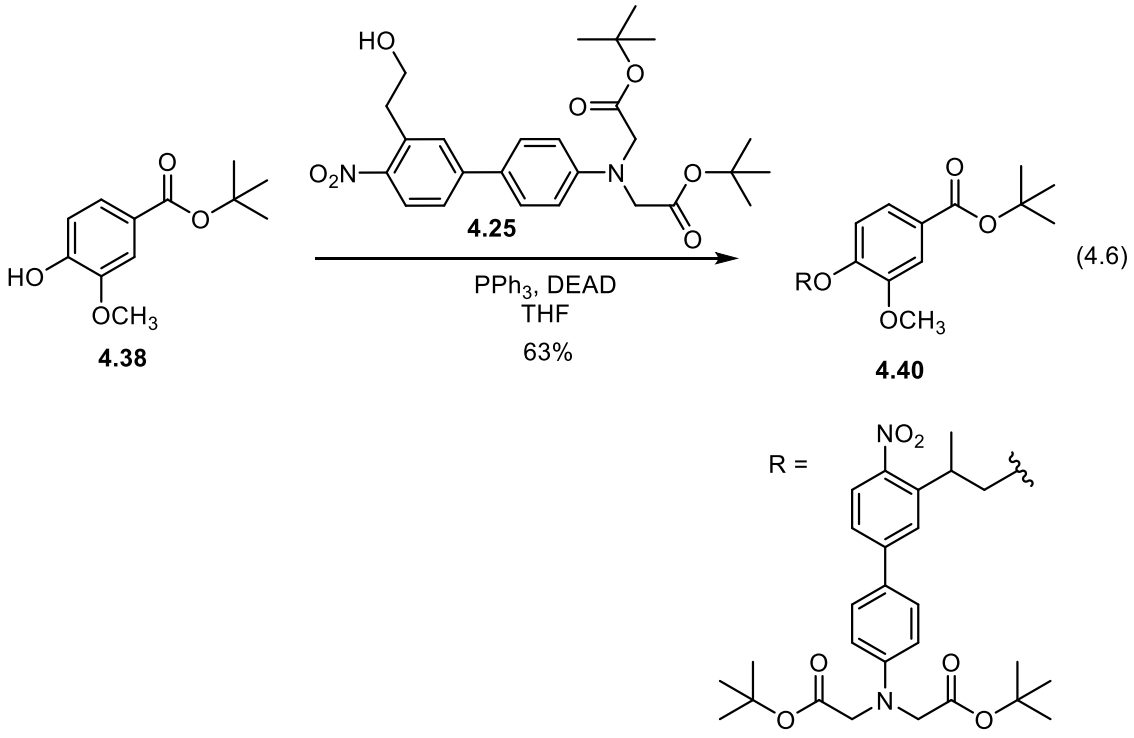

4.5.3 Synthesis of Caged Vanillic Acid Derivatives Summary and Conclusions

We successfully designed methods to cage vanillic acid at the carboxylic acid moiety or the phenol moiety. While we did not investigate other photocages on this system, we expect these methods to prepare carboxylic acid or phenol caged vanillic acid would be readily translatable to other systems if desired. Unfortunately, Zemelman discovered that the *vanO*/VanR operon/repressor pair was ill suited for our neuronal labeling method. The VanR protein did not sufficiently repress transcription of the fluorescent protein in the absence of vanillic acid, and significant production of GFP was observed. Therefore, we abandoned our efforts towards caged vanillic acid analogs **4.36** and **4.40**. We did not evaluate the aqueous solubility or the deprotection efficiencies of these compounds because they could not be used in our system. Instead we focused on using *tetO*/TetR in our expression gate system, and we moved on to preparing caged derivatives of doxycycline

(**4.1**) or anhydrotetracycline (**4.2**). Nevertheless, **4.36** and **4.40** represent novel photocaged compounds that would allow for a light-controlled cell labeling system.

4.6 Synthesis of Caged Tetracycline Derivatives

Our new goal became the preparation of a photocaged derivative of **4.1** or **4.2**. We began our investigations with **4.1**, because **NV-Dox** had already been demonstrated to work well for the TET_{ON} system. Due to the chemical complexity of **4.1**, we though it prudent to begin probing its reactivity through model systems instead of the more complex and light sensitive **CANBP** derivatives. Following the precedent from Cambridge,[261] we first set out to find conditions that would enable caging at the phenolic diketone moiety of **4.1**.

Our initial efforts to alkylate doxycycline proved fruitless. Treatment of **4.1** with MOMCl at 0 ˚C, room temperature, or 70 ˚C, lead to intractable mixtures with no mass hits characteristic of useful products by LCMS analysis (Equation 4.7). Changing the alkylating agent to benzyl bromide provided similar results (Equation 4.8) and attempts to increase the nucleophilicity of doxycycline (**4.1**) through treatment with sodium hydride also proved ineffective (Equation 4.9).

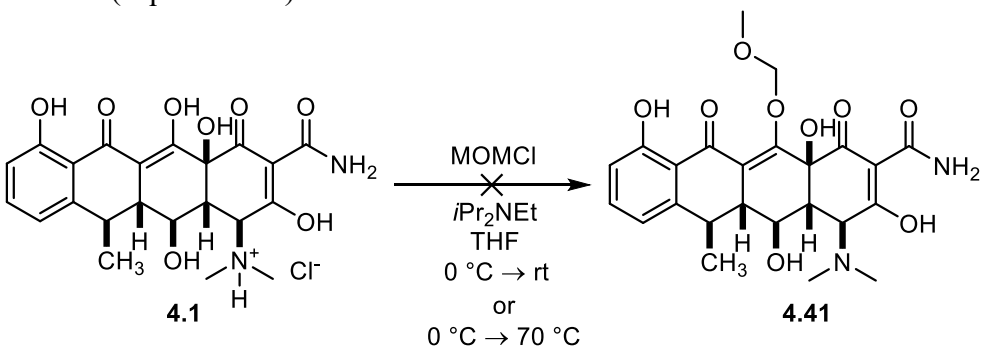

(4.7)

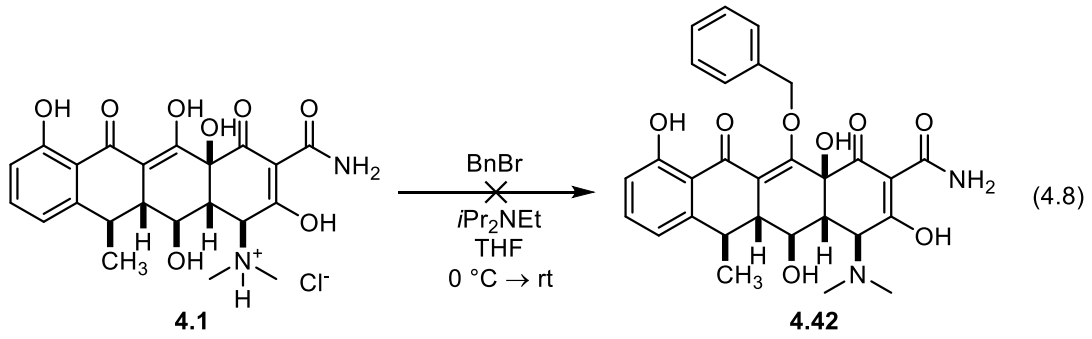

4.1 4.42 (4.8)

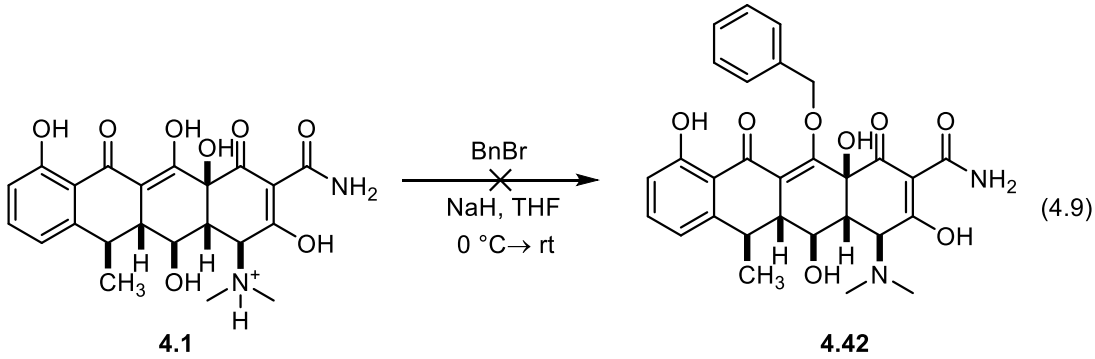

4.1 4.42 (4.9)

Alkylating doxycycline with halogen-based electrophiles was proving to be unproductive, so we changed strategies and attempted to functionalize doxycycline in a similar fashion to the procedure reported by Cambridge.[261] We used acetophenone (**4.43**) and **4.46** as starting points for alkylation model systems that would be similar to a photocage we could attach to doxycycline. The diazo compounds **4.45** and **4.47** were prepared through condensation of **4.43** or **4.46** with hydrazine (Equation 4.10) and then oxidation of the resulting hydrazone with MnO_2 (Equation 4.11). Unfortunately, treatment of doxycycline with freshly prepared **4.45** or **4.47** resulted in only decomposition of the materials and the formation of intractable mixtures (Equation 4.12).

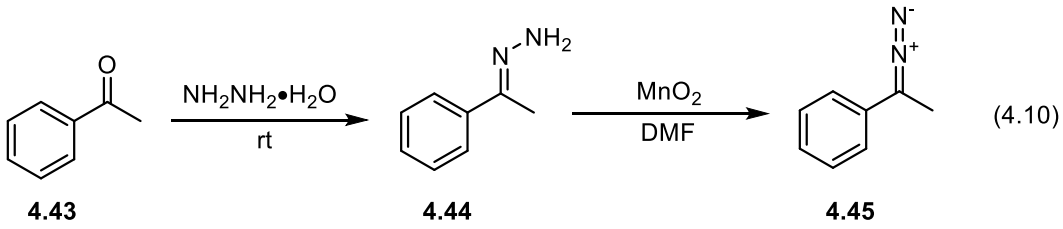

(4.10)

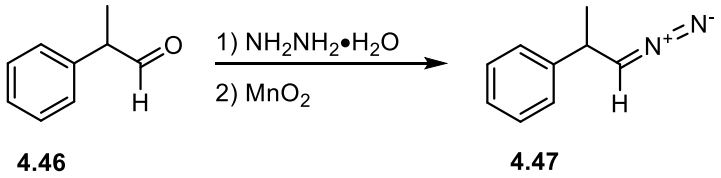

(4.11)

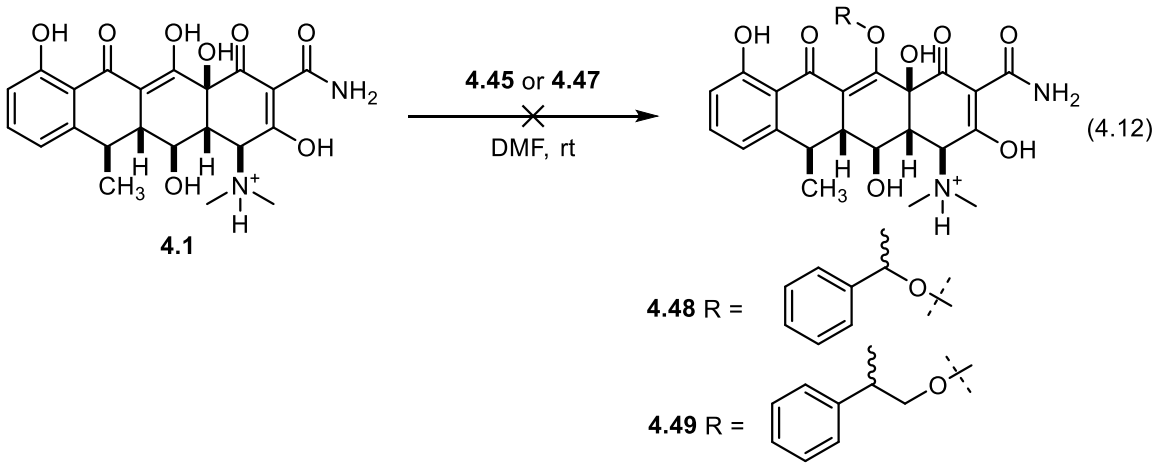

(4.12)

Doxycycline was proving difficult to alkylate with model systems, a problem we anticipated would be exacerbated by attempting to append the more structurally complicated light sensitive **CANBP** cage. Instead of attempting to alkylate **4.1**, we instead focused on acylation reactions. We speculated that attachment of the **CANBP** cage through a carbonate linker may be a more reliable strategy than alkylation of the complex ligand. With no literature precedent available for selectively acylating doxycycline, we again turned to a model system to establish the reactivity profile.

Following literature precedent from Tan and coworkers in their studies of selective diol acylations,[277] **4.1** was treated with propionyl chloride in the presence of *N*-methylimidazole (NMI) (20 mol%) (Equation 4.11). LCMS analysis of the reaction mixture revealed a mixture of mono- and bis-acylated doxycycline products that were inseparable by HPLC. While this model system did not lead to any structural information about the regiochemical outcome of the acylation, it did provide the first positive result towards caging doxycycline.

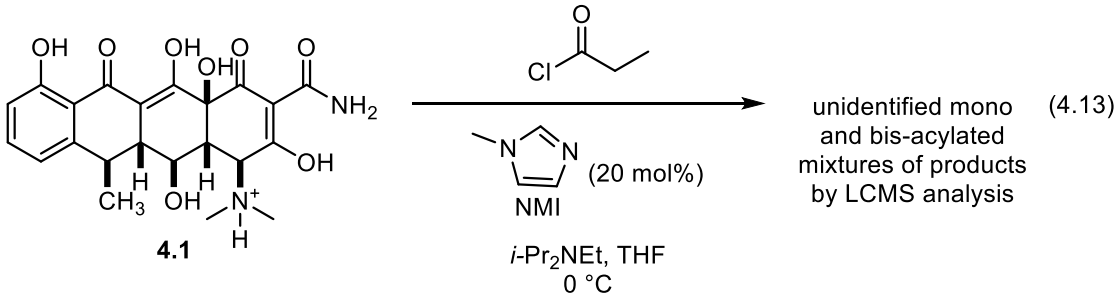

(4.13)

Heartened by the limited success of acylating **4.1** with propionyl chloride, we continued our studies using benzyl chloroformate (CbzCl) as a model that would more closely resemble the carbonate linker the cages **4.21** and **4.25** would require. Subjecting doxycycline to the same reactions conditions in THF or CH_3CN with CbzCl as the acylating reagent showed the major product to be a mono-acylated doxycycline derivate, along with other minor mono and bis-acylated products (Equation 4.14). After HPLC purification of the reaction mixture, we were able to isolate the major mono-acylated product, which was identified as **4.50** based on the downfield shift of the aromatic protons in the ^1H NMR spectrum.

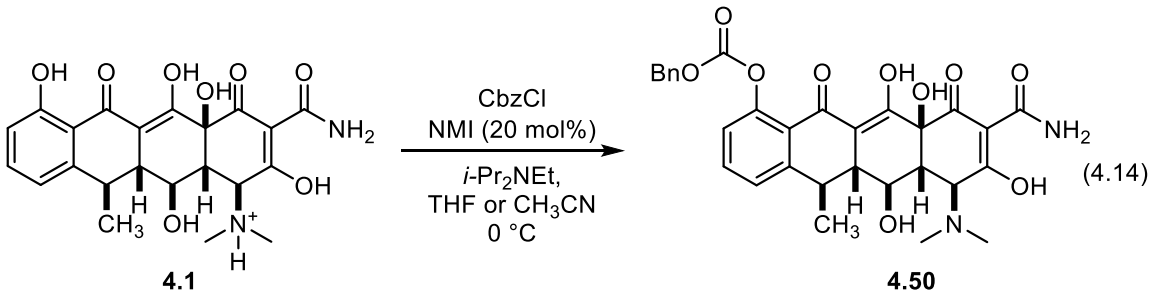

(4.14)

Interestingly, when *N*-methylimidazole was excluded from the reaction, the selectivity for the phenol acylated product decreased, and a mixture (ca 1:1) of mono acylated products was observed (Scheme 4.6). The exact role that N-methylimidazole is playing in this reaction is unknown. It was originally included due to its ability to act as a 1,2-diol activator through hydrogen bonding [277] with hopes that it would activate the enol moiety for acylation, instead, it increased the selectivity for the acylation of the phenol moiety. *N*-methylimidazole is also known to add to acyl chlorides to generate a more reactive acyl imidazolinium intermediate for acylation reactions, and it is possible that it is playing a similar function in this reaction. Regardless of its role, it is clear that the NMI increases the selectivity of the acylation.

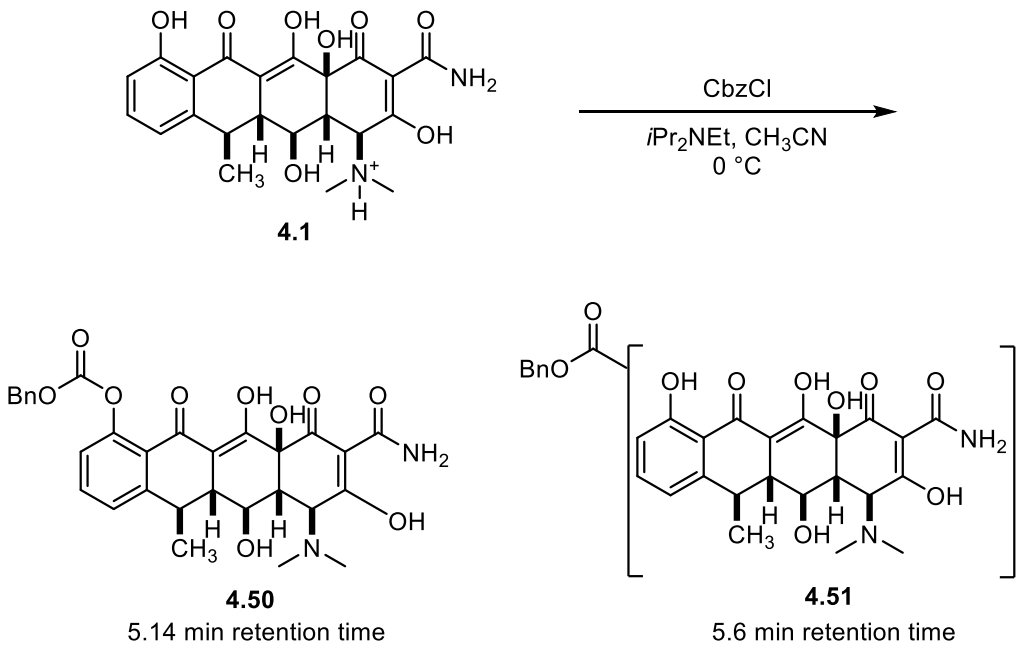

Scheme 4.6. Acylation of **4.1** with CbzCl in the absence of NMI.

While *N*-methylimidazole did improve the selectivity to provide one major product, the acylation still gave many other minor products with similar retention times that complicated the purification. Other efforts to increase the selectivity of the reaction were unsuccessful. A temperature screen revealed that no reaction occurred at –78 ˚C, while reactions at –30 ˚C and –15 ˚C provided comparable results to reactions performed at 0 ˚C. A small selection of solvents was screened including CH_3CN, THF, and CH_2Cl_2. While THF and CH_3CN provided comparable results, CH_2Cl_2 completely changed the selectivity of the reaction to a different mono-acylated isomer as the major product. Unfortunately, we were never able to isolate this product in sufficient purity to identify the structure.

After establishing a set of acylation conditions that offered some selectivity in functionalizing doxycycline, we turned our attention to attaching the desired photocages. As before, we employed the less advanced intermediate **4.16** as a model system. Conversion of **4.16** to the corresponding chloroformate through treatment with triphosgene

worked well, delivering **4.52** in ca. 90% purity based upon the ^{1}H NMR spectrum of the crude material (Equation 4.15). However, removal of residual triphosgene from the reaction mixture proved problematic, so we switched to preparing **4.52** through treatment with phosgene instead, which could be removed under reduced pressure (Equation 4.16).

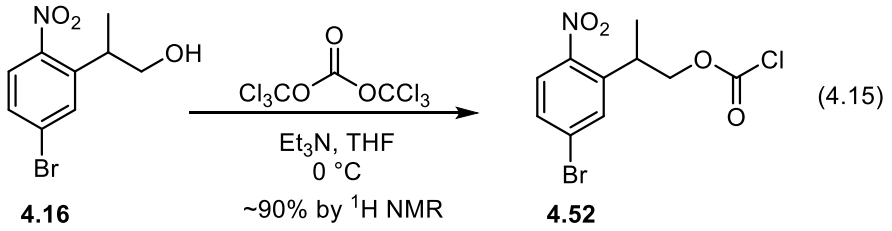

(4.15)

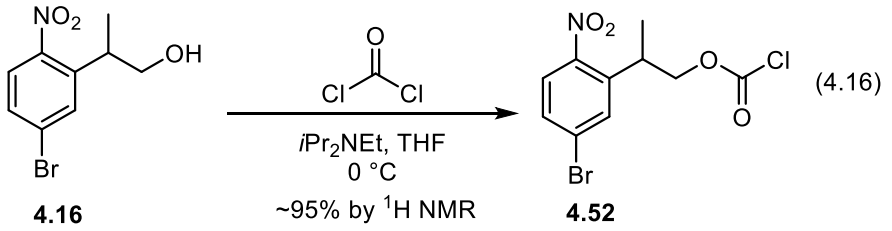

(4.16)

Gratifyingly, treating **4.1** with the freshly prepared chloroformate **4.52** in the presence of NMI demonstrated that the acylation conditions translated well from the CbzCl model system, delivering a mono-acylated **Dox** product as the major component, along with other minor acylation products and unreacted **4.1** (Equation 4.17). ^{1}H NMR analysis of the crude reaction mixture showed the presence of a product with aromatic protons shifted downfield, and we speculated that the phenol acylated **4.53** was the major product. We next attempted the reaction with the full CANBP cage **4.21** and again saw a similar product distribution as before, where the major product was assumed to be **4.54** (Equation 4.18). Unfortunately, all of our efforts to isolate material pure enough for biological purposes were not successful. The reaction mixture could not be purified by standard

chromatography with silica gel or neutral alumina. Furthermore, we were unable to remove the impurities via HPLC purification as well.

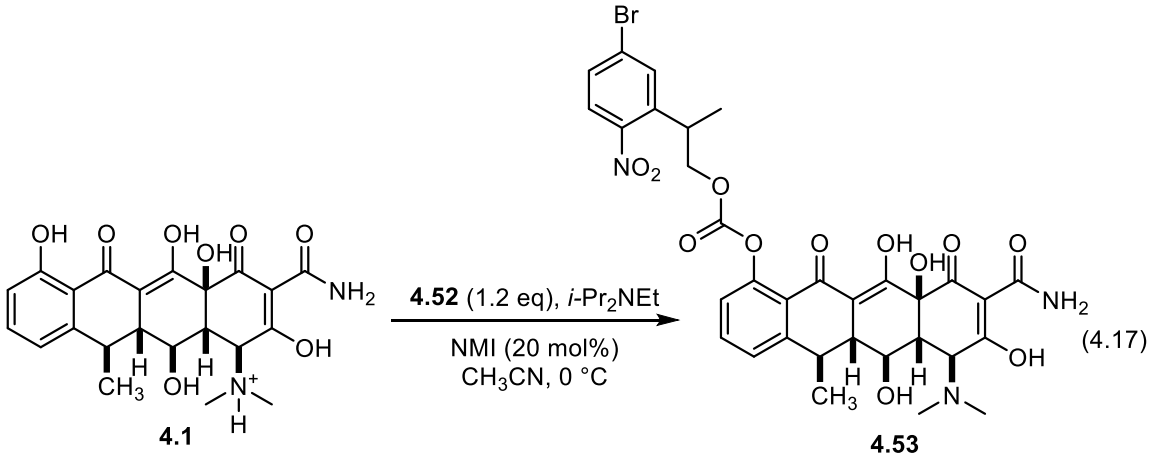

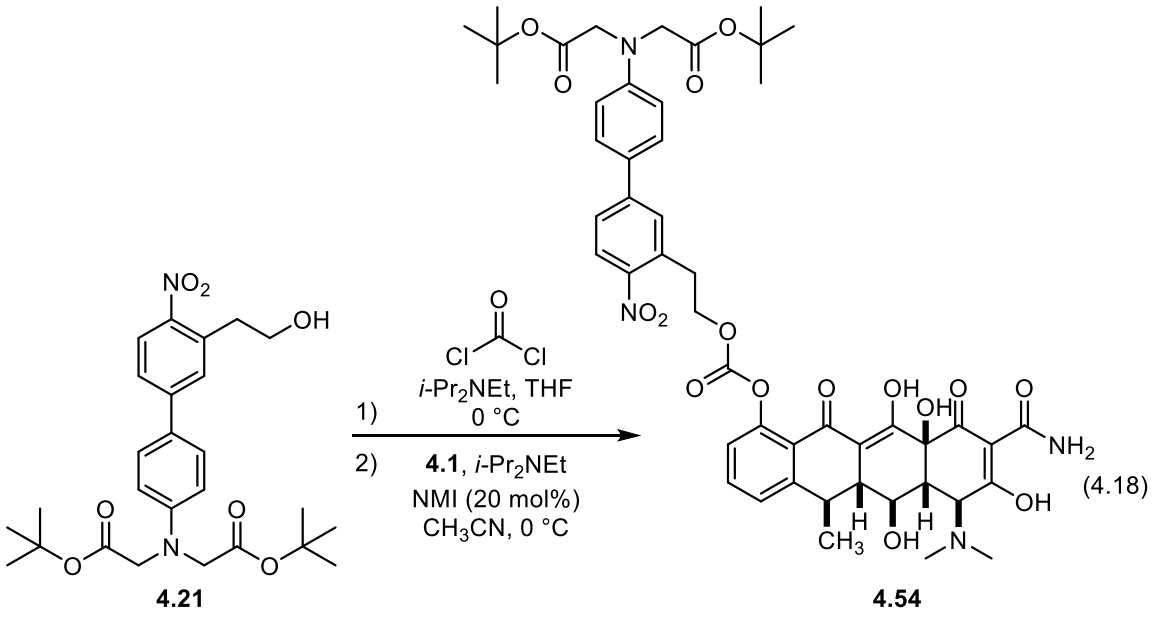

Due to the difficulty associated with purifying **4.54**. we directed our efforts to preparing a caged derivative of ATc (**4.2**), reasoning that its decreased polarity relative to doxycycline would facilitate purification. We attempted to prepare anhydrotetracycline

according to previously reported procedures[278] by heating tetracycline (**4.55**) and concentrated HCl in an alcoholic solvent under reflux; however we found the purity of the product to be highly variable. Following this procedure, we could isolate anhydrotetracycline in 80 – 93% purity based on the ^{1}H NMR spectrum (Scheme 4.7). Various attempts to recrystallize or purify the material by column chromatography were unavailing. While it was never confirmed, we speculated that the product was epimerizing under the reaction conditions, and the minor impurity was the epimeric product **4.56**. We circumvented this problem by running the reaction at room temperature rather than heating it under reflux (80 ˚C) (Equation 4.17). While the reaction time was significantly longer, requiring two days to go to completion, it proved to be a reliable, reproducible method to give anhydrotetracycline in excellent yield and purity on multigram scale.

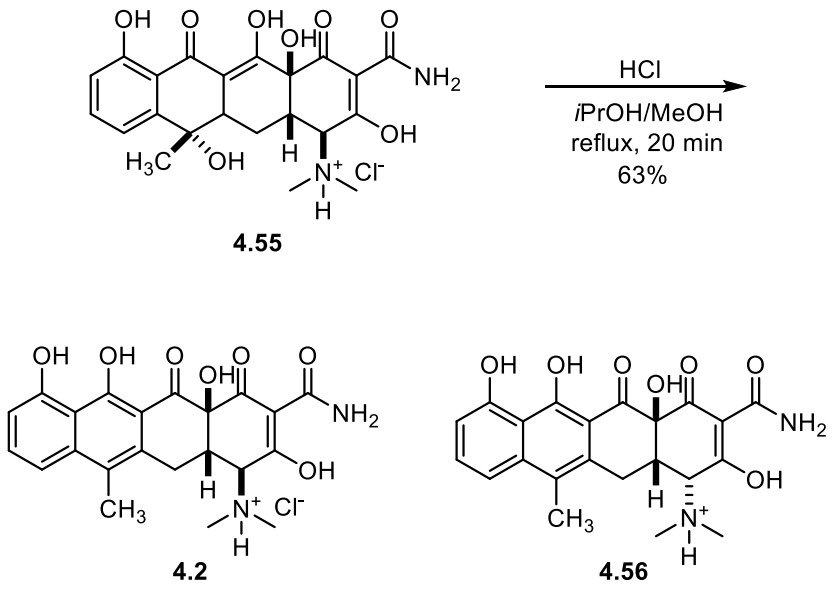

Scheme 4.7. Epimerization of ATc during the preparation from **4.55**

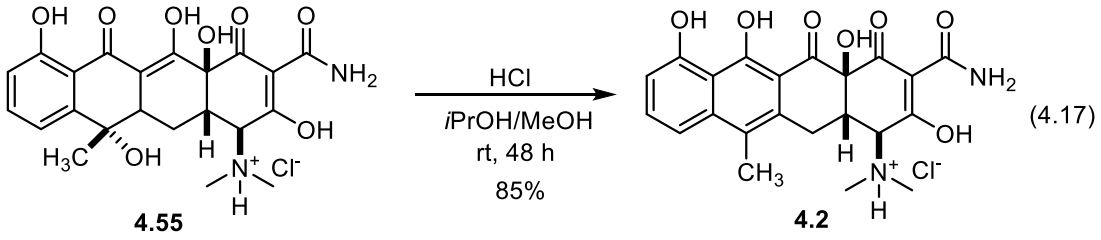

4.55 4.2 (4.17)

Treatment of anhydrotetracycline with benzyl chloroformate under the established acylation conditions for doxycycline revealed a similar product distribution by LCMS as seen with our doxycycline studies, with the major product having a mass corresponding to the mono-acylated product that we tentatively assigned as the phenol acylated product **4.57** (Equation 4.19). We next acylated anhydrotetracycline with chloroformate **4.52**, and to our delight, we found the reaction could be purified using standard chromatography (Equation 4.20). We isolated the desired product **4.58** in 12% yield, as well as some unidentified minor mono-acylated products. The majority of the material recovered from the reaction was unreacted anhydrotetracycline, as well ca. 50 mol % of **4.16**, which was attributed to be the result of incomplete formation of **4.52**.

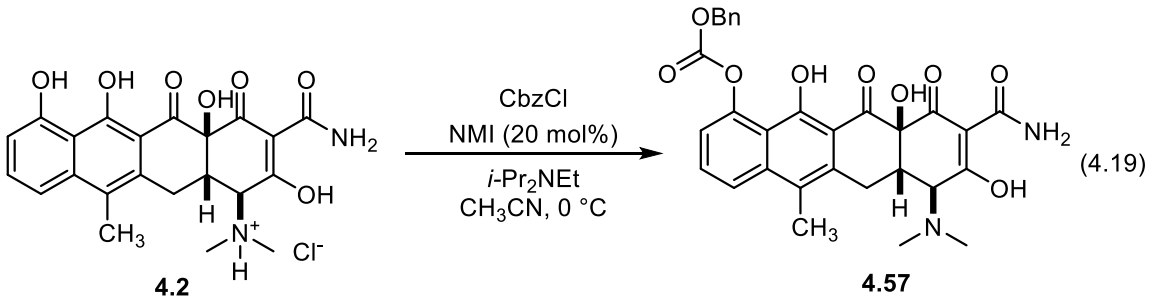

4.2 4.57 (4.19)

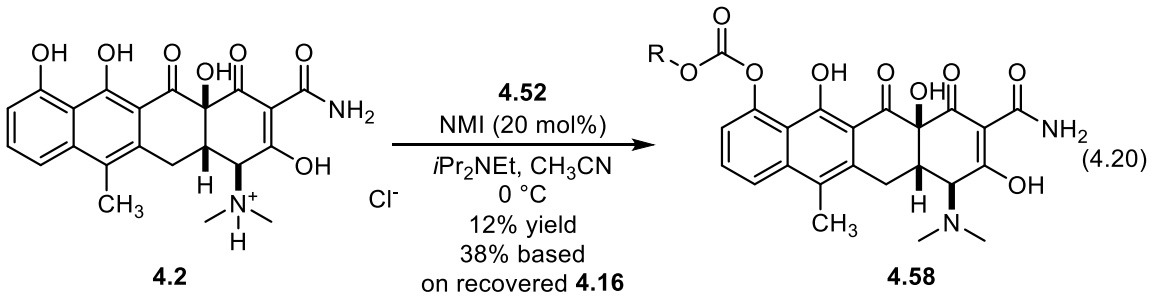

With conditions identified for acylating **4.2**, we had a clear path forward for installing the full **CANBP** photocages onto a tetracycline derivative. We began our studies with the nor-methyl **CANBP** cage **4.25**, reasoning it would be easier to purify due to the absence of diastereomeric products. Gratifyingly, we found that the acylation conditions developed for the various model systems translated well when chloroformate **4.59** was used, and the desired product **4.60** was isolated in 52% yield (Scheme 4.8). Removal of the *t*-butyl groups of **4.60** was accomplished through treatment with trifluoroacetic acid (TFA), which delivered the final caged ATc derivative **4.61** in quantitative yield.

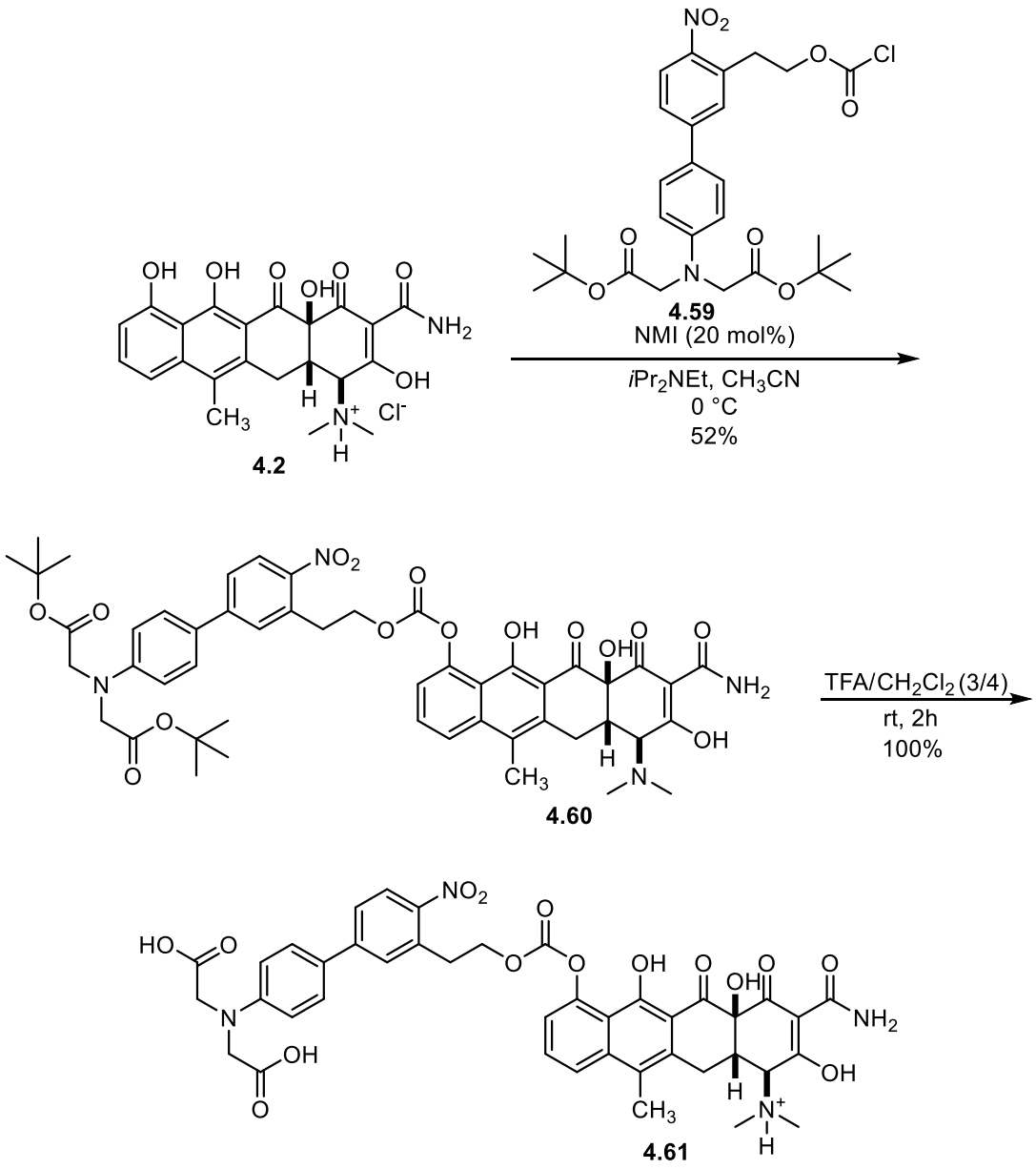

Scheme 4.8. Synthesis of caged ATc derivative **4.61**.

With **4.61** in hand, we began evaluating its possible use in our planned biological studies. To our dismay, we discovered that **4.61** is completely unstable in buffered aqueous solution, even in the absence of light. This was determined through control experiments of serial injections of an aqueous solution of **4.61** which had been protected from light onto

an analytical HPLC column. The caged compound **4.61** completely decomposed to **4.2** and **4.6-H** over the course of two hours. The instability of **4.61** was solvent dependent and we found that the compound was completely stable in organic solutions. Therefore, we assumed that carbonate linker was prone to hydrolysis. The poor stability of **4.61** has rendered this compound useless for our neuron labeling method and we were left with identifying a new strategy to cage anhydrotetracycline.

4.7 Summary and Future Directions

We have outlined a proposal for an exciting new method of identifying active neurons in the brain. If this method is successful, it could lead to a paradigm shift in the field of neurobiology and an unprecedented understanding of the brain. Unfortunately, so far, we have been unable to align the synthetic organic and neurobiology aspects of the project. That is to say, the synthetically accessible vanillic acid ligand is poorly behaved in the biological construct, and the biologically reliable tetracycline derivatives are challenging to selectively derivatize and purify. However, we think we have identified a clear path forward for preparing a water stable caged derivative of anhydrotetracycline.

Ethylene diamine carbamate linkers have been shown to be effective substitutes for carbonate linkers in the event of aqueous instability.[188] A recent example of this was demonstrated during a photocaging study of tamoxifen.[279,280] Upon irradiation of **4.63** and subsequent loss of CO_2, the by-products **4.64** and **4.65** were generated (Scheme 4.9). The carbamate **4.65** will then cyclize to form **4.66** and expel the leaving group, in this case **4.67**. This strategy should be readily applicable to the preparation of a caged derivative of **4.2** with a carbamate linker (Figure 4.6). We anticipate that the ATc derivative **4.68** would possess the necessary aqueous stability required for our studies, while maintaining a fast release rate of **4.2**.

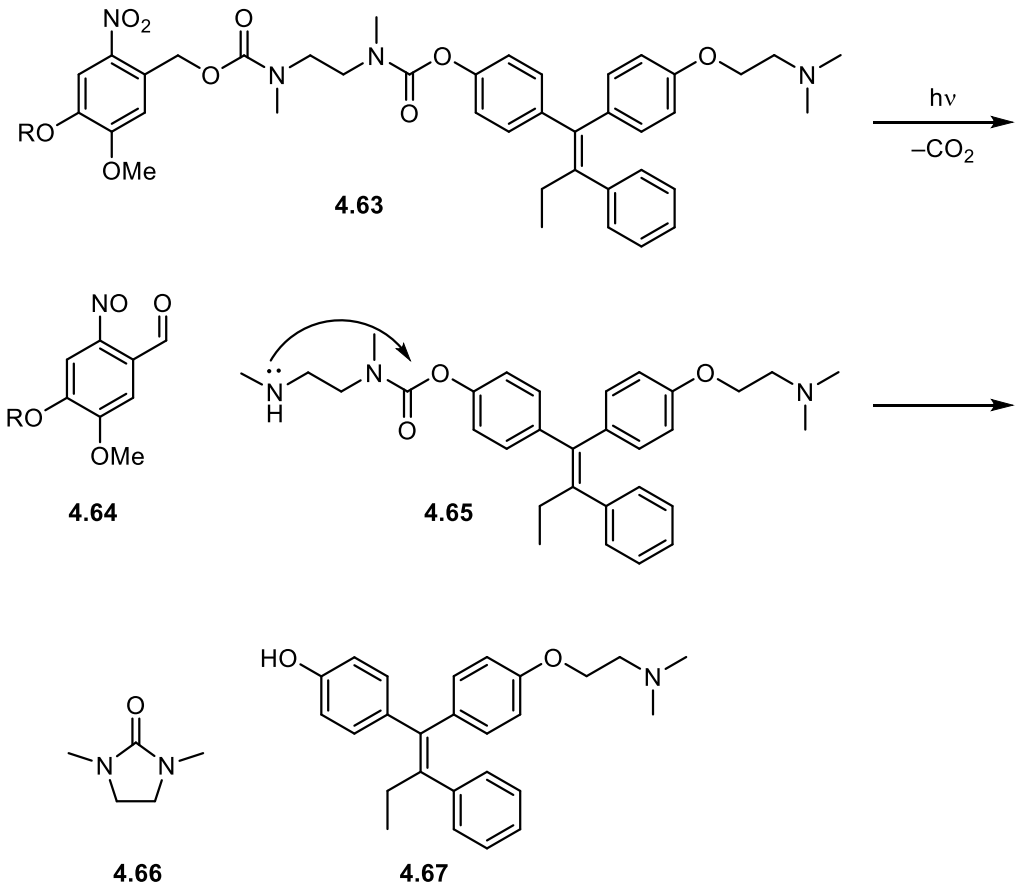

Scheme 4.9. Release of substrates from a photocage connected by an ethylene diamine carbamate linker.

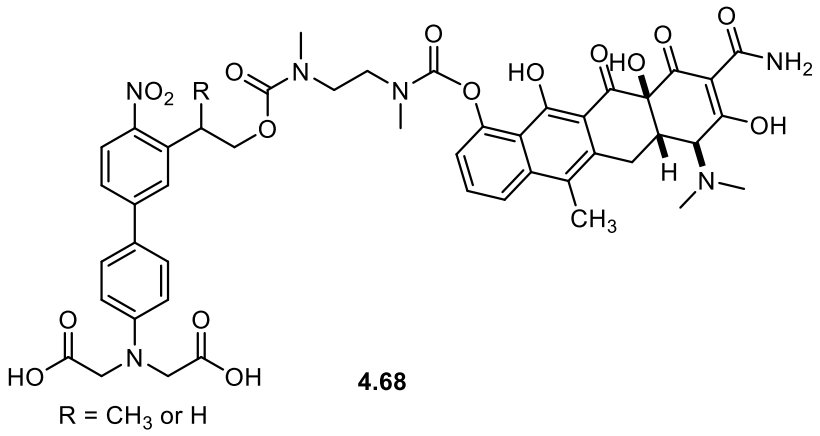

Figure 4.6 Carbamate linked caged ATc derivative.

Despite the instability of **4.61**, we were able to identify practical reaction conditions to selectively functionalize **4.2** and easily isolate the caged derivatives via standard chromatography. While we have not yet probed the general substrate scope this method, we expect this protocol to be readily applicable to other activated acylation reagents. Given the popularity and utility of the TET_{ON} gene expression system,[249,250,281] a general method to easily functionalize a tetracycline derivative would be valuable to the synthetic and biological communities. The deficiencies of the previous method for preparing light sensitive derivatives of **4.1** reported by Cambridge[261] further highlight the need for improvement. Thus, the preparation of **4.68** will also work towards establishing a general method for the preparation of caged derivatives of **4.2**. Once **4.68** is prepared, we can undertake the necessary solubility, stability, and deprotection experiments to test its viability for use in our labeling method.

PROGRESS TOWARDS THE TOTAL SYNTHESIS OF ALSTOSCHOLARISINE E

Chapter 5: Alstoscholarisines A–E – Isolation and Previous Syntheses

5.1 ISOLATION

Natural products that modulate the growth of neurons are quickly becoming a focus for the synthetic community.[282] Many neurogenic disorders, such as Alzheimer's and Parkinson's disease, are characterized by a progressive loss of neuronal activity. Consequently, novel therapies designed to restore neuronal viability or prevent neuronal decline are in high demand. The alstoscholarisines are five monoterpenoid indole alkaloids isolated from *Alstonia scholaris* collected in Yunnan Province, China by Luo in 2014 (Figure 5.1).[283]

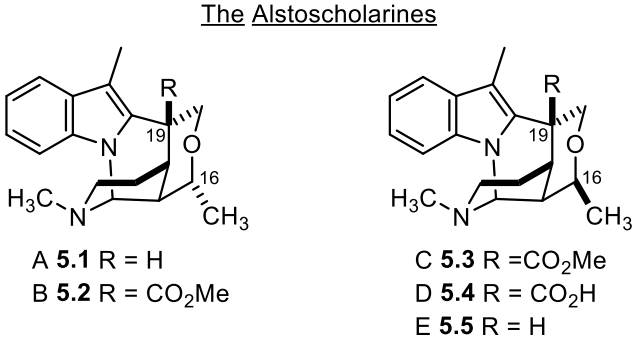

Figure 5.1. Alstoscholarisines A–E (**5.1–5.5**)

Alstoscholarisines A–E (**5.1**–**5.5**) share a pentacyclic core containing five contiguous stereocenters. They differ primarily in the presence or absence of a carboxyl moiety at C16, and the configuration of the methyl group at C19.[283] Alstoscholarisines A–E (**5.1**–**5.5**) were all found to promote neuronal stem cell (NSC) proliferation in a dosage dependent manner, with **5.1** being the most potent, functioning at a concentration of 0.1

μg/mL. Additionally, **5.1** was shown to promote NSC sphere formation and neuron differentiation. These compounds could play an important future role in discovering new treatments for neurodegenerative disorders such as Alzheimer's, Parkinson's, or Huntington's diseases.

The important biological activity and interesting structural features of the alstoscholarisines did not go unnoticed by the synthetic community, and there have been three reported syntheses of members of the alstoscholarisine family to date. Bihelovic and Ferjancic disclosed the first synthesis of (±)-alstoscholarisine A in 2016[284] and soon after, Yang reported an enantioselective synthesis of (–)-alstoscholarisine A.[285] Most recently, Weinreb pursued the more complex members of the alstoscholarisine family, and in 2017 reported syntheses of (±)-alstoscholarisine B and (±)-alstoscholarisine C.[286]

5.2 Previous Syntheses of Alstoscholarisine A

5.2.1 Bihelovic and Ferjancic's Synthesis of (±)-Alstoscholarisine A

Bihelovic and Ferjancic's synthesis commenced with the radical alkylation of skatole (**5.6**) using the xanthate ester **5.7**, followed by protection of the indole nitrogen to afford the known intermediate **5.9** (Scheme 5.1).[287] The ester enolate of **5.9** generated through treatment with lithium diisopropylamide (LDA) was allowed to react with aldehyde **5.10** to afford the aldol product **5.11**. This intermediate was immediately treated with sodium hydride, which triggered the migration of the indole nitrogen *t*-butylcarbamate (Boc) protecting group to the free alcohol **5.12**, and β-elimination of the newly formed carbonate delivered **5.13** in 75% yield from **5.9**. Interestingly, **5.13** was isolated primarily as the *E* isomer, with only minor amounts of the *Z* isomer detected. Next, palladium mediated removal of the allyl carbamate protecting group delivered **5.14** in 72% yield, and the stage was set for the investigation of the key domino cyclization cascade.

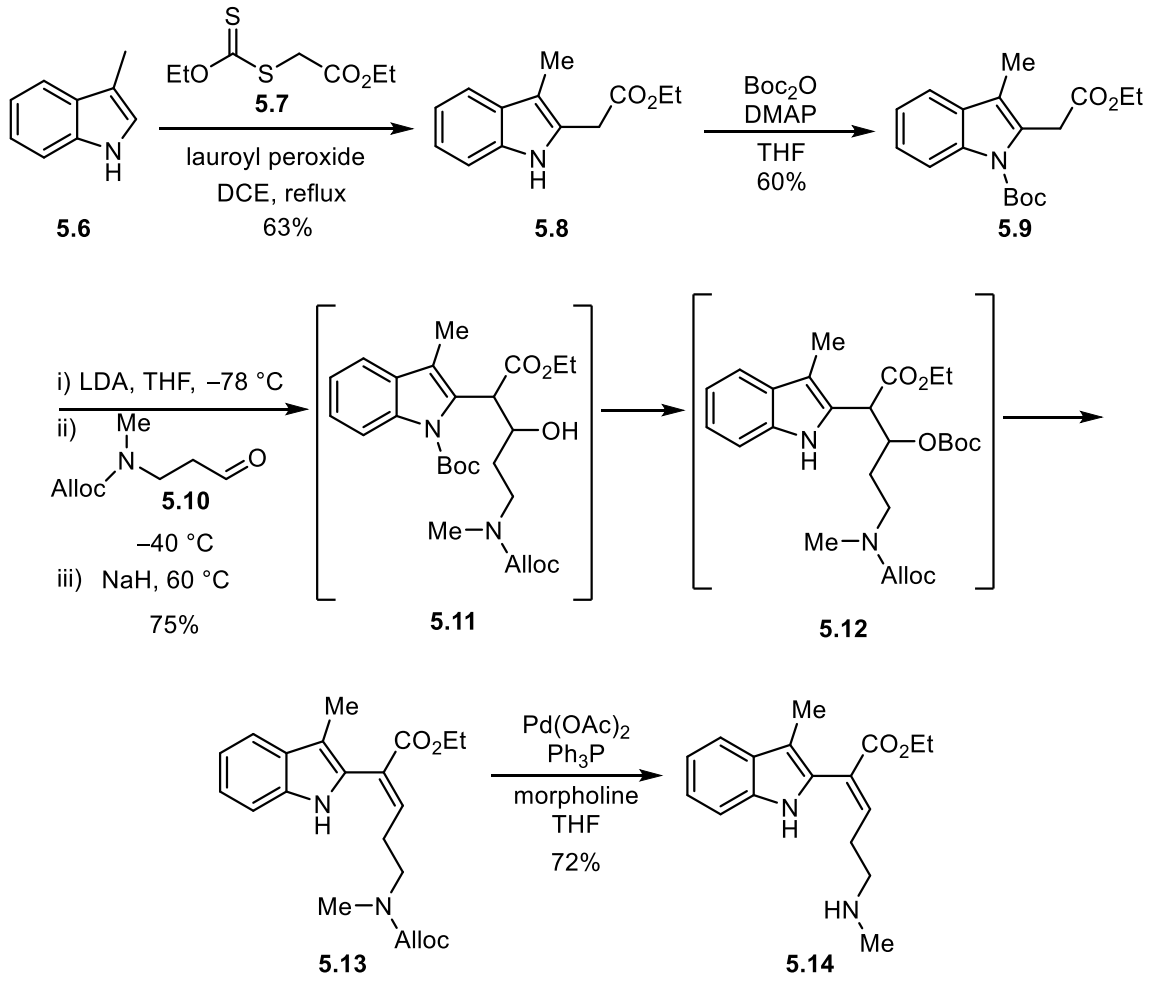

Scheme 5.1. Synthesis of **5.14**

With **5.14** prepared, the domino cyclization sequence was investigated. Initially, the cascade was attempted using ethyl propiolate (**5.15**), but, only Michael addition into the alkyne was observed (**5.16**). The reaction did not progress to intermediate **5.17** (Scheme 5.2). They hypothesized that the vinylogous carbamate **5.16** was not sufficiently nucleophilic to effect the second Michael addition and generate **5.17**. To address this issue, they planned instead to use an aliphatic enamine, to provide enhanced reactivity and possibly complete the desired cyclization.

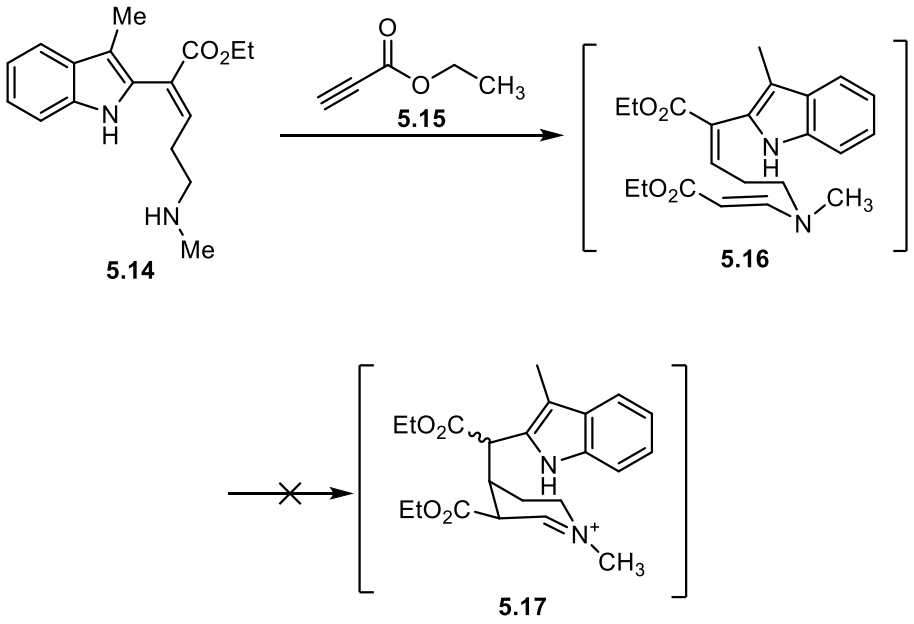

Scheme 5.2. Attempted domino cyclization sequence using **5.15**

Accordingly, 4-(phenylselanyl)butanal (**5.18**) was used as a synthon for 3-butenal, and when **5.14** was heated with **5.18** in CH_3CN in the presence of molecular sieves, it was smoothly converted to the tetracyclic products **5.21a,b** in a 1:1 ratio (Scheme 5.3). Fortunately, the ratio of **5.21a** and **5.21b** could be improved to 5:1 when DBU was added, and the reaction mixture was heated after the cyclization. In this fashion, the desired diastereomer **5.21a** was prepared in 71% yield (Equation 5.1).

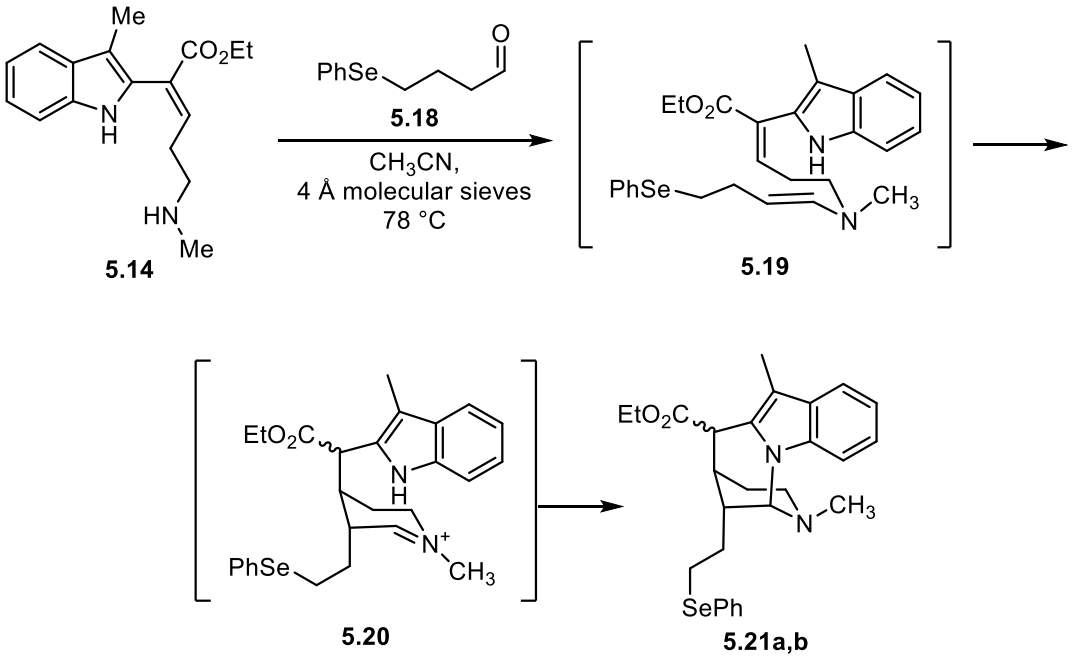

Scheme 5.3 Successful domino cyclization sequence using **5.14** and **5.18**

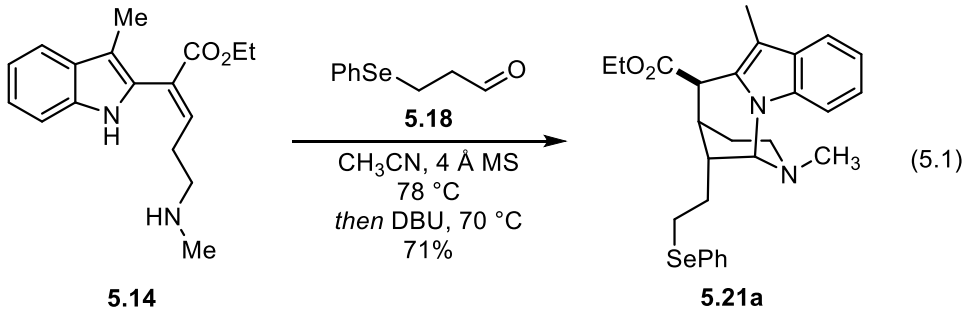

Interestingly, the selenium containing aliphatic side chain adopted an axial orientation in both **5.21a** and **5.21b**. The stereochemical outcome of the cyclization was rationalized to occur as the result of an equilibration between the enamine **5.23** and the iminium salts **5.22** and **5.20** (Scheme 5.4). Intermediate **5.20** is proposed to be thermodynamically more stable than **5.22**, due to the unfavorable gauche interactions present in **5.22** when the alkyl side chain is equatorial.

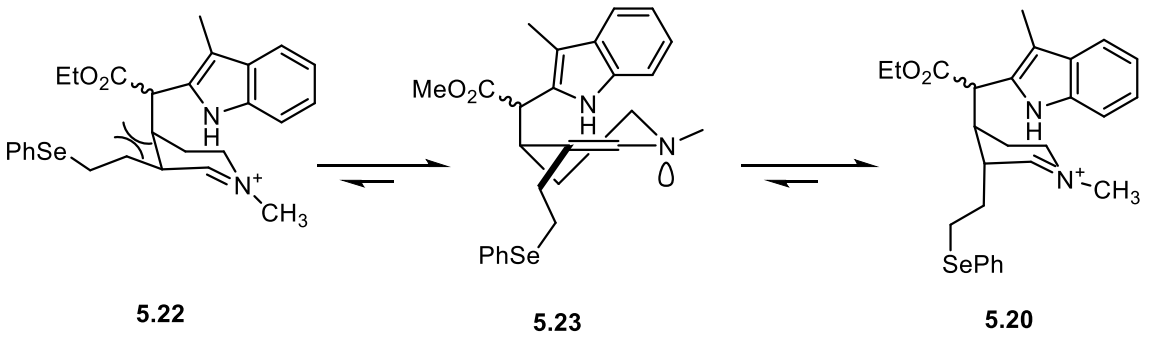

5.22 **5.23** **5.20**

Scheme 5.4. Equilibration between **5.22** and **5.20**.

With an efficient route to **5.21a** established, focus was shifted to the construction of the tetrahydropyran moiety of **5.1**. Toward this end, the selenide moiety of **5.21a** was oxidized with *meta*-chloroperoxybenzoic acid (*m*-CPBA), and the resulting selenoxide was eliminated to give olefin **5.24** in 83% yield. The ethyl ester was then reduced with diisobutylaluminum hydride (DIBAL) to afford the primary alcohol **5.25**. The terminal olefin of **5.25** was converted to the aldehyde **5.26** in two steps through dihydroxylation followed by diol cleavage with $Pb(OAc)_4$.

In order to form the desired tetrahydropyran, the axial aldehyde moiety of **5.26** required epimerization to the equatorial configuration. Unfortunately, **5.26** was unstable to a variety of basic conditions, possibly due to β-elimination of one of the indole moiety. Additionally, it seemed that the axial orientation of the aldehyde side chain of **5.26** was thermodynamically preferred because attempts to equilibrate it to the equatorial epimer were unsuccessful. Fortunately, when **5.26** was treated with DBU at room temperature, isomerization took place and the equatorial conformer was trapped as the mixture of hemiacetals **5.27**, which was immediately oxidized with Dess–Martin periodinane (DMP) to deliver **5.28** in 34% yield from **5.25**. The lactone **5.28** was converted to alstoscholarisine A (**5.1**) in two steps beginning with addition of MeLi to give hemiketal **5.29**, followed by

a diastereoselective ionic reduction with Et_3SiH and TMSOTf, where hydride delivery occurred from the convex face of the oxonium ion generated *in-situ*.

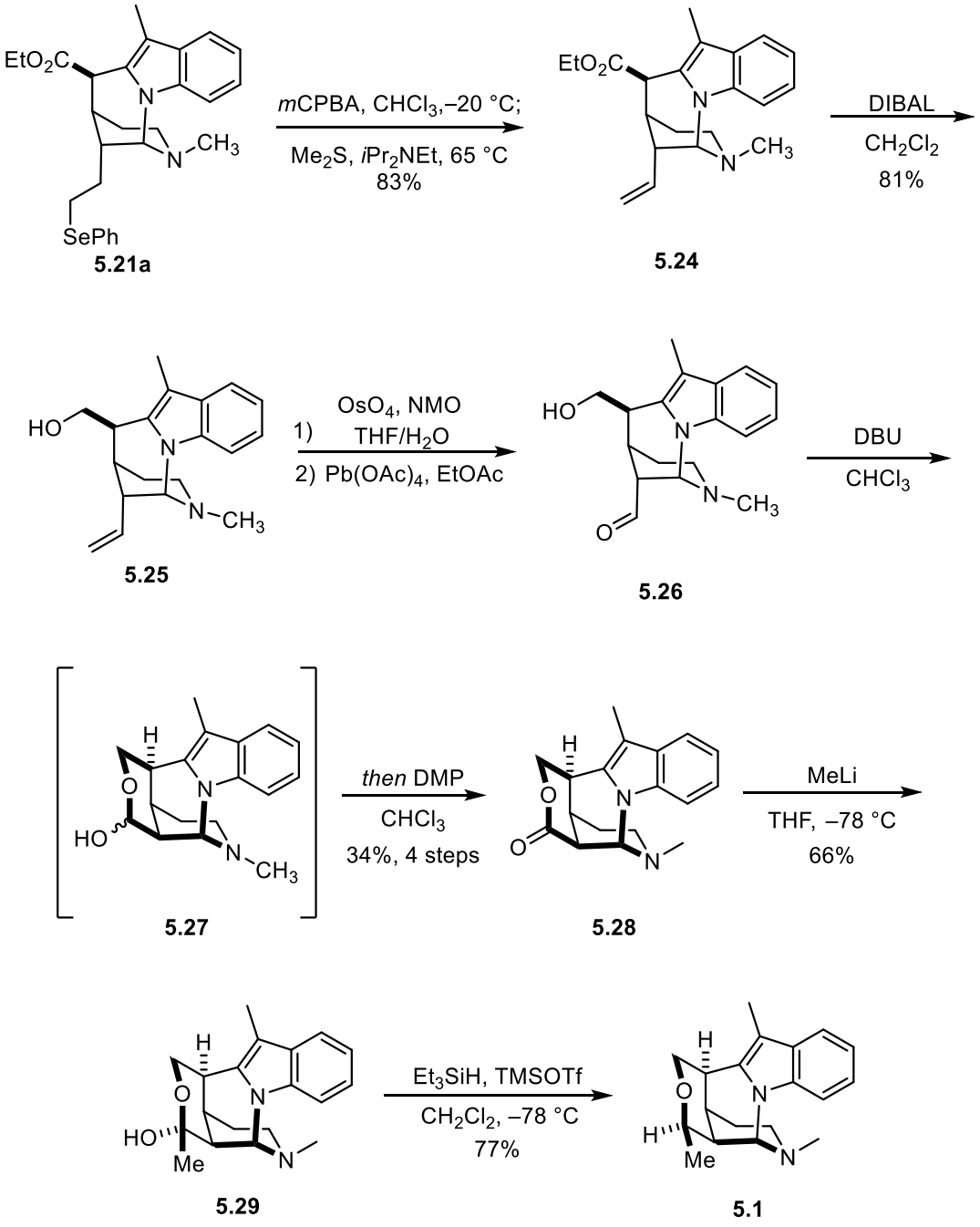

Scheme 5.5. Elaboration of **5.14** to alstoscholarisine A (**5.1**)

Bihelovic and Ferjancic completed the synthesis of (±)-alstoscholarisine A (**5.1**) in 13 steps and 1.7% overall yield from **5.5**. Their synthesis relied on an efficient domino sequence that quickly constructed the core of the natural product (**5.14** to **5.21a**, Equation 5.1). They were able to reach tetracyclic intermediate **5.21a**, in only five steps and good yield. Unfortunately, the construction of the tetrahydropyran ring was cumbersome, requiring seven steps, four of which were redox manipulations. Nevertheless, this synthesis is notable in that it represents the first successful approach to **5.1**.

5.2.2 Yang's Synthesis of (–)-Alstoscholarisine A

Yang's synthesis commenced with the preparation of the known butyrolactone **5.32**.[285] This starting material **5.32** was available in two steps and 40% yield from **5.30**, by a process involving ozonolysis of the terminal olefin to provide **5.31**, followed by addition of a vinyl Grignard reagent to the newly formed aldehyde and intramolecular cyclization to provide **5.32**.[288] The lactone **5.32** was then used to acylate the skatole (**5.5**) nitrogen atom under Lewis acidic conditions to provide **5.33** in 75% yield. This intermediate was the precursor for the first key step in Yang's enantioselective synthesis.

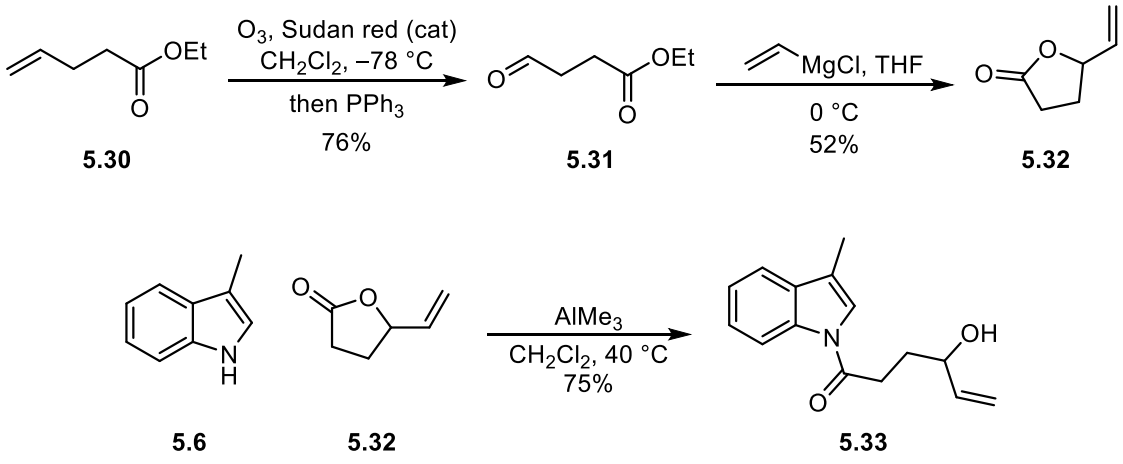

Scheme 5.6. Preparation of enantioselective Friedel–Crafts alkylation starting material.

An intramolecular cyclization of the allylic alcohol to the 2-position of **5.33** through a catalytic asymmetric Friedel–Crafts alkylation generated **5.34** in 75% yield and 99% ee. The terminal olefin of **5.34** was then dihydroxylated using OsO_4 to provide intermediate **5.35** as an inconsequential mixture (5:1) of diastereomers. The crude diol moiety was protected as the acetonide and the major diastereomer, **5.36**, was isolated in 75% yield and carried forward. Next, **5.36** was oxidized to the enone **5.37** through standard selenylation–elimination conditions. The enone **5.37** was used as a synthetic handle to install the remaining carbon framework of the natural product through a tandem Michael–aldol addition sequence. Copper iodide promoted the 1,4–addition of vinyl Grignard to **5.37**, and the resulting enolate was trapped with acetaldehyde to give **5.38** in 75% yield as a mixture (8:1) of diastereomers. The benzylic stereocenter of **5.37** was crucial to the success of the Michael–aldol sequence, as it directs the 1,4–addition, which in turn directs the stereochemistry of the aldol reaction. Yang did not report any additional details about the attempts to improve the diastereomeric mixture obtained during the conversion of **5.37** to **5.38**.

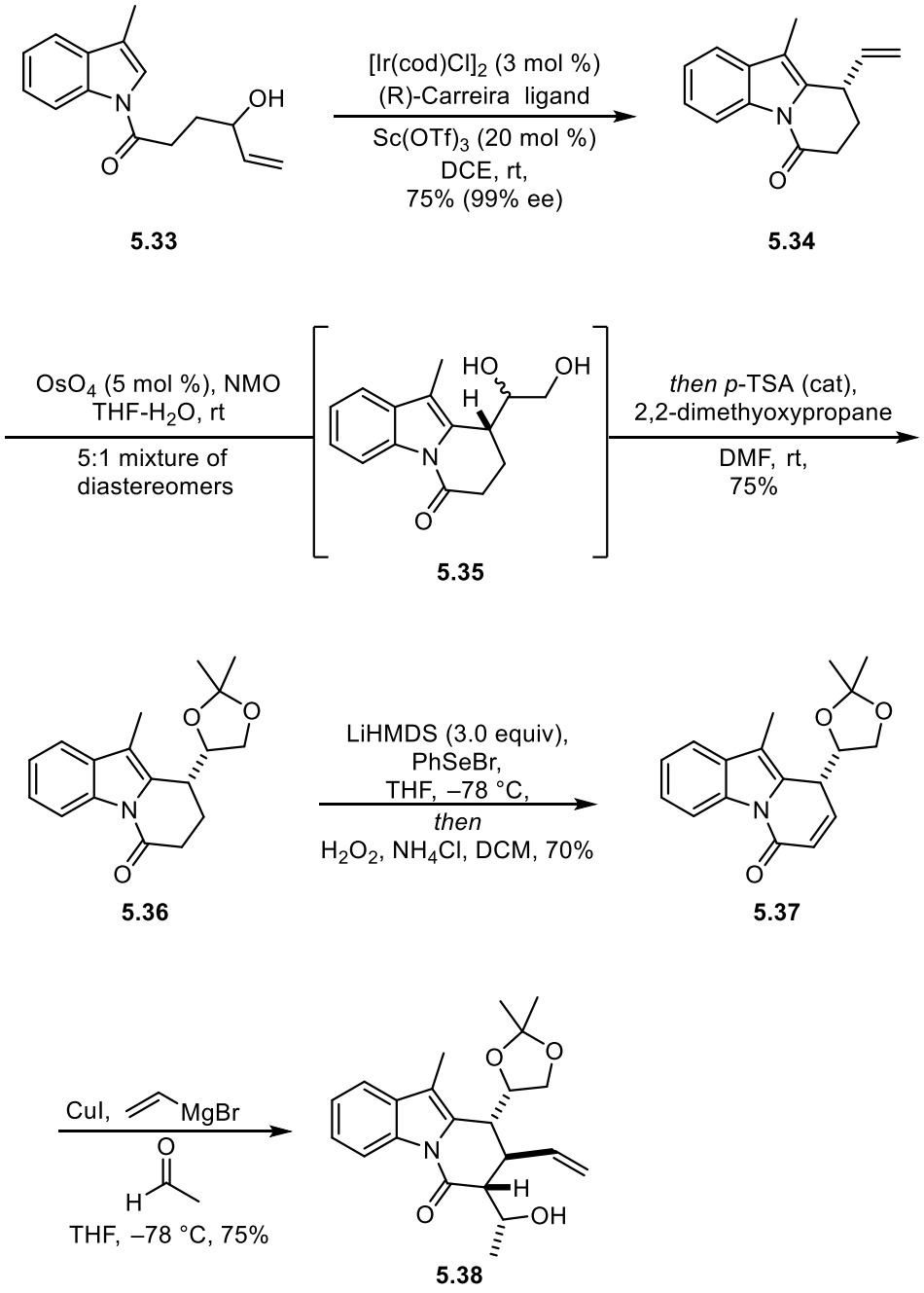

Scheme 5.7. Elaboration of **5.33** to **5.38**.

With the requisite stereocenters set and the carbon framework in place, focus was shifted to forming the final rings of **5.1**. The diol of **5.38** was unmasked under acidic

conditions, cleaved with $NaIO_4$, and the newly formed aldehyde was trapped as lactol **5.39** after intramolecular cyclization. The tetrahydropyran moiety was installed through an ionic reduction of the lactol **5.39** to form **5.40**. Hydroboration-oxidation of the terminal olefin of **5.40,** followed by oxidation of the primary alcohol with DMP afforded **5.41** in 81% yield. Finally, **5.41** was converted to **(–)-5.1** through a reductive amination-cyclization sequence with methylamine to install the final ring.

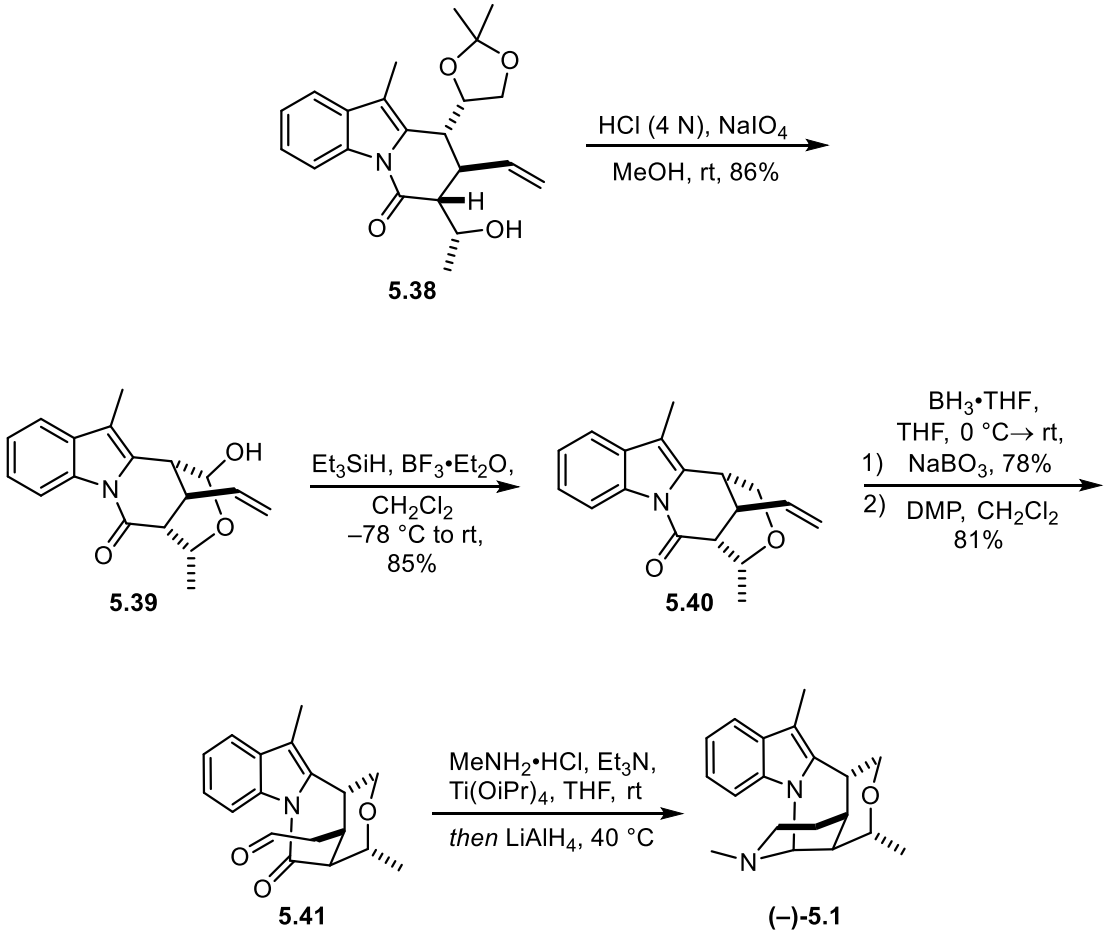

Scheme 5.8. Completion of **(–)-5.1** from **5.38**

Yang's synthesis of **(–)-5.1** was accomplished in 12 steps and 3% overall yield from **5.30**.[285] The highly selective intramolecular Friedel–Crafts alkylation proved to be a sound

strategy for the synthesis of **(–)-5.1**, as the stereocenter set during this initial cyclization directed the remaining carbon stereocenters later in the synthesis. Aside from having the only enantioselective approach to these natural products, Yang's synthesis is unique in his strategy for the late stage construction of piperidine ring (*i.e.* conversion of **5.41** to **5.1**). All other approaches to these natural products have instead constructed the tetrahydropyran moiety in the final step.

5.2.3 Weinreb's Synthesis of (±)-Alstoscholarisines B and C

Weinreb's synthesis of alstoscholarisines B (**5.2**) and C (**5.3**) commenced with the preparation of the Michael acceptor **5.45** (Scheme 5.9).[286] 2-Piperidone (**5.42**) was tosylated to give **5.43** (55%), which was then converted to **5.44** through treatment with excess lithium hexamethyldisilazide (LiHMDS) and sequential addition of allyl chloroformate followed by phenylselenium bromide. The selenide **5.44** was then oxidized and eliminated to afford Michael acceptor **5.45** in quantitative yield.

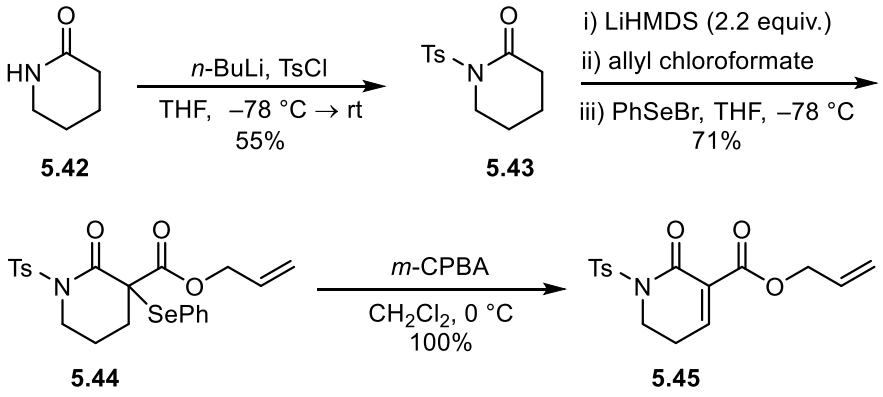

5.42 **5.43** **5.44** **5.45**

Scheme 5.9. Preparation of the Michael acceptor **5.45**

For the nucleophilic component of the planned conjugate addition with Michael acceptor **5.45**, Weinreb prepared **5.9** from **5.6** in the same manner as Bihelovic and

Ferjancic. The ester enolate of **5.9** was generated through treatment with lithium bis(trimethylsilyl)amide (LiHMDS) and then used in a Michael reaction with **5.45** to afford **5.46** in 69% yield as a complex mixture of stereoisomers (Scheme 5.10). Subjection of **5.46** to a one-pot C–allylation/decarboxylation process delivered **5.47** in 74% yield. This product was found to have a *trans*-configuration at C15 and C20, but it was a mixture of epimers at C16. The *N*-sulfonyllactam carbonyl moiety of **5.47** was reduced with DIBAL, and exposure of the aminal **5.48** to trifluoroacetic acid resulted in removal of the Boc protecting group and cyclization to afford **5.49** in 74% yield. The ester enolate of **5.49** was generated with LiHMDS and quenched with formaldehyde, and the resultant hydroxy methyl moiety was protected as the TBS ether delivering **5.50** in 80% yield.

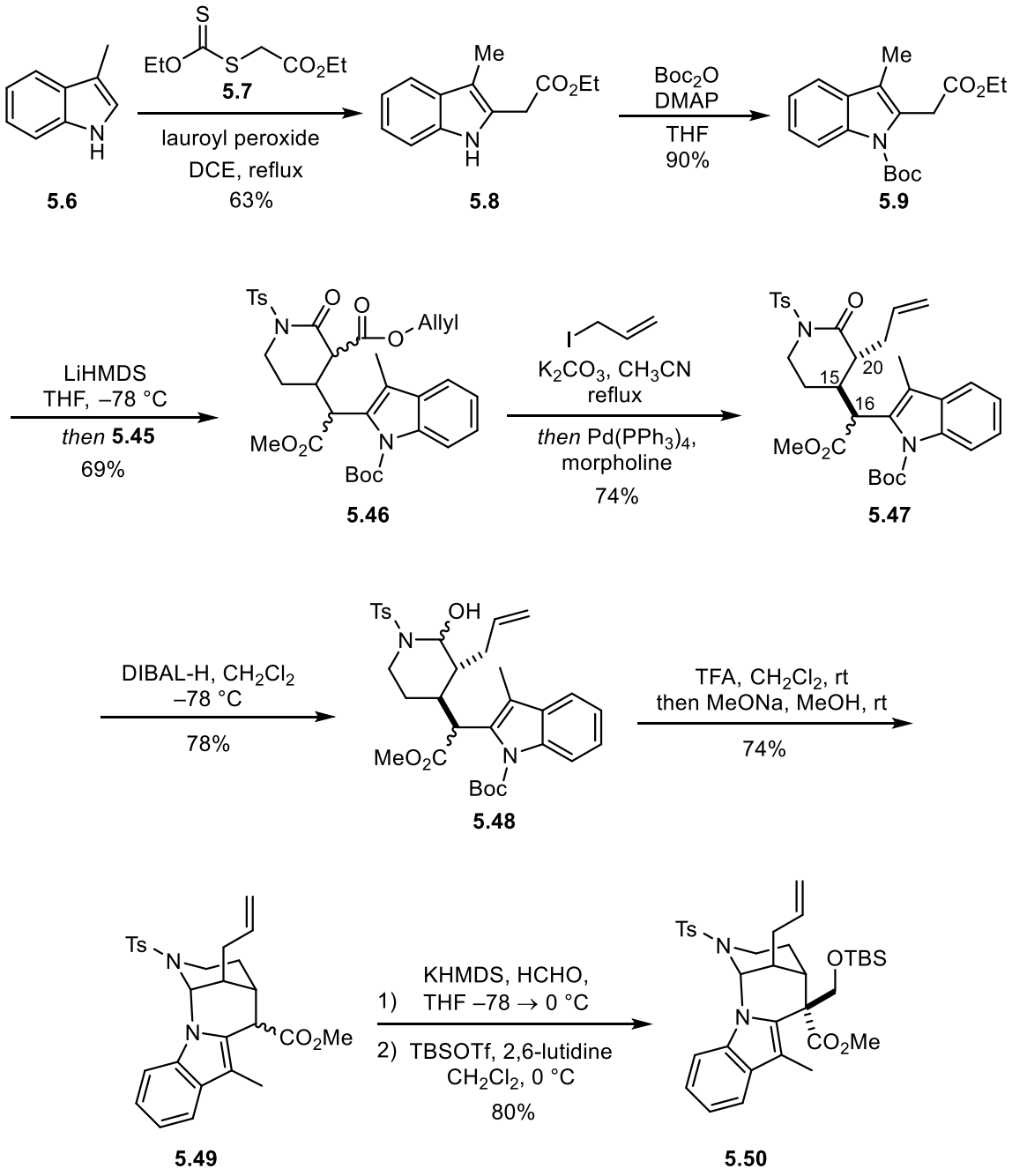

Scheme 5.10 Synthesis of the tetracyclic core **5.50** of **5.2** and **5.3**

After having constructed the tetracyclic core **5.50** of the target natural products, attention was turned to the construction of the remaining tetrahydropyran ring. The allyl

group of **5.50** was required to be converted into a formyl group. The olefin of **5.50** was transposed through a thermal ene reaction with diethyl diazocarboxylate (DEAD) to afford the allylhydrazine **5.51** in 77% yield (Scheme 5.11). The desired aldehyde was then prepared through dihydroxylation of **5.51** followed by cleavage of the resultant diol with $Pb(OAc)_4$ to afford **5.52** in 61% yield. The hydroxy methyl silyl ether protecting group was removed under acidic conditions to afford **5.53**, which only required epimerization of the axial aldehyde to form the tetrahydropyran ring.

Following a similar strategy to that used by Bihelovic and Ferjancic, **5.53** was treated with DBU to promote the formation of **5.54**, which cyclized to form a lactol that could be trapped as the acetate **5.55** with acetic anhydride. For the synthesis of alstoscholarisine C, **5.55** was reacted with $AlMe_3$ in the presence of TMSOTf to afford the methylated tetrahydropyran **5.56** as a single stereoisomer. This reaction presumably proceeds through the transfer of a methyl group from trimethylaluminum to the least hindered convex face of the intermediate oxocarbenium ion formed upon ionization of the acetate leaving group. Finally, alstoscholarisine C was completed through removal of the *N*-tosyl protecting group of **5.56**, followed by a reductive methylation, which delivered **5.3** in 60% yield.

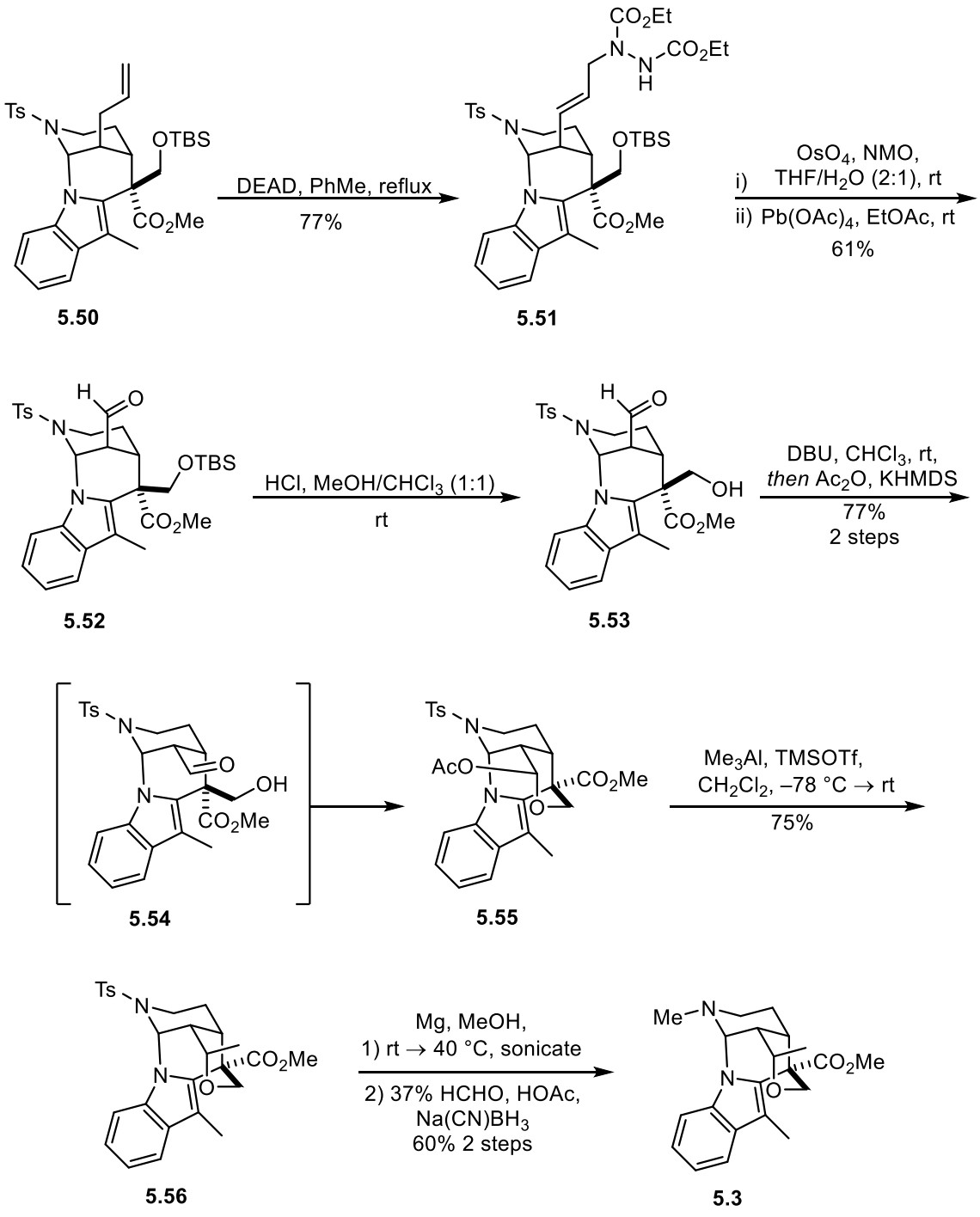

Scheme 5.11. Elaboration of **5.50** to (±)-alstoscholarisine C (**5.3**)

To complete the synthesis of alstoscholarisine B, **5.53** was converted to the lactol **5.57**, which was oxidized to the lactone **5.58** with iodobenzene diacetate/TEMPO (Scheme 5.12). Addition of methyllithium to **5.58** delivered **5.59** as a single stereoisomer, the absolute configuration of which was not determined. Subsequent ionic reduction of **5.59,** removal of the tosyl protecting group, and finally *N*-methylation afforded alstoscholarisine B (**5.2**).

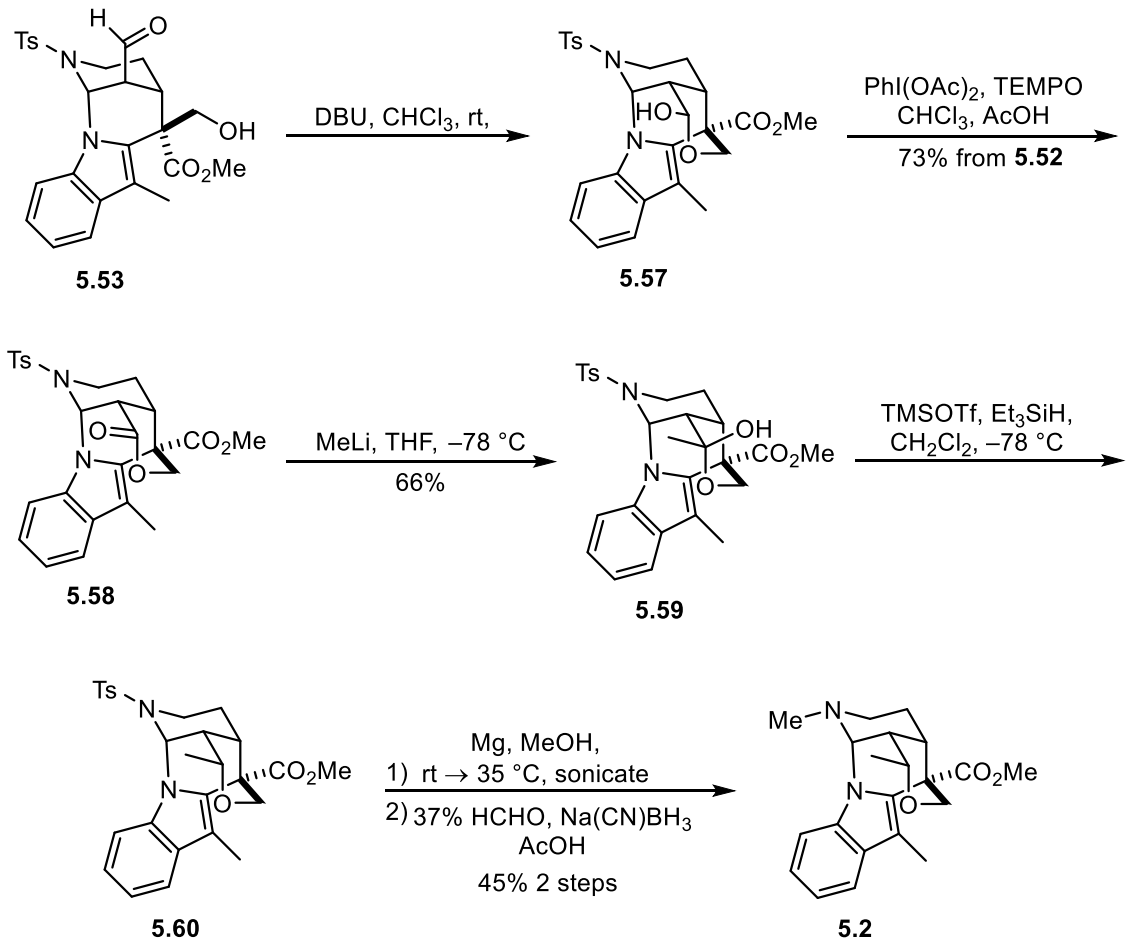

Scheme 5.12. Elaboration of **5.53** to **5.2**

Weinreb's syntheses of (±)-alstoscholarisines B (**5.2**) and C (**5.3**) proceeded in 20 and 17 steps respectively from **5.42**. These syntheses represent the first successful approaches to these natural products. Although there was no novel method showcased during the preparation of these molecules, the strategy to transpose the olefin of **5.50** through an ene reaction with DEAD (i.e. conversion of **5.50** to **5.51**, Scheme 5.10) was an interesting approach to convert the allyl group of **5.50** to a formyl group.

5.3 SUMMARY

There have been three reported syntheses of an alstoscholarisine natural product since their isolation in 2014.[283–286] Bihelovic and Ferjancic's synthesis of (±)-alstoscholarisine A (**5.1**) was the first reported synthesis of this natural product and they utilized an efficient domino cascade sequence to quickly construct the tetracyclic core of the molecule. Unfortunately, the construction of the remaining tetrahydropyran ring was less elegant, and detracted from the overall quality of their total synthesis. Nevertheless, they managed to complete a total synthesis of **5.1** relatively quickly, requiring only 13 steps in 1.7% overall yield. Yang also reported an efficient synthesis of alstoscholarisine A, with the added innovation of preparing **5.1** as a single enantiomer. While Yang's synthesis did not showcase any new chemistry, his key steps generally proceeded in good yield and selectivity. Weinreb's synthesis arguably also lacked innovation, but he did showcase a complicated conjugate addition (i.e. addition of **5.9** to **5.45** Scheme 5.8) and an interesting strategy to degrade an allyl group to a formyl group.

We began devising an approach to alstoscholarisine E (**5.5**) soon after the natural products were isolated. During the course of our planning, the total syntheses of alstoscholarisine A were reported by Bihelovic and Ferjancic and Yang. Despite the efficiencies of these routes, we believed that our approach offered significant

improvements over the previous reports, primarily because our planned route required only six steps to prepare **(±)-5.5**. Accordingly, we continued forward with our plan for a rapid synthesis of alstoscholarisine E.

Chapter 6: Progress Towards the Total Synthesis of Alstoscholarisine E

6.1 Synthetic Strategy

We envisioned a convergent synthesis of alstoscholarisine E (**6.1**) where **6.4** and **6.5** would be joined through a metal catalyzed coupling to give **6.3**, which could then be transformed to **6.1** in two steps through an olefin reduction followed by a reductive cyclization to form the final bridging aminal. Fragment **6.4** would be readily available through functionalization of 3-methylindole, and we planned to access **6.5** through a hetero-Diels–Alder (HDA) reaction of **6.6**. Previous studies in the Martin group demonstrated that **6.6** would be a suitable substrate for a HDA reaction;[289,290] however, our previous syntheses of compounds similar to **6.6** required seven steps to prepare. Given that a number of efficient syntheses of other members of this family of natural products have already been reported,[284,285] accessing **6.6** efficiently was paramount to the effectiveness of our overall approach. Thus, we devised a novel method to prepare **6.6** in step from the readily available starting materials **6.7**, **6.8**, **6.9**.

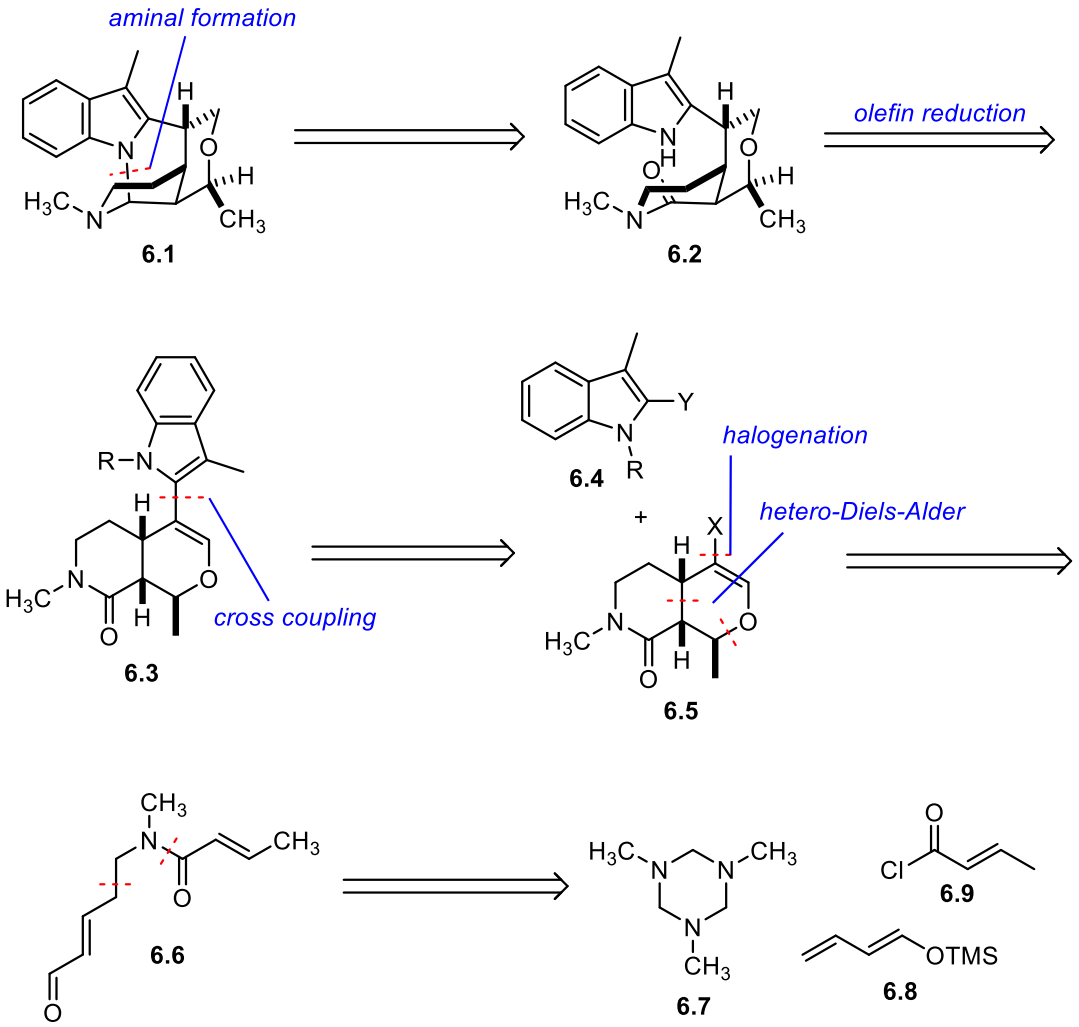

Scheme 6.1. Synthetic strategy for the preparation of alstoscholarisine E (**6.1**).

6.1.2 Martin Group Previous Work: Intramolecular Hetero-Diels–Alder Reactions

As part of our work in natural product synthesis, the Martin group became interested in the intramolecular Diels–Alder reactions of compounds such as **6.17**.[289–294] The preparation of the HDA precursor commenced from the protected propargyl alcohol **6.10**, the alkyne of which was lithiated with *n*-BuLi and reacted with ethylene oxide to generate **6.11** in 81% yield. Partial hydrogenation of the alkyne moiety of **6.11** proceeded smoothly, and the free alcohol of **6.12** was tosylated to give **6.13**. The activated tosyl

alcohol was then displaced with benzyl amine to afford **6.14,** which was acylated using **6.15** to afford the crotyl amide **6.16**. Finally, after removal of the methoxymethyl acetal (MOM) protecting group of **6.16**, Swern oxidation of resulting free alcohol delivered **6.17** in 7 steps and 39% overall yield from **6.10**.

At the time of these investigations, little was known about the intramolecular cyclization of trienes such as **6.17**. While many examples of intermolecular Diels–Alder reactions between an electron rich dieneophile with an α,β-unsaturated aldehyde as the diene component existed,[293] examples of intramolecular variants were sparse. Furthermore, **6.17** was also a unique intramolecular HDA substrate in that the diene and dieneophile were both electron deficient. Thus, it was notable that thermolysis of **6.17** (190 °C) delivered a 5:1 separable mixture of **6.18**:**6.19**, with the *cis*-cycloadduct **6.18** as the major component. With this proof of principle, we were then able to apply cycloadditions of this type towards several natural product syntheses.[293,294]

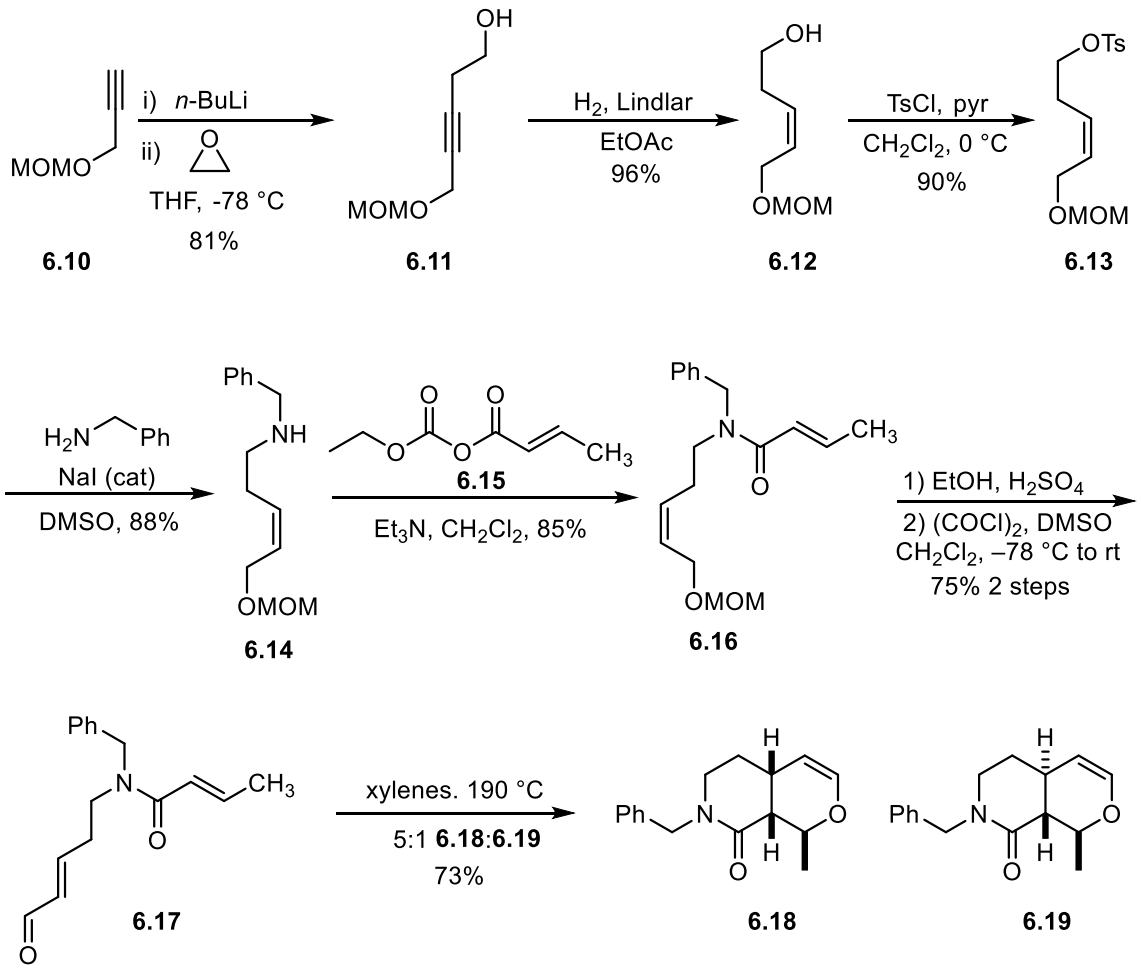

Scheme 6.2. Previous Martin group synthesis of intramolecular HDA precursors.

The preference for *cis*-fused bicyclic products during intramolecular Diels–Alder cycloadditions of trienes linked by ester and amide tethers has been observed in other independent investigations.[295–297] The interesting stereochemical outcome for these cyclizations prompted a number of theoretical mechanistic studies. The possible transition states that give rise to the *cis* and *trans* fused products **6.21** and **6.24** are depicted in scheme 6.3. The substrate is capable of cyclizing from a chair- (**6.22** and **6.25**) or boat-like (**6.20** and **6.23**) confirmation and there is an *endo* or *exo* arrangement possible for each. Theoretical mechanistic studies from our own lab[293] and later ones from Tanitillo and

Houk[298] on intramolecular cyclizations of this type were in agreement that *endo* geometries are favored over *exo* geometries, and that the boat-like conformations are preferred over the chair-like ones. However, these preferences can be influenced by the substituents present on the cycloaddition precursor of interest.[298] The preference for the boat-like conformation has been attributed to the ability of the amide group to maintain near planarity in these transition states, translating to better orbital overlap during the cyclization.[293] The orbital overlap between the diene and dienophile was determined to be maximized in the *endo*-boat-like transition state of type **6.23**, resulting in the *cis*-cycloadduct as the major product.[298] The results of these theoretical investigations were in good agreement with experimentally observed product ratios.[290,295,297]

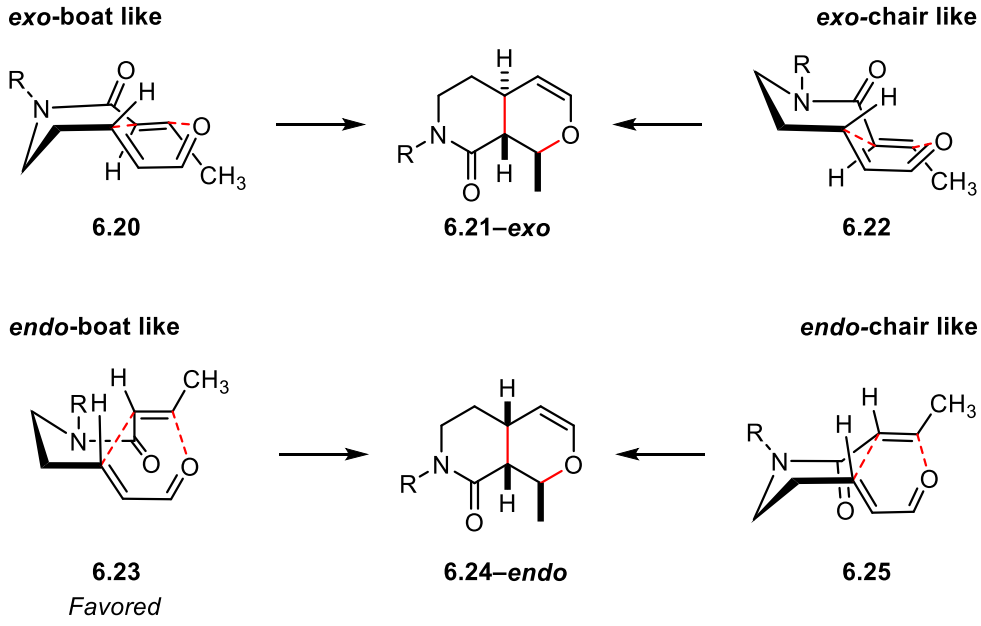

Scheme 6.3. Possible transition states for intramolecular HDA cycloadditions for amide tethered trienes.

6.2 One-Step Preparation of Hetero-Diels–Alder Precursor

Hexahydrotriazines **6.26** have been shown to breakdown to *N*-substituted-*N*-(chloromethyl)amides **6.29** upon reaction with acyl chlorides **6.27** (Scheme 2.4).[299,300] These reactive intermediates can be trapped with a nucleophile to quickly build chemical complexity. In this fashion, hexahydrotriazines can effectively act as synthons for *N*-acyliminium ions **6.28** that can be generated *in situ*.

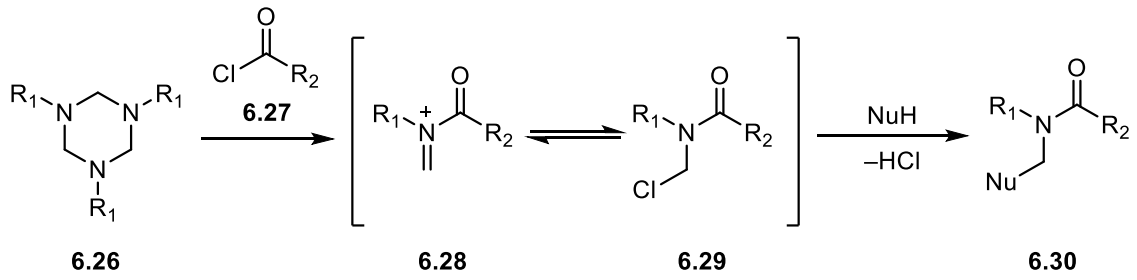

Scheme 6.4 General reactivity of hexahydrotriazines with acyl chlorides and nucleophilic capture of intermediates **6.28** or **6.29**.

We planned to harness this reactivity of hexahydrotriazines to develop an efficient preparation of **6.6** in one step. Accordingly, we attempted this reaction using conditions similar to those previously reported from our group for vinylogous Mannich reactions of *N*-acylated immium ions with silylenol ethers.[293] We first attempted this reaction at low temperature (–78 °C) with a dropwise addition of crotonyl chloride to a solution of **6.7** and **6.8** (Equation 6.1). We hoped that as the *N*-chloromethyl amide intermediate **6.29** was formed, nucleophile **6.8** would be present to intercept the reactive intermediate. Gratifyingly, we found that the reaction was successful, although the yield of **6.6** was poor (33%) and it was accompanied with a by-product that was difficult to remove.

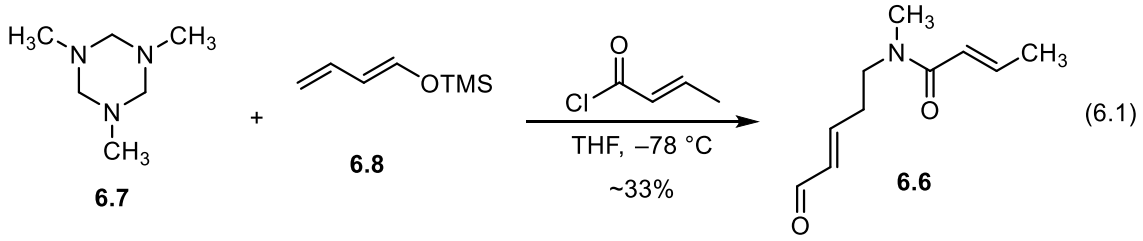

In order to optimize the yield of **6.6**, it was necessary to identify which step of the reaction was problematic. It was not clear if the formation of the *N*-chloromethyl amide intermediate **6.31** was not proceeding well or if the nucleophilic addition of **6.8** was problematic. Thus, we sought to identify reaction conditions that would lead to quantitative generation of the **6.31**. Interestingly, when **6.7** was treated with crotonyl chloride in THF at –78 °C, the major product was not the desired intermediate **6.31**, but rather the by-product **6.32**. We thought one easy solution to this problem would be to warm the reaction mixture. However, executing the same reaction at 0 °C led to a complex mixture of products, and it became clear that this reaction would require a screen of different temperatures and solvents.

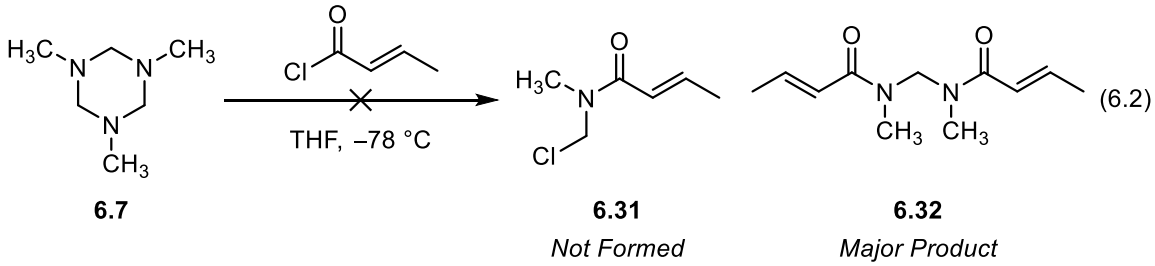

We turned to literature examples for the acylation of hexahydrotriazines and next investigated dichloromethane as a solvent for this reaction.[299,300] We discovered a positive correlation between temperature and product formation, and we found that heating the

reaction in a sealed tube at 50 °C afforded **6.31** (Equation 6.3). However, at lower temperatures (–78 or 0 °C) mixtures of **6.31** and **6.32** were observed.

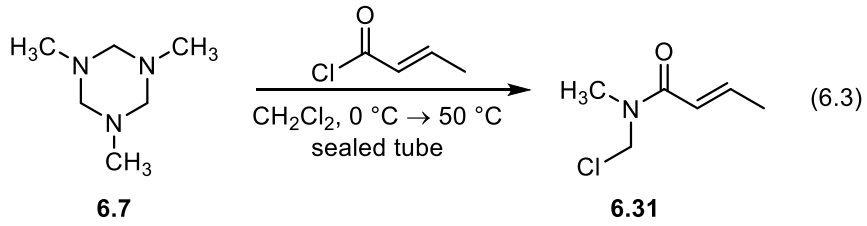

6.7 **6.31** (6.3)

With conditions identified for the formation of **6.31**, we returned to investigating the one-pot procedure to prepare **6.6**. On our second approach to this transformation, we applied a stepwise one-pot procedure where **6.31** was first generated quantitatively prior to the addition of nucleophile **6.8**. Fortunately, this proved to be an effective strategy, and we obtained **6.6** with an increased yield of 51%. However, significant formation of **6.32** was still observed (Equation 6.4). The presence of by-product **6.32** indicated that the formation of the *N*-chlormethyl amide intermediate was still problematic, and we sought to promote its formation through the addition of a Lewis acid. We discovered that inclusion of substoichiometric amounts of TMSOTf further enhanced the yield of **6.6**, but significant formation of **6.32** was still observed (Equation 6.5). This problem led us to return to our investigation of solvents for the formation of **6.31**. Since we previously observed a clear correlation between temperature and formation of **6.31**, we reasoned that a higher boiling solvent might be required. After a screening the reaction of **6.7**and **6.9** in THF, toluene, and acetonitrile at 70 °C, we discovered that acetonitrile gave complete conversion of **6.7** to **6.31** with minimal by-product formation (Equation 6.6). Interestingly, the reactions in THF or toluene (PhMe) led to unidentified mixtures of products at 70 °C, showing solvent is an important reaction parameter for this transformation.

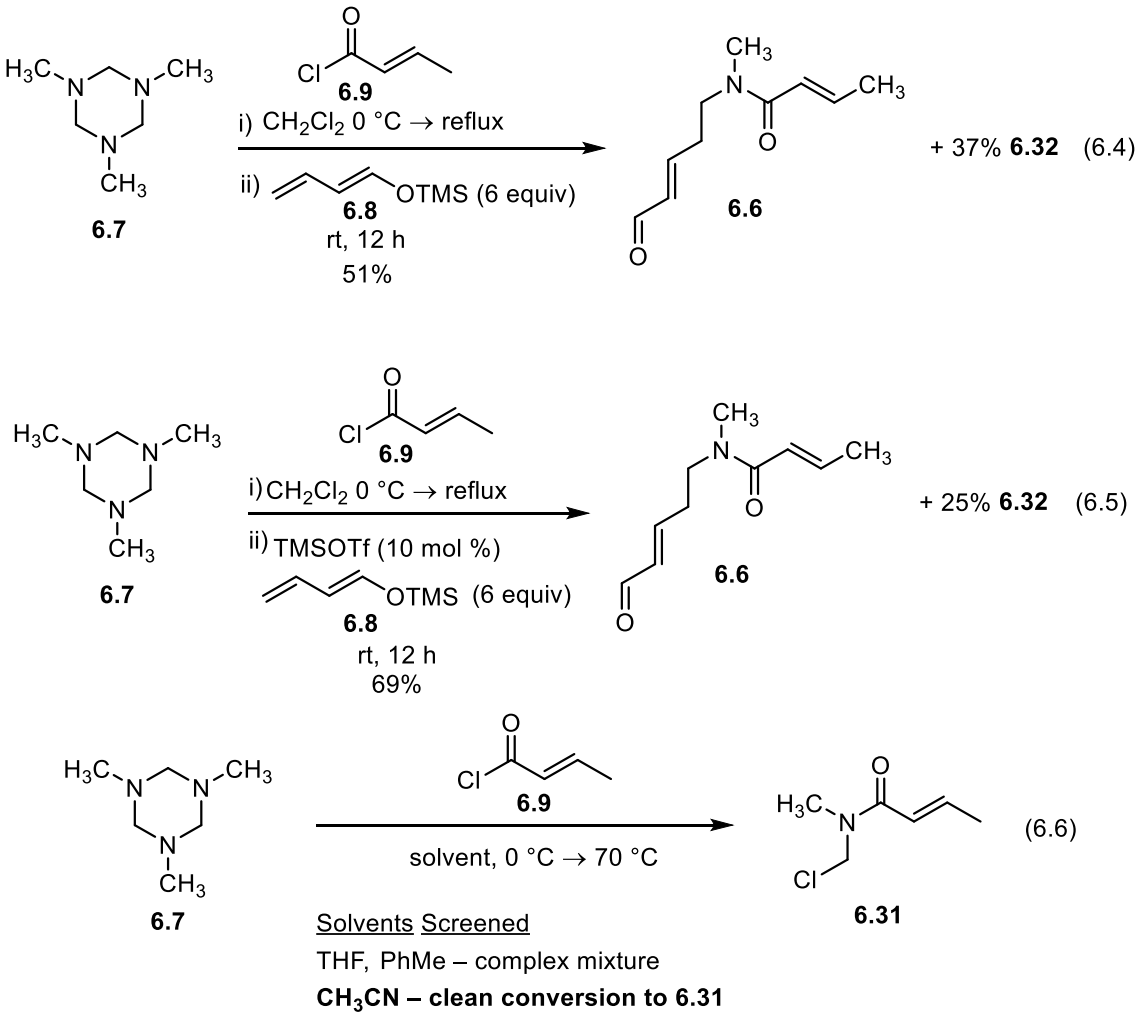

With a new set of conditions identified for the formation of **6.31**, we applied them to the one-pot transformation, and gratifyingly, **6.6** was obtained in 85% yield with minimal formation of by-product **6.32** (Equation 6.7). Furthermore, we found that this one-step preparation of the hetero-Diels-Alder precursor **6.6** was readily scalable to multigram quantities.

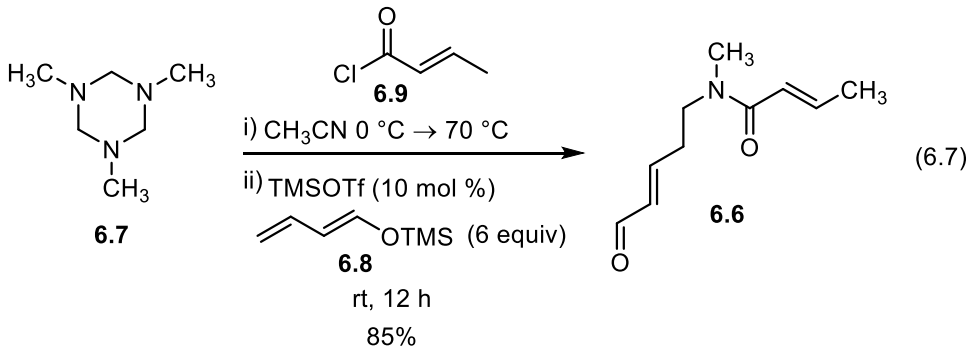

6.3 HETERO-DIELS-ALDER REACTION

With a scalable and reliable method to prepare **6.6** in place, we turned our attention to the intramolecular hetero-Diels-Alder reaction. Fortunately, we found that heating **6.6** in degassed xylenes at 190 °C delivered **6.33** and **6.34** as a mixture of *cis*:*trans* (7:1, **6.33**:**6.34**) cycloadducts as determined by the ^{1}H NMR spectrum of the crude reaction material. However, the yield of **6.33** was poor (35%), and the remainder of the recovered material from the reaction appeared to be derived from unreacted starting material and was deemed to be a decomposition by-product of **6.6**.

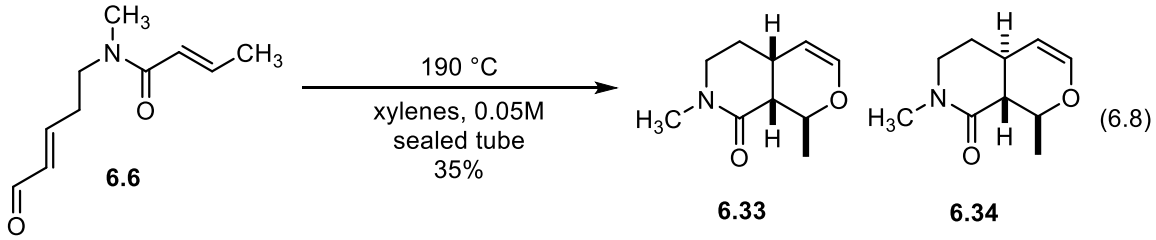

We speculated that the low yield of **6.33** was due to inefficient heating of the reaction vessel. Fortunately, changing the reaction set up from a cylindrical sealed tube to a sealed round bottom flask allowed for more efficient stirring and coverage of the reaction volume in the oil bath, and we were able to increase the yield of **6.33** to 58%. We found

that this reaction was sensitive to solvent volume, and when the concentration was increased to 0.05 M we observed diminished yields of **6.33** (45%).

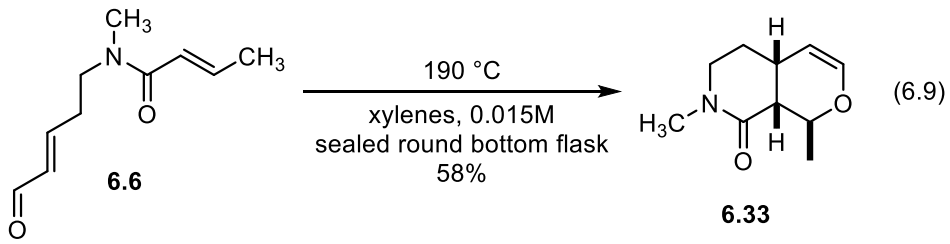

(6.9)

6.4 Halogenation of Hetero-Diels–Alder Product

Our next task was to derivatize **6.33** so that it could be used in a cross-coupling reaction with skatole. We set out to install a halogen atom at the β-position of the vinyl ether moiety of **6.33** through a previously reported method for the preparation of 2-haloglycals.[301] Following this method, **6.33** was treated with NBS and a catalytic amount of $AgNO_3$ in refluxing CH_3CN to afford **6.35** in 46% yield. We attempted to improve the yield of **6.35** through increasing the reaction time and stoichiometry of $AgNO_3$, but to no avail. When NIS was used in the reaction, the corresponding iodo-derivative **6.36** was obtained in 65% yield. This same trend of moderately increased yields for the preparation of iodoglycals over bromoglycals was observed in the original report as well.[301]

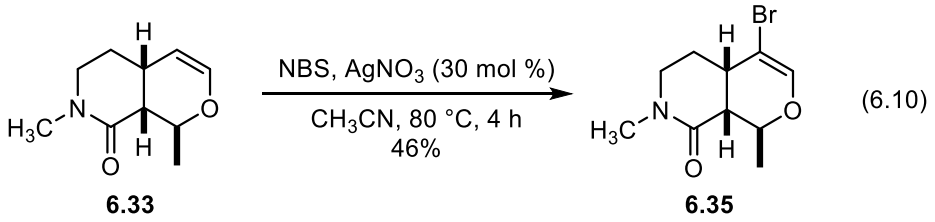

(6.10)

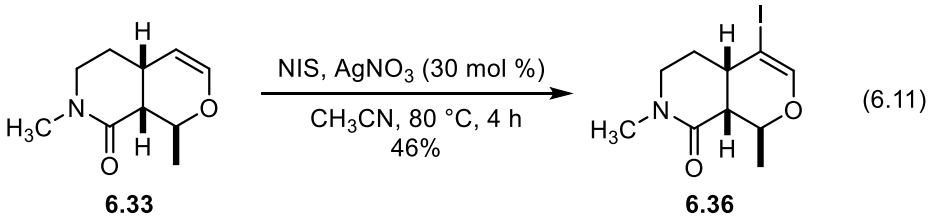

6.33 **6.36** (6.11)

Mechanistically, this reaction is proposed to proceed as outlined in Scheme 6.5. $AgNO_3$ activates the *N*-halosuccinimide reagent through coordination to one of the carbonyl oxygen atoms to form **6.38**. Nucleophilic attack by the vinyl ether **6.37** then generates intermediate **6.39**, which is trapped by the nitrate ion. Intermediate **6.41** then undergoes elimination to generate the β-halogenated vinyl ether **6.42**. A proton transfer between **6.40** and **6.43** will then regenerate succinimide **6.44** and $AgNO_3$, which can reenter the catalytic cycle.

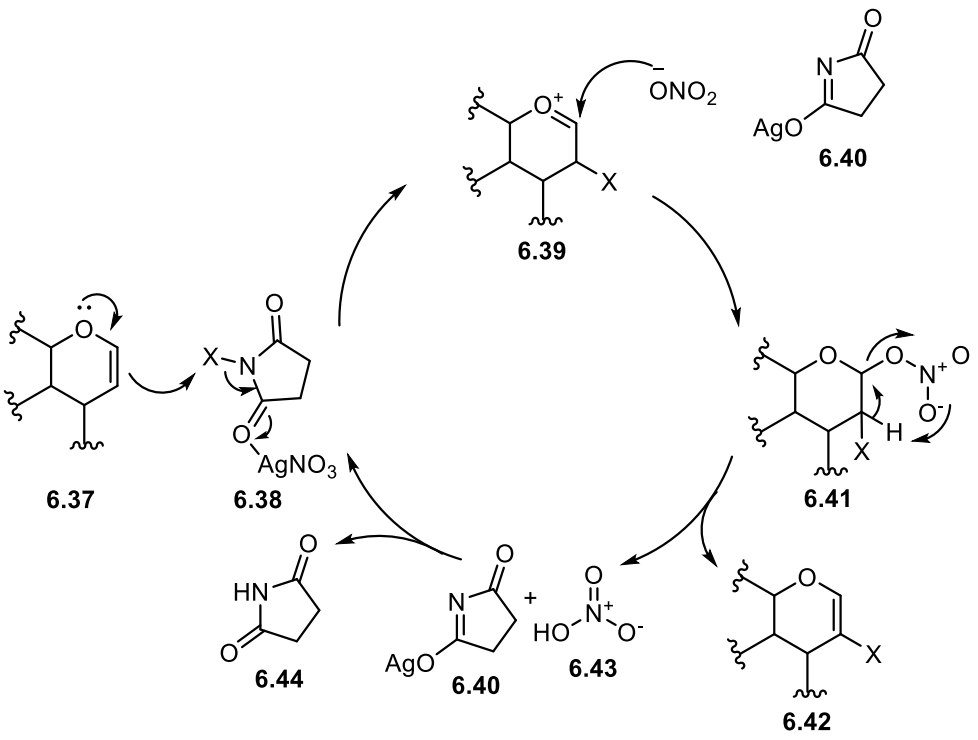

Scheme 6.5 Proposed mechanism for the halogenation of vinyl ethers by *N*-halosuccinimides and silver nitrate.

6.5 SKATOLE CROSS COUPLING EFFORTS

6.5.1 Direct C-2 Coupling to Skatole

We next investigated strategies to couple **6.35** and **6.36** with skatole (**6.45**). We were attracted to previously reported methods for the direct C-2 couplings of free N-H indole derivatives[302–305] because of the simplicity of the approach. While we were aware that these reactions had primarily been investigated for alkyl and aryl halide coupling partners, the possibility of directly coupling **6.35** or **6.36** with skatole (**6.45**) without the need for additional functionalization was a tempting prospect indeed. Following a previously reported method from Sames,[304] **6.35** and **6.45** were heated in dimethylacetamide in the presence of $Pd(OAc)_2$ and diisopropylamine, but unfortunately

no desired product **6.46** was obtained (Equation 6.12). Extending the reaction time to 36 hours or increasing the temperature up to 150 °C did not improve the outcome, and only decomposition of **6.35** was observed. We also attempted an alternative strategy for a C-2 coupling of N-H indole derivatives directed by norbornene.[302,303] Unfortunately, these conditions also did not form the desired product **6.46** (Equation 6.13).

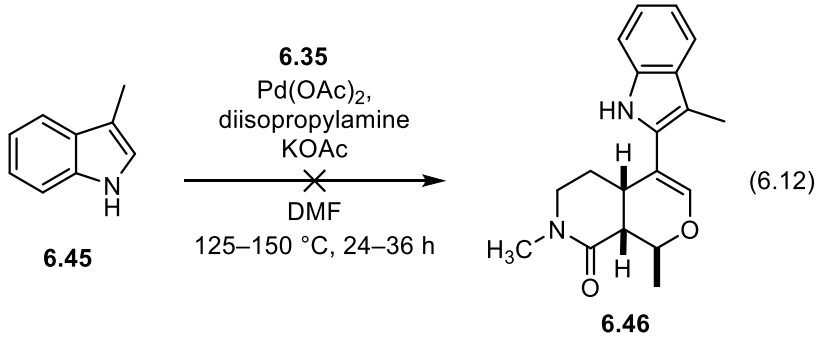

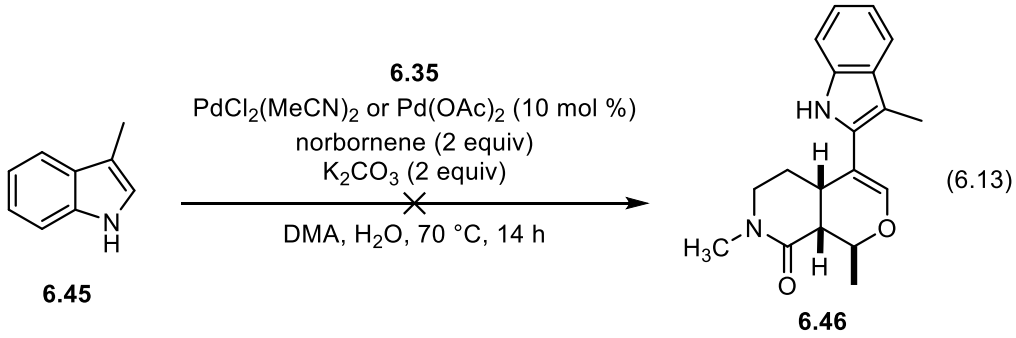

6.5.2 C-2 Lithiation of Skatole

Undeterred by the failures of these speculative strategies, we concluded that activation of the 2-position of **6.45** would be required to achieve our desired transformation. We pursued a strategy to derivatize **6.45** that would allow us to investigate multiple different approaches to join **6.35**/**6.36** and **6.45**. The directed C-2 lithiation of *N*-protected indole derivatives is well precedented,[306–308] and the lithiated intermediates **6.48** can be transmetallated with zinc **6.49**, boron **6.50**, or tin **6.51** reagents to give access to

Negishi, Suzuki, or Stille couplings, respectively (Scheme 6.6). Furthermore, there exists a variety of protecting groups available for the indole nitrogen atom that direct lithiation to the 2-position, including carboxyl (CO_2H), *tert*-butyloxycarbonyl (Boc), methoxymethyl acetal (MOM), and tosyl (SO_2PhMe), which provides us an additional element of flexibility when screening conditions to promote the desired coupling.

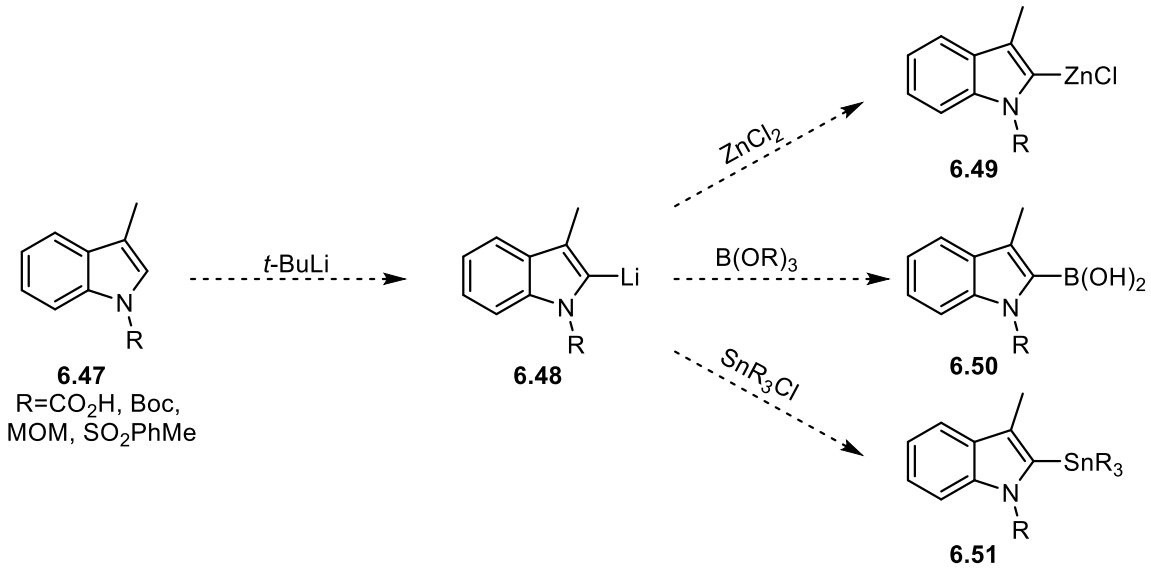

Scheme 6.6. C-2 -lithiation of skatole derivatives and transmetallation of **6.48**.

We commenced our cross-coupling investigations with Negishi reactions because it provided the opportunity for an efficient one-pot coupling sequence. We envisioned a strategy where the indole nitrogen of skatole (**6.45**) could be deprotonated, and then protected *in situ* with CO_2 to form **6.52**, which would then be lithiated at the 2-positon to give **6.53**. Subsequent transmetallation of **6.53** with zinc would form **6.54**, and introduction of a palladium catalyst and **6.35** or **6.36** would deliver the desired product **6.55** (Scheme 6.7). The relative instability of the carboxyl protecting group of **6.52** would also obviate

the need for a discrete deprotection step, making this approach a formal direct C-2 coupling of **6.35** or **6.36** to **6.45**.

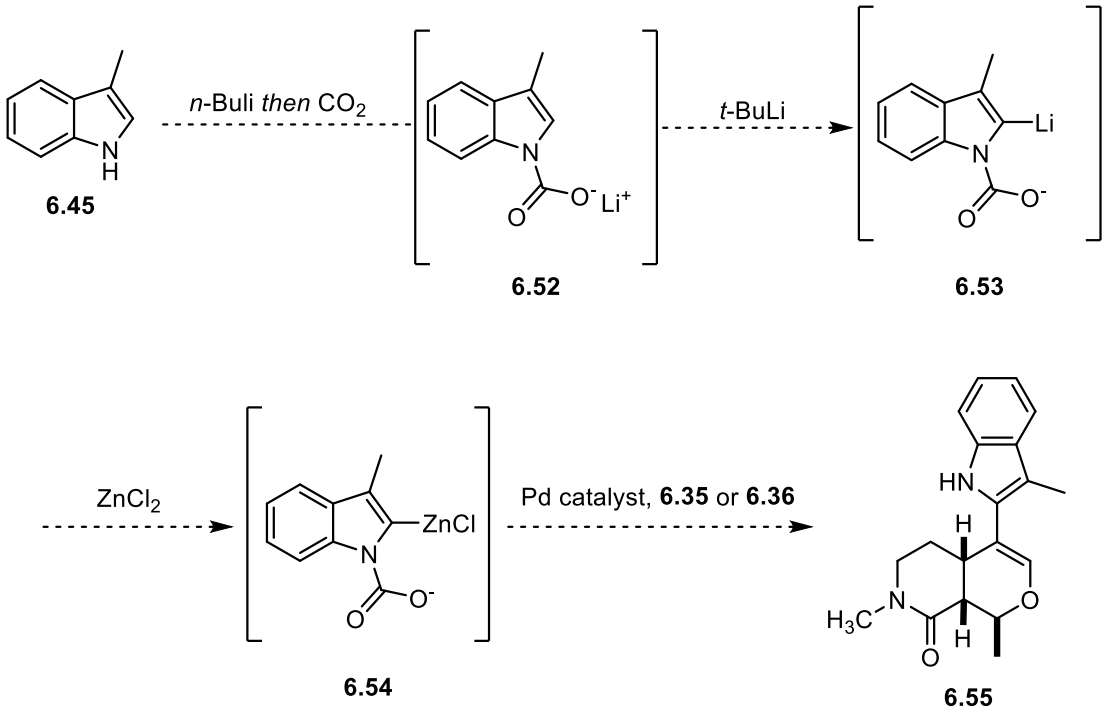

Scheme 6.7. Proposed one-pot sequence for Negishi coupling of **6.45** and **6.35** or **6.36**.

In order to effect the Negishi coupling between **6.35** and **6.45**, it was first necessary to identify suitable conditions for the formation of **6.52** and **6.53** (Scheme 6.8). After some experimentation, we found that deprotonation of **6.45** with *n*-BuLi followed by introduction of CO_2 gas led to good conversion to **6.52**. This intermediate was then treated with *t*-BuLi followed by quenching with D_2O to afford ca 80% of **6.56** as determined by the ^1H NMR spectrum of the crude reaction material.

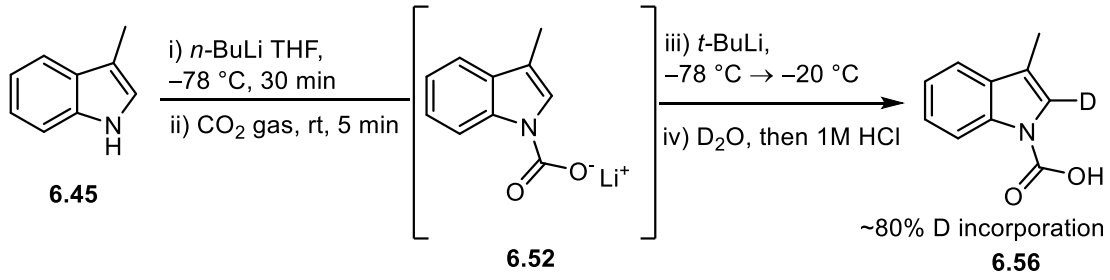

Scheme 6.8. C-2 lithiation of **6.52** and subsequent deuterium quenching.

With suitable conditions identified for the lithiation of **6.53**, we investigated the key Negishi coupling (Equation 6.14). Unfortunately, introduction of $Pd(PPh_3)_4$ and **6.35** to the reaction mixture after **6.53** was transmetallated with zinc did not result in formation of the desired product **6.55**, and mostly unreacted **6.35** was recovered. Increasing the reaction temperature to 80 °C showed no improvement. Because this one-pot five step sequence was a complicated procedure with multiple points at which the reaction could fail, we decided to take a more stepwise approach in hopes of identifying the problem.

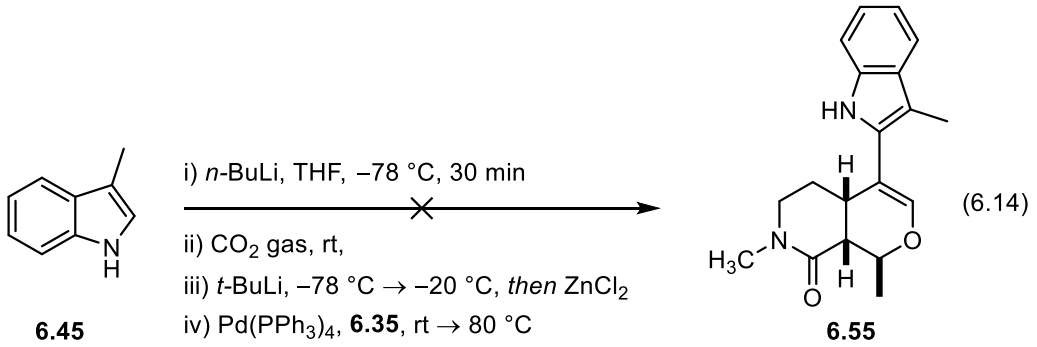

In order to simplify our procedure, we decided to abandon the use of the CO_2 protecting group for the indole nitrogen of **6.45**. Instead, we prepared the Boc protected derivative **6.57** in 90% yield through treatment of **6.45** with BoC-2O and 4-dimethylaminopyridine (DMAP) (Equation 6.15). We next verified the lithiation **6.57** after treatment with *t*-BuLi by quenching the reaction with CD_3OD, which afforded 85–90%

conversion to **6.58** based on the ^{1}H NMR spectrum of the crude reaction material (Equation 6.16). Furthermore, we observed similar conversions to **6.58** after the ltihiated intermediate was transmetalated with zinc, and the reaction was quenched with CD_3OD, providing evidence that formation of the zincated intermediate was not problematic (Equation 6.17).

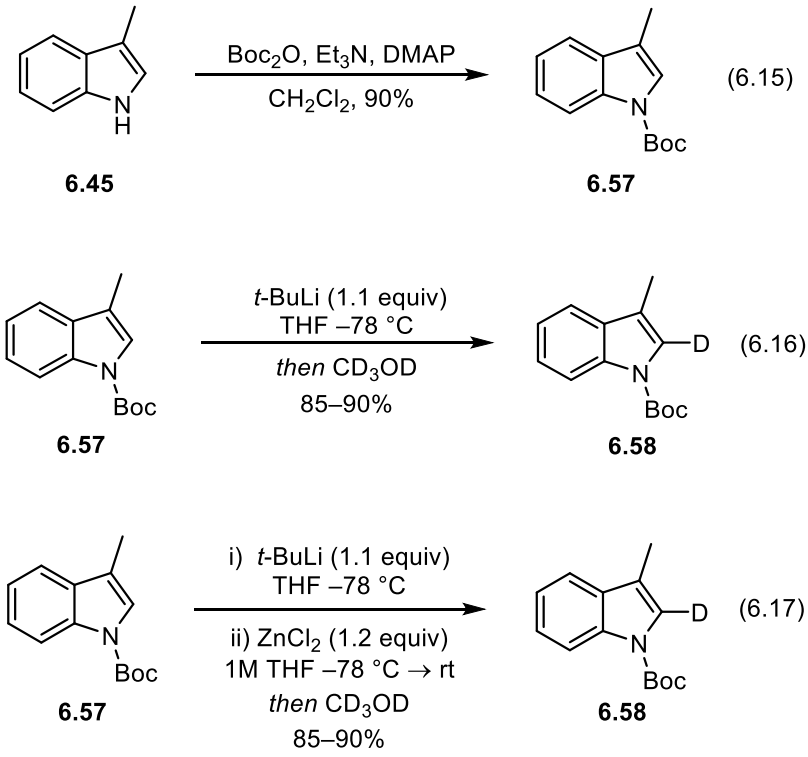

With the critical reaction parameters for the formation of the metallated intermediates established, we returned to the Negishi coupling reactions with **6.35** or **6.36** (Table 6.1). Attempting the coupling again in THF with $Pd(PPh)_3$ as the catalyst led to no desired product formation, even at temperatures up to 125 °C (Table 6.1, Entry 1). We speculated that the palladium tetrakis catalyst was too sterically encumbered or was not active enough to effectively promote the reaction, so we next investigated alternative palladium precatalysts and phosphine ligand systems. Knochel previously reported the combination of $Pd(dba)_2$ and P(*o*-fur)$_3$ to be effective conditions for promoting Negishi

couplings,[309] but, applying this combination to our system led to no product formation (Table 6.1, Entry 2). Similarly, Buchwald reported the combination of $Pd(dba)_2$ and the RuPhos ligand to be a potent catalyst for promoting Negishi couplings,[310] but again we observed no formation of **6.60** upon applying these conditions to our system (Table 6.1, Entry 3). Since we were observing no desired product formation in THF, we switched to dimethylacetamide as a solvent because it has been reported to be an effective solvent for Negishi couplings (Table 6.1, Entries 4–6).[309] Unfortunately, these efforts were also unsuccessful, and no formation of **6.60** was observed. The only major by-product we could identify from these reactions was the dehalogenated material **6.33**. While it is not exactly clear how this by-product would arise under the reaction conditions, phosphines have been shown to promote the dehydrohalogenation of 2-halogylcals, even in the absence of transition metal catalyst.[311] Furthermore, the Boc protecting group of **6.59** was not stable to the reaction conditions, and was cleaved during the course of the reaction.

Table 6.1. Negishi coupling conditions screened to form **6.60**

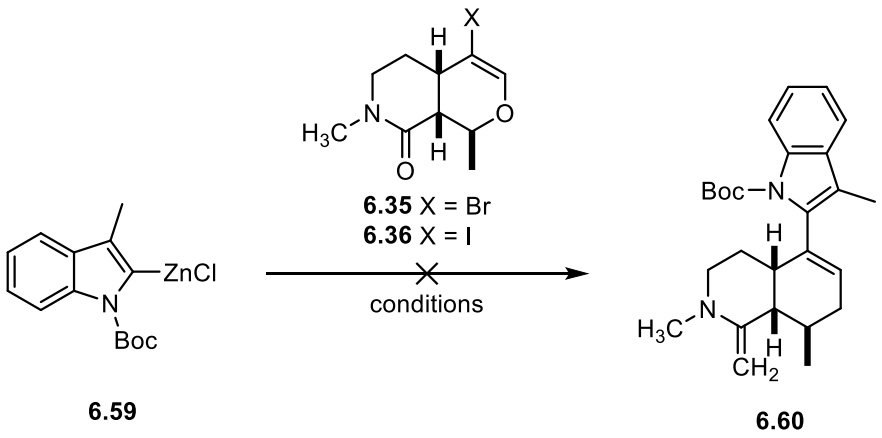

6.59 **6.60**

Entry	Catalyst	Ligand	Solvent	T °C
1	$Pd(PPh_3)_4$	–	THF	rt to 125
2	$Pd(dba)_2$	$P(o\text{-}fur)_3$	THF	rt to 125
3	$Pd(dba)_2$	RuPhos	THF	80
4	$Pd(PPh_3)_2Cl_2$	–	DMAc	80
5	$Pd(OAc)_2$	RuPhos	DMAc	80
6	$Pd(OAc)_2$	–	DMAc	80

The failure of all of our attempts to couple **6.35** or **6.36** to skatole led us to pursue a simpler a Negishi coupling model reaction as a proof of principle. Using the Negishi coupling reactions reported by Buchwald,[310] phenylzinc chloride (**6.61**) was heated with **6.36** in THF in the presence of $Pd(dba)_2$ and RuPhos to mixed results (Equation 6.18). While we did observe the formation of **6.62**, it was isolated in only 20% yield as part of an inseparable mixture (ca. 2:1) of unreacted **6.36** and **6.62**. The remainder of the material from the reaction contained numerous by-products that could not be identified. Despite the poor yield of **6.62**, this model reaction provided key evidence that **6.36** could in fact be

employed in a metal catalyzed cross coupling, although, it also suggested that a Negishi coupling may not be the best approach to join **6.36** and **6.45**.

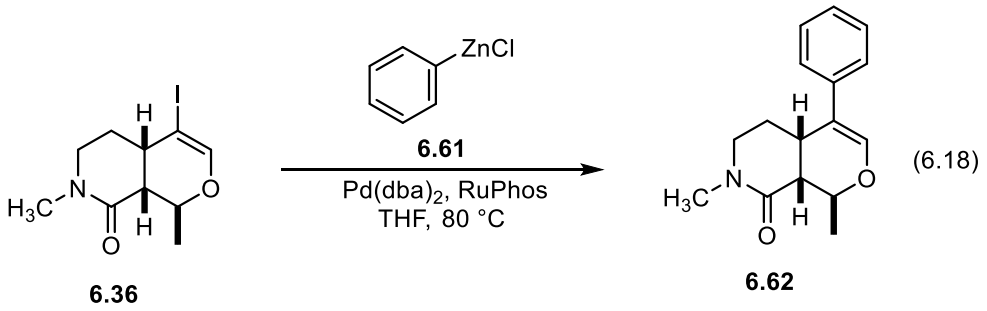

6.36 **6.62** (6.18)

We changed strategies and pursued a Suzuki coupling reaction to connect the two key fragments. We first explored a model Suzuki coupling between **6.36** and **6.63** to test the viability of **6.36** in these reactions. Fortunately, we found that **6.36** was converted to **6.64** in ca 33% yield, albeit as an inseperable mixture (3:1) of **6.36** and **6.64**. While the yield for this reaction was poor, we were heartened by the fact that there were few other by-products. This was sufficient proof of principle for us to move forward with our investigations.

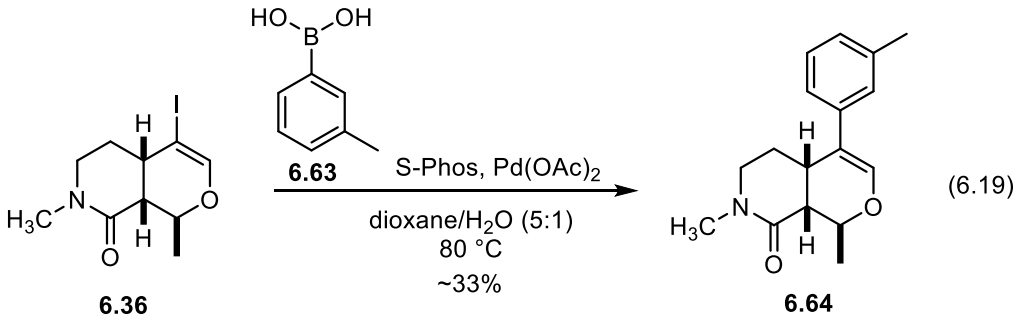

6.36 **6.64** (6.19)

Rather than attempt to optimize the yield of **6.64**, we were eager to move forward and test the coupling on our actual system. After some trial and error, we were able to

prepare **6.65** through lithiation of **6.57** followed by quenching with $B(OMe)_3$. Aqueous work up of the reaction then led to the formation of **6.65** in 85% yield. This boronic acid is unstable and was used immediately upon preparation in subsequent Suzuki couplings. Unfortunately, all of our efforts thus far have been unavailing. While we have not been able to probe this reaction extensively, our initial attempts have revealed the stability of **6.65** is problematic. Under the conditions outlined in Equations 6.21 and 6.22, the boronic acid **6.65** appears to decompose before the desired coupling can progress. Furthermore, the Boc protecting group of **6.65** is also unstable under these conditions, and skatole (**6.45**) is recovered from the reaction along with unreacted **6.35** or **6.36**. While these initial results are troubling, there are still a number of options available to couple skatole (**6.45**) and **6.36**, which will be discussed in the following section.

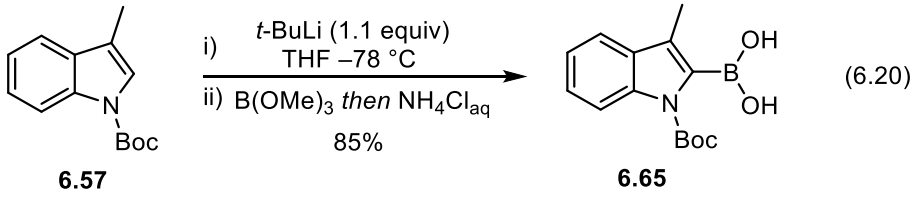

(6.20)

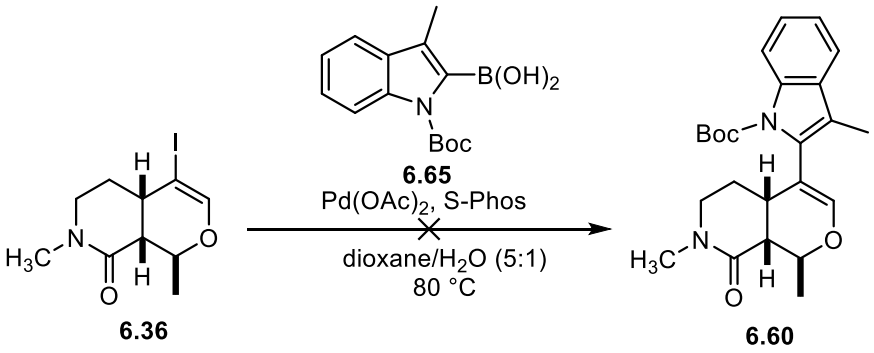

(6.21)

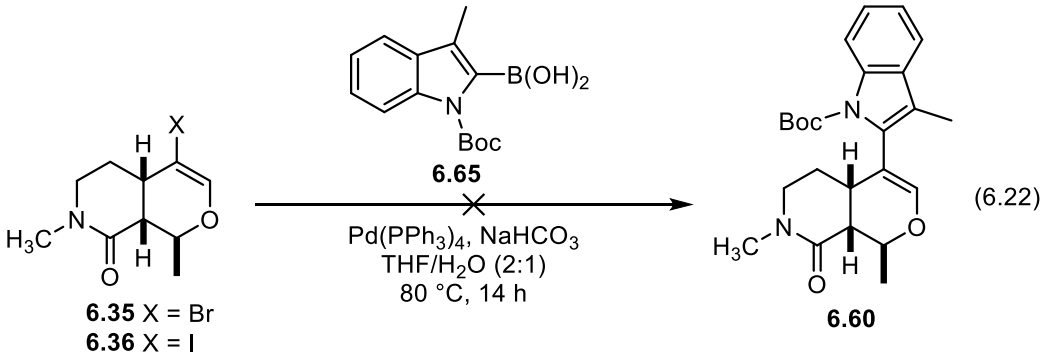

(6.22)

6.6 SUMMARY

In summary, we have proposed an efficient synthesis of alstoscholarisine E (**6.1**), which could require as few as six steps. We have demonstrated that the first three steps of this synthesis are feasible and proceed in good yield. An important feature of this work was the development of a high yielding, and scalable method to prepare hetero-Diels-Alder precursors such as **6.6** in one step. This represents a dramatic improvement over the previous syntheses of these substrates, which required seven total steps, and several of required purification via HPLC.[290] Acylation of **6.7** with **6.9** was shown to give **6.31**, which was alkylated with **6.8** to give the hetero-Diels–Alder precursor **6.6** in 86% yield in one chemical operation (Scheme 6.9). Thermolysis of **6.6** resulted in the intramolecular Diels–Alder cycloaddition to afford **6.33** in 58% yield. This product was then halogenated to give **6.36** in 65% yield. Although our efforts to couple **6.36** and skatole have to this point been unsuccessful, there remains a number of different strategies available to complete the desired transformation.

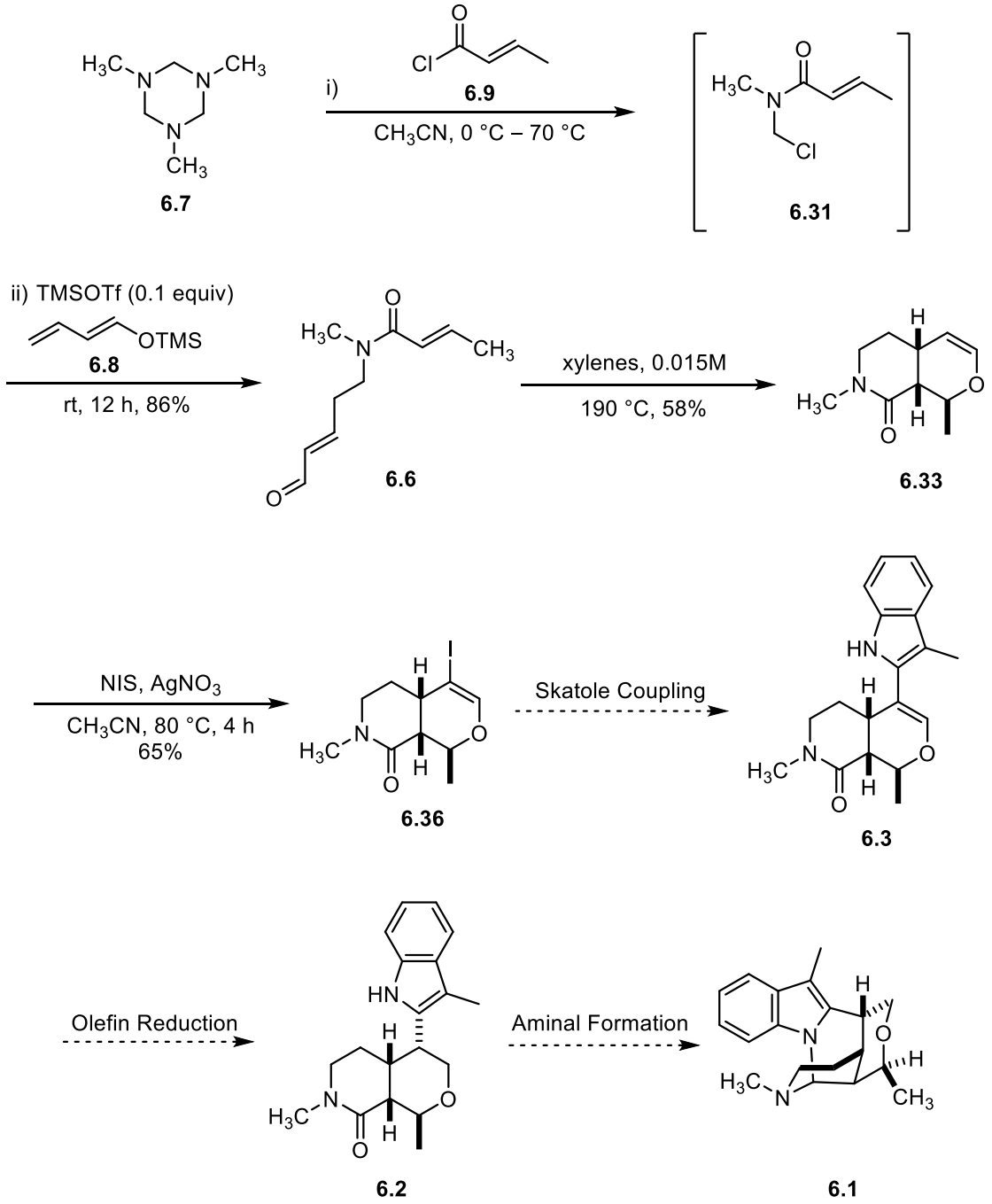

Scheme 6.9. Summary of progress towards the total synthesis of alstoscholarisine E.

6.7 Future Directions

The convergent synthetic strategy for joining the hetero-Diels–Alder product and skatole was attractive in its versatility. There exists a wide variety of strategies available to troubleshoot this transformation. Despite the failure of our initial attempts to couple **6.36** and **6.65**, the Suzuki reaction remains a promising strategy to join these two fragments. First, Suzuki reactions are well precedented for 2-haloglycals,[311] and while **6.36** is more hindered than previously reported substrates, the coupling of **6.36** and **6.63** (Equation 6.19) provides promising supporting evidence that **6.36** is a valid coupling partner. Our investigations have indicated that the instability of the boronic acid **6.65** is the primary reason for our inability to couple it with **6.36**. The instability of 2-heteroaryl boronic acids is well known, and there has been recent innovations in catalyst design to overcome this problem.[312] Buchwald reported the use of catalyst **6.68** for promoting Suzuki reactions of a variety of unstable boronic acids, including **6.66** (Equation 6.23). The reaction took place under mild conditions, and **6.66** was coupled with **6.67** to give **6.69** in 88% yield with no reported loss of the Boc protecting group.[312] Therefore, the instability of **6.65** does not seem an insurmountable problem, and application of these reaction conditions to our system could lead to desired formation of **6.60** (Equation 6.24).

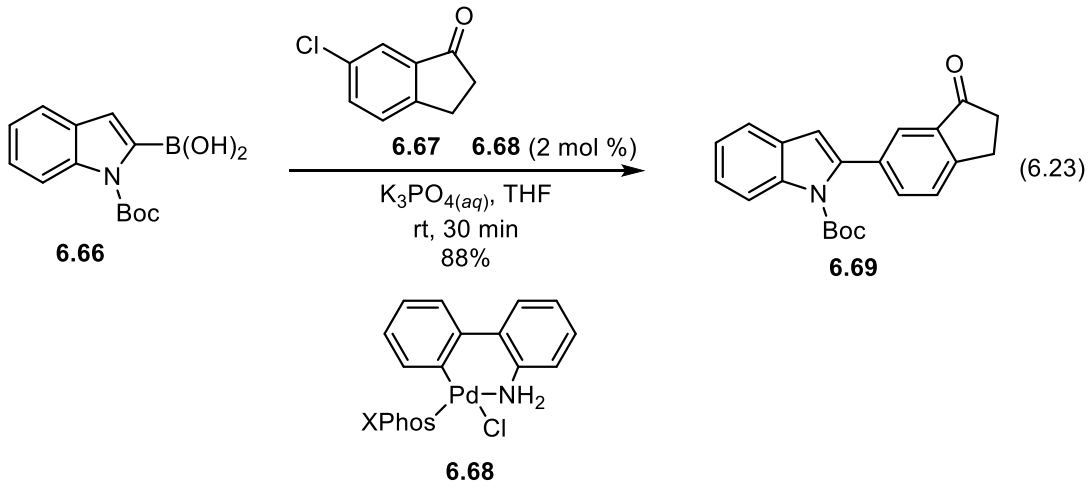

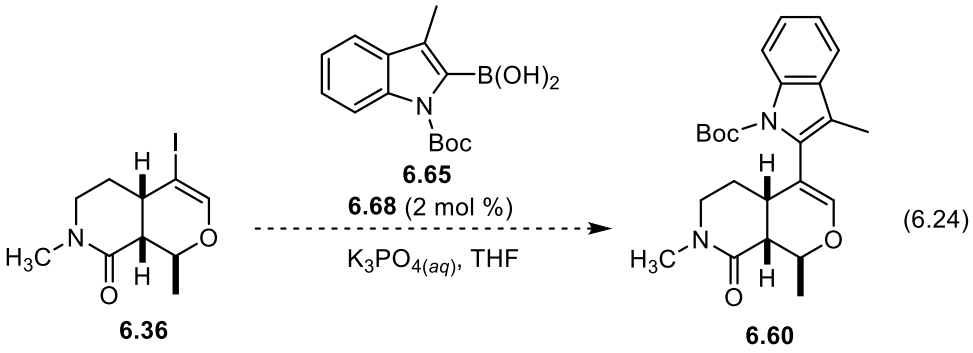

Another potential problem arises in that both of these coupling partners are sterically demanding substrates. The large Boc protecting group of **6.65** only exacerbates this issue. Hence, changing the indole nitrogen protecting group could be beneficial. Exploring the use of the MOM protected derivative **6.70** in a Suzuki reaction with **6.36** would be a worthwhile investigation (Equation 6.25).

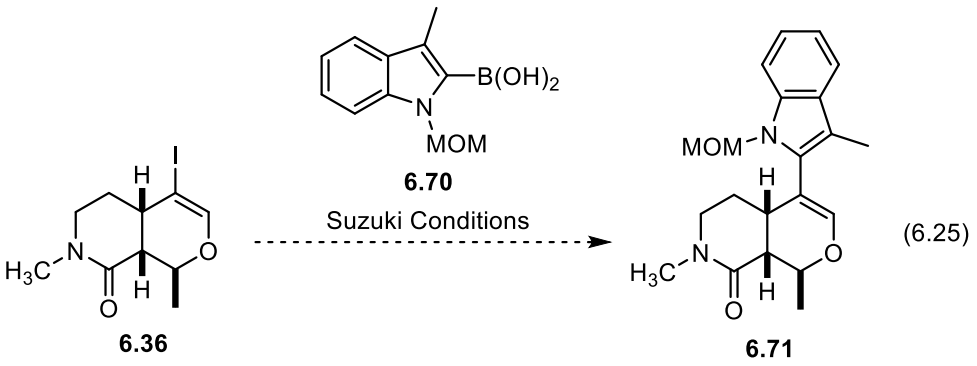

(6.25)

Although not ideal, one final strategy to investigate within Suzuki reactions would be to convert **6.36** to **6.71** and use it as a coupling partner with a 2-halogenated indole **6.72** (Scheme 6.10). While this strategy would add an additional step to the synthesis, it could solve the problem of the instability of the skatole boronic acid derivatives.

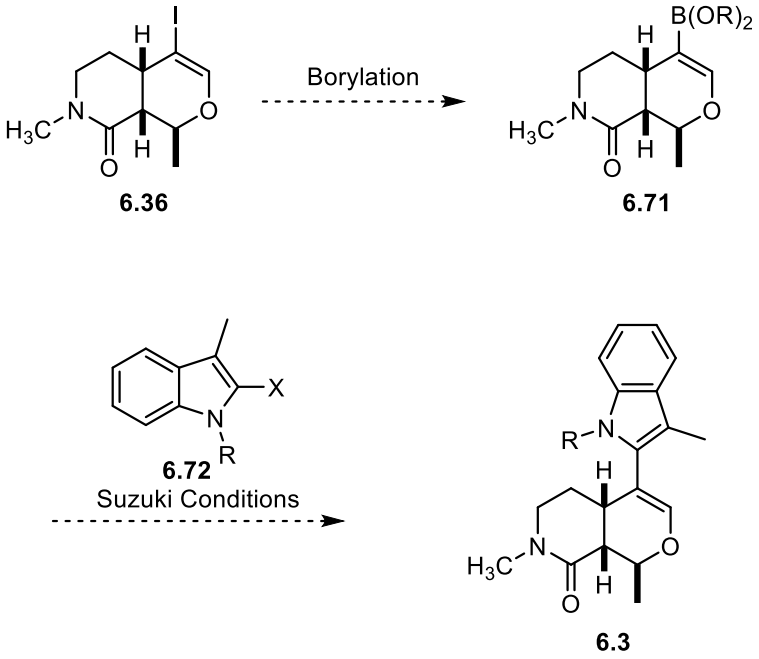

Scheme 6.10. Alternative Suzuki coupling strategy for connecting **6.36** and **6.72**.

Branching away from Suzuki reactions, there also exists the entire realm of Stille couplings to explore. The coupling partner **6.51** should be readily available from **6.48** and could be used in a coupling reaction with **6.36**, opening a different coupling strategy with reaction conditions to screen and optimize (Scheme 6.11). With the number of promising strategies available, we are confident that skatole (**6.4**) and the heteo-Diels–Alder product can be coupled, and the remaining steps of the synthesis could then be investigated.

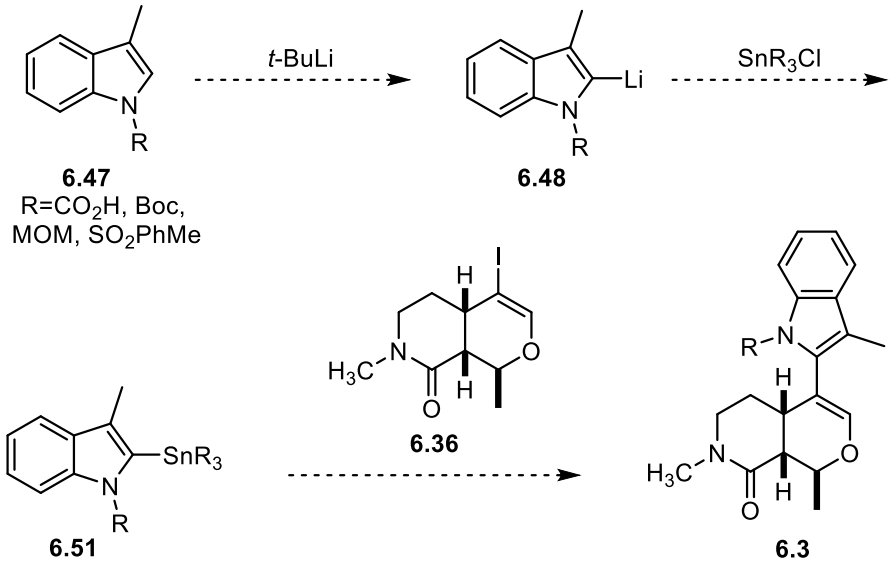

Scheme 6.11. Stille coupling strategy to prepare **6.3**.

Chapter 7 Experimental Procedures

7.1 General Experimental

Tetrahydrofuran and diethyl ether were dried by filtration through two columns of activated, neutral alumina according to the procedure described by Grubbs.[313] Methanol, acetonitrile and dimethylformamide were dried by filtration through two columns of activated molecular sieves, and toluene was dried by filtration through one column of activated, neutral alumina followed by one column of Q5 reactant. Benzene was distilled from sodium and benzophenone. Methylene chloride, diisopropylamine, triethylamine, and diisopropylethylamine were distilled from calcium hydride immediately prior to use. Pyridine was distilled from potassium hydroxide (KOH) and calcium hydride and stored over KOH pellets. All other reagents and solvents were reagent grade and were purchased and used as received unless otherwise noted. Reactions were performed under a nitrogen or argon atmosphere in round-bottom flasks sealed under rubber septa with magnetic stirring, unless otherwise noted. Water sensitive reactions were performed with flame- or oven-dried glassware, stir-bars, and steel needles. Reaction temperatures are reported as the temperatures of the bath surrounding the vessel. Sensitive reagents and solvents were transferred using plastic syringes and steel needles using standard techniques. Proton nuclear magnetic resonance (^{1}H NMR) and carbon nuclear magnetic resonance (^{13}C NMR) spectra were acquired in $CDCl_3$ unless otherwise noted. Chemical shifts are reported in parts per million (ppm, δ), downfield from tetramethylsilane (TMS, δ = 0.00 ppm) and are referenced to residual solvent ($CDCl_3$, δ = 7.26 ppm (1H) and 77.16 ppm (13C). Coupling constants (J) are reported in hertz (Hz) and the resonance multiplicity abbreviations used are: s, singlet; d, doublet; t, triplet; q, quartet; p, pentet; sex, sextet; sep, septet; dt, doublet

of triplets; dd, doublet of doublets; ddd, doublet of doublet of doublets; dddd, doublet of doublet of doublet of doublets; m, multiplet; comp, overlapping multiplets of magnetically non-equivalent protons. The abbreviations br and app stand for broad and apparent, respectively. Infrared (IR) spectra were obtained with a Thermo Scientific Nicolet IR-100 FT-IR series spectrometer as thin films on sodium chloride plates. Melting points were determined using a Thomas-Hoover Uni-melt capillary melting point apparatus. Thin-layer chromatography (TLC) was performed on EMD 60 F254 glass- backed pre-coated silica gel plates and were visualized using one or more of the following methods: UV light (254 nm) and staining with basic potassium permanganate (KMnO4) or acidic p-anisaldehyde (PAA). Flash chromatography was performed using glass columns and with Silicycle® SiliaFlash F60® (40-63 μm) silica gel eluting with the solvents indicated.

7.2 Experimental Procedures

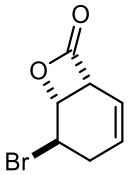

(1*S*,5*S*,6*S*)-5-Bromo-7-oxabicyclo[4.2.0]oct-2-en-8-one (2.59) (DK-3-118). *N*-Bromosuccinimide (3.871 g, 21.75 mmol) was added to a solution of 1,4-dihydrobenzoic acid (2.7 g, 21.8 mmol) and catalyst **2.94** (0.964 g, 2.18 mmol) in PhMe/CH_2Cl_2 (1:1) (220 mL) at –50 °C, and the solution was stirred for 14 h. The reaction was quenched with saturated aqueous Na_2SO_3 (150 mL), and the mixture was warmed to room temperature with vigorous stirring. The layers were separated and the aqueous layer was extracted with CH_2Cl_2 (3 x 75 mL). The combined organic layers were washed with 5% aqueous Na_2CO_3 (2 x 150 mL), dried ($MgSO_4$), filtered, and concentrated under reduced pressure. The crude residue was purified by column chromatography, eluting with hexanes/EtOAc (9:1) to give

3.1 g (70%) of **2.59** as a white solid: mp 96–98 °C: spectra matched the previously reported data;[19] ^{1}H NMR ($CDCl_3$, 400 MHz) δ ppm 6.10 – 6.00 (m, 1H), 5.90 (dddd, *J* = 9.9, 6.1, 1.8, 1.3 Hz, 1H), 4.94 (dd, *J* = 5.7, 3.1 Hz, 1H), 4.55 (q, *J* = 3.1 Hz, 1H), 4.28 (t, *J* = 6.1 Hz, 1H), 2.72 (comp, 2H); $[\alpha]^{25}_D$ –49.0 (c = 1.0, $CHCl_3$); HPLC (210 nm): OD-H (1% *i*-PrOH/hexanes, 1.0 mL/min) 16.6 min (major) 18.0 min (minor). **2.59** was recrystallized from hexanes (10 mg/100 mL) to give (1.9 g, 45%) of **2.59** as a single enantiomer. HPLC (210 nm): OD-H (1% *i*-PrOH/hexanes, 1.0 mL/min) 16.6 min

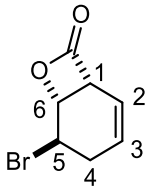

NMR Assigntment. ^{1}H NMR ($CDCl_3$, 400 MHz) δ ppm 6.10 – 6.00 (m, 1H, C2-H), 5.90 (dddd, *J* = 9.9, 6.1, 1.8, 1.3 Hz, 1H, C3-H), 4.94 (dd, *J* = 5.7, 3.1 Hz, 1H, C6-H), 4.55 (q, *J* = 3.1 Hz, 1H, C5-H), 4.28 (t, *J* = 6.1 Hz, 1H, C1-H), 2.72 (comp, 2H, C4-H)

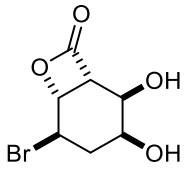

(1*R*,2*R*,3*S*,5*R*,6*R*)-5-Bromo-2,3-dihydroxy-7-oxabicyclo[4.2.0]octan-8-one (2.60) (DK-3-122). The olefin **2.59** (0.8 g, 3.9 mmol) was added to a solution of citric acid (0.824 g, 4.29 mmol), potassium osmate (0.143 g, 0.39 mmol, 0.1 mol %), and 4-methylmorpholine *N*-oxide (0.502 g, 4.29 mmol) in H_2O/*t*-BuOH (1:1) (16 mL) at 0 ˚C. The reaction mixture was stirred for 18 h, then solid sodium sulfite (500 mg) was added, and stirring was continued for 15 min at room temperature. The organic layer was removed under reduced pressure, and the aqueous layer was extracted with ethyl acetate (5 x 25

mL). The combined organic extracts were washed with brine (75 mL), dried ($MgSO_4$), filtered, and concentrated under reduced pressure. The crude material was recrystallized from ethanol to give 0.55 g (60%) of **2.60** as white crystals: mp 211–212˚C.^{1}H NMR (CD_3OD, 400 MHz,) δ ppm 4.51 (dd, *J* = 4.3, 1.2 Hz, 1 H), 4.13 (s, 1 H), 4.03 (dd, *J* = 9.59, 2.93 Hz, 1 H), 3.80 (ddd, *J* = 11.54, 9.59, 7.04 Hz, 1 H), 2.75 (m, 1 H), 2.67 (ddd, *J* = 14.18, 6.95, 5.09 Hz, 1 H), 2.11 (tdd, *J* = 11.80, 11.80, 2.70 Hz, 1 H). ^{13}C NMR (CD_3OD, 100 MHz) δ ppm 175.0, 83.1, 74.4, 72.6, 54.8, 49.8, 36.3; IR (film) 3380, 2955, 1711, 1439, 1261, 1202 cm^{-1}; mass spectrum (ESI) *m/z* 258.9576 $[M+Na]^+$, 260.9553$[M+Na]^+$ $[C_7H_9BrO_4$ $[M+Na]^+$ requires 258.9576, 260.9553].

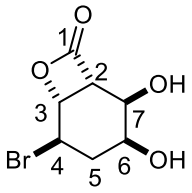

NMR Assignment. ^{1}H NMR (CD_3OD, 400 MHz) δ ppm 4.51 (dd, *J* = 4.30, 1.17 Hz, 1 H, C3-H) 4.13 (s, 1 H C7-H) 4.03 (dd, *J* = 9.59, 2.93 Hz, 1 H, C2-H) 3.80 (ddd, *J* = 11.54, 9.59, 7.04 Hz, 1 H, C4-H) 2.75 (ddd, *J* = 1.00 Hz, 1 H, C6-H) 2.67 (ddd, *J* = 14.18, 6.95, 5.09 Hz, 1 H, C5-H) 2.11 (tdd, *J* = 11.80, 11.80, 2.70, 0.80 Hz, 1 H, C5-H) ^{13}C NMR (400 MHz) 175.0 C1, 83.1 C3, 74.4 C7, 72.6 C6, 54.8 C4, 49.8 C2 36.3 C5-H

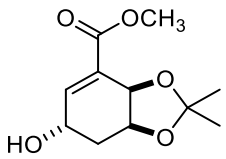

Methyl (3a*R*,6*S*,7a*S*)-6-hydroxy-2,2-dimethyl-3a,6,7,7a-tetrahydrobenzo-[d][1,3]dioxole-4-carbo-xylate (2.98) (DK-3-134). Diol **2.60** (0.258 g, 1.09 mmol) was added to a suspension of K_2CO_3 (0.225 g, 1.63 mmol) of MeOH (11 mL, 0.1 M), and the reaction was stirred for 2 h, whereupon, the solvent was removed under reduced pressure. The residue was redissolved in MeOH (5 mL) and excess K_2CO_3 was removed by vacuum filtration. The filtrate was evaporated under reduced pressure, and the crude triol **2.97** was carried in the next step without further purification. The crude **2.97** (0.205 g, 1.09 mmol) was suspended in CH_2Cl_2 (17 mL, 0.065M) containing 4 Å mol sieves (1 g). Camphorsulfonic acid (0.886 g, 3.82 mmol) and 2,2-dimethoxy propane (0.284 g, 0.35 mL, 2.73 mmol) were added, and the reaction was heated under reflux for 3 h, whereupon, it was cooled to room temperature and filtered. The filtrate was concentrated under reduced pressure, and the crude product was directly purified by column chromatography eluting with hexanes/EtOAc (1:1) to give 0.186 g (75%) of **2.98** as a white solid: mp 75–76 ˚C. ^{1}H NMR (400 MHz, $CDCl_3$) δ ppm 7.05 (dd, J = 5.2, 1.1 Hz, 1 H), 4.91 (d, J = 5.5 Hz, 1 H), 4.59 (tdt, J = 4.4, 2.4, 1.2,Hz, 1 H), 4.30-4.23 (m, 1 H), 3.81 (s, 3 H), 3.13 (d, J = 10.6 Hz, 1 H), 2.39 (dddd, J = 15.1, 4.4, 3.1, 1 Hz, 1 H), 1.98 (ddd, J = 15.1, 4.7, 2.5 Hz, 1 H), 1.43 (s, 3 H), 1.39 (s, 3 H). ^{13}C NMR ($CDCl_3$, 100 MHz) δ ppm 166.6, 139.7, 129.9, 109.9, 73.1, 71.0, 62.9, 52.2, 31.6, 28.2, 26.3.; IR (film) 3454, 2987, 2938, 1723, 1651, 1438, 1372, 1314, 1259, 1219 cm^{-1}; mass spectrum (ESI) *m/z* 251.0892 $[M+Na]^+$ [$C_{11}H_{16}O_5$ $[M+Na]^+$ requires 251.0890].

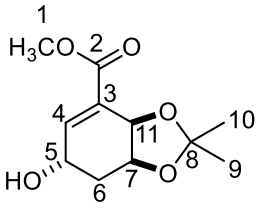

NMR Assignment. . ^{1}H NMR (400 MHz, $CDCl_3$) δ ppm 7.05 (dd, *J* = 5.18, 1.08 Hz, 1 H, C4-H) 4.91 (d, *J* = 5.5 Hz, 1 H, C11-H) 4.59 (tdt, *J* = 4.4, 2.4, 1.2,Hz, 1 H C5-H) 4.30-4.23 (m, 1 H C7-H) 3.81 (s, 3 H, C1-H) 3.13 (d, *J* = 10.6 Hz, 1 H, C5-OH) 2.39 (dddd, *J* = 15.1, 4.4, 3.1, 1 Hz, 1 H, C6-H) 1.98 (ddd, *J* = 15.1, 4.7, 2.5 Hz, 1 H, C6-H) 1.43 (s, 3 H, C10-H) 1.39 (s, 3 H, C9-3H) ^{13}C NMR (400 MHz) 166.6 C2, 139.7 C4, 129.9 C3, 109.9 C8, 73.1 C11, 71.0 C7, 62.9 C5, 52.2 C1, 31.6 C6, 28.2 C10, 26.3 C9

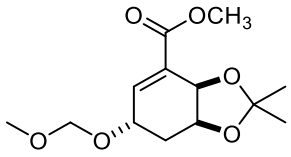

Methyl(3a*R*,6*S*,7a*S*)-6-(methoxymethoxy)-2,2-dimethyl-3a,6,7,7a,tetra-hydrobenzo[d][1,3]-dioxole-4-carboxylate (2.105) (DK-3-135). Chloromethyl methyl ether (0.105 g, 1.3 mmol) was added to a solution of **2.98** (0.150 g, 0.66 mmol) and diisopropylethylamine (0.25 g, 2.0 mmol) in CH_2Cl_2 (2.5 mL, 0.25 M), and the reaction was heated under reflux for 4 h. The solvent was removed under reduced pressure, and the reaction mixture was purified directly by column chromatography eluting with hexanes:EtOAc (7:3) to give 0.27 g (95%) of **2.98** as a white solid; mp 70–71 °C. ^{1}H NMR ($CDCl_3$, 400 MHz) δ ppm 7.12 (s, 1 H) 4.80 (d, *J* = 5.8 Hz, 1 H) 4.74 (s, 2 H) 4.32 - 4.20 (comp, 2 H) 3.81 (s, 3 H) 3.41 (s, 3 H) 2.21 (dt, *J* = 12.2, 5.1 Hz, 1 H) 1.76 (dt, *J* = 12.2, 10.3 Hz, 1 H) 1.49 (s, 3 H) 1.43 (s, 3 H) ^{13}C NMR ($CDCl_3$, 100 MHz) δ ppm 166.6, 139.73, 129.9, 109.9, 95.8, 73.1, 71.0, 62.9, 56.7, 52.2, 31.6, 28.2, 26.3; IR (film) 2987, 2938, 1723,

1651, 1438, 1372, 1314, 1259, 1219 cm^{-1}; mass spectrum (ESI) *m/z* 295.1158 $[M+Na]^+$, [$C_{13}H_{20}O_6$ $[M+Na]^+$ requires 295.1158].

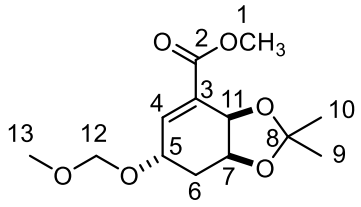

NMR Assignment ^{1}H NMR ($CDCl_3$, 400 MHz) δ ppm 7.12 (s, 1 H, C4-H) 4.80 (d, *J* = 5.8 Hz, 1 H, C11-H) 4.74 (s, 2 H, C12-H) 4.32– 4.20 (comp, 2 H, C5-H, C7-H) 3.81 (s, 3 H, C1-H) 3.41 (s, 3 H, C13-H) 2.21 (dt, *J* = 12.2, 5.1 Hz, 1 H, C6-H) 1.76 (dt, *J* = 12.2, 10.3 Hz, 1 H, C6-H) 1.49 (s, 3 H, C9-H) 1.43 (s, 3 H, C10-H) ^{13}C NMR ($CDCl_3$, 100 MHz) δ ppm 166.6 C2, 139.73 C4, 129.9 C3, 109.9 C8, 95.8 C12, 73.1 C11, 71.0 C7, 62.9 C5, 56.7 C13, 52.2 C1, 31.6 C6, 28.2 C10, 26.3 C9.

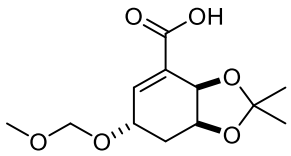

(3a*R*,6*S*,7a*S*)-6-(Methoxymethoxy)-2,2-dimethyl-3a,6,7,7a,tetrahydrobenzo-[d][1,3]dioxole-4-carboxylic acid (2.105) (DK-3-137). 1 M aq LiOH (0.72 mL, 0.72 mmol) was added to a solution of **2.98** (0.1 g, 0.36 mmol) in CH_3CN (3.6 mL, 0.1 M), and the reaction was stirred for 14 h. The solvent was removed under reduced pressure, and the residue was dissolved in EtOAc (5 mL). Amberlite® IR120 acidic resin was added until the pH was ca. 5. The solution was filtered, and the filtrate was concentrated under reduced pressure. The crude product was purified by column chromatography eluting with hexanes/EtOAc/AcOH (85:15:0.1) to give 0.081 g (87%) of **2.105** as a white solid; mp 74–75 ˚C. ^{1}H NMR ($CDCl_3$, 400 MHz) δ ppm 7.25 (d, *J* = 2.1 Hz, 1 H) 4.79 (d, *J* = 5.8 Hz, 1

H) 4.76 (d, *J* =1.7 Hz, 2 H) 4.33 (dt, *J* = 10.1, 5.1 Hz, 1 H) 4.30–4.24 (m, 1 H) 3.42 (s, 3 H) 2.23 (dt, *J* = 12.3, 5.1 Hz, 1 H) 1.81 (dt, *J* = 12.3, 10.1 Hz, 1 H) 1.51 (s, 3 H) 1.44 (s, 3 H) ^{13}C NMR ($CDCl_3$, 100 MHz) δ ppm 171.3, 135.5, 130.73, 121.1, 95.5, 86.1, 74.6, 72.4, 58.2, 32.3, 28.2, 26.3. IR (film) 3454, 2980, 2924, 1722, 1651, 1434, 1372, 1314, 1259, 1219 cm^{-1}; mass spectrum (ESI) *m/z* 257.10330 $[M–H]^–$, [$C_{12}H_{18}O_6$ $[M–H]^–$ requires 257.1031].

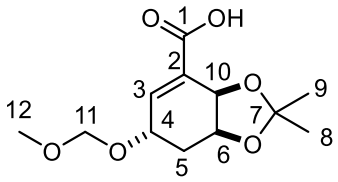

NMR Assignment. ^{1}H NMR ($CDCl_3$, 400 MHz) δ ppm 7.25 (d, *J* = 2.1 Hz, 1 H, C3-H) 4.79 (d, *J* = 5.8 Hz, 1 H, C10-H) 4.76 (d, *J* =1.7 Hz, 2 H, C11-H) 4.33 (dt, *J* = 10.1, 5.1 Hz, 1 H, C6-H) 4.30–4.24 (m, 1 H, C4-H) 3.42 (s, 3 H, C12-H) 2.23 (dt, *J* = 12.3, 5.1 Hz, 1 H, C5-H) 1.81 (dt, *J* = 12.3, 10.1 Hz, 1 H, C5-H) 1.51 (s, 3 H, C8-H) 1.44 (s, 3 H, C9-H) ^{13}C NMR ($CDCl_3$, 100 MHz) δ ppm 171.3 C1, 135.5 C3, 130.73 C2, 121.1 C7, 95.5 C11, 86.1 C10, 74.6 C4, 72.4 C6, 58.2 C12, 32.3 C5, 28.2 C8, 26.3 C9.

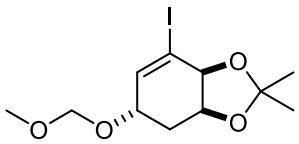

(3aS,5S,7aS)-7-iodo-5-(methoxymethoxy)-2,2-dimethyl-3a,4,5,7a-tetrahydrobenzo[d][1,3]dioxole (2.109) (DK-2-286) Oxalyl chloride (113 mg, 0.89 mmol) was added to a solution of carboxylic acid **2.105** (46 mg, 0.178 mmol) and DMF (2 µL ,0.017 mmol) in CH_2Cl_2 (0.6 mL) at 0 ˚C. The reaction was warmed to room temperature and stirred for 0.5 h, whereupon the solvent was removed under reduced

pressure. The crude residue was dissolved in CH_2Cl_2 (0.36 mL), and 2-mercaptopyridine *N*-oxide sodium salt (32 mg, 0.21 mmol), and 2,2,2-trifluoroethyl iodide (187 mg, 0.89 mmol) were added. The reaction vessel was sealed and irradiated with a 150 W electric flood lamp for 1 h. The solvent was removed under reduced pressure, and the crude reaction mixture was purified directly by column chromatography eluting with hexanes/EtOAc (95:5) to give 21 mg (34%) of **2.109** as a clear oil. ^{1}H NMR (400 MHz, $CDCl_3$) δ ppm 6.69 (d, *J* = 3.4 Hz, 1 H) 4.70 (s, 2 H) 4.51 (d, *J* = 5.8 Hz, 1 H) 4.34 (ddd, *J* = 8.0, 5.7, 4.1 Hz, 1 H) 4.08–4.03 (m, 1 H) 3.39 (s, 3 H) 2.21 (dt, *J* = 13.7, 4.8 Hz, 1 H) 1.99 (dt, *J* = 14.3, 6.7 Hz, 1 H) 1.53 (s, 3 H), 1.41 (s, 3H) ^{13}C NMR (100 MHz, $CDCl_3$) δ ppm 131.3, 120.1, 98.2, 96.1, 73.1, 71.0, 64.9, 52.2, 31.6, 28.2, 26.3

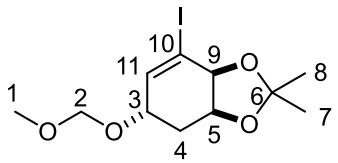

NMR Assignment. ^{1}H NMR (400 MHz, $CDCl_3$) δ ppm 6.69 (d, J = 3.4 Hz, 1 H, C11-H) 4.70 (s, 2 H, C2-H) 4.51 (d, J = 5.8 Hz, 1 H, C9-H) 4.34 (ddd, J = 8.0, 5.7, 4.1 Hz, 1 H, C3-H)) 4.08 – 4.03 (m, 1 H, C5-H) 3.39 (s, 3 H, C1-H) 2.21 (dt, J = 13.7, 4.8 Hz, 1 H, C4-H) 1.99 (dt, J = 14.3, 6.7 Hz, 1 H, C4-H) 1.53 (s, 3 H, C7-H), 1.41 (s, 3H, C8-H); ^{13}C NMR (100 MHz, CDCl3) δ ppm 131.3 C11, 120.1 C6, 98.2 C2, 96.1 C10, 73.1 C9, 71.0 C3, 64.9 C5, 52.2 C1, 31.6 C4, 28.2 C7, 26.3 C8

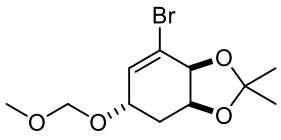

(3a*S*,5*S*,7a*S*)-7-Iodo-5-(methoxymethoxy)-2,2-dimethyl-3a,4,5,7a-tetrahydro-benzo-[d][1,3]dioxole (2.110) (DK-3-139). Carboxylic acid **2.99** (0.025 g, 0.1 mmol) dissolved in CH_2Cl_2 (0.5 mL) was added to a solution of EDCI•HCl (0.037 g, 0.19 mmol) and **2.78** (0.029 g, 0.19 mmol) in CH_2Cl_2 (1.5 mL) cooled to 0 C. The reaction was warmed to room temperature and stirred for 1.5 h, whereupon it was diluted with CH_2Cl_2 (5 mL) and the organic layer was washed with saturated NH_4Cl_{aq} (3 x 5 mL). The layers were separated, and the organic layer was dried ($MgSO_4$), filtered, and concentrated under reduced pressure to give crude **2.108,** which was used directly in the next step. The crude **2.108** was dissolved in Cl_3Br (2 mL) and irradiated with a 150 W electric flood lamp for 10 min. The solvent was removed under reduced pressure, and the crude material was purified by column chromatography eluting with hexanes/EtOAc (9:1) to give 0.016 g (55%) of **2.110** as a clear oil. ^{1}H NMR ($CDCl_3$, 400 MHz) δ ppm 6.39 (d, *J* = 3.4 Hz, 1 H) 4.70 (s, 2 H) 4.51 (d, *J* = 5.8 Hz, 1 H) 4.34 (ddd, *J* = 8.0, 5.7, 4.1 Hz, 1 H) 4.08–4.03 (m, 1 H) 3.39 (s, 3 H) 2.21 (dt, *J* = 13.7, 4.8 Hz, 1 H) 1.99 (dt, *J* = 14.3, 6.7 Hz, 1 H) 1.53 (s, 3 H), 1.41 (s, 3H) ^{13}C NMR (100 MHz, $CDCl_3$) δ ppm 134.3, 123.0, 110.0, 95.7, 76.0, 72.8, 70.9, 55.4, 31.7, 28.1, 26.2. IR (film): 2928, 2854, 1618, 1465, 1256, 1090, 837 cm^{-1}; mass spectrum (ESI) *m/z* 315.02080 $[M+Na]^+$, 317.01880 $[M+Na]^+$ [$C_{11}H_{17}BrO_4$ $[M+Na]^+$ requires 315.02082, 317.01878]. $[\alpha]^{25}_D$ –64.0 (c = 0.5, $CHCl_3$)

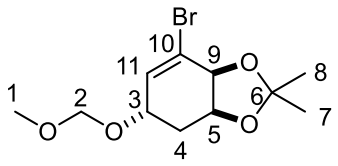

NMR Assignment. ^{1}H NMR ($CDCl_3$, 400 MHz) δ ppm 6.39 (d, *J* = 3.4 Hz, 1 H, C11-H) 4.70 (s, 2 H, C2-H) 4.51 (d, *J* = 5.8 Hz, 1 H, C9-H) 4.34 (ddd, *J* = 8.0, 5.7, 4.1 Hz, 1 H, C3-H) 4.08–4.03 (m, 1 H, C5-H) 3.39 (s, 3 H, C1-H) 2.21 (dt, *J* = 13.7, 4.8 Hz, 1 H, C-H) 1.99 (dt, *J* = 14.3, 6.7 Hz, 1 H, C4-H) 1.53 (s, 3 H, C7-H), 1.41 (s, 3H, C8-H) ^{13}C NMR (100 MHz, $CDCl_3$) δ ppm 134.3 C11, 123.0 C10, 110.0 C6, 95.7 C2, 76.0 C9, 72.8 C3, 70.9 C5, 55.4 C1, 31.7 C4, 28.1 C7, 26.2 C8.

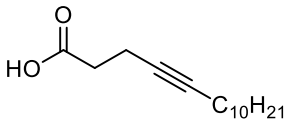

4-Pentadecynoic acid (2.164) (DK-4-293). *n*-Butyllithium (2.5 M in hexanes, 10.2 mL, 25 mmol) was added dropwise to a solution of pent-4-ynoic acid (**2.207**) (1.0 g, 10 mmol) in THF/HMPA (4:1) (100 mL) at –78 °C. The reaction was warmed to 0 °C and stirred for 2 h, whereupon it was cooled back to –78 °C, and iododecane (6.0 g, 22.4 mmol) was added dropwise. The reaction was slowly warmed to room temperature and stirred for 12 h, whereupon 2 M aq LiOH (100 mL) was added. The reaction was stirred for an additional 18 h, whereupon 6 M HCl was added until the reaction mixture was ca. pH 2. The layers were separated, and the aqueous portion was extracted with EtOAc (3 x 150 mL). The combined organic layers were washed with brine (5 x 100 mL), dried ($MgSO_4$), filtered, and concentrated under reduced pressure. The crude material was purified by column chromatography eluting with hexanes/EtOAc (9:1 → 3:1) to give 2.0 g (82%) of **2.208** as a white solid; mp 61–62 °C. ^{1}H NMR ($CDCl_3$, 400 MHz) δ 2.55 (dd, *J* = 14.5, 7.9 Hz, 2 H) 2.52 – 2.42 (comp, 2 H) 2.12 (tt, *J* = 7.0, 2.2 Hz, 2 H) 1.45 (dddd, J = 13.8, 6.5

Hz, 2 H)1.19 – 1.39 (comp, 14 H) 0.88 (t, J = 6.7 Hz, 3 H). ^{13}C NMR (100 MHz, $CDCl_3$) δ ppm 178.8, 81.7, 77.9, 34.2, 32.1, 29.8, 29.8, 29.6, 29.4, 29.1, 29.1, 22.9, 18.9, 14.7, 14.3; IR (film) 3450, 2980, 2924, 2354, 1745, 1421, 1384, 1314, 1259, 1215 cm^{-1}; mass spectrum (ESI) *m/z* 237.1860 $[M–H]^–$, [$C_{15}H_{26}O_2$ $[M–H]^–$ requires 237.1860]

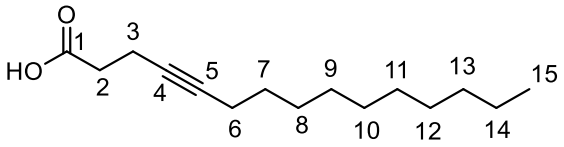

NMR Assignment. ^{1}H NMR ($CDCl_3$, 400 MHz) δ 2.55 (dd, J = 14.5, 7.9 Hz, 2 H, C2-H) 2.52 – 2.42 (comp, 2 H, C3-H) 2.12 (tt, J = 7.0, 2.2 Hz, 2 H, C6-H) 1.45 (dddd, J = 13.8, 6.5 Hz, 2 H, C7-H)1.19 – 1.39 (comp, 14 H, C8–C14-H) 0.88 (t, J = 6.7 Hz, 3 H, C15-H). ^{13}C NMR (100 MHz, $CDCl_3$) δ ppm 178.8 C1, 81.7 C4, 77.9 C5, 34.2 C2, 32.1, 29.8 C6, 29.8, 29.6, 29.4, 29.1, 29.1, 22.9, 18.9, 14.7, 14.3, C3,C6–C15

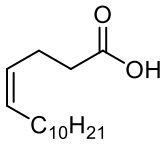

(*Z*)-Pentadec-4-enoic acid (2.158) (DK-3-263). $NaBH_4$ (0.480 g, 12.6 mmol) dissolved in EtOH (20 mL) was added to a suspension of $Ni(OAc)_2$•$4H_2O$ (3.14 g, 12.6 mmol) in EtOH (80 mL), and the reaction was stirred for 30 min at room temperature. Ethylenediamine (0.30 g, 5.04 mmol) was added, followed by a solution of **2.208** (1.0 g, 4.2 mmol) in EtOH (8 mL), and the reaction was placed under an atmosphere of H_2. The reaction was stirred for 1 h, and H_2O (60 mL) was then added. The reaction mixture was acidified with 1 M HCl until ca. pH 2, and the organic layer was removed under reduced pressure. The aqueous layer was extracted with Et_2O (5 x 100 mL), and the combined organic layers were washed with brine (2 x 250 mL), dried ($MgSO_4$), filtered, and

concentrated under reduced pressure. The crude product was purified by column chromatography, eluting with hexanes/EtOAc (9:1) to give 0.86 g (85%) of **9** as a pale yellow oil. ^{1}H NMR ($CDCl_3$, 400 MHz) δ 5.48 – 5.39 (m, 1 H), 5.38 – 5.28 (m, 1 H), 2.44 – 2.29 (comp, 4 H), 2.04 (dd, *J* = 7.2, 1.4 Hz, 2 H), 1.39 – 1.17 (comp, 17 H), 0.88 (t, *J* = 6.7 Hz, 3 H). ^{13}C NMR ($CDCl_3$, 100 MHz) δ 179.6, 131.9, 126.8, 34.1, 31.9, 29.7, 29.6, 29.6, 29.5, 29.3, 29.3, 27.2, 22.7, 22.5, 14.1. IR (film) 3454, 2987, 2913, 1719, 1634, 1435, 1370, 1310, 1225, 1216 cm^{-1}; mass spectrum (ESI) *m/z* 239.2017 $[M–H]^–$, [$C_{15}H_{28}O_2$ $[M–H]^–$ requires 239.2017]

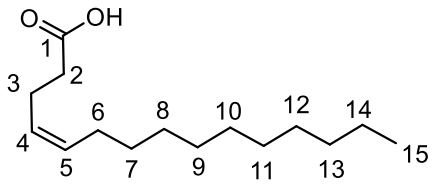

NMR Assignment. ^{1}H NMR ($CDCl_3$, 400 MHz) δ 5.48 – 5.39 (m, 1 H C4-H), 5.38 – 5.28 (m, 1 H, C5-H), 2.44 – 2.29 (comp, 4 H, C2-H, C3-H), 2.04 (dd, *J* = 7.2, 1.4 Hz, 2 H, C6-H), 1.39 – 1.17 (comp, 17 H C7–C14-H), 0.88 (t, *J* = 6.7 Hz, 3 H, C15-H). ^{13}C NMR ($CDCl_3$, 100 MHz) δ 179.6 C1, 131.9 C4, 126.8 C5, 34.1 C2, 31.9 C3, 29.7, 29.6, 29.6, 29.5, 29.3, 29.3, 27.2, 22.7, 22.5, 14.1.C6–C15

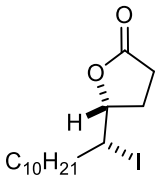

(*R*)-5-((*R*)-1-Iodoundecyl)dihydrofuran-2(3H)-one (2.156) (DK-3-217). *N*-iodosuccinimide (461 mg, 2.05 mmol) and iodine (43 mg, 0.171 mmol) were added to a solution of **2.158** (410 mg, 1.71 mmol) and **2.94** (76 mg, 0.171 mmol) in PhMe/CH_2Cl_2 (2:1) (60 mL) at –20 °C. The solution was stirred for 14 h, whereupon saturated aqueous

$Na_2S_2O_3$ (20 mL) was added, and the mixture was warmed to room temperature with vigorous stirring. The layers were separated, and the aqueous layer was extracted with CH_2Cl_2 (2 × 20 mL). The combined organic layers were dried (Na_2SO_4), filtered, and concentrated under reduced pressure. The crude residue was purified by column chromatography, eluting with hexanes/EtOAc (95:5) to give 530 mg (85%) of **2.156** as a colorless oil: ^{1}H NMR ($CDCl_3$, 400 MHz) δ ppm 4.36 (td, *J* = 7.4, 3.4 Hz, 1 H) 4.15 (dt, *J* = 10.0, 3.9 Hz, 1 H) 2.70 (ddd, *J* = 18.1, 10.6, 4.7 Hz, 1 H) 2.56 (ddd, *J* = 18.5, 10.1, 8.5 Hz, 1 H) 2.48–2.32 (m, 1 H) 2.11 (dddd, *J* = 13.1, 10.6, 8.3, 7.0 Hz, 1 H) 1.97–1.85 (m, 1 H) 1.81–1.71 (m, 1 H) 1.65–1.51 (m, 1 H) 1.44–1.16 (comp, 15 H) 0.88 (t, *J* = 6.7, 3 H). ^{13}C NMR ($CDCl_3$, 100 MHz) δ ppm 176.7, 82.1, 39.4, 35.8, 32.1, 29.8, 29.8, 29.8, 29.6, 29.5, 29.0, 28.9, 27.0, 22.9, 14.4. IR (film) 2969, 1762, 1469, 1166, 986 cm^{-1}; mass spectrum (ESI) *m/z* 389.0954 $[M+Na]^+$, [$C_{15}H_{27}IO_2$ $[M+Na]^+$ requires 389.0954]. $[\alpha]^{26}_D$ +11 (c = 0.5, $CHCl_3$). HPLC (254 nm): Whelk-O1 (8% *i*-PrOH / hexanes, 1.0 mL/min) 28.2 min (major), 39.9 min (minor); 95:5 er.

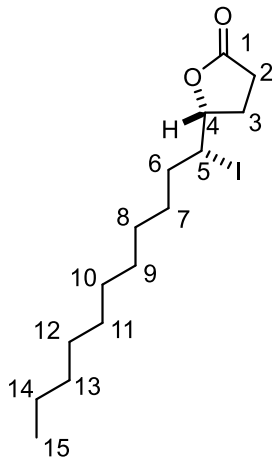

NMR Assignment. ^{1}H NMR ($CDCl_3$, 400 MHz) δ ppm 4.36 (td, *J* = 7.4, 3.4 Hz, 1 H, C5-H) 4.15 (dt, *J* = 10.0, 3.9 Hz, 1 H, C4-H) 2.70 (ddd, *J* = 18.1, 10.6, 4.7 Hz, 1 H, C2-H) 2.56 (ddd, *J* = 18.5, 10.1, 8.5 Hz, 1 H, C2-H) 2.48–2.32 (m, 1 H C3-H) 2.11 (dddd, *J* = 13.1, 10.6, 8.3, 7.0 Hz, 1 H, C3-H) 1.97–1.85 (m, 1 H C6-H) 1.81–1.71 (m, 1 H, C6-H) 1.65–1.51 (m, 1 H, C7-H) 1.44–1.16 (comp, 15 H, C7–C14-H) 0.88 (t, *J* = 6.7, 3 H, C15-H). ^{13}C NMR ($CDCl_3$, 100 MHz) δ ppm 176.7 C1, 82.1 C4, 39.4, 35.8, 32.1, 29.8, 29.8, 29.8, 29.6, 29.5, 29.0, 28.9, 27.0, 22.9, 14.4. C2,C3,C5–C15

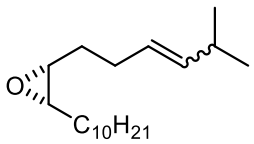

(2*S*,3*R*)-2-Decyl-3-(5-methylhex-3-en-1-yl)oxirane (2.166) (DK-3-256). DIBAL (1 M in hexanes, 0.6 mL, 0.6 mmol) was added dropwise to a solution of **2.158** (200 mg, 0.55 mmol) in Et_2O (6 mL) at –78 °C and the reaction was stirred for 2 h. The reaction mixture was added via cannula to a solution of isobutyltriphenylphosphonium bromide (500 mg. 1.28 mmol) and *n*-butyllithium (2.1 M in hexanes, 0.6 mL, 1.2 mmol) in THF (6 mL) that had been stirred for 45 min at 0 °C. The reaction was warmed to room temperature and stirred for 2 h. The solvent was removed under reduced pressure, and the solid was

suspended in hexanes (20 mL) and filtered. The filter cake was washed with additional hexanes (3 x 10 mL), and the filtrate was concentrated under reduced pressure. The crude residue was purified by column chromatography, eluting with hexanes/EtOAc (98:2) to give 95 mg (62%) of **2.166** as an inseparable mixture of *cis:trans* isomers (5:1) as a colorless oil. ^{1}H NMR ($CDCl_3$, 400 MHz) δ ppm 5.47–5.20 (comp, 2 H,) 2.95–2.89 (comp, 2H), 2.61 (dd, J = 13.5, 6.9 Hz, 1H), 2.27–2.14 (comp, 2H), 1.63–1.19 (comp, 20H), 0.96 (t *J* = 6.5 Hz, 6H), 0.88 (t, *J* = 6.7 Hz, 3H). ^{13}C NMR ($CDCl_3$, 100 MHz) δ 138.5, 138.4, 125.9, 125.8, 57.3, 56.8, 31.9, 29.6, 29.5, 29.3, 28.1, 27.9, 27.8, 26.6, 26.4, 24.4, 23.1, 22.7, 14.1. IR (film) 2987, 1643, 1465, 1256, 1090 cm^{-1}; mass spectrum (ESI) *m/z* 303.2663 $[M+Na]^+$, [$C_{19}H_{36}O$ $[M+Na]^+$ requires 303.2664]

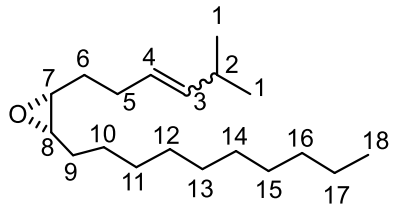

NMR Assignments. ^{1}H NMR ($CDCl_3$, 400 MHz) δ ppm 5.47–5.20 (comp, 2 H, C4-H, C3-H) 2.95–2.89 (comp, 2H, C8-H, C7-H), 2.61 (dd, J = 13.5, 6.9 Hz, 1H, C2-H), 2.27–2.14 (comp, 2H, C5-H), 1.63–1.19 (comp, 20H C6,C9–117-H), 0.96 (t *J* = 6.5 Hz, 6H, C1-H), 0.88 (t, *J* = 6.7 Hz, 3H, C18-H). ^{13}C NMR ($CDCl_3$,100 MHz) δ 138.5 C4, 138.4 C3, 125.9 C4, 125.8 C3, 57.3 C7, 56.8 C8, 31.9, 29.6, 29.5, 29.3, 28.1, 27.9, 27.8, 26.6, 26.4, 24.4, 23.1, 22.7, 14.1.C1,C2,C5,C6,C9–18

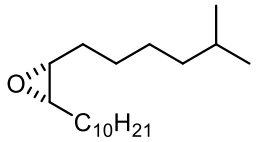

(2*S*,3*R*)-2-Decyl-3-(5-methylhexyl)oxirane, (+)-disparlure (2.111) (DK-4-281). PtO_2 (5 mg, 0.02 mmol) was added to a solution of **2.166** (50 mg, 0.18 mmol) in hexanes (1.5 mL) under an H_2 atmosphere. The reaction was stirred for 1 h, whereupon it was filtered, and the solvent was removed under reduced pressure. The crude residue was purified by column chromatography, eluting with hexanes/EtOAc (99:1) to give 45 mg (90%) of **2.11** as a colorless oil. The compound was consistent with the previously reported data.[166,172] $[\alpha]^{26}_{D}$ +0.8 (c = 0.3, $CHCl_3$). ^{1}H NMR (400 MHz, $CDCl_3$) δ 2.90 (p, *J* = 4.2 Hz, 2 H), 1.62 – 1.13 (comp, 28 H), 0.87 (d, *J* = 6.6 Hz, 6 H) ^{13}C NMR (126 MHz, $CDCl_3$) δ 57.4, 39.1, 32.1, 29.8, 29.7, 29.5, 28.1, 28.0, 28.0, 27.5, 27.0, 26.7, 22.8, 22.8, 22.8, 14.3.

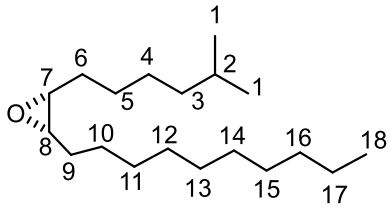

NMR Assignment. ^{1}H NMR (400 MHz, $CDCl_3$) δ 2.90 (p, *J* = 4.2 Hz, 2 H C8,C7-H), 1.62 – 1.13 (comp, 28 H C2–C18-H), 0.87 (d, *J* = 6.6 Hz, 6 H, C1-H)

Table 7.1 Comparison of ^{13}C NMR peaks of disparlure with reported literature values.

Grubbs[172]	**Prasad**[166]	**Wang**[147]	**Pandey**[314]	**Martin**	**Martin**
100 MHz	75 MHz	20 MHz	100 MHz	126 MHz	126 MHz
57.4	57.2	57.12	57.2	57.3	57.28
57.4	38.9	39.05	38.8	38.9	38.91
39.1	31.9	32.03	31.8	31.9	31.91
32.2	29.5	26.69	29.5	29.6	29.61
32.1	29.3	29.47	29.3	29.6	29.57
29.8	27.9	28	27.8	29.3	29.34
29.7	27.3	27.44	27.8	27.9	27.91
29.6	26.8	27.02	27.8	27.9	27.87
29.5	26.6	26.73	27.3	27.8	27.83
28.0 (3C)	22.6	22.68	26.8	27.3	27.34
27.5	22.5	14.15	26.5	26.9	26.87
27.4	14.1		26	26.6	26.61
26.8			22.6	22.7	22.69
26.2			22.6	22.6	22.63
22.8 (2C)			14.1	22.6	22.62
14.3				14.1	14.12

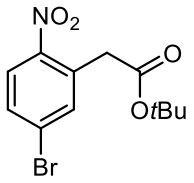

***tert*-Butyl 2-(5-bromo-2-nitrophenyl)acetate (4.15) (DK-3-211)** A solution of 4-bromonitrobenzene (5.00g, 24.8 mmol) and *tert*-butylchloroacetate (5.60 g, 37.2 mmol) in DMF (60 mL) was added via cannula to a stirred solution of *t*-BuOK (16.7 g, 148.8 mmol) in DMF (16.7 g, 148.8 mmol). The reaction was stirred at room temperature for 2 h, whereupon it was cooled to 0 °C and 1 M HCl (120 mL) was added. The mixture was extracted with EtOAc (3 x 150 mL) and the combined organic layers were washed with brine (3 x 150 mL). The organic layers were dried (Mg_2SO_4), filtered, and concentrated under reduced pressure. The crude mixture was purified by column chromatography, eluting with hexanes/EtOAc (95:5 to 90:10) to give 7.05 g (90%) of **4.15** as a yellow solid. The compound was consistent with the previously reported data.[221] ^{1}H NMR (400 MHz, $CDCl_3$) δ 7.96 (d, *J* = 8.5 Hz, 1H), 7.57 (dd, *J* = 8.5, 2.0 Hz, 1H), 7.48 (d, *J* = 2.0 Hz, 1H), 3.89 (s, 2H), 1.41 (s, 9H),

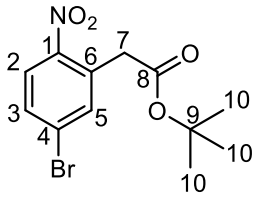

NMR Assignments. ^{1}H NMR (400 MHz, $CDCl_3$) δ 7.96 (d, *J* = 8.5 Hz, 1H, C2-H), 7.57 (dd, *J* = 8.5, 2.0 Hz, 1H, C3-H), 7.48 (d, *J* = 2.0 Hz, 1H, C5-H), 3.89 (s, 2H, C7-H), 1.41 (s, 9H, C10-H)

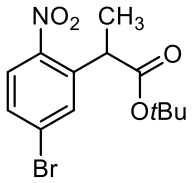

***tert*-Butyl-2-(5-bromo-2-nitrophenyl)propanoate (4.16) (DK-3-213)** Sodium hydride (60% dispersion in mineral oil, 0.75 g, 18.3 mmol) was added to a solution of **4.15** (6.21 g, 18.3 mmol) in THF (65 mL). Methyl iodide (5.3 g, 37.6 mmol) was added dropwise, and the reaction was stirred at room temperature for 14 h, whereupon, H_2O (60 mL) was added, and the layers were separated. The aqueous layer was extracted with EtOAc (3 x 100 mL) and the combined organic layers were washed with brine (2 x 100 mL), dried (Mg_2SO_4), filtered, and concentrated under reduced pressure. The crude material was purified by column chromatography, eluting with hexanes/EtOAc (95:5) to give 4.83 g (80%) of **4.16** as a yellow solid. The compound was consistent with the previously reported data.[221] ^{1}H NMR (400 MHz, $CDCl_3$) δ 7.81 (d, *J* = 8.5 Hz, 1H), 7.62 (d, *J* = 2.0 Hz, 1H), 7.54 (dd, *J* = 8.5, 2.0 Hz, 1H), 4.21 (q, *J* = 7.1 Hz, 1H), 1.57 (d, *J* = 7.1 Hz, 3H), 1.40 (s, 9H).

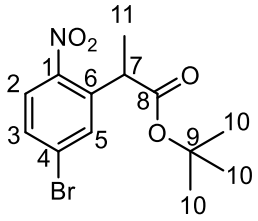

NMR Assignment. ^{1}H NMR (400 MHz, $CDCl_3$) δ 7.81 (d, *J* = 8.5 Hz, 1H, C2-H), 7.62 (d, *J* = 2.0 Hz, 1H, C3-H), 7.54 (dd, *J* = 8.5, 2.0 Hz, 1H, C3-H), 4.21 (q, *J* = 7.1 Hz, 1H, C7-H), 1.57 (d, *J* = 7.1 Hz, 3H, C11-H), 1.40 (s, 9H C10-H).

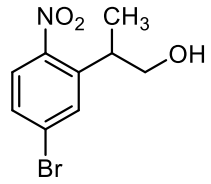

2-(5-Bromo-2-nitrophenyl)propan-1-ol (4.17) (DK-3-234) DIBAL (1 M in hexanes, 18.2 mL, 18.2 mmol) was added dropwise to a solution **4.16** (2.0 g, 6.06 mmol) in THF (76 mL) at 0 °C. The reaction was stirred for 3 h, whereupon, 6 M HCl (50 mL) was added slowly. The reaction mixture was extracted with EtOAc (3 x 150mL) and the combined organic layers were washed with a 10% aqueous solution of Rochelle's salt (3 x 50 mL), then dried (Mg_2SO_4), filtered, and concentrated under reduced pressure. The crude material was purified by column chromatography eluting with hexanes/EtOAc (9:1) to give 1.42 g (90%) of **4.17** as a red oil. The compound was consistent with the previously reported data.[221] ^{1}H NMR (400 MHz, $CDCl_3$) δ 7.66 (d, *J* = 8.7 Hz, 1H), 7.63 (d, *J* = 2.1 Hz, 1H), 7.49 (dd, *J* = 8.6, 2.1 Hz, 1H), 3.79 (ddd, *J* = 17.9, 10.8, 6.5 Hz, 2H), 3.55 (ddd, *J* = 13.8, 6.9 Hz, 1H), 1.33 (d, *J* = 6.9 Hz, 3H).

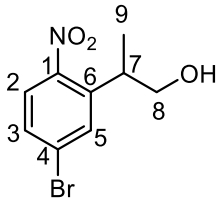

NMR Assignment. ^{1}H NMR (400 MHz, $CDCl_3$) δ 7.66 (d, *J* = 8.7 Hz, 1H C2-H), 7.63 (d, *J* = 2.1 Hz, 1H, C5-H), 7.49 (dd, *J* = 8.6, 2.1 Hz, 1H, C3-H), 3.79 (ddd, *J* = 17.9, 10.8, 6.5 Hz, 2H, C8-H), 3.55 (ddd, *J* = 13.8, 6.9 Hz, 1H, C7-H), 1.33 (d, *J* = 6.9 Hz, 3H, C9-H).

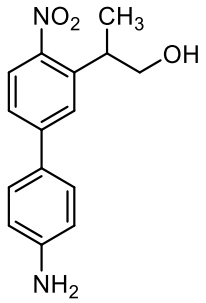

2-(4'-Amino-4-nitro-[1,1'-biphenyl]-3-yl)propan-1-ol (4.19) (DK-2-244). $Pd(OAc)_2$ (50.5 mg, 0.194 mmol) was added to a solution of **4.17** (505 mg, 1.95 mmol), 4-amino-phenyl boronic acid hydrochloride (404 mg, 2.3 mmol), K_2CO_3 (725 mg, 5.24 mmol), B_4NBr (626 mg, 1.94 mmol) in degassed EtOH/H_2O (2:1, 15 mL), and the reaction was heated under reflux for 3 h. Upon cooling to room temperature, H_2O (50 mL) was added and the mixture was extracted with EtOAc (3 x 50mL). The combined organic extracts were washed with brine (50 mL), dried (Mg_2SO_4), and concentrated under reduced pressure. The crude product was purified by column chromatography eluting with hexanes/EtOAc (7:3) to give 425 mg (81%) of **4.19** as an orange solid. The compound was consistent with the previously reported data.[221] ^{1}H NMR (400 MHz, CD_3OD) δ 7.81 (d, *J* = 8.5 Hz, 1H), 7.66 (d, *J* = 2.0 Hz, 1H), 7.54 (dd, *J* = 8.5, 2.0 Hz, 1H), 7.46 (d, *J* = 8.6 Hz, 2H), 6.79 (d, *J* = 8.6 Hz, 2H), 3.80 (dd, *J* = 10.8, 6.9 Hz, 1H), 3.70 (dd, *J* = 10.8, 6.4 Hz, 1H), 3.53 (dd, *J* = 13.6, 6.8 Hz, 1H), 1.36 (d, *J* = 6.9 Hz, 3H).

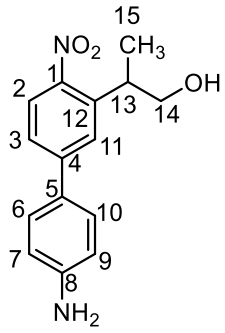

NMR Assignment. ^{1}H NMR (400 MHz, CD_3OD) δ 7.81 (d, *J* = 8.5 Hz, 1H, C2-H), 7.66 (d, *J* = 2.0 Hz, 1H, C11-H), 7.54 (dd, *J* = 8.5, 2.0 Hz, 1H, C3-H), 7.46 (d, *J* = 8.6 Hz, 2H, C6,C10-H), 6.79 (d, *J* = 8.6 Hz, 2H, C7,C9-H), 3.80 (dd, *J* = 10.8, 6.9 Hz, 1H, C14-H), 3.70 (dd, *J* = 10.8, 6.9 Hz, 1H, C14-H), 3.53 (dd, *J* = 13.6, 6.9 Hz, 1H, C13-H), 1.36 (d, *J* = 6.9 Hz, 3H, C15-H).

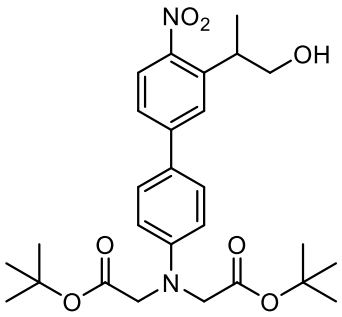

Di-*tert*-butyl 2,2'-((3'-(1-hydroxypropan-2-yl)-4'-nitro-[1,1'-biphenyl]-4-yl)-azanediyl)diacetate (4.21) (DK-4-156). *tert*-Butyl 2-bromoacetate (0.382 g, 0.289 mL, 1.96 mmol) was added to a solution of **4.19** (0.195 g, 0.717 mmol) and *i*-PrNEt$_2$ (0.279 g, 0.375 mL, 2.15 mmol) in DMF (10 mL). The reaction mixture was heated to 80 °C and stirred for 12 h, whereupon it was cooled to room temperature and quenched with saturated aqueous $NaHCO_3$ (10 mL). The mixture was extracted with EtOAc (3 x 20 mL), and the combined organic extracts were washed with brine (5 x 20 mL), dried (Mg_2SO_4), filtered, and concentrated under reduced pressure. The crude material was purified by column

chromatography eluting with hexanes/EtOAc (7:3) to afford 190 mg (45%) of **4.21** as an orange solid. The compound was consistent with the previously reported data.[221] ^{1}H NMR (400 MHz, $CDCl_3$) δ 7.85 (d, *J* = 8.5 Hz, 1H), 7.59 (d, *J* = 1.8 Hz, 1H), 7.51 – 7.46 (comp, 3H), 6.67 (d, *J* = 8.8 Hz, 2H), 4.06 (s, 4H), 3.86 – 3.82 (comp, 2H), 3.67 (dd, *J* = 13.3, 6.6 Hz, 1H), 1.48 (s, 18H), 1.37 (d, *J* = 6.9 Hz, 3H).

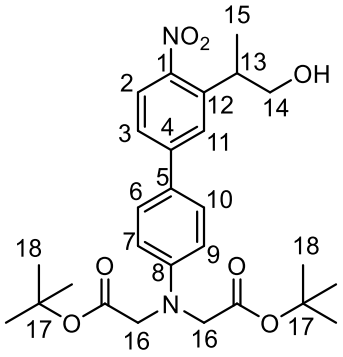

NMR Assignments. ^{1}H NMR (400 MHz, $CDCl_3$) δ 7.85 (d, *J* = 8.5 Hz, 1H, C2-H), 7.59 (d, *J* = 1.8 Hz, 1H, C11-H), 7.51 – 7.46 (comp, 3H, C6,C10,C3-H), 6.67 (d, *J* = 8.8 Hz, 2H, C7,C9-H), 4.06 (s, 4H, C16-H), 3.86–3.82 (comp, 2H, C14-H), 3.67 (dd, *J* = 13.3, 6.6 Hz, 1H, C13-H), 1.48 (s, 19H, C18-H), 1.37 (d, *J* = 6.9 Hz, 3H, C15-H).

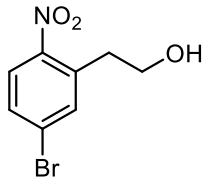

2-(5-Bromo-2-nitrophenyl)ethan-1-ol (4.23) (DK-5-219). DBAL (1 M in hexanes, 30.0 mL, 30.0 mmol) was added to a solution of **4.15** (3.15 g, 10 mmol) in THF (100 mL) at 0 °C. The was stirred for 3 h, whereupon, 6 M HCl (50 mL) was added slowly, and the layers were separated. The aqueous layer was washed with EtOAc (3 x 50 mL) and the combined organic layers were washed with a 10% aqueous solution of Rochelle's salt

(3 x 50 mL), then dried (Mg_2SO_4), filtered, and concentrated under reduced pressure. The crude material was purified by column chromatography eluting with hexanes/EtOAc (9:1) to give 2.2 g (90%) of **4.23** as a red-orange oil. ^{1}H NMR (400 MHz, $CDCl_3$) δ 7.83 (d, *J* = 8.7 Hz, 1H), 7.60 (d, *J* = 2.1 Hz, 1H), 7.53 (dd, *J* = 8.7, 2.2 Hz, 1H), 3.96 (t, *J* = 6.3 Hz, 2H), 3.16 (t, *J* = 6.3 Hz, 2H). ^{13}C NMR ($CDCl_3$,100 MHz) δ 148.2, 141.0, 131.6, 130.4, 127.5, 125.7, 67.6, 36.4. mass spectrum (ESI) *m/z* 268.0 $[M+Na]^+$, 270.0 $[M+Na]^+$ [$C_8H_8BrNO_3$ $[M+Na]^+$ requires 268.96 , 269.96].

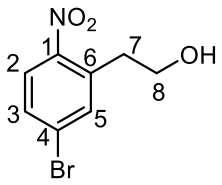

NMR Assignment. ^{1}H NMR (400 MHz, $CDCl_3$) δ 7.83 (d, *J* = 8.7 Hz, 1H, C2-H), 7.60 (d, *J* = 2.1 Hz, 1H, C5-H), 7.53 (dd, *J* = 8.7, 2.2 Hz, 1H, C3-H), 3.96 (t, *J* = 6.3 Hz, 2H, C8-H), 3.16 (t, *J* = 6.3 Hz, 2H, C7-H). ^{13}C NMR ($CDCl_3$,100 MHz) δ 148.2 C1, 141.0 C6, 131.6 C5, 130.4 C3, 127.5 C4, 125.7 C2, 67.6 C8, 36.4 C7.

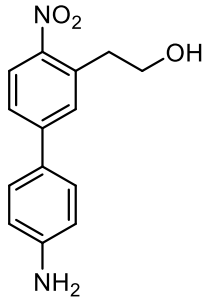

2-(4'-Amino-4-nitro-[1,1'-biphenyl]-3-yl)ethan-1-ol (4.24) (DK-5-209). $Pd(OAc)_2$ (50.5 mg, 0.194 mmol) was added to a solution of **4.23** (500 mg, 2.0 mmol), 4-amino-phenyl boronic acid hydrochloride (404 mg, 2.3 mmol), K_2CO_3 (725 mg, 5.24 mmol), B_4NBr (626 mg, 2.0 mmol) in degassed EtOH/H_2O (2:1, 15 mL), and the reaction

was heated under reflux for 3 h. Upon cooling to rt, H_2O (50 mL) was added and the mixture was extracted with EtOAc (3 x 50mL). The combined organic extracts were washed with brine (50 mL), dried (Mg_2SO_4), and concentrated under reduced pressure. The crude was purified by column chromatography eluting with hexanes/EtOAc (7:3) to give 425 mg (81%) of **4.24** as an orange solid. m.p. 162–163 °C. ^{1}H NMR (400 MHz, $CDCl_3$) δ 8.01 (d, *J* = 8.4 Hz, 1H), 7.52 (dd, *J* = 4.4, 2.0 Hz, 1H), 7.49 (d, *J* = 2.1 Hz, 1H), 7.43 (d, *J* = 8.7 Hz, 2H), 6.75 (d, *J* = 8.7 Hz, 2H), 3.98 (dd, *J* = 11.8, 6.2 Hz, 2H), 3.85 (s, 2H), 3.24 (t, *J* = 6.4 Hz, 2H). ^{13}C NMR (100MHz, $CDCl_3$) 147.2, 145.9, 139.0, 129.0, 127.3, 125.7, 125.2, 124.7, 115.4, 111.8, 68.1, 36.5. mass spectrum (ESI) *m/z* 258.1 $[M+H]^+$, [$C_{14}H_{14}N_2O_3$ $[M+H]^+$ requires 258.10].

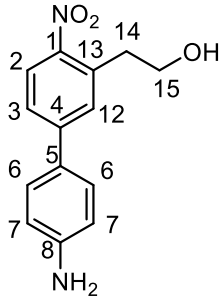

NMR Assignment. ^{1}H NMR (400 MHz, $CDCl_3$) δ 8.01 (d, *J* = 8.4 Hz, 1H, C2-H), 7.52 (dd, *J* = 4.4, 2.0 Hz, 1H, C3-H), 7.49 (d, *J* = 2.1 Hz, 1H, C12-H), 7.43 (d, *J* = 8.7 Hz, 2H, C6-H), 6.75 (d, *J* = 8.7 Hz, 2H, C7-H), 3.98 (dd, *J* = 11.8, 6.2 Hz, 2H, C15-H), 3.85 (s, 2H, NH2), 3.24 (t, *J* = 6.4 Hz, 2H, C14-H). ^{13}C NMR (100MHz, $CDCl_3$) 147.2 C1, 145.9 C4, 139.0 C8, 129.0 C6, 127.3 C3, 125.7 C2, 125.2 C7, 124.7 C5, 115.4 C12, 111.8 C13, 68.1 C15, 36.5 C14

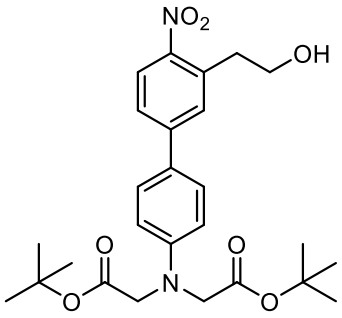

Di-*tert*-butyl 2,2'-((3'-(2-hydroxyethyl)-4'-nitro-[1,1'-biphenyl]-4-yl)azanediyl)diacetate (4.25) (DK-5-213). *tert*-Butyl 2-bromoacetate (0.280 g, 0.21 mL, 1.45 mmol) was added to a solution of **4.24** (0.150 g, 0.58 mmol) and *i*-PrNEt$_2$ (0.225 g, 0.3 mL, 1.74 mmol) in DMF (6 mL). The reaction mixture was heated to 80 °C and stirred for 12 h. Upon cooling to room temperature, the reaction was quenched with saturated aqueous $NaHCO_3$ (10 mL). The mixture was extracted with EtOAc (3 x 20 mL), and the combined organic extracts were washed with brine (5 x 20 mL), dried (Mg_2SO_4), filtered, and concentrated under reduced pressure. The crude material was purified by column chromatography eluting with hexanes/EtOAc (7:3) to afford 0.145 g (52%) of **4.25** as an orange solid. ^{1}H NMR (400 MHz, $CDCl_3$) δ 8.03 (d, *J* = 8.4 Hz, 1H), 7.58 – 7.46 (comp, 4H), 6.67 (d, *J* = 8.9 Hz, 2H), 4.06 (s, 4H), 3.99 (t, *J* = 6.4 Hz, 2H), 3.25 (t, *J* = 6.4 Hz, 2H), 1.48 (s, 18H). ^{13}C NMR (100MHz, $CDCl_3$) δ 169.7, 148.6, 148.4, 139.1, 145.8, 139.0, 128.2, 125.7, 125.2, 124.7, 112.6, 82.0, 68.1, 54.5, 30.9, 24.4; mass spectrum (ESI) *m/z* 486.2 $[M+H]^+$, [$C_{26}H_{34}N_2O_7$ $[M+H]^+$ requires 486.24].

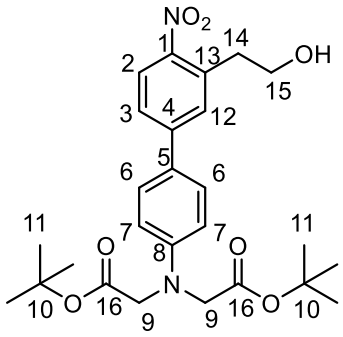

NMR Assignment. ^{1}H NMR (400 MHz, $CDCl_3$) δ 8.03 (d, *J* = 8.4 Hz, 1H, C2-H), 7.58 – 7.46 (comp, 4H, C3,C12,C6-H), 6.67 (d, *J* = 8.9 Hz, 2H, C7-H), 4.06 (s, 4H, C-H), 3.99 (t, *J* = 6.4 Hz, 2H, C15-H), 3.25 (t, *J* = 6.4 Hz, 2H, C14-H), 1.48 (s, 18H, C11-H). ^{13}C NMR (100MHz, $CDCl_3$) δ 169.7 C16, 148.6 C1, 148.4 C5, 139.1 C8, 139.0 C8, 128.2 C6, 125.7 C3, 125.2 C7, 124.7 C5, 112.6 C12, 82.0 C10, 68.1 C15, 54.5 C15, 30.9 C9, 24.4 C14.

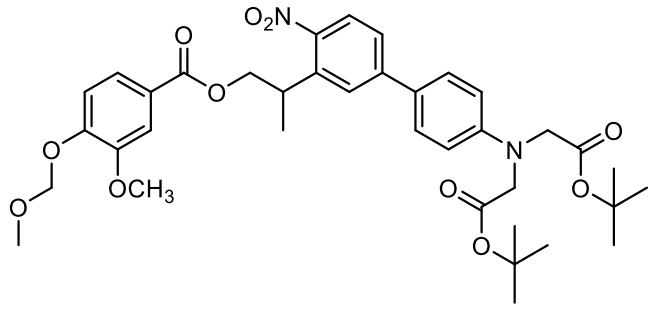

Di-*tert*-butyl 2,2'-((3'-(1-((3-methoxy-4-(methoxymethoxy)-benzoyl)oxy)-propan-2-yl)-4'-nitro-[1,1'-biphenyl]-4-yl)azanediyl)diacetate. (4.36) (DK-4-157). Triethylamine (0.04 g, 0.4 mmol) and DMAP (0.004 g, 0.03 mmol) were added to a solution of **4.21** (0.1 g, 0.2 mmol), **4.36** (0.042 g, 0.2 mmol), and 2,4,6-trichlorobenzoyl chloride (0.05 g, 0.2 mmol) in THF (2 mL) at 0 °C. The reaction was warmed to room temperature over 2 h and was stirred for an additional 2 h, whereupon it was diluted with

H_2O (5 mL) followed by EtOAc (5 mL). The layers were separated and the organic layer was dried (Na_2SO_4), filtered, and concentrated. The crude material was purified by column chromatography eluting with hexanes/EtOAc (9:1) to give 0.080 g of **4.36** as a yellow film. ^{1}H NMR (400 MHz, $CDCl_3$) δ 7.85 (dd, *J* = 8.5, 3.1 Hz, 1H), 7.66 – 7.41 (comp, 5H), 7.12 (d, *J* = 8.5 Hz, 1H), 6.66 (dd, *J* = 8.7, 4.5 Hz, 2H), 6.40 (s, 2H), 5.28 (d, *J* = 8.2 Hz, 2H), 4.50 (d, *J* = 6.9 Hz, 2H), 4.08–4.01 (comp, 3H), 3.90–3.79 (comp, 3H), 3.50 (d, *J* = 7.0 Hz, 2H), 1.53–1.42 (comp, 12H); mass spectrum (ESI) *m/z* 694.3 $[M+H]^+$, [$C_{37}H_{46}N_2O_{11}$ $[M+H]^+$ requires 694.31].

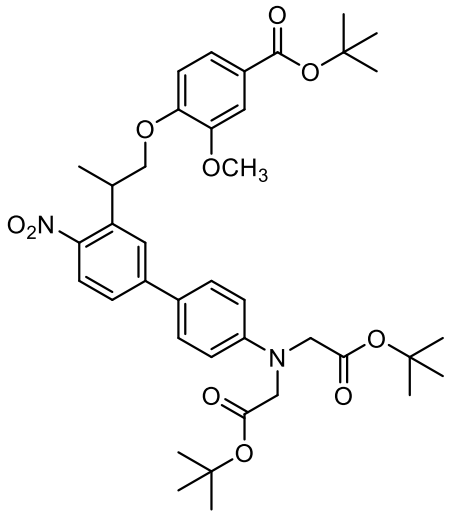

Di-*tert*-butyl 2,2'-((3'-(1-(4-(tert-butoxycarbonyl)-2-methoxyphenoxy)propan-2-yl)-4'-nitro-[1,1'-biphenyl]-4-yl)azanediyl)diacetate (4.40) (DK-4-153). Diethyl azodicarboxylate (DEAD) (0.016 g, 0.092 mmol) was added to a solution of **4.21** (0.046 g, 0.092 mmol), *tert*-butyl 4-hydroxy-3-methoxybenzoate (0.014 g, 0.062 mmol), and triphenylphosphine (0.024 g, 0.0923 mmol) in THF (0.6 mL), and the reaction stirred for 14 h. The solvent was removed under reduced pressure and the crude material was purified by column chromatography eluting with hexanes/EtOAc (90:10) to give 0.027 g (63%)of

4.40 as a yellow film. ^{1}H NMR (400 MHz, $CDCl_3$) δ 7.86 (d, *J* = 8.5 Hz, 1H), 7.82 (d, *J* = 1.8 Hz, 1H), 7.59 – 7.46 (comp, 5H), 6.85 (d, *J* = 8.4 Hz, 1H), 6.67 (d, *J* = 8.9 Hz, 2H), 4.33 (dd, *J* = 9.4, 5.0 Hz, 1H), 4.19 (dd, *J* = 9.4, 6.1 Hz, 1H), 4.08 (d, *J* = 12.4 Hz, 4H), 4.00 (dd, *J* = 12.1, 6.0 Hz, 1H), 3.81 (s, 3H), 1.63 – 1.42 (comp, 30H). ^{13}C NMR (100 MHz $CDCl_3$) δ 168.4, 164.7, 153.8, 150.8, 150.0, 149.6, 144.4, 142.3, 132.6, 131.3, 128.1, 127.6, 123.9, 123.3, 122.7, 117.9, 116.0, 114.1, 82.0, 75.1, 56.8, 52.0, 36.4, 28.4, 17.9; mass spectrum (ESI) *m/z* 706.3 $[M+H]^+$, [$C_{39}H_{50}N_2O_{10}$ $[M+H]^+$ requires 706.35].

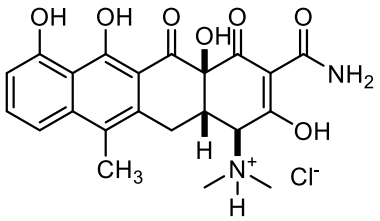

(1*S*,4a*S*,12a*S*)-3-Carbamoyl-2,4a,6,7-tetrahydroxy-*N*,*N*,11-trimethyl-4,5-dioxo-1,4,4a,5,12,12a-hexahydrotetracen-1-aminium (ATc-HCl, 4.2-HCl) (DK-4-241). Tetracycline (0.5 g, 1.04 mmol) was suspended in a solution of *i*-PrOH/HCl/MeOH (20:5:1) (6 mL) and stirred at room temperature for 48 h. The suspension was filtered, and the filter cake was washed with *i*-PrOH (3 x 5 mL) followed by Et_2O (2 x 5 mL). The filtered solid was collected and dried to give 0.440 (85%) of **4.2-HCl** as an orange solid. This sample was identical to commercially available **4.2-HCl**. ^{1}H NMR (400 MHz, CD_3OD) δ 7.59 (d, *J* = 7.9 Hz, 1H), 7.48 (dd, *J* = 8.5, 0.9 Hz, 1H), 6.89 (dd, *J* = 7.8, 0.8 Hz, 1H), 4.26 (d, *J* = 4.0 Hz, 1H), 3.63 (dd, *J* = 17.4, 4.9 Hz, 1H), 3.42 (dt, *J* = 9.2, 4.9 Hz, 1H), 3.09 (d, *J* = 25.4 Hz, 6H), 2.45 (s, 3H), mass spectrum (ESI) *m/z* 426.1 $[M+H]^+$, [$C_{22}H_{22}N_2O_7$ $[M+H]^+$ requires 426.14].

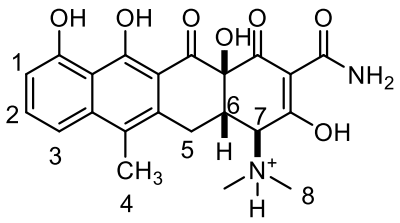

NMR Assignment. ^{1}H NMR (400 MHz, CD_3OD) δ 7.59 (d, *J* = 7.9 Hz, 1H, C3-H), 7.48 (dd, *J* = 8.5, 0.9 Hz, 1H, C2-H), 6.89 (dd, *J* = 7.8, 0.8 Hz, 1H, C1-H), 4.26 (d, *J* = 4.0 Hz, 1H, C7-H), 3.63 (dd, *J* = 17.4, 4.9 Hz, 1H, C6-H), 3.42 (dt, *J* = 9.2, 4.9 Hz, 1H, C5-H), 3.09 (comp, 7H, C8-H, C5-H), 2.45 (s, 3H, C4-H),

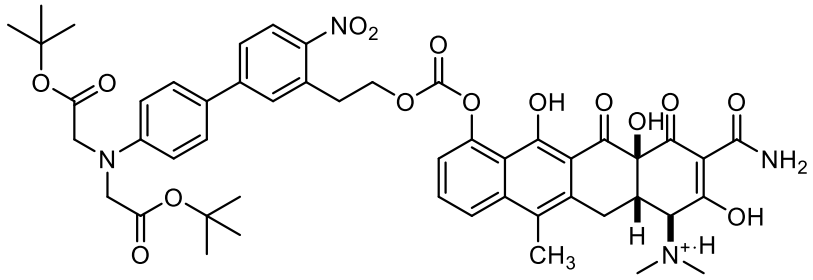

Di-*tert*-butyl 2,2'-((3'-(2-(((((6a*S*,7*S*,10a*S*)-9-carbamoyl-7-(dimethylamino)-8,10a,12-trihydroxy-5-methyl-10,11-dioxo-6,6a,7,10,10a,11-hexahydrotetracen-1-yl)oxy)carbonyl)oxy)ethyl)-4'-nitro-[1,1'-biphenyl]-4-yl)azanediyl)diacetate (4.61) (DK-4-289). A solution of *i*-$PrNEt_2$ (0.031 g, 0.24 mmol) and **4.25** (0.080 g, 0.16 mmol) in THF (0.8 mL) was added drop wise to a solution of phosgene (15% wt in PhMe, 0.527 g, 0.573 mL, 0.8 mmol) in THF (0.8 mL) at 0 °C and the reaction stirred for 0.5 h. The solvent was removed under reduced pressure and the crude material was dissolved in CH_3CN (0.75 mL), and added dropwise to a solution of **4.2-HCl** (0.061 g, 0.133 mmol), *N*-methylimidazole (0.002 g, 0.0267 mmol), and *i*-$PrNEt_2$ (0.038 g, 0.293 mmol) in CH_3CN (0.75 mL) at 0 °C. The reaction was stirred for 1 h, whereupon, the solvent was removed under reduced pressure, and the crude material was purified by chromatography eluting

with CH_2Cl_2/MeOH (98.5:1.5) to give 0.07 g (52%) of **4.61** as an orange solid. ^{1}H NMR (400 MHz, $CDCl_3$) δ 8.07 (d, *J* = 8.5 Hz, 1H), 7.87 (d, *J* = 8.8 Hz, 1H), 7.64–7.49 (comp, 5H), 7.10 (d, *J* = 7.2 Hz, 1H), 6.66 (d, *J* = 8.9 Hz, 2H), 6.02 (s, 1H), 4.63 (td, *J* = 6.5, 2.2 Hz, 2H), 4.06 (s, 4H), 3.62–3.18 (comp, 6H), 2.68 (m, 1H), 2.54 – 2.36 (comp, 9 H), 1.66 – 1.37 (comp, 18 H); mass spectrum (ESI) *m/z* 939.4 $[M+H]^+$, [$C_{22}H_{22}N_2O_7$ $[M+H]^+$ requires 939.36]

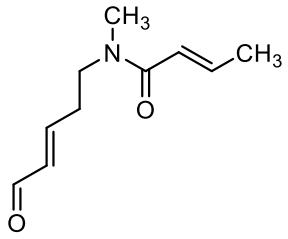

(*E*)-*N*-methyl-*N*-((*E*)-5-oxopent-3-en-1-yl)but-2-enamide (6.6) (DK-5-86). Crotonyl chloride (1.28 g, 12.2 mmol) was added drop wise to a solution of **6.7** (0.53 g, 4.1 mmol) in CH_3CN (15 mL) at 0 °C. The reaction was stirred for 0.5 h, and then heated under reflux for 1 h. After cooling to room temperature, TMSOTf (0.09 g, 0.5 mmol) and **6.8** (2.0 g, 14.3 mmol) were added, and the reaction was stirred for 14 h. The reaction was quenched with saturated aqueous NH_4Cl (20 mL) and the organic layer was removed under reduced pressure. The remaining aqueous layer was extracted with CH_2Cl_2 (3 x 40 mL) and the combined organic layers were washed with brine (2 x 50 mL), dried (Na_2SO_4), filtered, and concentrated under reduced pressure. The crude material was purified by chromatography eluting with hexanes/EtOAc (25:75) to afford 2.2 g of **6.6** as a yellow oil. ^{1}H NMR (400 MHz, $CDCl_3$) δ 9.50 (d, *J* = 7.9 Hz, 1H), 7.04–6.70 (comp, 2H), 6.31–6.06 (comp, 2H), 3.59 (dt, *J* = 13.9, 6.7 Hz, 2H), 3.15–2.93 (comp, 3H), 2.62 (dd, *J* = 13.9, 6.7 Hz, 2H), 1.89 (dd, *J* = 6.9, 1.7 Hz, 3H). ^{13}C NMR (100 MHz, $CDCl_3$) δ 192.7, 170.0, 154.0,

139.5, 131.7, 121.2, 47.4, 34.7, 29.4, 17.3; mass spectrum (ESI) *m/z* 182.1 $[M+H]^+$, [$C_{10}H_{15}NO_2$ $[M+H]^+$ requires 182.12]

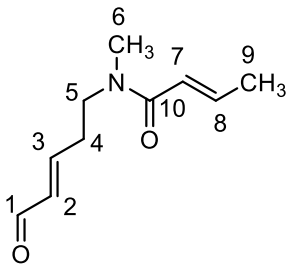

NMR Assignments. ^{1}H NMR (400 MHz, $CDCl_3$) δ 9.50 (d, *J* = 7.9 Hz, 1H, C1-H), 7.04–6.70 (comp, 2H, C3,C8-H), 6.31 – 6.06 (comp, 2H, C2,C7-H), 3.59 (dt, *J* = 14.3, 7.0 Hz, 2H, C5-H), 3.15–2.93 (comp, 3H C6-H), 2.62 (dd, *J* = 13.5, 6.4 Hz, 2H, C4-H), 1.89 (dd, *J* = 6.9, 1.7 Hz, 3H, C9). ^{13}C NMR (100 MHz, $CDCl_3$) δ 192.7 C1, 170.0 C10, 154.0 C3, 139.5 C8, 131.7 C2, 121.2 C7, 47.4 C6, 34.7 C5, 29.4 C4, 17.3 C9.

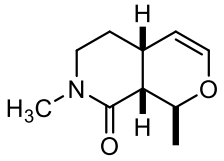

(**1S,4a*R*,8a*R*)-1,7-dimethyl-1,4a,5,6,7,8a-hexahydro-8H-pyrano[3,4-c]pyridin-8-one (6.33) (DK-5-63)** The triene **6.6** (0.5 g, 2.76 mmol) was dissolved in degassed xylenes (180 mL) and the reaction vessel was sealed and heated to 190 °C for 18 h. After cooling to room temperature, the solvent was removed under reduced pressure and the crude material was purified by chromatography eluting with hexanes/EtOAc (1:1 to 1:3) to give 0.29 g (58%) of **6.33**. as a gold oil. ^{1}H NMR (500 MHz, $CDCl_3$) δ 6.41 (dd, *J* = 6.2, 1.9 Hz, 1H), 4.84 (qd, *J* = 6.6, 3.8 Hz, 1H), 4.55 (dd, *J* = 5.8, 2.9 Hz, 1H), 3.39 (ddd, *J* =

11.9, 10.5, 4.5 Hz, 1H), 3.16 (dt, *J* = 12.0, 4.7 Hz, 1H), 2.95 (s, 3H), 2.78 – 2.67 (comp, *J* = 8.5, 2.7 Hz, 1H), 2.41 (dd, *J* = 5.6, 4.2 Hz, 1H), 1.99 (dddd, *J* = 13.8, 10.1, 5.1, 3.7 Hz, 1H), 1.88 – 1.75 (m, 1H), 1.36 (d, *J* = 6.7 Hz, 3H). ^{13}C NMR (125 MHz, $CDCl_3$) δ 171.0, 144.4 100.5, 70.2, 46.7, 44.4, 35.2, 27.1, 25.9, 18.2. mass spectrum (ESI) *m/z* 182.1 $[M+H]^+$, [$C_{10}H_{15}NO_2$ $[M+H]^+$ requires 182.12]

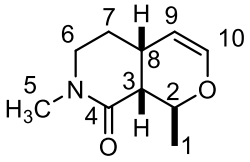

NMR Assignment. ^{1}H NMR (500 MHz, $CDCl_3$) δ 6.41 (dd, *J* = 6.4, 1.9 Hz, 1H, C10-H), 4.84 (qd, *J* = 6.4, 3.8 Hz, 1H, C9-H), 4.55 (dd, *J* = 5.7, 2.9 Hz, 1H, C2-H), 3.39 (ddd, *J* = 12.0, 10.5, 4.4 Hz, 1H, C6-H), 3.16 (dt, *J* = 12.0, 4.6 Hz, 1H, C6-H), 2.95 (s, 3H, C5-H), 2.78 – 2.67 (m, 1H, C8-H), 2.41 (dd, *J* = 5.7, 4.4 Hz, 1H, C3-H), 1.99 (dddd, *J* = 13.8, 10.1, 5.1, 3.7 Hz, 1H C7-H), 1.88 – 1.75 (m, 1H, C7-H), 1.36 (d, *J* = 6.7 Hz, 3H, C1-H).

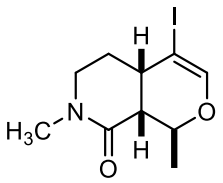

(1*S*,4a*S*,8a*R*)-4-Iodo-1,7-dimethyl-1,4a,5,6,7,8a-hexahydro-8H-pyrano[3,4-c]pyridin-8-one (6.36) (DK-5-175). *N*-Iodosuccinimide (0.5 g, 2.2 mmol) and $AgNO_3$ (0.01 g 0.55 mmol) were added to solution of **6.33** (0.39 g, 1.7 mmol) in CH_3CN (18 mL) at 80 °C and the reaction was stirred for 2 h. After cooling to room temperature, the solvent was removed under reduced pressure and the crude material was dissolved in CH_2Cl_2 (15 mL), and washed with H_2O (2 x 10 mL). The layers were separated and the organic layer

was dried (Na_2SO_4), filtered, and concentrated under reduced pressure. The crude material was purified by column chromatography eluting with hexanes/EtOAc (1:1 to 1:3) to give 0.35 g (67%) of **6.36** as a yellow oil.^{1}H NMR (400 MHz, $CDCl_3$) δ 6.71 (d, J = 1.8 Hz, 1H), 4.82 (qd, J = 6.6, 4.3 Hz, 1H), 3.73 (ddd, J = 6.7, 3.4, 1.7 Hz, 1H), 3.31 (ddd, J = 19.9, 11.3, 6.9 Hz, 2H), 3.12 (dt, J = 12.3, 5.0 Hz, 1H), 2.98–2.87 (comp, 3H), 2.76 – 2.69 (m, 1H), 2.55 (dt, J = 16.6, 8.3 Hz, 1H), 2.08 – 2.00 (comp, 2H), 1.88 – 1.80 (m, 1H), 1.35 (d, J = 6.6 Hz, 3H). ^{13}C NMR (100 MHz, $CDCl_3$) δ 169.7, 142.3, 76.0, 45.6, 44.7, 36.8, 34.5, 26.8, 19.1. mass spectrum (ESI) *m/z* 308.0 $[M+H]^+$, [$C_{10}H_{14}INO_2$ $[M+H]^+$ requires 308.01]

References

(1) Chung, W. J.; Vanderwal, C. D. Stereoselective Halogenation in Natural Product Synthesis. *Angew. Chem. Int. Ed.* **2016**, *55*, 4396–4434.

(2) Whitehead, D. C.; Yousefi, R.; Jaganathan, A.; Borhan, B. An Organocatalytic Asymmetric Chlorolactonization. *J. Am. Chem. Soc.* **2010**, *132*, 3298–3300.

(3) Murai, K.; Matsushita, T.; Nakamura, A.; Fukushima, S.; Shimura, M.; Fujioka, H. Asymmetric Bromolactonization Catalyzed by a C3-Symmetric Chiral Trisimidazoline. *Angew. Chem. Int. Ed.* **2010**, *49*, 9174–9177.

(4) Veitch, G. E.; Jacobsen, E. N. Tertiary Aminourea-Catalyzed Enantioselective Iodolactonization. *Angew. Chem. Int. Ed.* **2010**, *49*, 7332–7335.

(5) Zhang, W.; Zheng, S.; Liu, N.; Werness, J. B.; Guzei, I. A.; Tang, W. Enantioselective Bromolactonization of Conjugated (Z)-Enynes. *J. Am. Chem. Soc.* **2010**, *132*, 3664–3665.

(6) Zhou, L.; Tan, C. K.; Jiang, X.; Chen, F.; Yeung, Y. Y. Asymmetric Bromolactonization Using Amino-Thiocarbamate Catalyst. *J. Am. Chem. Soc.* **2010**, *132*, 15474–15476.

(7) Tan, C. K.; Zhou, L.; Yeung, Y. Amino-Thiocarbamate Catalyzed Asymmetric Bromolactonization of 1,2- Disubstituted Olefinic Acids. *Org. Lett.* **2011**, *13*, 2738–2741.

(8) Whitehead, D. C.; Fhaner, M.; Borhan, B. A Peptide Bromoiodinane Approach for Asymmetric Bromolactonization. *Tetrahedron Lett.* **2011**, *52*, 2288–2291.

(9) Tan, C. K.; Le, C.; Yeung, Y.-Y. Enantioselective Bromolactonization of Cis-1,2-Disubstituted Olefinic Acids Using an Amino-Thiocarbamate Catalyst. *Chem. Commun.* **2012**, *48*, 5793.

(10) Fang, C.; Paull, D. H.; Hethcox, J. C.; Shugrue, C. R.; Martin, S. F. Enantioselective Iodolactonization of Disubstituted Olefinic Acids Using a Bifunctional Catalyst. *Org. Lett.* **2012**, *14*, 6290–6293.

(11) Dobish, M. C.; Johnston, J. N. Achiral Counterion Control of Enantioselectivity in a Bronsted Acid-Catalyzed Iodolactonization. *J. Am. Chem. Soc.* **2012**, *134*, 6068–6071.

(12) Zhang, W.; Liu, N.; Schienebeck, C. M.; Decloux, K.; Zheng, S.; Werness, J. B.; Tang, W. Catalytic Enantioselective Halolactonization of Enynes and Alkenes. *Chem. Eur. J.* **2012**, *18*, 7296–7305.

(13) Murai, K.; Nakamura, A.; Matsushita, T.; Shimura, M.; Fujioka, H. C3-Symmetric Trisimidazoline-Catalyzed Enantioselective Bromolactonization of Internal Alkenoic Acids. *Chem. Eur. J.* **2012**, *18*, 8448–8453.

(14) Jiang, X.; Tan, C. K.; Zhou, L.; Yeung, Y. Y. Enantioselective Bromolactonization Using an S-Alkyl Thiocarbamate Catalyst. *Angew. Chem. Int. Ed.* **2012**, *51*, 7771–7775.

(15) Paull, D. H.; Fang, C.; Donald, J. R.; Pansick, A. D.; Martin, S. F. Bifunctional Catalyst Promotes Highly Enantioselective Bromolactonizations to Generate Stereogenic C-Br Bonds. *J. Am. Chem. Soc.* **2012**, *134*, 11128–11131.

(16) Tungen, J. E.; Nolsøe, J. M. J.; Hansen, T. V. Asymmetric Iodolactonization Utilizing Chiral Squaramides. *Org. Lett.* **2012**, *14*, 5884–5887.

(17) Oderinde, M. S.; Hunter, H. N.; Bremner, S. W.; Organ, M. G. Iodolactonization: Synthesis, Stereocontrol, and Compatibility Studies. *Eur. J. Org. Chem.* **2012**, No. 1, 175–182.

(18) Jaganathan, A.; Staples, R. J.; Borhan, B. Kinetic Resolution of Unsaturated Amides in a Chlorocyclization Reaction: Concomitant Enantiomer Differentiation and Face Selective Alkene Chlorination by a Single Catalyst. *J. Am. Chem. Soc.* **2013**, *135*, 14806–14813.

(19) Armstrong, A.; Braddock, C. D.; Jones, A. X.; Clark, S.; Braddock, D. C.; Jones, A. X.; Clark, S. Catalytic Asymmetric Bromolactonization Reactions Using $(DHQD)_2$PHAL-Benzoic Acid Combinations. *Tetrahedron Lett.* **2013**, *54*, 7004–7008.

(20) Arai, T.; Kajikawa, S.; Matsumura, E. The Role of Ni-Carboxylate during Catalytic Asymmetric Iodolactonization Using PyBidine-$Ni(OAc)_2$. *Synlett* **2013**, *24*, 2045–2048.

(21) Yousefi, R.; Ashtekar, K. D.; Whitehead, D. C.; Jackson, J. E.; Borhan, B. Dissecting the Stereocontrol Elements of a Catalytic Asymmetric Chlorolactonization: Syn Addition Obviates Bridging Chloronium. *J. Am. Chem. Soc.* **2013**, *135*, 14524–14527.

(22) Filippova, L.; Stenstrøm, Y.; Hansen, T. V. An Asymmetric Iodolactonization Reaction Catalyzed by a Zinc Bis-Proline-Phenol Complex. *Tetrahedron Lett.* **2014**, *55*, 419–422.

(23) Han, X.; Dong, C.; Zhou, H. B. C3-Symmetric Cinchonine-Squaramide-Catalyzed Asymmetric Chlorolactonization of Styrene-Type Carboxylic Acids with 1,3-Dichloro-5,5- Dimethylhydantoin: An Efficient Method to Chiral Isochroman-1-Ones. *Adv. Synth. Catal.* **2014**, *356*, 1275–1280.

(24) Nakatsuji, H.; Sawamura, Y.; Sakakura, A.; Ishihara, K. Cooperative Activation with Chiral Nucleophilic Catalysts and N-Haloimides: Enantioselective Iodolactonization of 4-Arylmethyl-4-Pentenoic Acids. *Angew. Chem. Int. Ed.* **2014**, *53*, 6974–6977.

(25) Parmar, D.; Maji, M. S.; Rueping, M. Catalytic and Asymmetric

Fluorolactonisations of Carboxylic Acids through Anion Phase Transfer. *Chem. Eur. J.* **2014**, *20*, 83–86.

(26) Egami, H.; Asada, J.; Sato, K.; Hashizume, D.; Kawato, Y.; Hamashima, Y. Asymmetric Fluorolactonization with a Bifunctional Hydroxyl Carboxylate Catalyst. *J. Am. Chem. Soc.* **2015**, *137*, 10132–10135.

(27) Woerly, E. M.; Banik, S. M.; Jacobsen, E. N. Enantioselective, Catalytic Fluorolactonization Reactions with a Nucleophilic Fluoride Source. *J. Am. Chem. Soc.* **2016**, *138*, 13858–13861.

(28) Kristianslund, R.; Aursnes, M.; Tungen, J. E.; Hansen, T. V. Squaramide Catalyzed Enantioselective Iodolactonization of Allenoic Acids. *Tetrahedron Lett.* **2016**, *57*, 5232–5236.

(29) Denmark, S. E.; Ryabchuk, P.; Burk, M. T.; Gilbert, B. B. Toward Catalytic, Enantioselective Chlorolactonization of 1,2-Disubstituted Styrenyl Carboxylic Acids. *J. Org. Chem.* **2016**, *81*, 10411–10423.

(30) Gelat, F.; Coffinet, M.; Lebrun, S.; Agbossou-niedercorn, F.; Michon, C.; Deniau, E. Tetrahedron : Asymmetry Regioselective Organocatalyzed Asymmetric Bromolactonization of Aryl Acrylate-Type Carboxylic Acids : A New Approach towards Enantioenriched 3-Substituted Isobenzofuranones. *Tetrahedron: Asymmetry* **2016**, *27*, 980–989.

(31) Aursnes, M.; Tungen, J. E.; Hansen, T. V. Enantioselective Organocatalyzed Bromolactonizations: Applications in Natural Product Synthesis. *J. Org. Chem.* **2016**, *81*, 8287–8295.

(32) Gelat, F.; Lebrun, S.; Henry, N.; Agbossou-Niedercorn, F.; Michon, C.; Deniau, E. Total Synthesis of (–)-Herbaric Acid through Organocatalyzed Asymmetric Halolactonization of Acrylate-Type Benzoic Acids. *Synlett* **2017**, *28*, 225–230.

(33) Salehi Marzijarani, N.; Yousefi, R.; Jaganathan, A.; Dilip Ashtekar, K.; Jackson, J. E.; Borhan, B. Absolute and Relative Facial Selectivities in Organocatalytic Asymmetric Chlorocyclization Reactions. *Chem. Sci.* **2018**, Advance Article, DOI: 10.1039/c7sc04430e.

(34) Kang, S. H.; Lee, S. B.; Park, C. M. Catalytic Enantioselective Iodocyclization of γ-Hydroxy-Cis-Alkenes. *J. Am. Chem. Soc.* **2003**, *125*, 15748–15749.

(35) Hennecke, U.; Müller, C. H.; Fröhlich, R. Enantioselective Haloetherification by Asymmetric Opening of Meso -Halonium Ions. *Org. Lett.* **2011**, *13*, 860–863.

(36) Huang, D.; Wang, H.; Xue, F.; Guan, H.; Li, L.; Peng, X.; Shi, Y. Enantioselective Bromocyclization of Olefins Catalyzed by Chiral Phosphoric Acid. *Org. Lett.* **2011**, *13*, 6350–6353.

(37) Zhao, Y.; Jiang, X.; Yeung, Y.-Y. Catalytic, Enantioselective, and Highly Chemoselective Bromocyclization of Olefinic Dicarbonyl Compounds. *Angew.*

Chem. Int. Ed. **2013**, *52*, 8597–8601.

(38) Ke, Z.; Tan, C. K.; Chen, F.; Yeung, Y. Y. Catalytic Asymmetric Bromoetherification and Desymmetrization of Olefinic 1,3-Diols with C2-Symmetric Sulfides. *J. Am. Chem. Soc.* **2014**, *136*, 5627–5630.

(39) Denmark, S. E.; Burk, M. T. Development and Mechanism of an Enantioselective Bromocycloetherification Reaction via Lewis Base/ Chiral Brønsted Acid Cooperative Catalysis. *Chirality* **2014**, *26*, 344–355.

(40) Soltanzadeh, B.; Jaganathan, A.; Staples, R. J.; Borhan, B. Highly Stereoselective Intermolecular Haloetherification and Haloesterification of Allyl Amides. *Angew. Chem. Int. Ed.* **2015**, *54*, 9517–9522.

(41) Zhou, P.; Cai, Y.; Zhong, X.; Luo, W.; Kang, T.; Li, J.; Liu, X.; Lin, L.; Feng, X. Catalytic Asymmetric Intra- and Intermolecular Haloetherification of Enones: An Efficient Approach to (−)-Centrolobine. *ACS Catal.* **2016**, *6*, 7778–7783.

(42) Ke, Z.; Tan, C. K.; Liu, Y.; Lee, K. G. Z.; Yeung, Y. Y. Catalytic and Enantioselective Bromoetherification of Olefinic 1,3-Diols: Mechanistic Insight. *Tetrahedron* **2016**, *72*, 2683–2689.

(43) Böse, D.; Denmark, S. E. Investigating the Enantiodetermining Step of a Chiral Lewis Base Catalyzed Bromocycloetherification of Privileged Alkenes. *Synlett* **2018**, *29*, 433–439.

(44) Zhou, L.; Chen, J.; Tan, C. K.; Yeung, Y. Y. Enantioselective Bromoaminocyclization Using Amino-Thiocarbamate Catalysts. *J. Am. Chem. Soc.* **2011**, *133*, 9164–9167.

(45) Egart, B.; Lentz, D.; Czekelius, C. Diastereoselective Bromocyclization of O-Allyl-N-Tosyl-Hydroxylamines. *J. Org. Chem.* **2013**, *78*, 2490–2499.

(46) Chen, F.; Tan, C. K.; Yeung, Y. Y. C2-Symmetric Cyclic Selenium-Catalyzed Enantioselective Bromoaminocyclization. *J. Am. Chem. Soc.* **2013**, *135*, 1232–1235.

(47) Zhou, L.; Tay, D. W.; Chen, J.; Leung, G. Y. C.; Yeung, Y.-Y. Enantioselective Synthesis of 2-Substituted and 3-Substituted Piperidines through a Bromoaminocyclization Process. *Chem. Commun.* **2013**, *6*, 4412–4414.

(48) Mizar, P.; Burrelli, A.; Günther, E.; Söftje, M.; Farooq, U.; Wirth, T. Organocatalytic Stereoselective Iodoamination of Alkenes. *Chem. Eur. J.* **2014**, *20*, 13113–13116.

(49) Tripathi, C. B.; Mukherjee, S. Catalytic Enantioselective Halocyclizations beyond Lactones: Emerging Routes to Enantioenriched Nitrogenous Heterocycles. *Synlett* **2014**, *25*, 163–169.

(50) Cai, Y.; Zhou, P.; Liu, X.; Zhao, J.; Lin, L.; Feng, X. Diastereoselectively

Switchable Asymmetric Haloaminocyclization for the Synthesis of Cyclic Sulfamates. *Chem. Eur. J.* **2015**, *21*, 6386–6389.

(51) Liu, W.; Pan, H.; Tian, H.; Shi, Y. Enantioselective 6-Exo-Bromoaminocyclization of Homoallylic N-Tosylcarbamates Catalyzed by a Novel Monophosphine-Sc(OTf) $_3$ Complex. *Org. Lett.* **2015**, *17*, 3956–3959.

(52) Jiang, H. J.; Liu, K.; Yu, J.; Zhang, L.; Gong, L. Z. Switchable Stereoselectivity in Bromoaminocyclization of Olefins: Using Brønsted Acids of Anionic Chiral Cobalt(III) Complexes. *Angew. Chem. Int. Ed.* **2017**, *56*, 11931–11935.

(53) Sawamura, Y.; Nakatsuji, H.; Sakakura, A.; Ishihara, K. "Phosphite–urea" Cooperative High-Turnover Catalysts for the Highly Selective Bromocyclization of Homogeranylarenes. *Chem. Sci.* **2013**, *4*, 4181.

(54) Sakakura, A.; Ukai, A.; Ishihara, K. Enantioselective Halocyclization of Polyprenoids Induced by Nucleophilic Phosphoramidites. *Nature* **2007**, *445*, 900–903.

(55) Samanta, R. C.; Yamamoto, H. Catalytic Asymmetric Bromocyclization of Polyenes. *J. Am. Chem. Soc.* **2017**, *139*, 1460–1463.

(56) Denmark, S. E.; Kuester, W. E.; Burk, M. T. Catalytic, Asymmetric Halofunctionalization of Alkenes-a Critical Perspective. *Angew. Chem. Int. Ed.* **2012**, *51*, 10938–10953.

(57) Neverov, A. A.; Brown, R. S. Br+ and I+ Transfer from the Halonium Ions of Adamantylideneadamantane to Acceptor Olefins. Halocyclization of 1,ω-Alkenols and Alkenoic Acids Proceeds via Reversibly Formed Intermediates. *J. Org. Chem.* **1996**, *61*, 962–968.

(58) Brown, R. S.; Nagorski, R. W.; McClung, R. E. D. D.; Aarts, G. H. M. M.; Klobukowski, M.; Bennet, A. J.; McDonald, R.; Santarsiero, B. D.; McClung, R. E. D. D.; Aarts, G. H. M. M.; et al. Stable Bromonium and Iodonium Ions of the Hindered Olefins Adamantylideneadamantane and Bicyclo[3.3.1]nonylidenebicyclo[3.3.1]nonane. X-Ray Structure, Transfer of Positive Halogens to Acceptor Olefins, and Ab Initio Studies. *J. Am. Chem. Soc.* **1994**, *116*, 2448–2456.

(59) Olah, G. A.; Bollinger, J. M. Stable Carbonium Ions. LVII.1a Halonium Ion Formation via Neighboring Halogen Participation. Trimethyl- and 1,1 -Dimethylethylenehalonium Ions. *J. Am. Chem. Soc.* **1968**, *90*, 947–953.

(60) Olah, G. A.; Bollinger, J. M. Stable Carbonium Ions. XLVIII. Halonium Ion Formation via Neighboring Halogen Participation. Tetramethylethylene Halonium Ions. *J. Am. Chem. Soc.* **1967**, *89*, 4744–4752.

(61) Olah, G. A.; Martin Bollinger, J.; Brinich, J. Stable Carbonium Ions. LXII. Halonium Ion Formation via Neighboring Halogen Participation:

Ethylenehalonium, Propylenehalonium, and 1,2-Dimethylethylenehalonium Ions. *J. Am. Chem. Soc.* **1968**, *90*, 2587–2594.

(62) Chen, G.; Ma, S. Enantioselective Halocyclization Reactions for the Synthesis of Chiral Cyclic Compounds. *Angew. Chem. Int. Ed.* **2010**, *49*, 8306–8308.

(63) Snyder, S. A.; Treitler, D. S.; Brucks, A. P. *Halonium-Induced Cyclization Reactions*; 2011; Vol. 44.

(64) Tan, C. K.; Zhou, L.; Yeung, Y. Y. Organocatalytic Enantioselective Halolactonizations: Strategies of Halogen Activation. *Synlett* **2011**, No. 10, 1335–1339.

(65) Tan, C. K.; Yeung, Y. Recent Advances in Stereoselective Bromofunctionalization of Alkenes Using N-Bromoamide Reagents. *Chem. Commun.* **2013**, *49*, 7985.

(66) Murai, K.; Fujioka, H. Recent Progress in Organocatalytic Asymmetric Halocyclization. *Heterocycles* **2013**, *87*, 763–805.

(67) Nolsøe, J. M. J.; Hansen, T. V. Asymmetric Iodolactonization: An Evolutionary Account. *Eur. J. Org. Chem.* **2014**, *2014*, 3051–3065.

(68) Wang, M.; Gao, L. X.; Mai, W. P.; Xia, A. X.; Wang, F.; Zhang, S. B. Catalyzed by Chiral Quaternary Ammonium Salts Derived from Cinchonidine Halolactonizations Are Useful Chemical Transformations for the Construction of Lactones from Olefinic Carboxylic Acids , Carboxylic Esters , and Amides . 1 In Extensive Studies on the. *J. Org. Chem.* **2004**, *69*, 2874–2876.

(69) Ashtekar, K. D.; Vetticatt, M.; Yousefi, R.; Jackson, J. E.; Borhan, B. Nucleophile-Assisted Alkene Activation: Olefins Alone Are Often Incompetent. *J. Am. Chem. Soc.* **2016**, *138*, 8114–8119.

(70) Brown, R. S. Investigation of the Early Steps in Electrophilic Bromination through the Study of the Reaction with Sterically Encumbered Olefins. *Acc. Chem. Res.* **1997**, *30*, 131–137.

(71) Lee, D. G.; Srinivasan, R. The Oxidation of Benzyldimethylamine by Bromine. *Can. J. Chem.* **1973**, *51*, 2546–2554.

(72) Volla, C. M. R.; Atodiresei, I.; Rueping, M. Catalytic C-C Bond-Forming Multi-Component Cascade or Domino Reactions: Pushing the Boundaries of Complexity in Asymmetric Organocatalysis. *Chemical Reviews*. 2014, pp 2390–2431.

(73) Ahmad, S. M.; Braddock, D. C.; Cansell, G.; Hermitage, S. A.; Redmond, J. M.; White, A. J. P. Amidines as Potent Nucleophilic Organocatalysts for the Transfer of Electrophilic Bromine from N-Bromosuccinimide to Alkenes. *Tetrahedron Lett.* **2007**, *48*, 5948–5952.

(74) Ikeuchi, K.; Ido, S.; Yoshimura, S.; Asakawa, T.; Inai, M.; Hamashima, Y.; Kan, T. Catalytic Desymmetrization of Cyclohexadienes by Asymmetric

Bromolactonization. *Org. Lett.* **2012**, *14*, 6016–6019.

(75) Armstrong, A.; Braddock, C. D.; Jones, A. X.; Clark, S.; Braddock, D. C.; Jones, A. X.; Clark, S. Catalytic Asymmetric Bromolactonization Reactions Using $(DHQD)_2PHAL$-Benzoic Acid Combinations. *Tetrahedron Lett.* **2013**, *54*.

(76) Hennecke, U.; Wilking, M. Desymmetrization as a Strategy in Asymmetric Halocyclization Reactions. *Synlett* **2014**, *25*, 1633–1637.

(77) Kaoru, F.; Manabu, N.; Yoshimitsu, N.; Takeo, K. Enantioselective Iodolactonization through Diastereotopic Group Differentiation. *Tetrahedron Lett.* **1990**, *31*, 3175–3178.

(78) Inoue, T.; Kitagawa, O.; Kurumizawa, S.; Ochiai, O.; Taguchi, T. Enantioselective Iodocarbocyclization of 4-Alkenylmalonate Derivatives Using a Chiral Titanium Complex. *Tetrahedron Lett.* **1995**, *64*, 40–4039.

(79) Kitagawa, O.; Taguchi, T. Iodocarbocyclization and Iodoaminocyclization Reactions Mediated by a Metallic Reagent. *Synlett* **1999**, *1999*, 1191–1199.

(80) Knowe, M. T.; Danneman, M. W.; Sun, S.; Pink, M.; Johnston, J. N. Biomimetic Desymmetrization of a Carboxylic Acid. *J. Am. Chem. Soc.* **2018**, *140*, 1998–2001.

(81) Xia, Q.-H.; Ge, H.-Q.; Ye, C.-P.; Liu, Z.-M.; Su, K.-X. Advances in Homogeneous and Heterogeneous Catalytic Asymmetric Epoxidation. *Chem. Rev.* **2005**, *105*, 1603–1662.

(82) Davis, R. L.; Stiller, J.; Naicker, T.; Jiang, H.; Jørgensen, K. A. Asymmetric Organocatalytic Epoxidations: Reactions, Scope, Mechanisms, and Applications. *Angew. Chem. Int. Ed.* **2014**, *53*, 7406–7426.

(83) Matsumoto, K. and Katsuki, T. (2010). Asymmetric Oxidations and Related Reactions. In Catalytic Asymmetric Synthesis, I. Ojima (Ed.)..

(84) Zhu, Y.; Wang, Q.; Cornwall, R. G.; Shi, Y. Organocatalytic Asymmetric Epoxidation and Aziridination of Olefins and Their Synthetic Applications. *Chem. Rev.* **2014**, *114*, 8199–8256.

(85) Jacobsen, E. N.; Zhang, W.; Muci, A. R.; Ecker, J. R.; Deng, L. Highly Enantioselective Epoxidation Catalysts Derived from 1,2-Diaminocyclohexane. *J. Am. Chem. Soc.* **1991**, *113*, 7063–7064.

(86) Jacobsen, E. N.; Zhang, W.; Güler, M. L. Electronic Tuning of Asymmetric Catalysts. *J. Am. Chem. Soc.* **1991**, *113*, 6703–6704.

(87) Katsuki, T. Mn-Salen Catalyst, Competitor of Enzymes, for Asymmetric Epoxidation. *J. Mol. Catal. A Chem.* **1996**, *113*, 87–107.

(88) Sawada, Y.; Matsumoto, K.; Katsuki, T. Titanium-Catalyzed Asymmetric Epoxidation of Non-Activated Olefins with Hydrogen Peroxide. *Angew. Chem.*

Int. Ed. **2007**, *46*, 4559–4561.

(89) Ratnayake, R.; Lacey, E.; Tennant, S.; Gill, J. H.; Capon, R. J. Kibdelones: Novel Anticancer Polyketides from a Rare Australian Actinomycete. *Chem. Eur. J.* **2007**, *13*, 1610–1619.

(90) Winter, D. K.; Sloman, D. L.; Porco Jr., J. A.; Online, V. A. Polycyclic Xanthone Natural Products: Structure, Biological Activity and Chemical Synthesis. *Nat. Prod. Rep.* **2013**, *30*, 382.

(91) Winter, D. K.; Endoma-Arias, M. A.; Hudlicky, T.; Beutler, J. A.; Porco, J. A. Enantioselective Total Synthesis and Biological Evaluation of (+)-Kibdelone A and a Tetrahydroxanthone Analogue. *J. Org. Chem.* **2013**, *78*, 7617–7626.

(92) Rujirawanich, J.; Kim, S.; Ma, A. J.; Butler, J. R.; Wang, Y.; Wang, C.; Rosen, M.; Posner, B.; Nijhawanc, D.; Ready, J. M. Synthesis and Biological Evaluation of Kibdelone C and Its Simplified Derivatives. *J. Am. Chem. Soc.* **2016**, *138*, 10561–10570.

(93) Sloman, D. L.; Bacon, J. W.; Porco, J. A. Total Synthesis and Absolute Stereochemical Assignment of Kibdelone C. *J. Am. Chem. Soc.* **2011**, *133*, 9952–9955.

(94) Butler, J. R.; Wang, C.; Bian, J.; Ready, J. M. Enantioselective Total Synthesis of (–)-Kibdelone C. *J. Am. Chem. Soc.* **2011**, *133*, 9956–9959.

(95) Klosowski, D. W.; Martin, S. F. Enantioselective Synthesis of F-Ring Fragments of Kibdelone C via Desymmetrizing Bromolactonization of 1,4-Dihydrobenzoic Acid. *Synlett* **2018**, *29*, 430–432.

(96) Ciesielski, J.; Canterbury, D. P.; Frontier, A. J. β-Iodoallenolates as Springboards for Annulation Reactions. *Org. Lett.* **2009**, *11*, 4374–4377.

(97) Froese, J.; Endoma-Arias, M. A. a; Hudlicky, T. Processing of O -Halobenzoates by Toluene Dioxygenase. the Role of the Alkoxy Functionality in the Regioselectivity of the Enzymatic Dihydroxylation Reaction. *Org. Process Res. Dev.* **2014**, *18*, 801–809.

(98) Yang, J.; Knueppel, D.; Cheng, B.; Mans, D.; Martin, S. F. Approaches to Polycyclic 1,4-Dioxygenated Xanthones. Application to Total Synthesis of the Aglycone of IB-00208. *Org. Lett.* **2015**, *17*, 114–117.

(99) Knueppel, D.; Yang, J.; Cheng, B.; Mans, D.; Martin, S. F. Total Synthesis of the Aglycone of IB-00208. *Tetrahedron* **2015**, *71*, 5741–5757.

(100) Blumberg, S.; Martin, S. F. Synthesis of the Pentacyclic Core of Citreamicin η. *Org. Lett.* **2017**, *19*, 790–793.

(101) Nicolaou, K. C.; Li, A. Total Syntheses and Structural Revision of α- and β-Diversonolic Esters and Total Syntheses of Diversonol and Blennolide C. *Angew.*

Chem. Int. Ed. **2008**, *47*, 6579–6582.

(102) Rich, R. H.; Lawrence, B. M.; Bartlett, P. A. Synthesis of (–)-2-Chloroshikimic Acid. *J. Org. Chem.* **1994**, *59*, 693–694.

(103) Rich, R. H.; Lawrence, B. M.; Bartlett, P. A. Synthesis of (-)-2-Chloroshikimic Acid. *J. Org. Chemisry* **1994**, *59*, 693–694.

(104) Johnson, R. G.; Ingham, R. K. The Degradation Of Carboxylic Acid Salts By Means Of Halogen - The Hunsdiecker Reaction. *Chem. Rev.* **1956**, *56*, 219–269.

(105) McKillop, A.; Bromley, D.; Taylor, E. C. Thallium in Organic Synthesis. VI. Synthesis of Primary Aliphatic Bromides. *J. Org. Chem.* **1969**, *34*, 1172–1173.

(106) Cristol, S.; Firth, Jr., W. Communications. A Convenient Synthesis of Alkyl Halides from Carboxylic Acids. *J. Org. Chem.* **1961**, *26*, 280–280.

(107) Barton, D. H. R.; Crich, D.; Motherwell, W. B. The Invention of New Radical Chain Reactions. Part VIII. Radical Chemistry of Thiohydroxamic Esters; A New Method For The Generation of Carbon Radicals From Carboxylic Acids. *Tetrahedron* **1985**, *41*, 3901–3924.

(108) Conly, J. C. Applications of the Hunsdiecker Silver Salt Degradation. The Preparation of Dibromides and Tribromides 1. *J. Am. Chem. Soc.* **1953**, *75*, 1148–1150.

(109) Wang, Z.; Zhu, L.; Yin, F.; Su, Z.; Li, Z.; Li, C. Silver-Catalyzed Decarboxylative Chlorination of Aliphatic Carboxylic Acids. *J. Am. Chem. Soc.* **2012**, *134*, 4258–4263.

(110) Kochi, J. K. A New Method for Halodecarboxylation of Acids Using Lead(IV) Acetate. *J. Am. Chem. Soc.* **1965**, *87*, 2500–2502.

(111) Concepcion, J. I.; Francisco, C. G.; Freire, R.; Hernandez, R.; Salazar, J. A.; Suarez, E. Iodosobenzene Diacetate, an Efficient Reagent for the Oxidative Decarboxylation of Carboxylic Acids. *J. Org. Chem.* **1986**, *51*, 402–404.

(112) Carbain, B.; Hitchcock, P. B.; Streicher, H. New Aspects of the Hunsdiecker-Barton Halodecarboxylation-Syntheses of Phospha-Shikimic Acid and Derivatives. *Tetrahedron Lett.* **2010**, *51*, 2717–2719.

(113) Kuehne, M. E.; Lambert, B. F. 1,4-Dihydrobenzoic Acid. *Org. Synth.* **1963**, *43*, 22.

(114) Kolb, H. C.; VanNieuwenhze, M. S.; Sharpless, K. B. Catalytic Asymmetric Dihydroxylation. *Chem. Rev.* **1994**, *94*, 2483–2547.

(115) Dupau, P.; Epple, R.; Thomas, A. A.; Fokin, V. V.; Sharpless, K. B. Osmium-Catalyzed Dihydroxylation of Olefins in Acidic Media: Old Process, New Tricks. *Adv. Synth. Catal.* **2002**, *344*, 421–433.

(116) Liebhold, A.; Mastro, V.; Schaefer, P. W. Learning from the Legacy of Leopold Trouvelot. *Bull. Entomol. Soc. Am.* **1989**, *35*, 20–22.

(117) Journal, S.; Sep, N.; Liebhold, A. M.; Halverson, J. A.; Northeasternforest, G. A. E. Gypsy Moth Invasion in North America : A Quantitative Analysis. *J. Biogeogr.* **1992**, *19*, 513–520.

(118) Tobin, P. C.; Sharov, A. A.; Liebhold, A. A.; Leonard, D. S.; Roberts, A. E.; Learn, M. R. Management of the Gypsy Moth through a Decision Algorithm under the STS Project. *Am. Entomol.* **2004**, *50*, 200–209.

(119) Liebhold, A. M.; Tobin, P. C. Population Ecology of Insect Invasions and Their Management. *Annu. Rev. Entomol.* **2008**, *53*, 387–408.

(120) Iwaki, S.; Marumo, S.; Saito, T.; Yamada, M.; Kazumasa, K. Synthesis and Activity of Optically Active Disparlure. *J. Am. Chem. Soc.* **1974**, *96*, 7842–7844.

(121) Graham, S.; Prestwich, G. Synthesis and Inhibitory Properties of Pheromone Analogs for the Epoxide Hydrolase of the Gypsy Moth. *J. Org. Chem.* **1994**, *59*, 2956–2966.

(122) Chan, T. H.; Chang, E. Synthesis of Alkenes from Carbonyl Compounds and Carbanic Alpha to Silicon. III. Full Report and Synthesis of the Sex Pheromone of Gypsy Moth. *J. Org. Chem.* **1974**, *39*, 3264–3268.

(123) Mori, K.; Takigawa, T.; Matsui, M. Stereoselective Synthesis of Optically Active Disparlure, the Pheremone of the Gypsy Moth. *Tetrahedron Lett.* **1976**, *44*, 3953–3956.

(124) Farnum, D. G.; Veysoglu, T.; Cardé, A. M.; Duhl-Emswiler, B.; Pancoast, T. A.; Reitz, T. J.; T. Cardé, R. A Stereospecific Synthesis of (+)-Disparlure, Sex Attractant of the Gypsy Moth. *Tetrahedron Lett.* **1977**, *18*, 4009–4012.

(125) Tolstikov, G. A.; Odinokov, V. N.; Galeeva, R. I.; Bakeeva, R. S. A New Selective Synthesis of Racemic Disparlure, the Sex Pheromone of Gypsy Moth (Porthetria Dispar L.). *Tetrahedron Lett.* **1978**, No. 21, 1857–1858.

(126) Pirkle, W. H.; Rinaldi, P. L. Synthesis and Enantiomeric Purity Determination of the Optically Active Epoxide Disparlure, Sex Pheromone of the Gypsy Moth. *J. Org. Chem.* **1979**, *44*, 1025–1028.

(127) Mori, K.; Takigawa, T.; Matsui, M. Pheromone Synthesis. XXV. Stereoselective Synthesis of Both Enantiomers of Disparlure, the Pheromone of the Gypsy Moth. *Tetrahedron* **1979**, *35*, 833–837.

(128) Rossiter, B. E.; Katsuki, T.; Sharpless, K. B. Asymmetric Epoxidation Provides Shortest Routes to Four Chiral Epoxy Alcohols Which Are Key Intermediates in Syntheses of Methymycin, Erythromycin, Leukotriene C-1, and Disparlure. *J. Am. Chem. Soc.* **1981**, *103*, 464–465.

(129) Mori, K.; Ebata, T. Synthesis of Optically Active Pheromones with an Epoxy Ring, (+)-Disparlure and the Saltmarsh Caterpillar Moth Pheromone [(Z,Z)-3,6-Cis-9,10-Epoxyheneicosadiene]. *Tetrahedron Lett.* **1981**, *22*, 4281–4282.

(130) Markgraf, H. J.; Lusskin, S. I.; McDonald, E. C.; Volpp, B. D. Synthesis of (±)-disparlure. *J. Chem. Ecoo* **1983**, *9*, 211–218.

(131) Brown, H. C.; Basavaiah, D. Pheromone Synthesis via Organoboranes: A Convenient Stereospecific Synthesis of Racemic Disparlure, the Sex Pheromone of the Gypsy Moth (Porthetria Dispar L). *Synthesis (Stuttg).* **1983**, *4*, 283–284.

(132) Koumaglo, K.; Chan, T. H. Regioselection in the Alkylation of Trimethylsilylallyl Anion - Stereoselective Synthesis of Disubstituted Alkenes. *Tetrahedron Lett.* **1984**, *25*, 717–720.

(133) Guoqiang, L.; Biqi, W.; Lingyu, L.; Xianqing, W.; Weishan, Z. Studies on the Identification and Synthesis of Insect Pheromone XVI. Synthesis of the Optical Active Sex Pheromone of Gypsy Moth and Its Three Optical Isomers. *Acta Chim. Sin.* **1984**, *42*, 797–804.

(134) Mori, K.; Ebata, T. Pheromone Synthesis. 86. Synthesis of Optically Active Pheromones with an Epoxy Ring, Dispalure. *Tetrahedron* **1986**, *42*, 3471–3478.

(135) Masaki, Y.; Serizawa, Y.; Nagata, K.; Oda, H.; Nagashima, H.; Kaji, K. Synthesis of Chiral 1,2-Diols and Related Compounds of Biological Activities via Stepwise Ring Fission of 5-Alkyl-6,8-dioxabicyclo[3.2.1]octane Skeleton. *Tetrahedron Lett.* **1986**, *27*, 231–234.

(136) Jigajinni, V. B.; Wightman, R. H. An Enantiospecific Synthesis of (+)-Disparlure from Carbohydrate Precursors. *Carbohydrate Research*. 1986, pp 145–148.

(137) Sato, T.; Itoh, T.; Fujisawa, T. Diastereoselective α-Alkylation of β-Hydroxy Sulfoxides and Its Application to the Synthesis of (+)- and (3)-Disparlure. *Tetrahedron Lett.* **1987**, *28*, 5677–5680.

(138) Wei-Shan, Z.; Zhi-Min, W.; Guo-Qiang, L. Synthesis of (7R, 8S)-(+)-and (7S, 8R)- (-) -Sex Pheromone of Gypsy Moth and Stereochemistry of β-H Ydroxysilane. *Acta Chim. Sin.* **1987**, *45*, 40–46.

(139) Pikul, S.; Kozlowska, M.; Jurczak, J. Total Synthesis of (+)-Disparlure. *Tetrahedron Lett.* **1987**, *28*, 2627–2628.

(140) Kametani, T.; Tsubuki, M.; Honda, T. A Formal Synthesis of (+)-Disparlure from an Optically Active 2-Furylcarbinol. *Chem. Pharm. Bull.* **1988**, *36*, 3706–3709.

(141) Satoh, T.; Oohara, T.; Ueda, Y.; Yamakawa, K. The Practical Procedure for a Preparation of 1-Chloroalkyl P-Tolyl Sulfoxides in High Optically Active Form: A Very Short Synthesis of Optically Active Disparlure. *Tetrahedron Lett.* **1988**, *29*, 313–316.

(142) Marczak, S.; Masnyk, M.; Wicha, J. Synthesis of (+)-Disparlure Using the Reaction of 6-Methylheptyl Phenyl Sulphone with Trimethylsilyl Ethylene Oxide and Asymmetric Epoxidation. *Tetrahedron Letters*. 1989, pp 2845–2846.

(143) Odinokov, V. N.; Akhmetova, V. R.; Khasanov, K. D.; Abduvakhabov, A. A.; Kuchin, A. V.; Andreeva, N. I.; Tolstikov, G. A. Synthesis of (7R,SS)-(+)-Cis-2-Methyl-7,8-Epoxyoctadecane - the Sex Pheromone of Porthetria Dispar. *Chem. Nat. Compd.* **1989**, *25*, 610–613.

(144) Satoh, T.; Oohara, T.; Ueda, Y.; Yamakawa, K. A Novel Approach to the Asymmetric Synthesis of Epoxides, Allylic Alcohols, .alpha.-Amino Ketones, and .alpha.-Amino Aldehydes from Carbonyl Compounds through .α,β-Epoxy Sulfoxides Using the Optically Active *p*-Tolylsulfinyl Group To Introduce Chirality *J. Org. Chem.* **1989**, *54*, 3130–3136.

(145) Prestwich, G. D.; Graham, S. M.; Kuo, J.; Vogt, R. G. Tritium Labeled Enantiomers of Disparlure. Synthesis and in Vitro Metabolism. *J. Am. Chem. Soc.* **1989**, *111*, 636–642.

(146) Kang, S.-K.; Kim, Y.-S.; Lim, J.-S.; Kim, K.-S.; Kim, S.-G. Synthesis of Chiral Epoxy Alcohols: Synthesis of (+)-Disparlure. *Tetrahedron Letters*. 1991, pp 363–366.

(147) Keinan, E.; Sinha, S. C.; Sinha-Bagchi, A.; Zhi-Min, W.; Xiu-Lian, Z.; Sharpless, K. B. B. Synthesis of All Four Isomers of Disparlure Using Osmium-Catalyzed Asymmetric Dihydroxylation. *Tetrahedron Lett.* **1992**, *33*, 6411–6414.

(148) Brevet, J.-L.; Mori, K. Pheromone Snythesis. CXXXIX. Enzymatic Preparation of (2S,3R)-4-Acetoxy-2,3-Epoxybutan-1-Ol and Its Conversion to the Epoxy Pheromones of the Gypsy Moth and the Ruby Tiger Moth. *Synthesis*. **1992**, 1007–1012.

(149) Fukusaki, E.; Senda, S.; Nakazono, Y.; Yuasa, H.; Omata, T. Large-Scale Preparation of (+)-Disparlure, the Gypsy Moth Pheromone, by a Practical Chemico-Enzymatic Procedure. *J. Ferment. Bioeng.* **1992**, *73*, 284–286.

(150) Tsuboi, S.; Furutani, H.; Ansari, M. H. H.; Sakai, T.; Utaka, M.; Takeda, A. Highly Enantioselective Reduction of 3-Chloro-2-Oxoalkanoates with Fermenting Bakers' Yeast. A New Synthesis of Optically Active 3-Chloro-2-Hydroxyalkanoates and Glycidic Esters. *J. Org. Chem.* **1993**, *58*, 486–492.

(151) Ko, S. Y. Y. Cis-Epoxides via Sharpless' Asymmetric Dihydroxylation Reaction: Synthesis of (+)-Disparlure. *Tetrahedron Lett.* **1994**, *35*, 3601–3604.

(152) Paolucci, C.; Mazzini, C.; Fava, A. Dihydro- and Tetrahydrofuran Building Blocks from 1,4:3,6-Dianhydrohexitols. 2. Synthesis of Acetal, Alcohol, Diol, Epoxide, Hydrocarbon, and Lactone Pheromones. *J. Org. Chem.* **1995**, *60*, 169–175.

(153) Curci, R.; D'Accolti, L.; Fiorentino, Mi.; Rosa, A. Enantioselective Epoxidation of Unfunctionalized Alkenes Using Dioxiranes Generated in Situ. *Tetrahedron Lett.* **1995**, *36*, 5831–5834.

(154) Sinha-Bagchi, a.; Sinha, S. C.; Keinan, E. A Practical Approach to

Enantiomerically Pure Cis-Epoxides. Synthesis of (+)-Disparlure. *Tetrahedron Asymmetry* **1995**, *6*, 2889–2892.

(155) Oliver, J. E.; Waters, R. M.; Harrison, D. J. Semiochemicals via Epoxide Inversion. *J. Chem. Ecol.* **1996**, *22*, 287–294.

(156) Li, L. H. H.; Wang, D.; Chan, T. H. H. Asymmetric Epoxidation of Nearly Symmetrical Cis-Alkenes. Sharpless Epoxidation of (1,2-Dialkyl)vinylsilanols. *Tetrahedron Lett.* **1997**, *38*, 101–104.

(157) Tsuboi, S.; Yamafuji, N.; Utaka, M. Lipase-Catalyzed Kinetic Resolution of 3-Chloro-2-Hydroxyalkanoates. Its Application for the Synthesis of (-)-Disparlure. *Tetrahedron Asymmetry* **1997**, *8*, 375–379.

(158) Bykov, V. I. I.; Butenko, T. a a; Petrova, E. B. B.; Finkelshtein, E. S. S. Synthesis of Z-Isomeric Insect Sex Pheromone Components via Ethenolysis of 1,5-Cyclooctadiene. *Tetrahedron* **1999**, *55*, 8249–8252.

(159) Kametani, T.; Tsubuki, M.; Tatsuzaki, Y.; Honda, T. Synthesis of Optically Active 2-Furylmethanols as Useful Chiral Building Blocks and Its Application to the Synthesis of (5R,6S)-6-Acetoxyhexadecan-5-Olide and (+)-Disparlure. *J. Chem. Soc. Perkin Trans. 1* **1990**, 639–646.

(160) Marshall, J. a.; Jablonowski, J. a.; Jiang, H. Total Synthesis of the Gypsy Moth Pheromones (+)- and (-)-Disparlure from a Single Nonracemic Alpha-Silyloxy Allylic Stannane. *J. Org. Chem.* **1999**, *64*, 2152–2154.

(161) Hu, S.; Jayaraman, S.; Oehlschlager, a. C. An Efficient Enantioselective Synthesis of (+)-Disparlure. *J. Org. Chem.* **1999**, *64*, 3719–3721.

(162) Fukusaki, E.; Satoda, S.; Senda, S.; Omata, T. Lipase-Catalyzed Kinetic Resolution of 2, 3-Epoxy-1-Tridecanol and Its Application to Facile Synthesis of (+)-Disparlure. *J. Biosci. Bioeng.* **1999**, *87*, 103–104.

(163) Inkster, J. A. H.; Ling, I.; Honson, N. S.; Jacquet, L.; Gries, R.; Plettner, E. Synthesis of Disparlure Analogues, Using Resolution on Microcrystalline Cellulose Triacetate-I. *Tetrahedron Asymmetry* **2005**, *16*, 3773–3784.

(164) Koumbis, A. E.; Chronopoulos, D. D. A Short and Efficient Synthesis of (+)-Disparlure and Its Enantiomer. *Tetrahedron Lett.* **2005**, *46*, 4353–4355.

(165) Zhang, S.; Sun, H.; Li, B. Asymmetric Total Synthesis of (+)-Disparlure: (+)-(7R,8S)-Cis -7,8-Epoxy-2-Methyloctodecane. *Acta Chim. Sin.* **2007**, No. 21, 2433–2436.

(166) Prasad, K. R. R.; Anbarasan, P. Enantiodivergent Synthesis of Both Enantiomers of Gypsy Moth Pheromone Disparlure. *J. Org. Chem.* **2007**, *72*, 3155–3157.

(167) Kovalenko, V. N.; Masalov, N. V.; Kulinkovich, O. G. Synthesis of (+)-Disparlure from Diethyl (−)-Malate via Opening and Fragmentation of the Three-Membered

Ring in Tertiary Cyclopropanols. *Russ. J. Org. Chem.* **2009**, *45*, 1318–1324.

(168) Kim, S. G. G. Concise Total Synthesis of (+)-Disparlure and Its Trans-Isomer Using Asymmetric Organocatalysis. *Synthesis.* **2009**, No. 14, 2418–2422.

(169) Chen, H.; Gong, Y.; Gries, R. M.; Plettner, E. Synthesis and Biological Activity of Conformationally Restricted Gypsy Moth Pheromone Mimics. *Bioorganic Med. Chem.* **2010**, *18*, 2920–2929.

(170) Dubey, A. K.; Chattopadhyay, A. An Enantiodivergent Synthesis of Both (+)- and (-)-Disparlure from (R)-2,3-Cyclohexylideneglyceraldehyde. *Tetrahedron Asymmetry* **2011**, *22*, 1516–1521.

(171) Wang, Z.; Zheng, J.; Huang, P. Asymmetric Synthesis of Both Enantiomers of Disparlure. *Chinese J. Chem.* **2012**, *30*, 23–28.

(172) Herbert, M. B.; Marx, V. M.; Pederson, R. L.; Grubbs, R. H. Concise Syntheses of Insect Pheromones Using Z-Selective Cross Metathesis. *Angew. Chem. Int. Ed.* **2013**, *52*, 310–314.

(173) Bethi, V.; Kattanguru, P.; Fernandes, R. A. Domino Recombinant γ-Isomerization and Reverse Wacker Oxidation of γ-Vinyl-γ-Butyrolactone: Synthesis of (+)-Trans-, (–)- and (+)-Disparlures. *Eur. J. Org. Chem.* **2014**, *2014*, 3249–3255.

(174) Prestwich, G.; Graham, S.; Konig, W. Enatioselective Opening of (+)- Disparlure and (–)-Disparlure by Epoxide Hydrase in Gypsy-Moth Antennae. *J. Chem. Soc.* **1989**, *9*, 575–577.

(175) Avedissian, H.; Sinha, S. C.; Yazbak, A.; Sinha, A.; Neogi, P.; Sinha, S. C.; Keinan, E. Total Synthesis of Asimicin and Bullatacin. *J. Org. Chem.* **2000**, *65*, 6035–6051.

(176) Sajiki, H.; Hattori, K.; Hirota, K. Highly Chemoselective Hydrogenation with Retention of the Epoxide Function Using a Heterogeneous Pd/C-Ethylenediamine Catalyst and THF. *Chem. Eur. J.* **2000**, *6*, 2200–2204.

(177) Fujisawa, T.; Sato, T.; Kawara, T.; Naruse, K. One-Pot Synthesis of (*Z*)-Alkenoic Acids. *Chem. Lett.* **1980**, 1123–1124.

(178) Müller, D. S.; Marek, I. Copper Mediated Carbometalation Reactions. *Chem. Soc. Rev.* **2016**, *45*, 4552–4566.

(179) Normant, J. F.; Alexakis, A. Carbometallation (C-Metallation) of Alkynes: Stereospecific Synthesis of Alkenyl Derivatives. *Synthesis* **1981**, *11*, 841–870.

(180) *Modern Organocopper Chemistry*, Illustrated.; Krause, N., Ed.; John Wiley & Sons, 2002.

(181) Marek, I.; Minko, Y. Carbometallation Reactions. In *Metal Catalyzed Cross-Coupling Reactions*; 2013; Vol. 3, pp 763–874.

(182) Nakamura, E.; Mori, S.; Nakamura, M.; Morokuma, K. Theoretical Studies on the

Addition of Polymetallic Lithium Organocuprate Clusters to Acetylene. Cooperative Effects of Metals in a Trap-and-Bite Reaction Pathway. *J. Am. Chem. Soc.* **1997**, *119*, 4887–4899.

(183) House, H. O.; Chu, C. Y.; Wilkins, J. M.; Umen, M. J. The Chemistry of Carbanions. XXVII. Convenient Precursor for the Generation of Lithium Organocuprates. *J. Org. Chem.* **1975**, *40*, 1460–1469.

(184) Bertz, S. H.; Vellekoop, A. S.; Smith, R. A. J.; Snyder, J. P. Preparation of Ethereal Lithium Dimethylcuprates (Me2CuLi)2 and Me2CuLi•LiI Displaying Narrow Line Width 13C NMR Resonances. *Organometallics* **1995**, *14*, 1213–1220.

(185) Surry, D. S.; Spring, D. R. The Oxidation of Organocuprates—an Offbeat Strategy for Synthesis. *Chem. Soc. Rev.* **2006**, *35*, 218–225.

(186) Klosowski, D. W.; Martin, S. F. Synthesis of (+)-Disparlure via Enantioselective Iodolactonization. *Org. Lett.* **2018**, *20*, 1269–1271.

(187) Yu, H.; Li, J.; Wu, D.; Qiu, Z.; Zhang, Y. Chemistry and Biological Applications of Photo-Labile Organic Molecules. *Chem. Soc. Rev.* **2010**, *39*, 464–473.

(188) Bochet, C. G. Photolabile Protecting Groups and Linkers. **2002**, No. September 2001, 125–142.

(189) Mayer, G.; Heckel, A. Biologically Active Molecules with a " Light Switch " Angewandte. *Angew. Chem. Int. Ed.* **2006**, *45*, 4900–4921.

(190) Young, D. D.; Deiters, A. Photochemical Activation of Protein Expression in Bacterial Cells. *Angew. Chem. Int. Ed.* **2007**, *46*, 4290–4292.

(191) Shao, Q.; Xing, B. Photoactive Molecules for Applications in Molecular Imaging and Cell Biology. **2010**, 2835–2846.

(192) Pelliccioli, A. P.; Wirz, J. Photoremovable Protecting Groups: Reaction Mechanisms and Applications. *Photochem. Photobiol. Sci.* **2002**, *1*, 441–458.

(193) Klán, P.; Bochet, C. G.; Givens, R.; Rubina, M.; Popik, V.; Kostikov, A.; Wirz, J.; Klán, P.; Šolomek, T.; Bochet, C. G.; et al. Photoremovable Protecting Groups in Chemistry and Biology: Reaction Mechanisms and Efficacy. *Chem. Rev.* **2013**, *113*, 119–1191.

(194) Givens, R. S.; Rubina, M.; Wirz, J. Applications of P-Hydroxyphenacyl (pHP) and Coumarin-4-Ylmethyl Photoremovable Protecting Groups. *Photochem. Photobiol. Sci.* **2012**, *11*, 472.

(195) *Dynamic Studies in Biology: Phototriggers, Photoswitches and Caged Biomolecules*; Goeldner, M., Givens, R., Eds.; John Wiley & Sons, 2006.

(196) Barltrop, J. A.; Schofield, P. Photosensitive Protecting Groups. *Tetrahedron Lett.* **1962**, No. 16, 697–699.

(197) Barton, D. H. R.; Chow, Y. L.; Cox, A.; Kirby, G. W. Photosensitive Protection of Functional Groups. *Tetrahedron Lett.* **1962**, *3*, 1055–1057.

(198) Sheehan, J. C.; Wilson, R. M. Photolysis of Desyl Compounds. A New Photolytic Cyclization. *J. Am. Chem. Soc.* **1964**, *86*, 5277–5281.

(199) Patchornik, A.; Amit, B.; Woodward, R. B. Photosensitive Protecting Groups. *J. Am. Chem. Sociely* **1970**, *92*, 6333–6335.

(200) Barltrop, J. A.; Plant, P. J.; Schofield, P. Photosensitive Protective Groups. *Chem. Commun.* **1966**, *0,* 822–823.

(201) Givens, R. S.; Conrad II, P. G.; Yousef, A. L.; Lee, J.-I. Photoremovable Protecting Groups. In *CRC Handbook of Organic Photochemistry and Photobiology, Volumes 1 & 2, Second Edition*; Horspool, W., Lenci, F., Eds.; CRC Press: Boca Raton, 2003.

(202) Wang, P. Photolabile Protecting Groups: Structure and Reactivity. *Asian J. Org. Chem.* **2013**, *2*, 452–464.

(203) Šolomek, T.; Mercier, S.; Bally, T.; Bochet, C. G. Photolysis of Ortho-Nitrobenzylic Derivatives: The Importance of the Leaving Group. *Photochem. Photobiol. Sci.* **2012**, *11*, 548.

(204) Šolomek, T.; Bochet, C. G.; Bally, T. The Primary Steps in Excited-State Hydrogen Transfer: The Phototautomerization of O-Nitrobenzyl Derivatives. *Chem. Eur. J.* **2014**, *20*, 8062–8067.

(205) Il'ichev, Y. V.; Schworer, M. A.; Wirz, J. Photochemical Reaction Mechanisms of 2-Nitrobenzyl Compounds: Methyl Ethers and Caged ATP. *J. Am. Chem. Soc.* **2004**, *126*, 4581–4595.

(206) Kohl-Landgraf, J.; Buhr, F.; Lefrancois, D.; Mewes, J. M.; Schwalbe, H.; Dreuw, A.; Wachtveitl, J. Mechanism of the Photoinduced Uncaging Reaction of Puromycin Protected by a 6-Nitroveratryloxycarbonyl Group. *J. Am. Chem. Soc.* **2014**, *136*, 3430–3438.

(207) Schaper, K.; Etinski, M.; Fleig, T. Theoretical Investigation of the Excited States of 2-Nitrobenzyl and 4,5-Methylendioxy-2-Nitrobenzyl Caging Groups. *Photochem. Photobiol.* **2009**, *85*, 1075–1081.

(208) Zuman, P.; Shah, B. Addition, Reduction, and Oxidation Reactions of Nitrosobenzene. *Chem. Rev.* **1994**, *94*, 1621–1641.

(209) Zou, K.; Todd Miller, W.; Givens, R. S.; Bayley, H. Caged Thiophosphotyrosine Peptides. *Angew. Chem. Int. Ed.* **2001**, *40*, 3049–3051.

(210) Zou, K.; Cheley, S.; Givens, R. S.; Bayley, H. Catalytic Subunit of Protein Kinase A Caged at the Activating Phosphothreonine. *J. Am. Chem. Soc.* **2002**, *124*, 8220–8229.

(211) Schwörer, M.; Wirz, J. Photochemical Reaction Mechanisms of 2-Nitrobenzyl Compounds in Solution, I. 2-Nitrotoluene: Thermodynamic and Kinetic Parameters of Theaci-Nitro Tautomer. *Helv. Chim. Acta* **2001**, *84*, 1441–1458.

(212) Cameron, J. F.; Fréchet, J. M. J. Photogeneration of Organic Bases from O-Nitrobenzyl-Derived Carbamates. *J. Am. Chem. Soc.* **1991**, *113*, 4303–4313.

(213) Neenan, T. X.; Houlihan, F. M.; Reichmanis, E.; Kometani, J. M.; Bachman, B. J.; Thompson, L. F. Photo- and Thermochemistry of Select 2,6-Dinitrobenzyl Esters in Polymer Matrices: Studies Pertaining to Chemical Amplification and Imaging. *Macromolecules* **1990**, *23*, 145–150.

(214) Momotake, A.; Lindegger, N.; Niggli, E.; Barsotti, R. J.; Ellis-Davies, G. C. R. The Nitrodibenzofuran Chromophore: A New Caging Group for Ultra-Efficient Photolysis in Living Cells. *Nat. Methods* **2006**, *3*, 35–40.

(215) Schäfer, F.; Joshi, K. B.; Fichte, M. A. H.; MacK, T.; Wachtveitl, J.; Heckel, A. Wavelength-Selective Uncaging of Da and dC Residues. *Org. Lett.* **2011**, *13*, 1450–1453.

(216) Mahmoodi, M. M.; Abate-Pella, D.; Pundsack, T. J.; Palsuledesai, C. C.; Goff, P. C.; Blank, D. A.; Distefano, M. D. Nitrodibenzofuran: A One-and Two-Photon Sensitive Protecting Group That Is Superior to Brominated Hydroxycoumarin for Thiol Caging in Peptides. *J. Am. Chem. Soc.* **2016**, *138*, 5848–5859.

(217) Hasan, A.; Foote, R. S.; Cornwell, P.; Isham, K. R.; Gigerich, H.; Stengele, K.-P.; Pfleiderer, W.; Sachleben, R. A. Photolabile Protecting Groups for Nucleosides:synthesis and Photodeprotection Rates. *Tetrahedron* **1997**, *53*, 4247–4264.

(218) Beier, M.; Hoheisel, J. D. Production by Quantitative Photolithographic Synthesis of Individually Quality Checked DNA Microarrays. *Nucleic Acids Res.* **2000**, *28*, e11.

(219) Berroy, P.; Viriot, M. L.; Carré, M. C. Photolabile Group for 5′-OH Protection of Nucleosides: Synthesis and Photodeprotection Rate. *Sensors Actuators, B Chem.* **2001**, *74*, 186–189.

(220) Bhushan, K. R. Light-Directed Maskless Synthesis of Peptide Arrays Using Photolabile Amino Acid Monomers. *Org. Biomol. Chem.* **2006**, *4*, 1857.

(221) Donato, L.; Mourot, A.; Davenport, C. M.; Herbivo, C.; Warther, D.; Léonard, J.; Bolze, F.; Nicoud, J. F.; Kramer, R. H.; Goeldner, M.; et al. Water-Soluble, Donor – Acceptor Biphenyl Derivatives in the 2-(O-Nitrophenyl) Propyl Series: Highly Efficient Two-Photon Uncaging of the Neurotransmitter γ-Aminobutyric Acid at λ = 800 nm. *Angew. Chem. Int. Ed.* **2012**, *51*, 1840–1843.

(222) Amit, B.; Ben-Efraim, D. A.; Patchornik, A. Light-Sensitive Amides. The Photosolvolysis of Substituted 1-Acyl-7-Nitroindolines. *J. Am. Chem. Soc.* **1976**,

98, 843–844.

(223) Amit, B.; Patchornik, A. The Photorearrangement of N-Substituted Ortho-Nitroanilides and Nitroveratramides. A Potential Photosensitive Protecting Group. *Tetrahedron Lett.* **1973**, *14*, 2205–2208.

(224) Cohen, A. D.; Helgen, C.; Bochet, C. G.; Toscano, J. P. The Mechanism of Photoinduced Acylation of Amines by N-Acyl-5,7- Dinitroindoline as Determined by Time-Resolved Infrared Spectroscopy. *Org. Lett.* **2005**, *7*, 2845–2848.

(225) Papageorgiou, G.; Corrie, J. E. T. Synthesis of an Anionically Substituted Nitroindoline-Caged GABA Reagent That Has Reduced Affinity for GABA Receptors. *Tetrahedron* **2007**, *63*, 9668–9676.

(226) Pass, S. H.; Amit, B.; Patchornik, A. Racemization-Free Photochemical Coupling of Peptide Segments. *J. Am. Chem. Soc.* **1981**, *103*, 7674–7675.

(227) Trigo, F. F.; Papageorgiou, G.; Corrie, J. E. T.; Ogden, D. Laser Photolysis of DPNI-GABA, a Tool for Investigating the Properties and Distribution of GABA Receptors and for Silencing Neurons in Situ. *J. Neurosci. Methods* **2009**, *181*, 159–169.

(228) Park, C. H.; Givens, R. S. New Photoactivated Protecting Groups. 6. P-Hydroxyphenacyl: A Phototrigger for Chemical and Biochemical Probes. *J. Am. Chem. Soc.* **1997**, *119*, 2453–2463.

(229) Givens, R. S.; Park, C. H. P-Hydroxyphenacyl ATP: A New Phototrigger. *Tetrahedron Lett.* **1996**, *37*, 6259–6262.

(230) Zabadal, M.; Pelliccioli, A. P.; Klán, P.; Wirz, J. 2,5-Dimethylphenacyl Esters: A Photoremovable Protecting Group for Carboxylic Acids. *J. Phys. Chem. A* **2001**, *105*, 10329–10333.

(231) Klán, P.; Zabadal, M.; Heger, D. 2,5-Dimethylphenacyl as a New Photoreleasable Protecting Group for Carboxylic Acids. *Org. Lett.* **2000**, *2*, 1569–1571.

(232) Tseng, S. S.; Ullman, E. F. Elimination Reactions Induced by Photoenolization of O-Alkylbenzophenones. *J. Am. Chem. Soc.* **1976**, *98*, 541–544.

(233) Atemnkeng, W. N.; Louisiana, L. D.; Yong, P. K.; Vottero, B.; Banerjee, A. 1-[2-(2-Hydroxyalkyl)phenyl]ethanone: A New Photoremovable Protecting Group for Carboxylic Acids. *Org. Lett.* **2003**, *5*, 4469–4471.

(234) Pirrung, M. C.; Roy, B. G.; Gadamsetty, S. Structure-Reactivity Relationships in (2-Hydroxyethyl)benzophenone Photoremovable Protecting Groups. *Tetrahedron* **2010**, *66*, 3147–3151.

(235) Pika, J.; Konosonoks, A.; Robinson, R. M.; Singh, P. N. D.; Gudmundsdottir, A. D. Photoenolization as a Means to Release Alcohols. *J. Org. Chem.* **2003**, *68*, 1964–1972.

(236) Givens, R. S.; Matuszewski, B. Photochemistry of Phosphate Esters: An Effecient Method for Generation of Electrophiles. *J. Am. Chem. Soc.* **1984**, *106*, 6860–6861.

(237) Fournier, L.; Aujard, I.; Le Saux, T.; Maurin, S.; Beaupierre, S.; Baudin, J. B.; Jullien, L. Coumarinylmethyl Caging Groups with Redshifted Absorption. *Chem. Eur. J.* **2013**, *19*, 17494–17507.

(238) Schmidt, R.; Geissler, D.; Hagen, V. Kinetics Study of the Photocleavage of (Coumarin-4-Yl) Methyl Esters. *J. Phys. Chem. A* **2005**, *109*, 5000–5004.

(239) Schmidt, R.; Geissler, D.; Hagen, V.; Bendig, J. Mechanism of Photocleavage of (Coumarin-4-Yl)methyl Esters. *J. Phys. Chem. A* **2007**, *111*, 5768–5774.

(240) Hagen, V.; Kilic, F.; Schaal, J.; Dekowski, B.; Schmidt, R.; Kotzur, N. [8-[Bis(carboxymethyl)aminomethyl]-6-Bromo-7-Hydroxycoumarin-4-Yl]methyl Moieties as Photoremovable Protecting Groups for Compounds with COOH, NH 2, OH, and C-O Functions. *J. Org. Chem.* **2010**, *75*, 2790–2797.

(241) Fonseca, A. S. C.; Gonçalves, M. S. T.; Costa, S. P. G. Photocleavage Studies of Fluorescent Amino Acid Conjugates Bearing Different Types of Linkages. *Tetrahedron* **2007**, *63*, 1353–1359.

(242) Shembekar, V. R.; Chen, Y.; Carpenter, B. K.; Hess, G. P. A Protecting Group for Carboxylic Acids That Can Be Photolyzed by Visible Light. *Biochemistry* **2005**, *44*, 7107–7114.

(243) Shembekar, V. R.; Chen, Y.; Carpenter, B. K.; Hess, G. P. Coumarin-Caged Glycine That Can Be Photolyzed within 3 μs by Visible Light. *Biochemistry* **2007**, *46*, 5479–5484.

(244) Olson, J. P.; Kwon, H. B.; Takasaki, K. T.; Chiu, C. Q.; Higley, M. J.; Sabatini, B. L.; Ellis-Davies, G. C. R. Optically Selective Two-Photon Uncaging of Glutamate at 900 Nm. *J. Am. Chem. Soc.* **2013**, *135*, 5954–5957.

(245) Fournier, L.; Gauron, C.; Xu, L.; Aujard, I.; Saux, T. Le; Gagey-eilstein, N.; Maurin, S.; Dubruille, S.; Baudin, J.; Bensimon, D.; et al. A Blue-Absorbing Photolabile Protecting Group for in Vivo Chromatically Orthogonal Photoactivation. *ACS Chem. Biol.* **2013**, *8*, 1528–1536.

(246) Goswami, P. P.; Syed, A.; Beck, C. L.; Albright, T. R.; Mahoney, K. M.; Unash, R.; Smith, E. A.; Winter, A. H. BODIPY-Derived Photoremovable Protecting Groups Unmasked with Green Light. *J. Am. Chem. Soc.* **2015**, *137*, 3783–3786.

(247) Sitkowska, K.; Feringa, B. L.; Szymański, W. Green-Light-Sensitive BODIPY Photoprotecting Groups for Amines. *J. Org. Chem.* **2018**, *83*, 1819–1827.

(248) Gardner, L.; Deiters, A. Light-Controlled Synthetic Gene Circuits. *Curr. Opin. Chem. Biol.* **2012**, *16*, 292–299.

(249) Deiters, A. Light Activation as a Method of Regulating and Studying Gene

Expression. *Curr. Opin. Chem. Biol.* **2009**, *13*, 678–686.

(250) Weber, W.; Fussenegger, M. Artificial Mammalian Gene Regulation Networks-Novel Approaches for Gene Therapy and Bioengineering. *J. Biotechnol.* **2002**, *98*, 161–187.

(251) Weber, W.; Fux, C.; Daoud-El Baba, M.; Keller, B.; Weber, C. C.; Kramer, B. P.; Heinzen, C.; Aubel, D.; Bailey, J. E.; Fussenegger, M. Macrolide-Based Transgene Control in Mammalian Cells and Mice. *Nat. Biotechnol.* **2002**, *20*, 901–907.

(252) Gitzinger, M.; Kemmer, C.; El-Baba, M. D.; Weber, W.; Fussenegger, M. Controlling Transgene Expression in Subcutaneous Implants Using a Skin Lotion Containing the Apple Metabolite Phloretin. *Proc. Natl. Acad. Sci.* **2009**, *106*, 10638–10643.

(253) Gitzinger, M.; Kemmer, C.; Fluri, D. A.; Daoud El-Baba, M.; Weber, W.; Fussenegger, M. The Food Additive Vanillic Acid Controls Transgene Expression in Mammalian Cells and Mice. *Nucleic Acids Res.* **2012**, *40*.

(254) Weber, W.; Fussenegger, M. Approaches for Trigger-Inducible Viral Transgene Regulation in Gene-Based Tissue Engineering. *Curr. Opin. Biotechnol.* **2004**, *15*, 383–391.

(255) Saenger, W.; Orth, P.; Kisker, C.; Hillen, W.; Hinrichs, W. The Tetracycline Repressor-A Paradigm for a Biological Switch. *Angew. Chem. Int. Ed.* **2000**, *39*, 2042–2052.

(256) Chopra, I.; Roberts, M. Tetracycline Antibiotics: Mode of Action, Applications, Molecular Biology, and Epidemiology of Bacterial Resistance. *Microbiol. Mol. Biol. Rev.* **2001**, *65*, 232–260.

(257) Gossen, M.; Freundlieb, S.; Bender, G.; Müller, G.; Hillen, W.; Bujard, H. Transcriptional Activation by Tetracyclines in Mammalian Cells. *Science,* **1995**, *268*, 1766–1769.

(258) Gossen, M.; Bujard, H. Anhydrotetracycline, a Novel Effector for Tetracycline Controlled Gene Expression Systems in Eukaryotic Cells. *Nucleic Acids Res.* **1993**, *21*, 4411–4412.

(259) Gossen, M.; Bonin, A. L.; Freundlieb, S.; Bujard, H. Inducible Gene Expression Systems for Higher Eukaryotic Cells. *Curr. Opin. Biotechnol.* **1994**, *5*, 516–520.

(260) Cambridge, S. B.; Geissler, D.; Keller, S.; Cürten, B. A Caged Doxycycline Analogue for Photoactivated Gene Expression. *Angew. Chem. Int. Ed.* **2006**, *45*, 2229–2231.

(261) Cambridge, S. B.; Geissler, D.; Calegari, F.; Anastassiadis, K.; Hasan, M. T.; Stewart, A. F.; Huttner, W. B.; Hagen, V.; Bonhoeffer, T. Doxycycline-Dependent Photoactivated Gene Expression in Eukaryotic Systems. *Nat. Methods* **2009**, *6*, 527–531.

(262) Gardner, L.; Zou, Y.; Mara, A.; Cropp, T. A.; Deiters, A. Photochemical Control of Bacterial Signal Processing Using a Light-Activated Erythromycin. *Mol. Biosyst.* **2011**, *7*, 2554–2557.

(263) Zheng, J.; Sagar, V.; Smolinsky, A.; Bourke, C.; LaRonde-LeBlanc, N.; Cropp, T. A. Structure and Function of the Macrolide Biosensor Protein, MphR(A), with and without Erythromycin. *J. Mol. Biol.* **2009**, *387*, 1250–1260.

(264) Kramer, B. P.; Viretta, A. U.; Baba, M. D. E.; Aubel, D.; Weber, W.; Fussenegger, M. An Engineered Epigenetic Transgene Switch in Mammalian Cells. *Nat. Biotechnol.* **2004**, *22*, 867–870.

(265) Carrillo-Reid, L.; Yang, W.; Kang Miller, J.; Peterka, D. S.; Yuste, R. Imaging and Optically Manipulating Neuronal Ensembles. *Annu. Rev. Biophys.* **2017**, *46*, 271–293.

(266) Markram, H. Seven Challenges for Neuroscience. *Funct. Neurol.* **2013**, *28*, 145–151.

(267) Mayr, B.; Montminy, M. Transcriptional Regulation by the Phosphorylation-Dependent Factor Creb. *Nat. Rev. Mol. Cell Biol.* **2001**, *2*, 599–609.

(268) Leclercq, R. Mechanisms of Resistance to Macrolides and Lincosamides: Nature of the Resistance Elements and Their Clinical Implications. *Clin. Infect. Dis.* **2002**, *34*, 482–492.

(269) Orth, P.; Schnappinger, D.; Hillen, W.; Saenger, W.; Hinrichs, W. Structural Basis of Gene Regulation by the Tetracycline Inducible Tet Repressor-Operator System. *Nat. Struct. Biol.* **2000**, *7*, 215–219.

(270) Martínez, Á. T.; Speranza, M.; Ruiz-Dueñas, F. J.; Ferreira, P.; Camarero, S.; Guillén, F.; Martínez, M. J.; Gutiérrez, A.; Del Río, J. C. Biodegradation of Lignocellulosics: Microbial, Chemical, and Enzymatic Aspects of the Fungal Attack of Lignin. *Int. Microbiol.* **2005**, *8*, 195–204.

(271) Thanbichler, M.; Iniesta, A. A.; Shapiro, L. A Comprehensive Set of Plasmids for Vanillate - And Xylose-Inducible Gene Expression in Caulobacter Crescentus. *Nucleic Acids Res.* **2007**, *35*, 1–16.

(272) Werten, S.; Dalm, D.; Palm, G. J.; Grimm, C. C.; Hinrichs, W. Tetracycline Repressor Allostery Does Not Depend on Divalent Metal Recognition. *Biochemistry* **2014**, *53*, 7990–7998.

(273) Meis, A. R. Unpublished results

(274) Orth, P.; Cordes, F.; Schnappinger, D.; Hillen, W.; Saenger, W.; Hinrichs, W. Conformational Changes of the Tet Repressor Induced by Tetracycline Trapping. **1998**, *2*, 439–447.

(275) Dos Santos, H. F.; De Almeida, W. B.; Zerner, M. C. Conformational Analysis of

the Anhydrotetracycline Molecule: A Toxic Decomposition Product of Tetracycline. *J. Pharm. Sci.* **1998**, *87*, 190–195.

(276) Neises, B.; Steglich, W. Simple Method for the Esterification of Carboxylic Acids. *Angew. Chem. Int. Ed.* **1978**, *17*, 522–524.

(277) Sun, X.; Lee, H.; Lee, S.; Tan, K. L. Catalyst Recognition of Cis-1,2-Diols Enables Site-Selective Functionalization of Complex Molecules. *Nat. Chem.* **2013**, *5*, 790–795.

(278) Miller, M. W.; Hochstein, F. A. Isolation and Characterization of Two New Tetracycline Antibiotics. *J. Org. Chem* **1962**, *27*, 2525–2528.

(279) Wong, P. T.; Roberts, E. W.; Tang, S.; Mukherjee, J.; Cannon, J.; Nip, A. J.; Corbin, K.; Krummel, M. F.; Choi, S. K. Control of an Unusual Photo-Claisen Rearrangement in Coumarin Caged Tamoxifen through an Extended Spacer. *ACS Chem. Biol.* **2017**, *12*, 1001–1010.

(280) Faal, T.; Wong, P. T.; Tang, S.; Coulter, A.; Chen, Y.; Tu, C. H.; Baker, J. R.; Choi, S. K.; Inlay, M. a. 4-Hydroxytamoxifen Probes for Light-Dependent Spatiotemporal Control of Cre-ER Mediated Reporter Gene Expression. *Mol. BioSyst.* **2015**, *11*, 783–790.

(281) Deiters, A. Principles and Applications of the Photochemical Control of Cellular Processes. *ChemBioChem*. 2010, pp 47–53.

(282) Wilson, R. M.; Danishefsky, S. J. Applications of Total Synthesis to Problems in Neurodegeneration: Fascinating Chemistry along the Way. *Acc. Chem. Res.* **2006**, *39*, 539–549.

(283) Yang, X. W.; Yang, C. P.; Jiang, L. P.; Qin, X. J.; Liu, Y. P.; Shen, Q. S.; Chen, Y. Bin; Luo, X. D. Indole Alkaloids with New Skeleton Activating Neural Stem Cells. *Org. Lett.* **2014**, *16*, 5808–5811.

(284) Bihelovic, F.; Ferjancic, Z. Total Synthesis of (±)-Alstoscholarisine A. *Angew. Chem. Int. Ed.* **2016**, *55*, 2569–2572.

(285) Liang, X.; Jiang, S.-Z.; Wei, K.; Yang, Y.-R. Enantioselective Total Synthesis of (−)-Alstoscholarisine A. *J. Am. Chem. Soc.* **2016**, *138*, 2560–2562.

(286) Mason, J. D.; Weinreb, S. M. Total Syntheses of the Monoterpenoid Indole Alkaloids (±)-Alstoscholarisine B and C. *Angew. Chem. Int. Ed.* **2017**, *56*, 16674–16676.

(287) Huang, J.; Zhao, L.; Liu, Y.; Cao, W.; Wu, X. Enantioselective Intermolecular Formal [3 + 3] Cycloaddition of 2,3-Disubstituted Indoles with Acrolein. *Org. Lett.* **2013**, *15*, 4338–4341.

(288) Helmboldt, H.; Aho, J. E.; Pinko, P. M. Synthetic Studies toward Pectenotoxin 2. Part II. Synthesis of the CDE and CDEF Ring Systems. *Org. Lett.* **2008**, *10*, 4183–

4185.

(289) Martin, S. F.; Benage, B. Applications of Intramolecular Diels–Alder Reactions of Heterodienes. Facile Syntheses of The Heteroyohimbine Alkaloids Tetrahydroalstonine and Akuammigine. *Tetrahedron Lett.* **1984**, *25*, 4863–4866.

(290) Martin, S. F.; Benage, B.; Williamson, S. A.; Brown, S. P. Applications of the Intramolecular Diels-Alder Reactions of Heterodienes to the Syntheses of Indole Alkaloids. *Tetrahedron* **1986**, *42*, 2903–2910.

(291) Martin, S. F.; Tu, C. yun; Kimura, M.; Simonsen, S. H. Intramolecular [4 + 2] Cycloadditions as a General Strategy for Alkaloid Synthesis. A Novel Formal Synthesis of Lycorine. *J. Org. Chem.* **1982**, *47*, 3634–3643.

(292) Martin, S. F.; Williamson, S. A.; Gist, R. P.; Smith, K. M. Aspects of the Intramolecular Diels-Alder Reactions of Some 1,3,9-Trienic Amides, Amines, and Esters. An Approach to the Pentacyclic Skeleton of the Yohimboid Alkaloids. *J. Org. Chem.* **1983**, *48*, 5170–5180.

(293) Martin, S. F.; Hunter, J. E.; Benage, B.; Geraci, L. S.; Mortimore, M.; Hunter, J. E.; Mortimore, M. Unified Strategy for Synthesis of Indole and 2-Oxindole Alkaloids. *J. Am. Chem. Soc.* **1991**, *113*, 6161–6171.

(294) Martin, S. F. Natural Products and Their Mimics as Targets of Opportunity for Discovery. *J. Org. Chem.* **2017**, *82*, 10757–10794.

(295) Miró, J.; Sánchez-Roselló, M.; Sanz, Á.; Rabasa, F.; Del Pozo, C.; Fustero, S. Tandem Cross Enyne Metathesis (CEYM)-Intramolecular Diels-Alder Reaction (IMDAR). An Easy Entry to Linear Bicyclic Scaffolds. *Beilstein J. Org. Chem.* **2015**, *11*, 1486–1493.

(296) Kim, P.; Nantz, M. H.; Kurth, M. J.; Olmstead, M. M. Intramolecular Diels−Alder Reactions of Decatrienoates: Remote Stereocontrol and Conformational Activation. *Org. Lett.* **2000**, *2*, 1831–1834.

(297) Jung, M. E.; Huang, A.; Johnson, T. W. Unusual Diastereoselectivity in Intramolecular Diels-Alder Reactions of Substituted 3,5-Hexadienyl Acrylates. Preference for a Boatlike Structure of the Six-Atom Tether due to Ester Overlap. *Org. Lett.* **2000**, *2*, 1835–1837.

(298) Tantillo, D. J.; Houk, K. N.; Jung, M. E. Origins of Stereoselectivity in Intramolecular Diels-Alder Cycloadditions of Dienes and Dienophiles Linked by Ester and Amide Tethers. *J. Org. Chem.* **2001**, *66*, 1938–1940.

(299) Amoroso, R.; Cardillo, G.; Tomasini, C.; Tortoreto, P. A New Route to the Synthesis of Amino Acids through the Mercury Cyclization of Chiral Amidals. *J. Org. Chem.* **1992**, *57*, 1082–1087.

(300) Gronowitz, S.; Lidert, Z. A Convenient Synthesis of N-Substituted N-Chloromethyl Carboxamides. *Synthesis* **1979**, *1979*, 810.

(301) Dharuman, S.; Vankar, Y. D. N -Halosuccinimide/AgNO3-Efficient Reagent Systems for One-Step Synthesis of 2-Haloglycals from Glycals: Application in the Synthesis of 2C-Branched Sugars via Heck Coupling Reactions. *Org. Lett.* **2014**, *16*, 1172–1175.

(302) Della Ca, N.; Fontana, M.; Motti, E.; Catellani, M. Pd/Norbornene: A Winning Combination for Selective Aromatic Functionalization via C-H Bond Activation. *Acc. Chem. Res.* **2016**, *49*, 1389–1400.

(303) Gao, Y.; Zhu, W.; Yin, L.; Dong, B.; Fu, J.; Ye, Z.; Xue, F.; Jiang, C. Palladium-Catalyzed Direct C2-Arylation of Free (N H) Indoles via Norbornene-Mediated Regioselective C H Activation. *Tetrahedron Lett.* **2017**, *58*, 2213–2216.

(304) Jiao, L.; Bach, T. Palladium-Catalyzed Direct 2-Alkylation of Indoles by Norbornene-Mediated Regioselective Cascade C-H Activation. *J. Am. Chem. Soc.* **2011**, *133*, 12990–12993.

(305) Wang, X.; Gribkov, D. V.; Sames, D. Phosphine-Free Palladium-Catalyzed C-H Bond Arylation of Free (N-H)-Indoles and Pyrroles. *J. Org. Chem.* **2007**, *72*, 1476–1479.

(306) Enders, J. C. D.; Mehta, S. V. L. G.; Overman, R. N. L. E.; Polanc, A. P. S.; Editor, S.; Maes, B. U. W. *Topics in Heterocyclic Chemistry Series*; 2012.

(307) Ila, H.; Markiewicz, J. T.; Malakhov, V.; Knochel, P. Metalated Indoles, Indazoles, Benzimidazoles, and Azaindoles and Their Synthetic Applications. *Synthesis* **2013**, *45*, 2343–2371.

(308) Gribble, G. W.; Keavy, D. J.; Davis, D. A.; Saulnier, M. G.; Pelcman, B.; Barden, T. C.; Sibi, M. P.; Olson, E. R.; Belbruno, J. J. Syntheses and Diels–Alder Cycloaddition Reactions of 4H-Furo[3,4-B]indoles. A Regiospecific Diels–Alder Synthesis of Ellipticine. *J. Org. Chemisry* **1992**, *57*, 5878–5891.

(309) Haas, D.; Hammann, J. M.; Greiner, R.; Knochel, P. Recent Developments in Negishi Cross-Coupling Reactions. *ACS Catal.* **2016**, *6*, 1540–1552.

(310) Milne, J. E.; Buchwald, S. L. An Extremely Active Catalyst for the Negishi Cross-Coupling Reaction. *J. Am. Chem. Soc.* **2004**, *126*, 13028–13032.

(311) Cobo, I.; Matheu, M. I.; Castill, S.; Boutureira, O.; Davis, B. G. Phosphine-Free Suzuki À Miyaura Cross-Coupling in Aqueous Media Enables Access to 2- C -Aryl-Glycosides. **2013**, *500*, 2010–2013.

(312) Kinzel, T.; Zhang, Y.; Buchwald, S. A New Palladium Precatalyst for the Suzuki Coupling of Unstable Boronic Acids. *J. Am. Chem. Soc.* **2010**, *132*, 14073–14075.

(313) Pangborn, A. B.; Giardello, M. A.; Grubbs, R. H.; Rosen, R. K.; Timmers, F. J. Safe and Convenient Procedure for Solvent Purification. *Organometallics* **1996**, *15*, 1518–1520.

(314) Garg, Y.; Kumar Tiwari, A.; Kumar Pandey, S. Enantioselective Total Synthesis of Cis-(+)- and Trans-(+)-Disparlure. *Tetrahedron Lett.* **2017**, *58*, 3344–3346.